

University of Southampton Research Repository ePrints Soton

Copyright © and Moral Rights for this thesis are retained by the author and/or other copyright owners. A copy can be downloaded for personal non-commercial research or study, without prior permission or charge. This thesis cannot be reproduced or quoted extensively from without first obtaining permission in writing from the copyright holder/s. The content must not be changed in any way or sold commercially in any format or medium without the formal permission of the copyright holders.

When referring to this work, full bibliographic details including the author, title, awarding institution and date of the thesis must be given e.g.

AUTHOR (year of submission) "Full thesis title", University of Southampton, name of the University School or Department, PhD Thesis, pagination

University of Southampton

Faculty of Engineering and the Environment

Bioenergy and Organic Resources Group

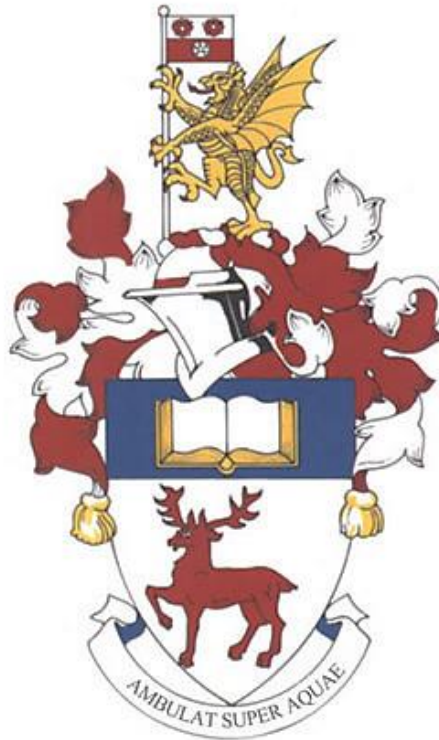
Anaerobic digestion of marine microalgae

By

Keiron Philip Roberts

Thesis for the degree of Doctor of Philosophy

May 2015



Declaration of authorship

I Keiron Philip Roberts declare that this thesis and the work presented in it are my own and have been generated by me as the result of my own original research.

Title: Anaerobic digestion of marine microalgae.

I confirm that:

1. This work was done wholly or mainly while in candidature for a research degree at this University;
2. Where any part of this thesis has previously been submitted for a degree or any other qualification at this University or any other institution, this has been clearly stated;
3. Where I have consulted the published work of others, this is always clearly attributed;
4. Where I have quoted from the work of others, the source is always given. With the exception of such quotations, this thesis is entirely my own work;
5. I have acknowledged all main sources of help;
6. Where the thesis is based on work done by myself jointly with others, I have made clear exactly what was done by others and what I have contributed myself;
7. Parts of this work have been published as:

Roberts, K. P., et al. (2016). "Quantification of methane losses from the acclimatisation of anaerobic digestion to marine salt concentrations." Renewable Energy **86**: 497-506.

Signed:.....

Date:.....

Abstract

Anaerobic digestion is a simple and energetically efficient way in comparison to some other biofuel methods of producing renewable energy from a range of biomass types. Although digestion of micro-algal biomass was first suggested in the 1950s, only a few studies have been conducted for assessment of its performance. This work assessed the potential for energy recovery from microalgae via anaerobic digestion for both freshwater and marine species.

This research screened seven laboratory-grown marine and freshwater microalgal species (*Nannochloropsis. oculata*, *Thalassiosira . pseudonana*, *Dunaliella. salina*, *Rhododomas sp*, *Isochrysis. galbana*, *Chlorella. vulgaris* and *Scenedesmus sp*) and two samples from large-scale cultivation systems for their suitability as a substrate for anaerobic digestion. Biochemical methane production and a theoretical maximum growth yield of each species were employed to offer a means of comparing methane productivity per unit of cultivation under standard conditions. The data generated were useful in determining suitable species to culture and digest under continuous operation.

A review of the literature highlighted a gap in the knowledge for the continuous digestion of different marine micro-algal species, as well as the potential inhibitory effect of high salinities on the anaerobic digestion process to non-acclimatised systems run under continuous operation. Addition of total salt $\geq 10\text{g L}^{-1}$ caused reactor failure, supporting the findings of the literature review. It was possible, however, to gradually adapt the inoculum to marine concentrations of chloride salts (31.1 g L^{-1}) with $<7\%$ difference in specific methane production of controls. Addition of sulphate showed competition between methanogens and sulphate-reducing bacteria with further minor losses in methane yield. There was up to 60% reduction in SMP for the highest sulphate loaded reactors, however, the population successfully adapted to sulphate concentrations above those typically found in seawater and showed gaseous H_2S productivity in proportion to the applied sulphate load. This suggests that the effects of marine concentrations of chloride and sulphate salts can be overcome by a gradual acclimatisation.

The selected algal species *I. galbana* and *D. salina* were continuously cultivated in a photobioreactor under low and high sulphate media and continuously digested using the salt adapted inoculum. The specific methane production for *I. galbana* and *D. salina* was 0.19 and 0.23 L CH₄ g⁻¹ VS, with a VS destruction of 32% and 50% respectively. Addition of a high SO₄ grown *D. salina* as a feed resulted in a reduction of SMP to 0.19 L CH₄ g⁻¹ VS with an increase in H₂S production. Losses in total solids and sulphur were observed under continuous study due to oxidation of H₂S and struvite precipitation within the reactors, which was not observed under batch analysis. This highlights the importance in conducting continuous studies over batch, as these effects can be overlooked.

Acknowledgements

Throughout the emotional rollercoaster that is a PhD I have had the fortune to work with and meet many fantastic people whom have helped and guided me along in what appears at times, the long lonely road of academic research.

I would like to give my heartfelt thanks and appreciation to Dr. Sonia Heaven and Prof. Charles Banks, whom without their perseverance, patience and professionalism in developing and guiding myself as a researcher, I would never have had the opportunity to start, or dedication to finish a PhD. Thank you for putting up with my terrible spelling.

My appreciation and thanks to Dr. Yue Zhang for her valuable advice, keen eye for detail and kind words throughout the PhD.

My thanks and appreciation to Dr. Dominic Mann or all the help you have given me within the laboratory and Pilar Pascual-Hidalgo for training me on almost every piece of analytical equipment we have access too. A special thank-you for the lengthy conversations we used to have around the GC.

I must give a massive thank-you to everyone within the Bioenergy and Organic Resources Research Group, and my friends within the office for all your help, advice, proofreading and discussions over coffee/ beer.

Thanks to the EPSRC and the All Gas project for funding me throughout my studies to enable me to conduct my research and visit distant places.

Thanks to the “Magnolia Army”, Alisdair and the late Phil all of whom encouraged each other to pursue a PhD and stick with academia, at the last count 5 out of 8 are now Dr’s.

Lastly I would like to give my thanks and congratulate my wife Lauren, and my family, particularly my father, for putting up with me talking about “poo” all the time. Your unwavering encouragement, patience and help have helped power me through, and without you I doubt I would have had the determination to finish.

Table of Contents

1. Background	1
1.1 Energy crisis	1
1.2 Biofuels	4
1.2.1 First generation biofuels	5
1.2.2 Second generation biofuels	7
1.2.3 Third generation biofuels	8
1.2.4 Anaerobic digestion.....	9
1.3 Aims and objectives	10
2. Literature review	13
2.1 Algae	13
2.1.1 Aquatic photosynthesis	14
2.1.2 Nutrients	18
2.1.3 Commercial applications of macro and microalgae.....	22
2.1.4 Commercial and large scale algal culturing	24
2.2 Algae and biofuels	29
2.2.1 Macro algae as a feedstock for biofuels	31
2.3 Algal species examined	33
2.3.1 <i>Chlorella vulgaris</i>	33
2.3.2 <i>Scenedesmus spp.</i>	34
2.3.3 <i>Nannochloropsis oculata</i>	35
2.3.4 <i>Isochrysis galbana</i>	36
2.3.5 <i>Dunaliella salina</i>	37
2.3.6 <i>Thalassiosira pseudonana</i>	38
2.3.7 <i>Rhodomonas spp.</i>	39
2.4 Anaerobic digestion	39

2.4.1	Hydrolysis	40
2.4.2	Acidogenesis.....	41
2.4.3	Acetogenesis.....	42
2.4.4	Methanogenesis	43
2.4.5	Environmental factors that influence anaerobic digestion...	44
2.4.6	Potential inhibitors for the AD of marine microalgae	47
2.4.7	Sulphur and sulphate	51
2.4.8	C/N and algae digestion.....	56
2.4.9	Anaerobic digestion of algae	58
2.4.10	Conclusions from the literature review.....	71
3.	Methodology	74
3.1	General.....	74
3.2	Culture media and feedstocks	74
3.2.1	Jaworski's Medium (JM).....	75
3.2.2	Almeria Culture medium	76
3.2.3	Low Sulphate medium	77
3.3	Culturing algae	80
3.3.1	Photobioreactor Design	83
3.3.2	Growth rate.....	86
3.3.3	Algae examined	88
3.3.4	Large-scale algal harvesting.....	89
3.4	Basic analysis.....	90
3.4.1	pH	90
3.4.2	Alkalinity.....	90
3.4.3	Volatile fatty acids (VFA).....	91

3.4.4	Total Kjeldahl Nitrogen (TKN) and total ammonia nitrogen (TAN)	92
3.4.5	Total solids and volatile solids	92
3.4.6	Total Suspended Solids	93
3.4.7	VS destruction	94
3.4.8	Determination of solids loss	94
3.4.9	Cell number	94
3.4.10	Light metal cations by Flame Absorption Spectrometry	95
3.4.11	Elemental composition	95
3.4.12	Calorific value	96
3.4.13	Theoretical methane potential, Buswell equation	96
3.4.14	Gas volume and composition	96
3.4.15	Sulphide analysis	99
3.4.16	Total soluble sulphide - calculated	99
3.4.17	Soluble sulphide - ion selective electrode	100
3.4.18	Soluble sulphate	101
3.5	Anaerobic digestion	103
3.5.1	Biochemical methane potential assay	104
3.5.2	Simulated SMY	105
4.	Experimental Results	107
4.1	Algal characterisation	107
4.1.1	Introduction	107
4.1.2	Growth rates and growth yields	108
4.1.3	Sulphate and growth rate/ yield for marine microalgae	112
4.1.4	Optimum concentration of JM	120
4.1.5	Characterisation of freshwater and marine microalgae	122

4.1.6	BMP and theoretical energy values	125
4.1.7	Methane production kinetics	129
4.1.8	Growth yield and effect on overall methane productivity ..	132
4.1.9	Discussion of algal screening	133
4.1.10	Conclusions from algal screening	138
4.2	Acclimatisation of municipal wastewater bio-solids to salt	140
4.2.1	Introduction	140
4.2.2	Substrate characteristics	142
4.2.3	Phase 1 – preliminary trial	144
4.2.4	Phase 2 and Phase 3.....	148
4.2.5	Digestate solids content.....	158
4.2.6	Phase 4 – Sulphate addition.....	165
4.2.7	Concluding remarks	181
4.3	Large scale algal growth and continuous digestion	182
4.3.1	Introduction	182
4.3.2	Continuous algal growth	182
4.3.3	Cultivation results and discussion	183
4.3.4	Continuous algal digestion.....	186
4.3.5	Results and discussion	187
4.3.6	Continuous digestion study.....	190
4.3.7	Continuous digestion discussion	204
4.3.8	Concluding remarks	212
5.	Conclusions and further work.....	215
5.1	Conclusions	215
5.1.1	Algal growth and characterisation	215
5.1.2	Acclimatisation to chloride and sulphate salts.....	216

5.1.3	Continuous digestion of <i>D. salina</i> and <i>I. galbana</i>	217
5.2	Further work	218
6.	References	219

Table of Figures and Tables

Figures

FIGURE 1 FOSSIL FUEL PRICE BETWEEN 1950 AND 2008 (SHAFIEE AND TOPAL, 2010).....	3
FIGURE 2 FOSSIL FUEL PRICE BETWEEN 1950 AND 2008 CORRECTED FOR INFLATION (SHAFIEE AND TOPAL, 2010).	3
FIGURE 3 GLOBAL ENERGY USAGE (CHUM ET AL., 2011)	5
FIGURE 4 GLOBAL BIOENERGY USAGE (CHUM ET AL., 2011)	5
FIGURE 5 GLOBAL BIOETHANOL PRODUCTION (AJANOVIC, 2011).....	7
FIGURE 6 GLOBAL BIODIESEL PRODUCTION (AJANOVIC, 2011).....	7
FIGURE 7 – RESEARCH OUTLINE AND PLAN FOR THE FOLLOWING PHD.	12
FIGURE 8 – PHYLOGENETIC TREE OF LIFE, WITH COLOURED BOXES DENOTING DIVERSITY IN PIGMENTATION. THE ANIMAL AND PLANT KINGDOMS ARE CIRCLED IN GREEN AND RED RESPECTIVELY (SCHLARB-RIDLEY, 2011).....	14
FIGURE 9– (P) RESPONSE OF CHANGING LIGHT INTENSITY ON PHOTOSYNTHESIS. THE RATE OF INCREASE IS A, THE COMPENSATION IRRADIANCE WHERE PHOTOSYNTHESIS IS EQUAL TO RESPIRATION. R IS RESPIRATION RATE, E_k IS WHERE PHOTOSYNTHESIS BECOMES LIGHT SATURATED, P_{MAX} IS WHERE THE RATE OF PHOTOSYNTHESIS BECOMES SATURATED. P_G AND P_N ARE GROSS AND NET PHOTOSYNTHESIS RESPECTIVELY (KAISER ET AL., 2005A).	16
FIGURE 10 - DETERMINATION OF THE INFLUENCE OF % OF OXYGEN WITHIN INJECTED GAS AND BIOMASS YIELD AT AN IRRADIANCE OF $300 \text{ MMOL M}^{-2} \text{ S}^{-1}$ (MOLINA ET AL., 2001).	18
FIGURE 11 – FRACTIONS OF DIFFERENT CARBONATE SPECIES AT CHEMICAL EQUILIBRIUM. INCREASING PH ALTERS THE STOICHIOMETRY OF DISSOLVED INORGANIC CARBON FROM CO_2 AT A PH OF 0-8, HCO_3^- AT A PH OF 4-11 AND CO_3^{2-} AT 7-14 (FLEISCHER ET AL., 1996).	19
FIGURE 12 – SPECIFIC GROWTH RATE OF <i>D. SALINA</i> AS A FUNCTION OF THE SULPHATE CONCENTRATION IN THE CULTURE MEDIUM (GIORDANO ET AL., 2000).....	21
FIGURE 13 – GLOBAL SECURITY THREAT OF FRESHWATER AS A RESOURCE, IMAGE TAKEN FROM VOROSMARTY ET AL. (2010).....	22
FIGURE 14 – SCHEMATIC OF A SIMPLE RACEWAY POND (SINGH AND SHARMA, 2012), IMAGE OF RACEWAY PONDS IN ALMERIA, SOUTHERN SPAIN.	25
FIGURE 15 – SCHEMATIC OF ATYPICAL FLAT PLATE PHOTOBIOREACTOR USED WITHIN A LABORATORY SETTING (SINGH AND SHARMA, 2012).	26
FIGURE 16 - SERPENTINE TUBULAR REACTOR USED AT ALMERIA IN SOUTHERN SPAIN. THE SOLAR RECEIVER RETURNS ON TOP OF ITSELF CAUSING SHADED REGIONS FROM DAYLIGHT (FERNANDEZ ET AL., 2001)	27
FIGURE 17 – MICROSCOPE IMAGE OF <i>CHLORELLA SP.</i>	33
FIGURE 18 – MICROSCOPE IMAGE OF <i>SCENEDESMUS SP.</i>	34
FIGURE 19 – MICROSCOPE IMAGE OF <i>NANNOCHLOROPSIS SP.</i>	35

FIGURE 20 – <i>ISOCHRYSIS GALBANA</i> (THRONDSEN, 1997).	36
FIGURE 21 – <i>DUNALIELLA SALINA</i> .	37
FIGURE 22 – SEM IMAGE OF <i>THALASSIOSIRA PSEUDONANA</i> .	38
FIGURE 23 - <i>RHODOMONAS SP</i> (THRONDSEN, 1997).	39
FIGURE 24 A SCHEMATIC PATHWAY OF THE ANAEROBIC CONVERSION OF BIOMASS TO METHANE ADAPTED FROM DEMIREL AND SCHERER (2008).	40
FIGURE 25 RELATIVE GROWTH RATES OF PSYCHROPHILIC, MESOPHILIC AND THERMOPHILIC METHANOGENS (LETTINGA ET AL., 2001).	45
FIGURE 26 PATHWAYS FOR SULPHUR REDUCTION AND OXIDATION (MUYZER AND STAMS, 2008).	52
FIGURE 27 – COMPETITION OF THE PATHWAYS BETWEEN SRB AND METHANOGENIC ARCHAEA.	53
FIGURE 28 – FRACTIONS OF SULPHIDE SPECIES PRESENT WITHIN AN ANAEROBIC DIGESTER IN AQUEOUS SOLUTION AS A FUNCTION OF PH AT 25°C, IMAGE ADAPTED FROM BLUNDEN AND ANEJA (2008).	55
FIGURE 29 ALGAL STARTER CULTURES GROWING IN THE LABORATORY.	81
FIGURE 30 – 25 L CULTURING VESSELS.	82
FIGURE 31 – SCHEMATIC OF BUBBLE COLUMN USED TO GROW ALGAE FOR BMP EXAMINATION.	82
FIGURE 32 – ABOVE, PHOTO OF CONSTRUCTED PHOTOBIOREACTOR, AND BELOW SCHEMATIC OF THE SERPENTINE TUBULAR PHOTOBIOREACTOR USED FOR THE CONTINUOUS GROWTH OF MARINE MICROALGAE.	84
FIGURE 33 ALGAL CULTURES IN SIDE ARM FLASKS FOR GROWTH RATE DETERMINATION ...	87
FIGURE 34 – RELATIONSHIP BETWEEN THE GROWTH LIMITING FACTOR (S) AND THE SPECIFIC GROWTH RATE AS A % OF THE MAXIMUM GROWTH RATE UNDER IDEAL CONDITIONS FOR THE MONOD EQUATION MODEL (MONOD, 1949).	88
FIGURE 35 – POWERFUGE PILOT CENTRIFUGE SETUP TO CENTRIFUGE LAB GROWN MICROALGAE.	89
FIGURE 36 – UKRAINIAN MILK CREAMER.	90
FIGURE 37 – CSTR DESIGN FOR SEMI CONTINUOUS ANAEROBIC DIGESTION STUDIES (JIANG ET AL., 2012).	103
FIGURE 38 2 LITRE CSTR	104
FIGURE 39 CALIBRATION CURVES FOR TSS G L ⁻¹ AND ABSORBANCE AT AN OPTICAL DENSITY OF 680 FOR EACH SPECIES GROWN ON JM. (A) <i>SCENEDESMUS SP</i> , (B) <i>C. VULGARIS</i> , (C) <i>D. SALINA</i> , (D) <i>RHODODOMAS SP</i> , (E) <i>I. GALBANA</i> , (F) <i>N. OCVLATA</i> , (G) <i>T. PSEUDONANA</i> .	109
FIGURE 40 RESULTS FOR GROWTH OF FRESHWATER MICROALGAE CULTIVATED ON JM AND MARINE MICROALGAE CULTIVATED ON JM UNDER BOTH FRESH WATER AND MARINE MEDIA WITH USSS IN G TSS L ⁻¹ .	110
FIGURE 41 FLOW DIAGRAM OF THE SO ₄ ANALYSIS EXPERIMENT FOR EACH SULPHATE CONCENTRATION.	113
FIGURE 42 FINAL GROWTH YIELDS (A-C) AND CELL NUMBERS (D- F) FOR THE FOUR GENERATION RUNS WITH <i>D. SALINA</i> , <i>N. OCVLATA</i> AND <i>I. GALBANA</i> GROWN ON JM AND	

ARTIFICIAL SALT WITH DIFFERENT CONCENTRATIONS OF SO ₄ . KINETIC GROWTH RATE FOR THE FOURTH GENERATION RUN DETERMINED BY OD IN FIGURES G-I.....	115
FIGURE 43 SULPHATE CONCENTRATION IN MG L ⁻¹ FOR THE END OF EACH GENERATIONAL RUN.....	118
FIGURE 44 CULTURES POST GROWTH FOR <i>D. SALINA</i> UNDER BATCH CONDITIONS FOR THE SO ₄ CONCENTRATION STUDY. (A) FIRST GENERATION OF <i>D. SALINA</i> WITH DECREASING SULPHATE CONCENTRATION FROM LEFT TO RIGHT, (B) FINAL GENERATION OF <i>D. SALINA</i> WITH DECREASING SULPHATE CONCENTRATION FROM LEFT TO RIGHT, (C) CLUMPED ORGANIC MATTER IN FAILED FINAL CULTURE OF <i>D. SALINA</i> AT 0.1% SULPHATE.	119
FIGURE 45 GROWTH RATES OF <i>D. SALINA</i> GROWN ON SALT FORMULATION AS DESCRIBED IN SECTION 3.2.3 AND DIFFERING TOTAL CONCENTRATIONS OF JM.	121
FIGURE 46 28-DAY BMP CUMULATIVE NET SPECIFIC METHANE YIELD OF MARINE AND FRESHWATER MICROALGAE, (A) AND (B) 90-DAY BMP TEST	126
FIGURE 47 88 - DAY BMP CUMULATIVE NET SPECIFIC METHANE YIELD OF MARINE AND FRESHWATER MICROALGAE	127
FIGURE 48 CUMULATIVE NET SPECIFIC METHANE YIELD OF MARINE AND FRESHWATER MICROALGAE (AVERAGE OF EXPERIMENTAL DATA POINTS FOR REPLICATES) WITH KINETIC MODELS	131
FIGURE 49 INCREMENTAL INCREASES IN TOTAL SALT CONTENT IN FEED AND IN DIGESTER CONTENTS DURING PHASE 2 AND PHASE THREE.	141
FIGURE 50 SMP AND VBP FOR PHASE 1 REACTORS. VERTICAL DOTTED LINES INDICATE SALT SPIKING AND/OR START OF SALT SUPPLEMENTATION TO FEED ON DAY 13 AND CESSATION OF FEEDING FOR R3-6 ON DAY 35	145
FIGURE 51 PH (A), TAN (B), IA/PA RATIO (C), TOTAL ALKALINITY (D), PARTIAL ALKALINITY (E), INTERMEDIATE ALKALINITY (F). VERTICAL DOTTED LINES INDICATE SALT SPIKING AND/OR START OF SALT SUPPLEMENTATION TO FEED ON DAY 13 AND CESSATION OF FEEDING FOR R3-6 ON DAY 35.	146
FIGURE 52 (A) TOTAL VFA G L ⁻¹ , VFA SPECIES FOR REACTORS: R1 (B), R2 (C), R3 (D), R4 (E), R5 (F), R6 (G), R7 (H), R8 (I), R9 (J) AND R10 (K). VERTICAL DOTTED LINES INDICATE SALT SPIKING AND/OR START OF SALT SUPPLEMENTATION TO FEED ON DAY 13 AND CESSATION OF FEEDING FOR R3-6 ON DAY 35	148
FIGURE 53 TS % WW AND VS % WW	148
FIGURE 54 (A) VBP, (B) %CH ₄ , (C) SMP, (D) AVERAGE SMP. BLACK VERTICAL LINES DENOTE THE END OF PHASES. THE FIRST LINE IS THE END OF PHASE 2 WHERE REACTORS 1-8 ARE SPIKED WITH CHLORIDE SALTS, WITH THE RIGHT LINE THE POINT WHERE REACTORS R1 – R8 ARE BROUGHT UP TO 31.1G L ⁻¹ TOTAL SALT.....	150
FIGURE 55 (A) TS %WW, (B) VS% WW, (C) VS AS A % OF TS AND (D) % VS DESTRUCTION. BLACK VERTICAL LINES DENOTE THE END OF PHASES. THE FIRST LINE IS THE END OF PHASE 2 WHERE REACTORS 1-8 ARE SPIKED WITH CHLORIDE SALTS, WITH THE RIGHT LINE THE POINT WHERE REACTORS R1 – R8 ARE BROUGHT UP TO 31.1G L ⁻¹ TOTAL SALT.	152

FIGURE 56 (A) PH, (B) AMMONIA, (C) TOTAL VFA CONTENT, (D) TOTAL ALKALINITY, (E) PARTIAL ALKALINITY, (F) INTERMEDIATE ALKALINITY AND (G) IA/PA RATIO. BLACK VERTICAL LINES DENOTE THE END OF PHASES. THE FIRST LINE IS THE END OF PHASE 2 WHERE REACTORS 1-8 ARE SPIKED WITH CHLORIDE SALTS, WITH THE RIGHT LINE THE POINT WHERE REACTORS R1 – R8 ARE BROUGHT UP TO 31.1G L ⁻¹ TOTAL SALT.....	156
FIGURE 57 VFA PROFILES FOR R1 – R10. BLACK VERTICAL LINES DENOTE THE END OF PHASES. THE FIRST LINE IS THE END OF PHASE 2 WHERE REACTORS 1-8 ARE SPIKED WITH CHLORIDE SALTS, WITH THE RIGHT LINE THE POINT WHERE REACTORS R1 – R8 ARE BROUGHT UP TO 31.1G L ⁻¹ TOTAL SALT.....	158
FIGURE 58 MODELLED SALT LOSS DATA WITH ACTUAL ADDITIONAL ASH CONTENT COMPARED TO CONTROL FOR EACH DUPLICATE OF THE SALT SUPPLEMENTED REACTORS. WHERE EXTRA ASH IS THE DIFFERENCE BETWEEN THE CONTROL GROUP TS AND THE SALT SPIKED REACTORS TS.	160
FIGURE 59A SHOWS FOULING OF REACTOR SURFACES PRIOR TO CLEANING WITH DETERGENT AND HOT WATER. FIGURE 11B SHOWS SALT DEPOSITS AFTER DETERGENT, HOT WATER, MECHANICAL CLEANING AND AN INITIAL RINSE WITH SULPHURIC ACID.	160
FIGURE 60 AVERAGE WEEKLY VBP (A), AND SMP (B), AND WEEKLY %CH ₄ CONTENT OF THE BIOGAS (C) FOR THE SULPHATE ADDITION REACTORS.....	166
FIGURE 61 (A) TS% WW, (B) VS% WW AND (C) %VS DESTRUCTION.....	168
FIGURE 62 (A) PH, (B) TAN, (C) TOTAL ALKALINITY, (D) PARTIAL ALKALINITY, (E) INTERMEDIATE ALKALINITY, (F) IA/PA AND (G) TOTAL VFA FOR THE REACTORS WITHIN PHASE 4.	171
FIGURE 63 (A) VFA F1, (B) VFA F2, (C) VFA F3, (D) VFA F4, (E) VFA F5, (F) VFA F6, (G) VFA F7 AND (H) VFA F8 FOR PHASE 4.....	173
FIGURE 64 MEASURED AND CALCULATED VALUES FOR SOLUBLE SULPHIDE AT DIFFERENT SULPHATE CONCENTRATIONS.	173
FIGURE 65 HYDROGEN SULPHIDE PRODUCTION GRAPHS FOR PHASE 4. (A) H ₂ S PPMV (B) VOLUMETRIC H ₂ S PRODUCTION (C) SOLUBLE H ₂ S (D) SOLUBLE HS ⁻ (E) TOTAL DISSOLVED SULPHIDE (F) H ₂ S PPMV/SO ₄ ADDITION (G) COD/ SO ₄ (H) % REMOVAL OF SULPHUR	177
FIGURE 66 (A), PRE INOCULATION WITH <i>I. GALBANA</i> SHOWING THE AIRLIFT, (B) POST INOCULATION WITH <i>I. GALBANA</i> , (C) FOULING HAS BEGUN TO OCCUR WHERE THE PLASTIC FOLLOWERS ARE FAILING TO CLEAN THE REACTOR IN THE CENTRAL PART OF THE TUBES.....	184
FIGURE 67 TSS OF PBR FOR THE SPECIES <i>I. GALBANA</i> AND <i>D. SALINA</i> . DOTTED VERTICAL LINES REPRESENT POINTS WHERE BIOFOULING OCCURRED SUFFICIENTLY TO REDUCE YIELDS PRIOR TO STOPPING.	185
FIGURE 68 WEEKLY AVERAGES (A) BIOGAS, (B) BIOGAS G ⁻¹ VS, (C) SMP, (D) RESIDUAL BIOGAS PRODUCTION. ERROR BARS SHOW THE RANGE OF THE DATA.	191
FIGURE 69 (A) % TS AND VS OF THE DIGESTATE WW, (B) % VS DESTRUCTION. ERROR BARS SHOW THE RANGE OF THE DATA.	192

FIGURE 70 (A) AMMONIA, (B) PH, (C) ALKALINITY, (D) IA:PA, (E) TOTAL VFA, (F) <i>I. GALBANA</i> VFA, (G) <i>D. SALINA</i> VFA, (H) <i>D. SALINA</i> SO ₄ VFA. ERRORBARS SHOW THE RANGE OF THE DATA.	194
FIGURE 71 (A) BIOCHEMICAL METHANE POTENTIAL OF CELLULOSE CONTROL AND MILLBROOK DIGESTATE AS A BLANK. (B) BIOCHEMICAL METHANE POTENTIAL OF <i>I. GALBANA</i> , <i>D. SALINA</i> AND <i>D.SALINA</i> SO ₄ CONTINUOUSLY CULTIVATED IN A PBR. (C) METHANE PRODUCTION FOR THE TMP CALCULATED FROM THE EA, THE FINAL BMP VALUES FROM GRAPH B, AND THE AVERAGE FOR THE LAST HRT FOR THE SMP FROM THE CONTINUOUS DIGESTION ANALYSIS WITHIN THIS SECTION. ERROR BARS SHOW THE RANGE OF THE DATA.	196
FIGURE 72 CUMULATIVE NET SPECIFIC METHANE YIELD OF MARINE MICROALGAE (AVERAGE OF EXPERIMENTAL DATA POINTS FOR REPLICATES) WITH KINETIC MODELS. (A) <i>I. GALBANA</i> , (B) <i>D. SALINA</i> AND (C) <i>D. SALINA</i> SO ₄	197
FIGURE 73 AVERAGE IN-SITU RESIDUAL BIOGAS PRODUCTION POST-FEEDING FOR THE DIGESTERS <i>D. SALINA</i> , <i>D. SALINA</i> SO ₄ AND <i>I. GALBANA</i>	199
FIGURE 74 DESIGN OF MASS BALANCE IMPLEMENTED TO DETERMINE THE REMOVAL RATE OF SULPHUR EQUATIONS WITHIN SECTION 3.4.	202
FIGURE 75 (A) PPMV H ₂ S, (B) L H ₂ S G ⁻¹ VS ADDED, (C) MG L ⁻¹ H ₂ S SOLUBLE, (D) MG L ⁻¹ TOTAL SULPHIDE SOLUBLE, (E) PERCENTAGE REMOVAL OF SULPHUR. ERROR BARS SHOW THE RANGE OF THE DATA.	203
FIGURE 76 IMAGES OF DEPOSITS WITHIN THE ANAEROBIC DIGESTERS FOR LOW SULPHATE <i>D. SALINA</i> ON THE LEFT (A AND C), AND HIGH SULPHATE FED <i>D. SALINA</i> REACTORS ON THE RIGHT (B AND D).	209
FIGURE 77 OPTICAL MICROSCOPE IMAGES OF THE FEEDSTOCK'S PRE AND POST DIGESTION.	211

Tables

TABLE 1 – MEAN COMPOSITION OF PRIMARY COMPONENTS OF MARINE PHYTOPLANKTON, ADAPTED FROM (SARMIENTO AND GRUBER., 2006).....	18
TABLE 2 – MAXIMUM DISTANCE BETWEEN THE EXIT OF THE AIRLIFT COLUMN AND THE ENTRANCE (M) BASED ON EQUATIONS 2.1 AND 2.3.....	29
TABLE 3 OPTIMUM TEMPERATURE RANGES FOR THE GROWTH OF METHANE PRODUCING ARCHAEA ADAPTED FROM GERARDI (2003)	45
TABLE 4 – OBSERVED EFFECTS OF THE LIGHT METAL IONS NA, MG, CA AND K ON METHANE PRODUCTION FROM LARGE SCALE AD FACILITIES (MCCARTY, 1964).	49
TABLE 5 – SUMMARY OF ANAEROBIC TREATMENT OF HIGH SALINITY WASTEWATER AND SUBSTRATES WITH SUCCESSFUL <50% INHIBITED METHANOGENS. TABLE ADAPTED FROM LEFEBVRE AND MOLETTA (2006) AND FEIJOO ET AL. (1995).	50

TABLE 6 – FREE ENERGY CHANGES FOR REMINERALISATION REACTIONS (MOREL AND HERING, 1993).	53
TABLE 7 METHANE PRODUCTION AND OPERATIONAL CONDITIONS FOR THE ANAEROBIC DIGESTION OF MICROALGAE. ALL RESULTS REPORTED ARE THE MAXIMUM SMP REPORTED AND THE CONDITIONS TO WHICH THEY WERE REACHED.	61
TABLE 8 – JAWORSKI’S MEDIUM (JM).....	75
TABLE 9 – COMPOSITION OF CULTURE MEDIUM USED IN RACEWAY PONDS IN ALMERIA SPAIN (INFORMATION PROVIDED BY JOSE LOUIS MENDOZA MARTIN).	76
TABLE 10 – SULPHATE CONCENTRATION OF LOW SULPHUR GROWTH CULTURE MEDIA EXPERIMENTS FOR MARINE ALGAE.....	77
TABLE 11 – SYNTHETIC WASTEWATER COMPOSITION AS DESCRIBED BY WHALLEY ET AL. (2013) AND ALI (2014).....	78
TABLE 12 – TRACE ELEMENT SOLUTION	78
TABLE 13 – ARTIFICIAL SEAWATER CONSISTING OF THE 6 MAIN IONS FOUND IN SEAWATER, USED WITHIN THE SULPHATE GROWTH EXPERIMENTS AND CONTINUOUS CULTIVATION OF MARINE MICROALGAE FOR CONTINUOUS DIGESTION (BROWN ET AL., 2005).....	79
TABLE 14 – SULPHATE CONCENTRATIONS AND ADDITIONS.	79
TABLE 15 – OVERALL HYDRAULIC DESIGN OF THE PHOTOBIOREACTOR. THE TOTAL VOLUME HAS BEEN ESTIMATED WITH A HEADER TANK VOLUME OF APPROXIMATELY 20L.	85
TABLE 16 DETERMINATION OF FLOW TYPE USING THE REYNOLDS EQUATION. TURBULENT FLOW SHOULD HELP PREVENT SEDIMENTATION AND INCREASE MIXING ENABLING MOVEMENT BETWEEN LIGHT AND DARK AREAS.	85
TABLE 17 – DETERMINATION OF THE SIZE OF MICRO-EDDIES USING EQUATIONS FROM FERNÁNDEZ ET AL. (2001).	86
TABLE 18 PARAMETERS USED TO IDENTIFY METAL CATIONS USING THE AA.....	95
TABLE 19 SOLUBLE SULPHIDE STANDARDS.	101
TABLE 20 GROWTH RATES AND YIELDS OF SIX MICROALGAE CULTIVATED ON JM IN DEIONISED WATER ONLY FOR FRESH WATER SPECIES AND DEIONISED WATER AND USSS FOR MARINE SPECIES.....	111
TABLE 21 FINAL TSS G L ⁻¹ AND CELL NUMBER FOR THE SPECIES <i>N. OCVLATA</i> , <i>D. SALINA</i> ANF <i>I. GALBANA</i> AT THE SO ₄ CONCENTRATIONS OF 0.195, 1.95, 3.9 AND 19.5 MG SO ₄ L ⁻¹ FOR EACH GENERATIONAL RUN.....	116
TABLE 22 GROWTH RATES OF <i>D. SALINA</i> , <i>N. OCVLATA</i> AND <i>I. GALBANA</i> FOR THE FOUR SULPHATE CONCENTRATIONS 19.5, 3.9, 1.95 AND 0.195 MG SO ₄ L ⁻¹ DETERMINED FROM THE FOURTH GENERATION RUN.	120
TABLE 23 GROWTH YIELDS OF <i>D. SALINA</i> AFTER 14 DAYS GROWING ON VARIOUS STRENGTHS OF JM.	122
TABLE 24 CHARACTERISTICS OF 8 MICRO-ALGAL SAMPLES.....	124
TABLE 25 BMP, TMP AND CALORIFIC VALUES	128
TABLE 26 METHANE YIELDS AND KINETIC CONSTANTS OBTAINED FROM MODELLING.....	130

TABLE 27 GROWTH RATES AND GROWTH YIELDS (FROM SECTION 4.1.2) WITH POTENTIAL METHANE PRODUCTION PER LITRE OF CULTURE PER DAY FOR SELECTED SAMPLES OF FRESHWATER AND MARINE MICROALGAE.	133
TABLE 28 – EXPERIMENTAL DESIGN FOR EACH OF THE FOUR MAIN PHASES.	141
TABLE 29 RESULTS OF CHARACTERISATION OF THE SYNTHETIC WASTEWATER.	142
TABLE 30 DRIED SALT SAMPLES CORRECTION AND OBSERVED % MASS OF METAL IONS IN SALT STOCK SOLUTION MEASURED USING THE AA.	143
TABLE 31 MASS OF COMPONENTS WITHIN THE SYNTHETIC FEED REQUIRED FOR STRUVITE FORMATION DETERMINED FROM THE SYNTHETIC WASTEWATER RECIPE IN SECTION 3.	162
TABLE 32 AVERAGE VALUES FOR KEY MONITORING PARAMETERS IN THE LAST 20 DAYS OF PHASE 2.....	163
TABLE 33 AVERAGE VALUES FOR KEY MONITORING PARAMETERS IN THE LAST 20 DAYS OF PHASE 3.....	164
TABLE 34 AVERAGE VALUES FOR KEY MONITORING PARAMETERS IN THE LAST 21 DAYS OF PHASE 4.....	178
TABLE 35 CHARACTERISTICS OF THE ALGAL PASTE HARVESTED FROM CONTINUOUS GROWTH.	189
TABLE 36 METHANE YIELDS AND KINETIC CONSTANTS OBTAINED FROM MODELLING.....	198
TABLE 37 TMP, BMP, SMP AND CALORIFIC VALUES	199
TABLE 38 CORRECTION OF TMP USING VS DESTRUCTION UNDER CSTR OPERATION.....	200

Nomenclature

AD	Anaerobic Digestion,
ASW	Artificial seawater from Sigma products,
BMP	Biochemical methane potential,
BOD	Biochemical oxygen demand
CCAP	Culture Collection of Algae and Protozoa,
Chl a	Chlorophyll a,
COD	Chemical oxygen demand,
DW	Dry Weight,
EPA	Eicosapentaenoic acid,
EA	Elemental analysis
EU	European Union,
FW	Fresh water,
GC,	Gas chromatograph,
HRT	Hydraulic Retention Time
JM	Jaworskis Media,
IEA	International Energy Agency,
IPCC	Intergovernmental Panel on Climate Change,
LED	Light emitting diode,
LCA	Life cycle assessment,
Mb day ⁻¹	Million barrels per day,
MSW	Municipal Solids Waste,
OLR	Organic Loading Rate,
PAR	Photosynthetically active radiation,
PBR	Photobioreactor,
PCE	Photoconversion efficiency,
PFD	Photon flux density,
POM,	Particulate organic matter,
PS σ	Photosystem 1 or 2,
RPM	Revolutions per minute,
SMP	Specific methane production,
SMY	Specific Methane Yield,
STP	Standard Temperature and Pressure,
TAN	Total Ammonia Nitrogen,
TCV	Theoretical calorific value,
TMP	Theoretical methane potential,
TOC	Total organic carbon,
TKN	Total Kjeldahl Nitrogen,
TS	Total Solids,
USSS	Ultramarine Synthetic Sea Salt (Bristol)
VBP	Volumetric biogas production,
VFA	Volatile fatty acids,
VS	Volatile solids,

VS_i Volatile solids inoculum,
VS_s Volatile solids substrate,
WW Wet weight,

CHAPTER 1

1. Background

1.1 Energy crisis

Fossil fuels are integral to the modern economy and way of life, but reserves of coal, oil and natural gas are being utilised at an ever-increasing rate, with reserves currently predicted to be depleted by 2112 (Shafiee and Topal, 2009). Currently the majority of the energy consumed globally is from non-renewable sources, with the UK share at 97% of total consumption (RCEP, 2004). Demand for crude oil is set to increase from 87 million barrels a day (Mb day^{-1}) to 99 Mb day^{-1} by 2035 at a conservative estimate (Goldthau and Sovacool, 2012). While new reserves are being discovered such as in Kent, many are in locations such as the Arctic and Antarctic which are technically and politically challenging to access. Increasing demand is coupled with increasing atmospheric CO_2 concentrations from pre-industrial concentrations of less than 240 ppm to 388 ppm and rising, leading to perturbation of the global climate (Meehl et al., 2007). Increasing demand for energy is being driven by a growing population and the increasing energy consumption of the developing world with its growing economies. Energy requirements are predicted to increase by 30% by 2035, with 90% of this increase coming from non-Organisation for Economic Co-operation and Development (OECD) countries, particularly China (IEA, 2006, Meehl et al., 2007, Guillard and Ryther, 1962).

Alternative energy sources are therefore required to help meet the growing demand and to mitigate the depletion of fossil fuel resources and the increase in anthropogenic CO_2 . Currently several options are available or in development to provide large scale energy to the public.

Of these nuclear power is currently the cleanest in terms of anthropogenic CO_2 emissions. It also occupies the smallest land area per energy output in relation to coal, gas and oil power stations as well as renewable energy sources. It does however; require a high initial and running capital coupled with high post use remediation than for fossil fuel sources. While it can be argued that the risk involved in the use of nuclear technology is low there

Chapter 1

is public concern over its use. Due to historical and recent nuclear accidents such as Windscale in the United Kingdom, Three Mile Island in the United States, Chernobyl in the Ukraine and most recently Fukushima in Japan. Development over the last two decades has thus been limited. America has the greatest number of nuclear power stations and output at 30% of the world's total nuclear power capacity, but no new stations have been constructed in the USA since 1996. In some countries the use of nuclear power has been discouraged, limiting the development of new nuclear technologies. In contrast France has managed to reduce its previously high dependence on fossil fuels with the use of nuclear power providing over 78% of its total electrical energy needs (IAEA, 2014). Nuclear fusion is a technology that has yet to be mastered, and made energy efficient. Hydroelectric power is location dependent, requires high reserves of water, and can cause ecological loss and changes in land use. Wind and tidal turbines are dependent on the weather and cannot supply current or predicted future requirements. Photovoltaics are dependent on irradiance and do not offer a continuous supply of power as they do not work at night (Sims et al., 2007). Geothermal power is also location dependent requiring high temperature aquifers. These latter technologies can only address the issue of electric power and not that of liquid fuels.

The past 40 years have also seen fluctuations and a general increase in the price and availability of our conventional energy sources as shown in Figure 1, with two major fuel crises occurring in 1973 and 1979 permanently increasing the price of fuel (Figure 1). When inflation is taken into account as shown in Figure 2, oil and natural gas had returned to pre fuel crisis within seven years, with coal taking twenty years to recover. Increasing difficulty finding and extracting fuels has driven the increase in fuel prices over the last 15 years with no sign of respite.

The majority of the world's liquid fuels are sourced from politically unstable countries such as Iran and Algeria, which historically and recently have had internal problems with political tensions with the western countries. Recently the USA has increased in-country drilling operations and is currently one of the single biggest suppliers of liquid fuels in the world. Political tensions between Europe, USA and Russia over the Ukraine and Syria have resulted in USA flooding the market with oil, reducing the price per barrel to ~\$60 per barrel as of writing this introduction. This is primarily an economic weapon of the

West against Russia as oil and gas account for 80% of Russia's exports and a substantial proportion of its GDP.

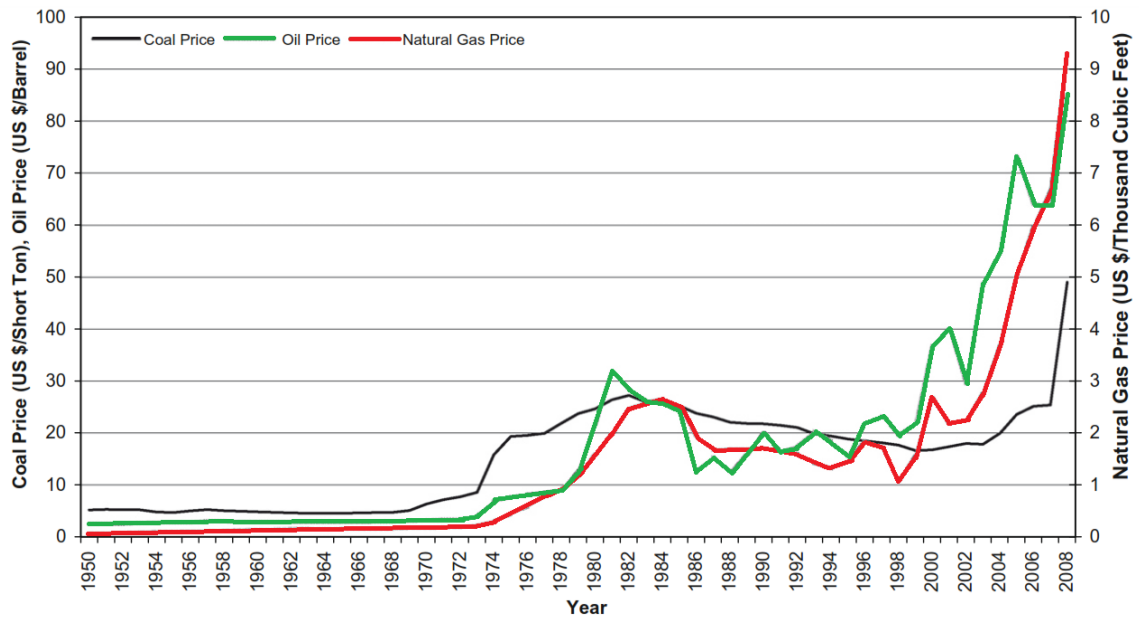


Figure 1 Fossil fuel price between 1950 and 2008 (Shafiee and Topal, 2010).

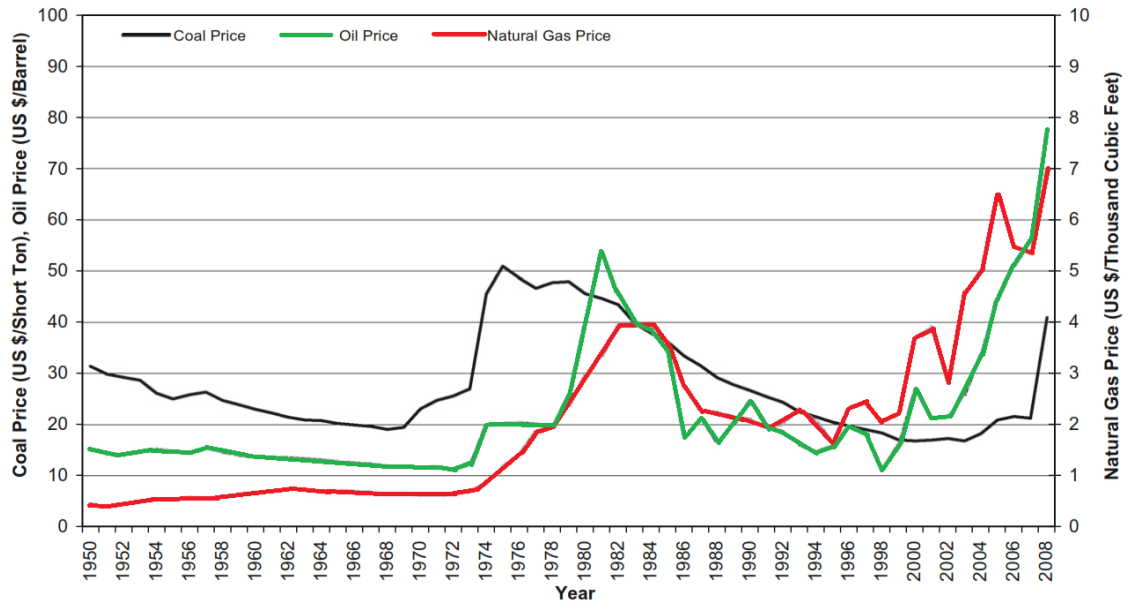


Figure 2 Fossil fuel price between 1950 and 2008 corrected for inflation (Shafiee and Topal, 2010).

To mitigate price increases and maintain energy security, political stability and sustainability requires the development of the alternative fuel sources mentioned above, a decrease in the demand for fossil fuels, and management and education on the use of fuels (Spicer, 1988, Shafiee and Topal, 2010). Given the range of demands and pressures, it is likely that a combination of energy sources is the best option to maintain energy security and stability of supply (Kiryama and Kajikawa, 2014).

1.2 Biofuels

Fuels derived from organic biomass are collectively known as biofuels, and traditionally come from two main sources: agricultural crops and woody material grown specifically for fuel use; and waste organic material/-agricultural residues (Spicer, 1988, Chum et al., 2011, Demirbaş, 2001). The energy within these biomasses can be released by a number of different processes. These include enzymatic breakdown and fermentation for biomasses high in sugar/ cellulose/ lignin to produce ethanol or heat via combustion; transesterification of high oil biomass for biodiesel production; anaerobic digestion of biomass in digesters or in landfill to produce biogas and pyrolysis and gasification to produce liquid, gas and solid carbon fuels (Demirbaş, 2001). Unlike most other renewable energy sources (with the exception of hydroelectric), the energy within biofuels and biomass can be easily stored until demand requires it, eliminating the mismatches between production and demand which are typical of wind and solar power (Milledge, 2010a). It can also be easily transported and used within vehicles using conventional methods with little adaption. The global renewable energy sector as of 2011 is less than 13% of global energy consumption, of which 80% is from bioenergy (Figure 3). Of this fraction 87% is from wood sources and 13% from alternative biomass sources (Figure 4). This is primarily due to the high demand for wood within the developing world to fuel homes (Chum et al., 2011).

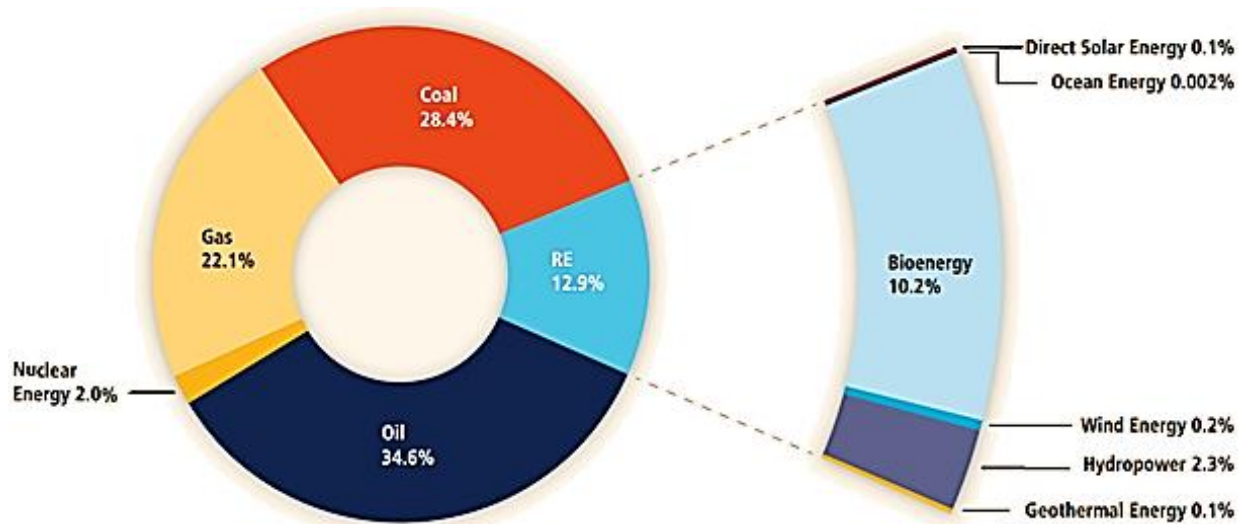


Figure 3 Global energy usage (Chum et al., 2011)

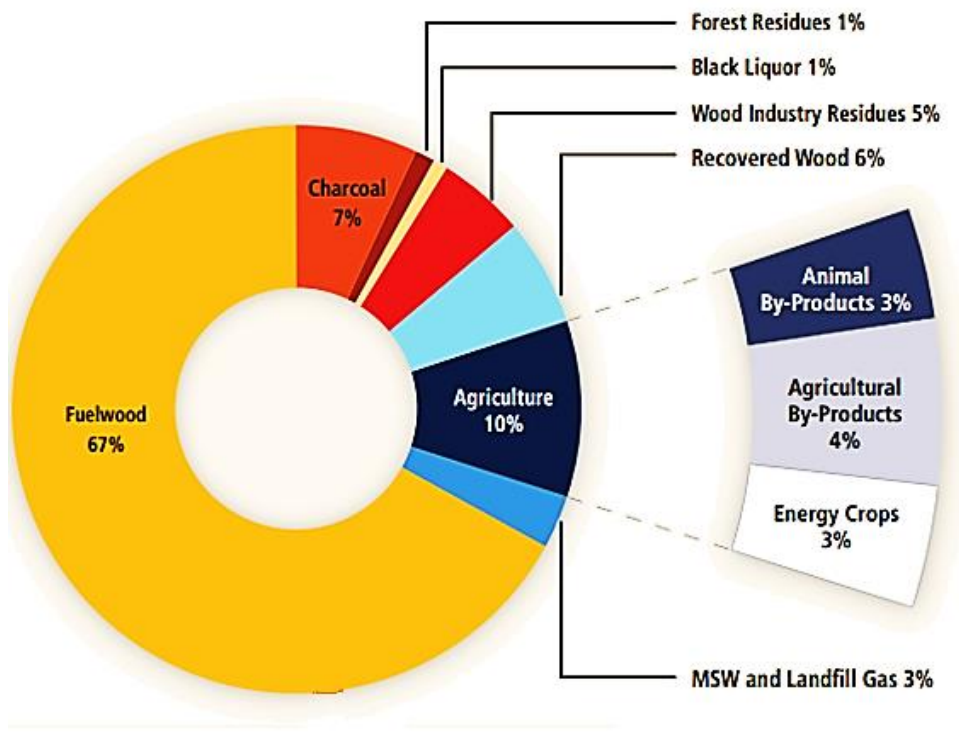


Figure 4 Global bioenergy usage (Chum et al., 2011)

1.2.1 First generation biofuels

First generation biofuels are made from edible sugars/starch or oil-containing parts of the plant, such as bioethanol from sugars and biodiesel from oils, with preferred feedstocks deriving from rapeseed, sugarcane, sunflowers, corn, soybean and wheat (Ajanovic,

2011). Biofuels from first generation crops can have an energy output greater than the energy used to cultivate, grow, harvest and produce the fuel. For bioethanol the energy output has been reported as around 25% and for biodiesel 93% more than the energy used to develop the fuel (Hill et al., 2006). Until relatively recently biofuels have not been economically viable on a global scale, with bioethanol being popular only among South American countries. With government subsidies for “greener” fuels, however, biofuels have become an increasingly popular alternative to fossil fuels. This increase is further driven by the European Union’s (EU) target of 10% of all transportation fuels being derived from biofuels by 2020. As a result of these pressures global bioethanol production has almost tripled over a seven year period and biodiesel seeing an eightfold increase (Figure 5 and Figure 6) (Joel C, 1979, Ajanovic, 2011). This is one factor that has driven the development of the US Energy Independence and Security Act (EISA) to promote the production of clean renewable fuels, in addition to the need to mitigate any instability in fuel supply by increasing the efficiency of products, vehicles and buildings (USA Congress 2007). This increase in usage, however, presents both practical and ethical problems. If all of the United States corn and soybean production were converted to biofuels only 12% of gasoline and 6% of diesel global demands would be met (Hill et al., 2006). The ethical implications are that arable land used for food produce would be converted to energy production, removing a large proportion of the potential global food supply and consuming scarce fresh water, and only mitigating a fraction of the growing fuel demands. Modern renewables are growing faster than any other energy form, but their absolute volumes are still well below that of any single fossil fuel (Guillard and Ryther, 1962, Ajanovic, 2011). There has been an increase in land use for biofuel crops of 14 million hectares over the last decade, with increased cropping intensity creating 42 million hectares of extra crop land for food production (Langeveld et al., 2014). First generation biofuels have been a hotly debated area due primarily to this food vs fuel debate, and to the effect of potential changes in land use such as deforestation due to potential increases. It is this speculation, uncertainty and difficulty in predicting the socioeconomic and ecological effect of first generation biofuels that has caused a recent decline in public popularity (Upham et al., 2009, Havlík et al., 2011).

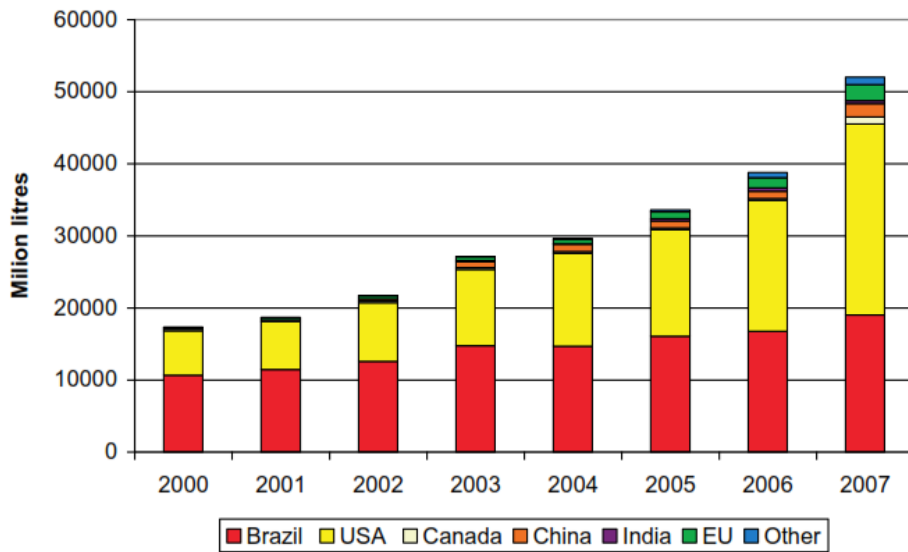


Figure 5 Global bioethanol production (Ajanovic, 2011)

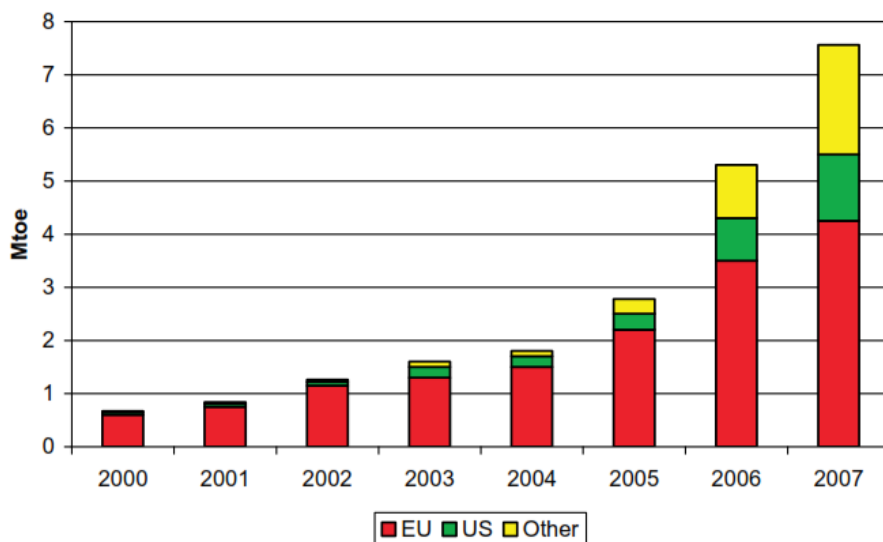


Figure 6 Global biodiesel production (Ajanovic, 2011)

1.2.2 Second generation biofuels

Second generation biofuels originate from the use of lignocellulose agricultural wastes and forest residue biomass, primarily organic material that is not used for consumption (Guillard and Ryther, 1962). Wood fuel and woody biomass makes up over 87% of the total annual global biomass used for energy (Chum et al., 2011). Unlike first generation biofuels that produce simple sugars, second generation fuels utilise the cellulose and

hemicellulose protected by lignin which are difficult to retrieve and require energy consuming pre-treatments to release them. Second generation fuels could eventually compete for arable land and impact upon food production and consume fresh water supplies potentially affecting biodiversity and nutrient supply. As a result alternative biofuel sources should also be sought, and these have already been described as third generation biofuels consisting of micro and macro algae instead of arable crops or lignocellulose terrestrial plants.

1.2.3 Third generation biofuels

Proposals for the use of algae as a biofuel were put forward in the late 1950's by Golueke et al. (1957) and were based on the breakdown of the carbohydrate fraction of the organism by anaerobic digestion for biogas production. The US Government's Aquatic Species Program (USA Congress 2007) was the most comprehensive effort to industrialise the use of algae as a biofuel. The program lasted from 1978-1996, but ceased due to the decreasing price of oil and increased stability in the Middle East (Thomas et al., 1984). Recent increases in fuel costs, however, and in fuel insecurity due to the highly fluid global political situation have driven interest back to algal fuels.

Third generation biofuels can occupy non arable land and utilise waters unsuitable for human or farming consumption such as wastewater effluent. Using marine organisms could relieve issues related to the use of arable land, and make use of water supplies that cannot be utilised for consumption such as salt water aquifers, marginal land and coastal regions. This could reduce the ethical implications associated with first and second generation biofuels; as well as alleviating certain land use and water supply issues. Estimates of potential microalgal yields per unit area are up to 30 times greater than that of traditional first generation biofuels, reducing the amount of land required for equivalent biomass production (Chisti, 2007). Currently, however, plant and animal materials are used for biofuels, but algae are not used on an industrial scale, due to the inherent difficulties in growth and harvesting.

1.2.4 Anaerobic digestion

Anaerobic digestion is the breakdown of organic material in the absence of oxygen by fermentative bacteria and methanogenic archaea to produce biogas consisting of methane and carbon dioxide. It has been suggested that this may be a more efficient way of converting the energy within some forms of biomass, particularly algae compared to ethanol and biodiesel production from this substrate (Ward et al., 2014, Sialve et al., 2009, Heaven et al., 2011). Microalgae can be cultivated on wastewater to reduce its chemical oxygen demand (a measure of organic pollution), and be fed to existing anaerobic digesters increasing the carbon content available for the conversion of biomass into biogas. This potentially offers a combined effect of reducing the requirement for further wastewater treatment and increasing the methane production.

The use of marine species of algae which can be cultivated on saline waters not suitable for irrigation or consumption, removes competition for fresh water. Using marginal lands not suitable for agriculture or regions with salt water lakes or salinas microalgae can be cultivated and used for biofuel production, with anaerobic digestion being one of the simplest methods of energy extraction (Zamalloa et al., 2011, Collet et al., 2011). The use of marine species, however, may give rise to inhibitory effects associated with the culture medium salinity which can dehydrate methanogens (Chen et al., 2008). Previous studies have reported inhibitory effects at salinities lower than that of average seawater concentrations, however, other studies report that adaptation to high salinities can occur. Large volumes of adapted digestate are not often readily available and it is therefore necessary to adapt an inoculum prior to the digestion of any marine species of microalgae suspended within a saline medium. The chemical compositions of the marine micro algal cell have been often reported to create potential inhibition due to the high nitrogen content potentially creating a high ammonia environment within the reactor. This coupled with the salinity effects suggests that the experimentation should be run under mesophilic conditions, as thermophilic reactors are more sensitive to environmental change and require a greater parasitic energy to heat, and psychrophilic reactors will potentially grow and adapt too slowly over the course of a single PhD (Chernicharo, 2007, Gerardi, 2003). This may reduce the methane yield, while the cell wall structure may limit degradation (Markou et al., 2012).

Chapter 1

Currently the majority of data gathered on the AD of marine microalgae has focussed on batch analysis within the mesophilic range of operating conditions (Ward et al., 2014). Limited research has been conducted into its methane potential under continuous operation and the compounded effects that can occur from the potentially inhibitory components within the substrate. This research therefore aimed to investigate the methane production potential of marine microalgae by mesophilic anaerobic digestion under both batch and continuous digestion, and evaluated the potential inhibitory effects of saline substrates on the methanogenic consortium. The specific aim and objectives are outlined below and developed within the literature review, with the research plan outlined in

Figure 7.

1.3 Aims and objectives

The aim of this research was to determine the feasibility of digesting marine microalgae for biogas production.

Objectives:

- Research the current literature on the anaerobic digestion of marine substrates, with a particular focus on marine microalgae and identify the potential inhibitory substrates within the feedstock.
- Characterise selected marine and freshwater microalgae to identify potential suitable species for biogas production.
- Determine the methane yields of selected marine and freshwater microalgae using batch analysis and select suitable strains for continuous cultivation and digestion under continuous operation.
- Conduct continuous anaerobic digestion studies to acclimatise an anaerobic inoculum from a readily-available large-scale source to high (marine) concentrations of chloride and sulphate salts.
- Grow selected marine microalgal species from the algal screening continuously on low/no sulphur containing culture medium.
- Conduct semi-continuous anaerobic digestion studies on selected strains of marine microalgae grown under low sulphur conditions using the salt-acclimatised inoculum to determine their biodegradability.

Chapter 1

- Grow marine micro algae on ocean concentrations of chloride and sulphate salts for continuous digestion.
- Continue the semi-continuous anaerobic digestion studies on the selected strain of microalgae grown under seawater concentrations of sulphur.

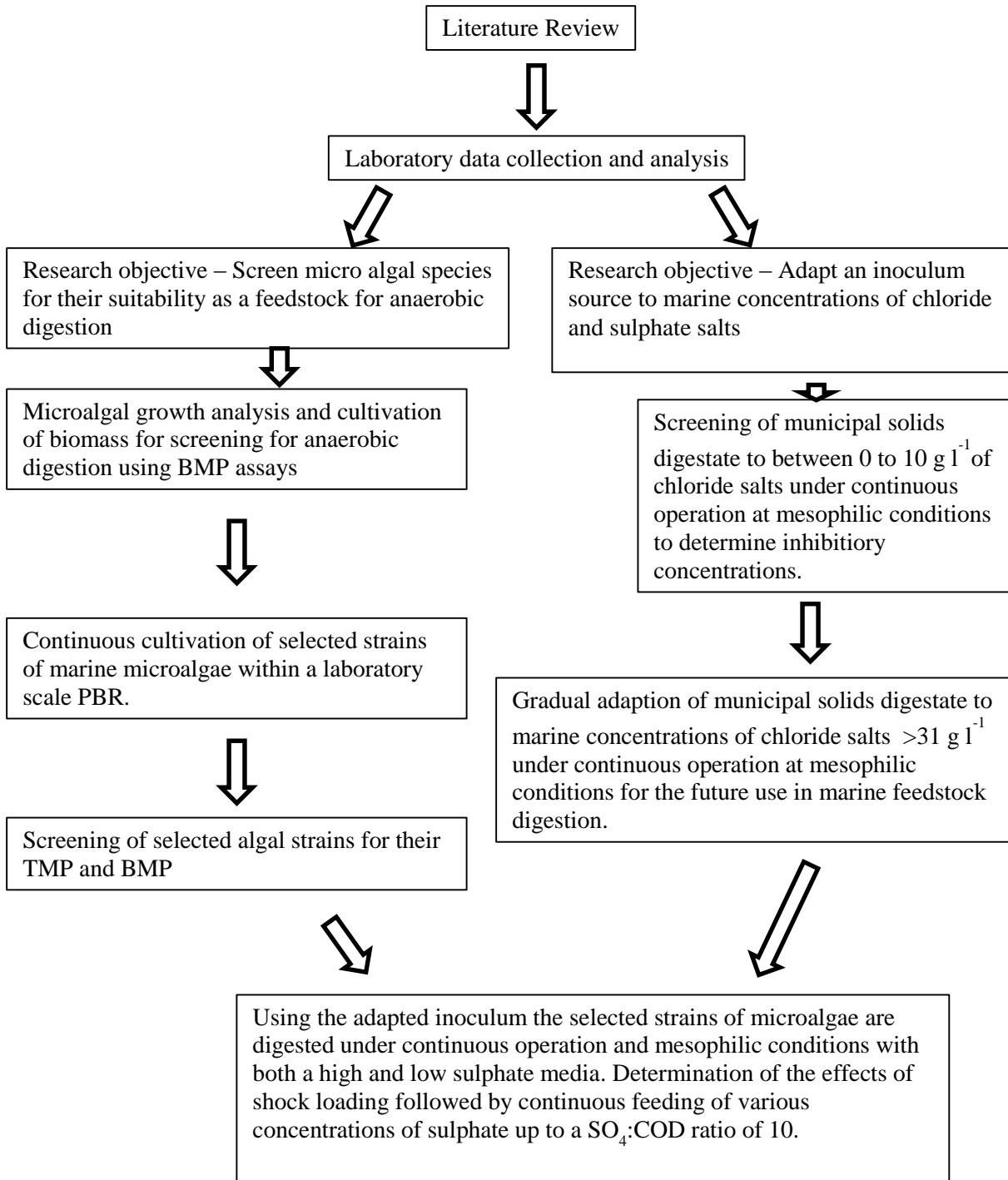


Figure 7 – Research outline and plan for the following PhD.

CHAPTER 2

2. Literature review

This chapter summarises key literature on the anaerobic digestion of marine microalgae for the production of biogas, reviewing and identifying the gaps within the subject area

2.1 Algae

The oceans provide approximately 40-50% of the total primary production of the globe ($40 - 50 \text{ Pg C year}^{-1}$) yet the total plant biomass of the aquatic system is around 1% of that of the terrestrial environment with $1 - 2 \times 10^{15} \text{ g C}$ compared to $600 - 1000 \times 10^{15} \text{ g C}$ (Falkowski and Raven, 2007). This shows how efficient small masses of aquatic photoautotrophs are for primary productivity. The reason for this difference is due to the short lifespan of microalgae (~1 week) and the downwelling/settling of dead material removing the biomass from the ocean and depositing it as a sediment on the ocean floor. Algae are a heterogeneous assemblage of marine and freshwater organisms that vary in size from single celled organisms to giant seaweeds. There is a high diversity in the natural environment, as shown in Figure 8 where algal groups occupy 19 branches, with the entirety of land plants dominating just one branch (Schlarb-Ridley, 2011). Microalgae consist of both photosynthetic protists, which are eukaryotes and the prokaryotic cyanobacteria, also known as the blue green algae (Graham et al., 2009). As a result of this diversity species are mainly classified by ecological traits, with genetic identification becoming an increasingly popular method. Algae lack the large organelles and reproductive features of land plants, making them highly different to terrestrial plants. This simplicity in their composition enables them to have a higher photosynthetic efficiency capable of drawing down a high volume of CO_2 in relation to their mass (Graham et al., 2009).

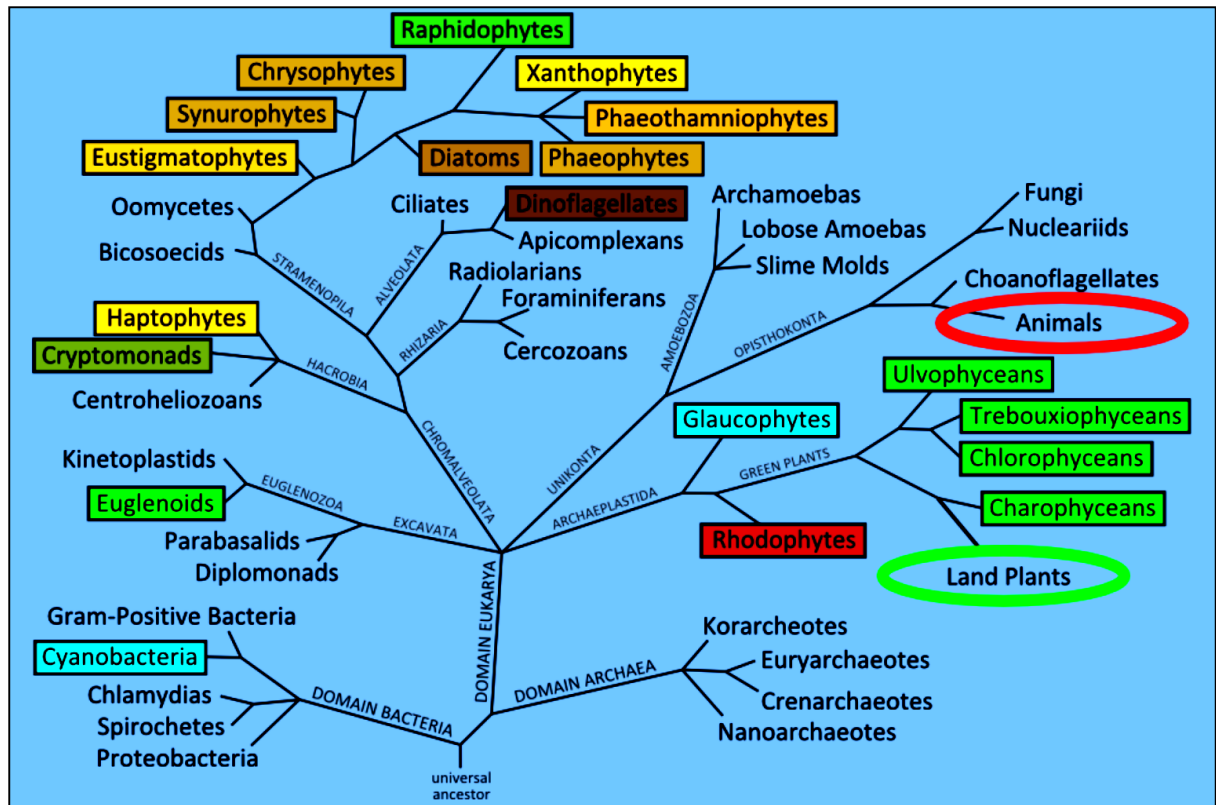
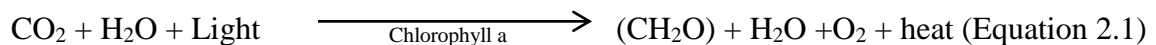


Figure 8 – Phylogenetic tree of life, with coloured boxes denoting diversity in pigmentation. The animal and plant kingdoms are circled in green and red respectively (Schlarb-Ridley, 2011).

2.1.1 Aquatic photosynthesis

Photosynthesis is the formation of chemical bond energy within an organic compound by the utilisation of light energy and the fixation of CO_2 . This can use natural or artificial light sources. The process is complex and not yet fully understood, but the simple generally accepted reversible equation is shown in Equation 2.1 (Falkowski and Raven, 2007).



Photoautotrophic organisms are only able to utilise around 45% of incoming insolation. This is at a wavelength of 400-700 nm within the visual spectrum and is known as photosynthetically available radiation (PAR) (Kirk, 1994). The photosynthetic electron transport chain (PET) consists of two pigment protein complexes known as photosystem I and photosystem II (PSI, PSII). PSI absorbs photons directing the excitation energy to

reaction centre complexes within PSII. Within this reaction centre the photon energy is converted to electrochemical energy which in turn drives PET (Suggett et al., 2007). The rate of photosynthesis generally depends on a light dependent and a light independent step. The light dependent step is limited by the quantity of light harvested by the cell and its chloroplasts, and the size of the functional area of PSII within the cell, as well as the number of reaction sites (Suggett et al., 2007). One photon of light can only influence one molecule which creates a rate limiting variable: this is known as the Stark-Einstein Law (Falkowski and Raven, 2007, Kirk, 1994).

2.1.1.1 Maximum algal growth yield

It is important when considering reported values for algal growth and productivity to define a maximum theoretical rate of algal growth that cannot currently be exceeded, as a basis for determining the credibility of the literature in question.

It has been reported that 8-12 photons are required to fix one carbon atom, with the general consensus that 12 are required on average (Wilhelm and Jakob, 2011, Williams and Laurens, 2010, Weyer et al., 2010). This gives rise to a maximum potential yield on the basis of photon flux. Assuming an average insolation of $\sim 1000 \text{ W m}^{-2}$ and $4.2 \mu\text{mol m}^{-2} \text{ s}^{-1}$ per W m^{-2} with 12 photons required per carbon atom, 3.5×10^{-4} moles of carbon are fixed every second. Assuming an average daily insolation period of 12 hours 15.12 moles of carbon are fixed per day. If losses due to respiration and fluorescence (as heat) are taken into account, $\sim 22\%$ of the photons will be utilised, fixing a maximum of 40 g C m^{-2} (Wilhelm and Jakob, 2011). This theoretical maximum can be further reduced by other abiotic and biotic factors such as nutrient availability, temperature, inorganic carbon availability, salinity, competition within a mixotrophic environment, predation, photo-limitation, photo-inhibition and photo transmission efficiency (Weyer et al., 2010, Long et al., 1994). It is this photosynthetic solar energy conversion efficiency that ultimately determines the yield of micro algal biomass and biofuel production. Therefore the maximum reported growth cannot exceed $40 \text{ g of C fixed m}^{-2} \text{ day}^{-1}$ (Stephenson et al., 2011).

Increasing the light intensity can increase photosynthetic yields, but this is ultimately limited by other variables. Figure 9 shows the effect of increasing the light intensity on the overall yield, which increases linearly until reaching a plateau when photo-inhibition

occurs. Any increase beyond P_{\max} will yield no increases in algal production. An excess in irradiance beyond P_{\max} can cause photo-inhibition and death of the cells, reducing the overall yield. This is due to the sensitivity of photosystem II to high irradiances, denaturing this system. This does not mean that the overall yield obtained in practice cannot be increased, however, as other abiotic and biotic variables such as CO_2 can be manipulated and optimised. Inorganic carbon can be under saturated within marine environments in comparison to terrestrial systems due to terrestrial weathering and the high salinity of marine systems, and the concentration may be too low to saturate the first enzyme in the dark reaction shown in Equation 2.2 (Kaiser et al., 2005b, Kirk, 1994, Kaiser et al., 2005a). It is the combination of several abiotic factors that are of great interest to biological engineers in producing systems that enable the maximum growth of algae for economic solutions to the energy crisis.

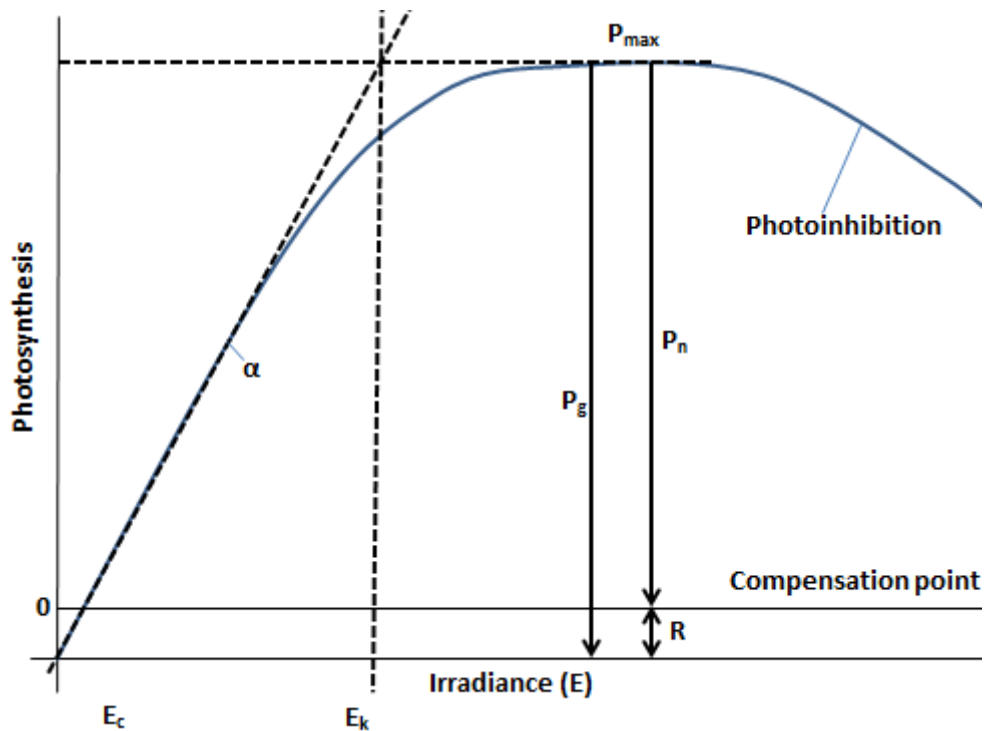
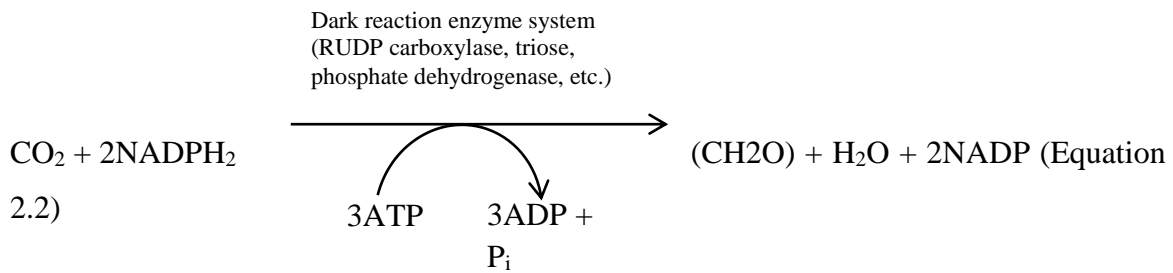


Figure 9– (P) response of changing light intensity on photosynthesis. The rate of increase is α , the compensation irradiance where photosynthesis is equal to respiration. R is respiration rate, E_k is where photosynthesis becomes light saturated, P_{\max} is where the rate of photosynthesis becomes saturated. P_g and P_n are gross and net photosynthesis respectively (Kaiser et al., 2005a).



A major by-product of photosynthesis is oxygen. Oxygen is essential for cellular respiration, but saturated concentrations above that of the atmosphere cause a reduction in photosynthetic activity due to inhibition of the Ribulose-1,5-bisphosphate carboxylase oxygenase enzyme (RUBISCO) inhibiting the fixation of inorganic carbon. Oxygen can become toxic at concentrations greater than 4 to 5 times saturation at $20 \pm 2^\circ\text{C}$, reducing the growth rate and yield significantly. Molina et al. (2001) showed that the ideal oxygen concentration is $\sim 20\%$ v/v with a linear decline with increasing oxygen content, as shown in Figure 10; this value is similar to atmospheric concentration.

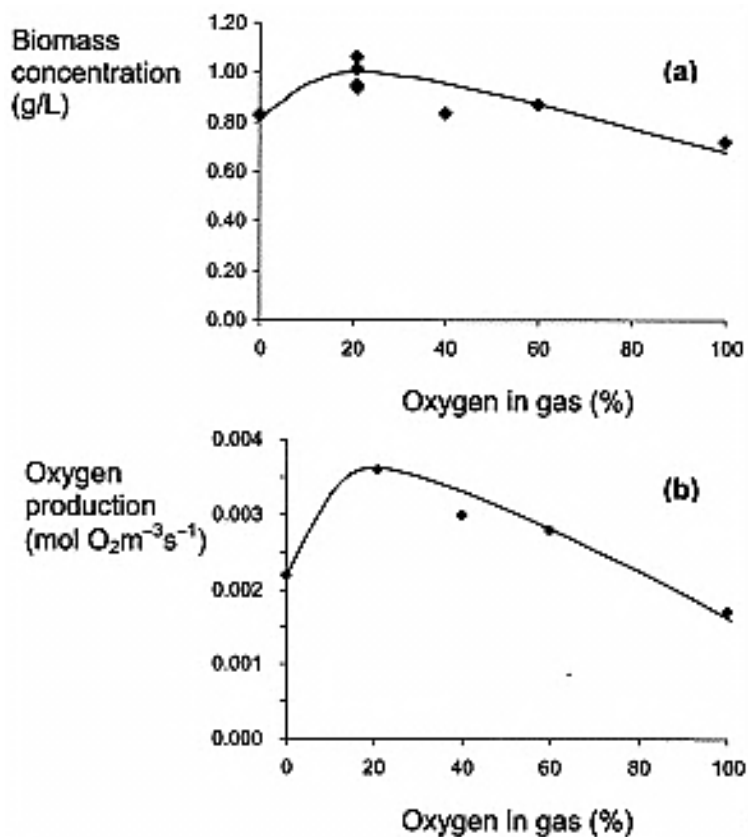


Figure 10 - Determination of the influence of % of oxygen within injected gas and biomass yield at an irradiance of $300 \mu\text{mol m}^{-2} \text{s}^{-1}$ (Molina et al., 2001).

Mendoza et al. (2013) reported that oxygen super saturation during algal cultivation led to a marked reduction in biomass productivity, which was more severe if pure CO_2 was used to replenish inorganic carbon and remove O_2 than if flue gas was used due to the greater stripping potential of the larger volume of flue gas. They found that the energy requirement to remove sufficient oxygen was more than compensated by the growth yield making this an important variable to control for efficient energetic algal growth.

2.1.2 Nutrients

Several key elements constitute the majority of the macronutrients of microalgae, making up over 0.5% dry weight (DW) in each case. In descending order these are carbon, oxygen, nitrogen, phosphorus and sulphur following the Redfield ratio of 106C: 16N: (16Si siliceous organisms only) 1P: 0.7S when grown at their maximum growth rate with luxury uptake (Graham et al., 2009, Redfield, 1958). The average stoichiometry of the primary components of marine algae is shown in Table 1. Micronutrients such as zinc, copper, molybdenum, cobalt, manganese and iron are also required, but only in trace amounts and primarily for enzymatic activity, although these nutrients can become inhibitory and toxic at high concentrations.

Table 1 – Mean composition of primary components of marine phytoplankton, adapted from (Sarmiento and Gruber., 2006)

Organic matter component	Composition	Reference
Carbohydrate	$\text{C}_6\text{H}_{10}\text{O}_5$	(Anderson, 1995)
Lipid	$\text{C}_{40}\text{H}_{34}\text{O}_2$	and (Laws, 1991) (Hedges et al., 2002)
	$\text{C}_{3.83}\text{H}_{6.05}\text{O}_{1.25}\text{N}$	
Protein	$\text{C}_{106}\text{H}_{168}\text{O}_{34}\text{N}_{28}\text{S}$	

Dissolved inorganic carbon is utilised by photoautotrophic organisms by RUBISCO. At typical fresh water and marine pH values of 7.5-8.4, CO_2 concentrations are relatively low compared to the other inorganic forms of carbon, at around 0.01-10% of total inorganic carbon. Extracellular carbonic anhydrase converts H_2CO_3 into CO_2 and water as

described by the following equilibrium reaction (Martin and Tortell, 2006, Falkowski and Raven, 2007):



This facilitates the diffusion of CO_2 within the cell by supersaturating the concentration outside the cell. Shifting the equilibrium of inorganic carbon to the right as shown in Figure 11 (Fleischer et al., 1996).

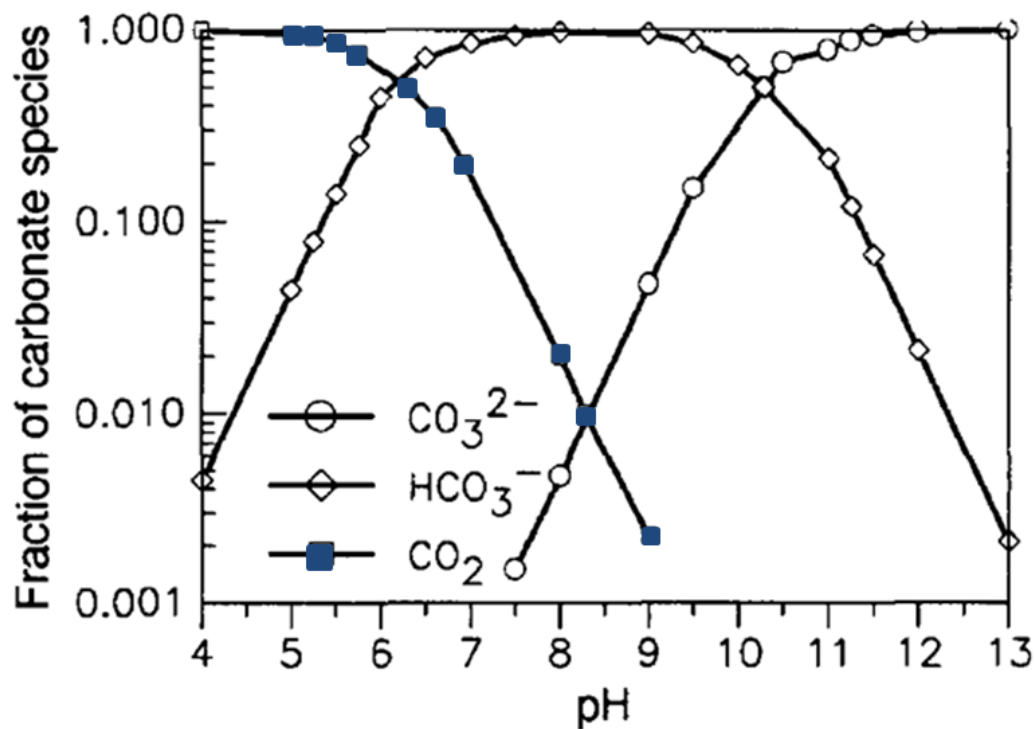


Figure 11 – Fractions of different carbonate species at chemical equilibrium. Increasing pH alters the stoichiometry of dissolved inorganic carbon from CO_2 at a pH of 0-8, HCO_3^- at a pH of 4-11 and CO_3^{2-} at 7-14 (Fleischer et al., 1996).

The majority of nitrogen in aquatic systems exists as dissolved nitrogen gas (N_2), ammonium ions (NH_4^+), Nitrite (NO_2^-) and Nitrate (NO_3^-). The remainder consists of dissolved organic nitrogen such as urea and amino acids.

2.1.2.1 Sulphur

Sulphur is one of the main ions in seawater, with an average concentration of 9.05×10^2 mg S L⁻¹. It occurs primarily as sulphate with an average seawater concentration of 2800 SO₄ mg L⁻¹ (Brown et al., 2005). Primarily used in proteins as shown in Table 1, it is also excreted as the aerosol dimethylsulphide when the organism becomes stressed, particularly by light. The average sulphur content of marine algae ranges from 1.5-16 mg g⁻¹ dry weight, following the Redfield Ratio (Grobbelaar, 2007). This sulphur fraction may become problematic in the anaerobic digestion of marine algae as explored later within this chapter; for this reason it may be advantageous to grow marine algae on a low sulphur culture medium. Wheeler et al. (1982) managed successfully to culture marine algae in their synthetic marine water at 180 mg SO₄ L⁻¹, at over ten times lower concentrations of SO₄ than in seawater. This was on a batch basis, however, and continuous cultures may fail due to the washout of sulphur from the system. Giordano et al. (2000) grew several generations of *D. salina* at various sulphate concentrations. They found that at sulphate concentrations below 9.6 mg SO₄ L⁻¹ there was a dramatic decrease in the growth rate as shown in Figure 12. This was considered to be caused by a substantial decline in RUBISCO and chlorophyll *a/b* binding proteins. Gilbert et al. (1997) and Ferreira and Teixeira (1992) also found that RUBISCO decreased dramatically in terrestrial plants in low/ absent sulphur concentrations, decreasing the rate of photosynthesis. The reduction in photosynthesis will lead to a decline in biomass production with the Calvin cycle becoming inactivated, as the oxygen producing pathway is inhibited, but cellular respiration continues causing cell death (Zhang et al., 2002). Giordano et al. (2000) suggested that with the onset of sulphur limitation RUBISCO and chlorophyll binding proteins may act as a reservoir of fixed sulphur, initially preventing the decline in specific growth rate. After several generations, however, sulphur limitation will become apparent. This is highly species dependent and requires investigation of individual species to determine the cumulative effect of reduced sulphates on growth rate and biomass composition.

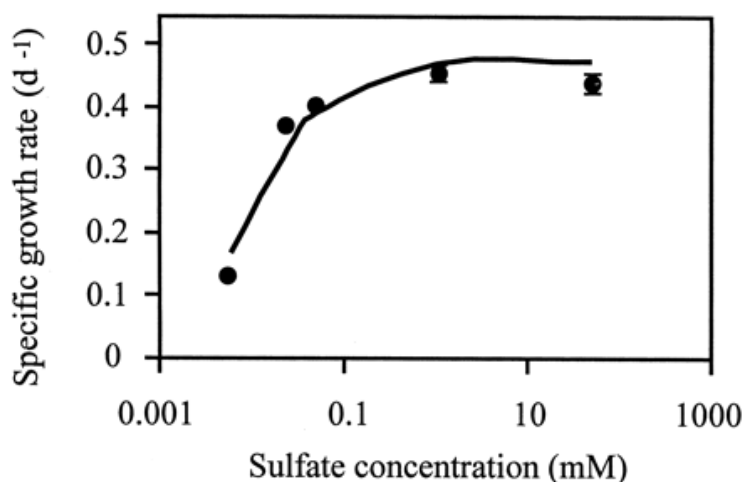


Figure 12 – Specific growth rate of *D. salina* as a function of the sulphate concentration in the culture medium (Giordano et al., 2000).

2.1.2.2 Fertilisers

Nitrogen and phosphorus are often added as a fertiliser for the growth of microalgae with phosphorus often added to excess. The supply of nutrients, balancing growth with costs is critical in enabling an economic system for the efficient growth of biomass and high value products (Mayers et al., 2014, Milledge, 2010b). The depletion of a single nutrient, typically nitrogen is often used to increase the lipid content of the microalgae while reducing the growth rate and yield (Adams and Bugbee, 2014). This is discussed further in section 2.2.

2.1.2.3 Commercial operation

At a commercial scale the main requirements for algal growth are space, water supply, and the nutrients mentioned above. It has been suggested that the growth of microalgae exclusively for biofuels could not be feasible unless algal growth was a by-product of wastewater treatment or high value products (Lundquist et al., 2010). The availability of nutrient sources, CO₂ supply, suitable water sources and space may be the largest constraint on algal growth systems, limiting suitable growth sites to a few areas (Pate et al., 2011). The use of fresh water for algal growth would add to the cost, and contribute to the global security threat of water as a resource; 80% of the world's population resides in regions where fresh water supply is of concern, as shown in Figure 13 (Vorosmarty et al., 2010). Some authors have suggested that microalgae require much less water than traditional biofuel from fuel crops, with fuel crops requiring approximately 10,000 litres

of water per litre of biofuel, with microalgae at 1.5 litres of water per litre of biofuel (De Fraiture et al., 2008, Wijffels and Barbosa, 2010). This however, does not take into account evaporative loss, with the water requirements for microalgae likely to be much greater when is taken into account. The purpose of this research was to investigate the suitability of marine/ brackish species of microalgae for anaerobic digestion, thus potentially making alternative water resources and space available for large-scale culturing, as previous research has primarily focused on fresh water and waste water streams.

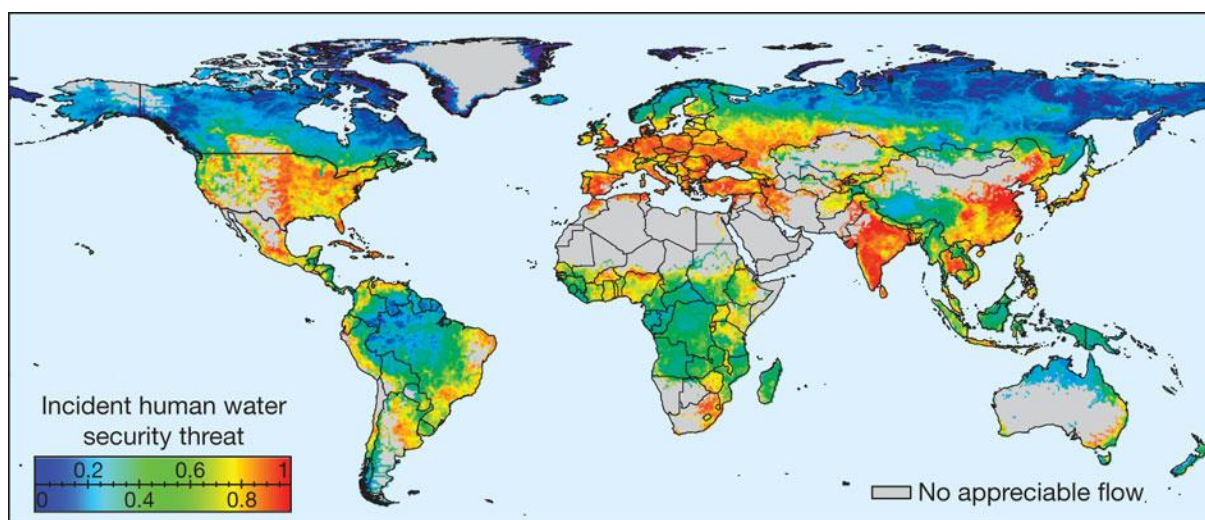


Figure 13 – Global security threat of freshwater as a resource, image taken from Vorosmarty et al. (2010).

2.1.3 Commercial applications of macro and microalgae

Traditionally, macro and micro algae have been cultivated and harvested for food consumption and as a soil enhancer. Macro and microalgae are widely cultivated for use in nutraceuticals, pharmaceuticals and as a food source for humans, animals and agriculture. Macro algae are known to have been a part of human diets since 600 BC and were traditionally consumed as a vegetable in eastern Asia (Patarra et al., 2011, Tabarsa et al., 2012). The first reported use of microalgae for food dates back 2000 years to the Chinese who used *Nostoc* to survive during periods of famine (Spolaore et al., 2006). In the 1950s a dramatic increase in world population led to a decrease in protein supply which led to the suggestion of using algal biomass high in protein as a substitute, while

the last 70 years have seen a rise in the commercial production of algae as a feedstock (Becker, 2007).

The inherently high costs of cultivating microalgae have steered development away from food and biofuels to high value molecules, primarily fatty acids, pigments, phycobiliproteins and stable isotope biochemicals. Carotenoids, in particular β - Carotene, are abundant in microalgae forming up to 14% of *D. salina* dry weight. β - Carotene is used as a pigment food colorant and nutrient supplement in animal feeds with prices ranging from \$300 - \$3000 kg⁻¹ depending on purity (Becker, 2004, Spolaore et al., 2006). Polyunsaturated fatty acids (PUFAs) are traditionally sourced from marine fish such as cod. Fish cannot synthesise PUFA but accumulate them from smaller fish that graze on algae which produce PUFA. Due to the possibility of bioaccumulation of toxins such as mercury within fish up the food chain, particularly in cod and tuna which are tertiary predators the use of algae as a source of PUFAs has increased. The application of fish oil as an additive is limited due to its fishy smell and taste as well as its poor oxidative stability. As such the use of microalgae as a commercial source of PUFAs may be a logical alternative to the use of fish oil (Luiten et al., 2003, Medina et al., 1998).

Microalgae are capable of incorporating the stable isotopes ¹³C, ¹⁵N and ²H from relatively inexpensive inorganic molecules into high value amino acids, carbohydrates, lipids and nucleic acids for use in scientific analysis, with prices ranging from \$260 – 28000 g⁻¹ of material (Spolaore et al., 2006).

It is suggested that the development of biorefineries for high value products of this type from algae will bring with it the technology required to reduce the costs of growing and harvesting algae for use as an economically competitive biofuel substrate (Milledge, 2011). Algal biodiesel will need to be sold at a maximum of \$0.5 L⁻¹ to be competitive with current liquid fossil fuels, and estimates for the cost of producing microalgae for biodiesel are currently a factor of ten above this (Chisti, 2008). This low value is directing research towards the high value products that can yield returns up to 60,000 times greater than that of biofuel production. If algae is cultivated and harvested at the yields required for biofuel production, the value of certain by-products mentioned are unlikely to remain high in value as the excess supply into the market could reduce their value.

2.1.4 Commercial and large scale algal culturing

As microalgae are generally grown in suspension in water, several types of growth system have been developed over the last 50 years in an attempt to maximise yields, and minimise contamination/ predation and energy input. As mentioned above the main factors affecting growth other than the culture medium itself are irradiance, CO₂ and O₂ concentration as well as mixing. Each of the systems discussed below has several strengths and weaknesses associated with its operation. All systems ultimately have the major downstream problem of removing the suspended algal biomass from the culture media in an energetically efficient way.

Several methods currently exist to cultivate microalgae: these include open lake/ pond type systems referred to as a static pond or raceway ponds with motion is utilised and closed systems referred to as photobioreactors (PBR). This review concentrates primarily on enclosed PBR systems.

2.1.4.1 Open Raceways

The cheapest and easiest method of algal cultivation is by open raceway. These can either be dug into the ground with or without a waterproof liner or raised above the ground in a water tight vessel, although it has been suggested that the use of liners or raising the pond can make the system economically unfeasible (Milledge, 2013). Their design is simple as shown in Figure 14. A paddle wheel is used to mix and may help the system to remove excess O₂ and replenish CO₂. Some systems inject CO₂ in the sump to supplement the dissolved carbon and use pH as an indicator of when to supply CO₂, with an increase in pH causing an injection of gas (Mendoza et al., 2013). A potential problem with this system is mixing away from the paddle wheel as the system can be classed as turbulent, but minimal mixing can occur between the surface and depth limiting the total microalgae's exposure to irradiance and preventing the degassing of O₂ during peak irradiance hours.

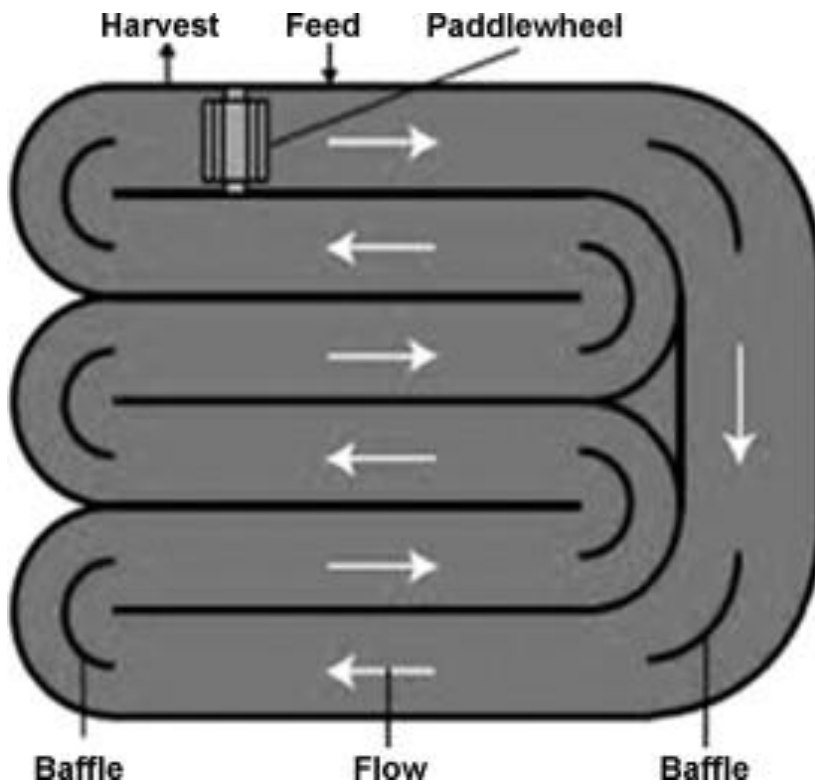


Figure 14 – Schematic of a simple raceway pond (Singh and Sharma, 2012), image of raceway ponds in Almeria, Southern Spain.

2.1.4.2 Flat panel photobioreactor

A common laboratory-sized system, it is the simplest system to model and analyse shown in Figure 15. The irradiance can be maintained relatively constant throughout the system minimising the effects of internal shading and attenuation. This system can mimic environmental effects and has a high level of control which is difficult to get with an open

system. Flat plate PBR, however, are less likely to be used on a commercial scale due to the high costs involved in their manufacturing, materials and maintenance.

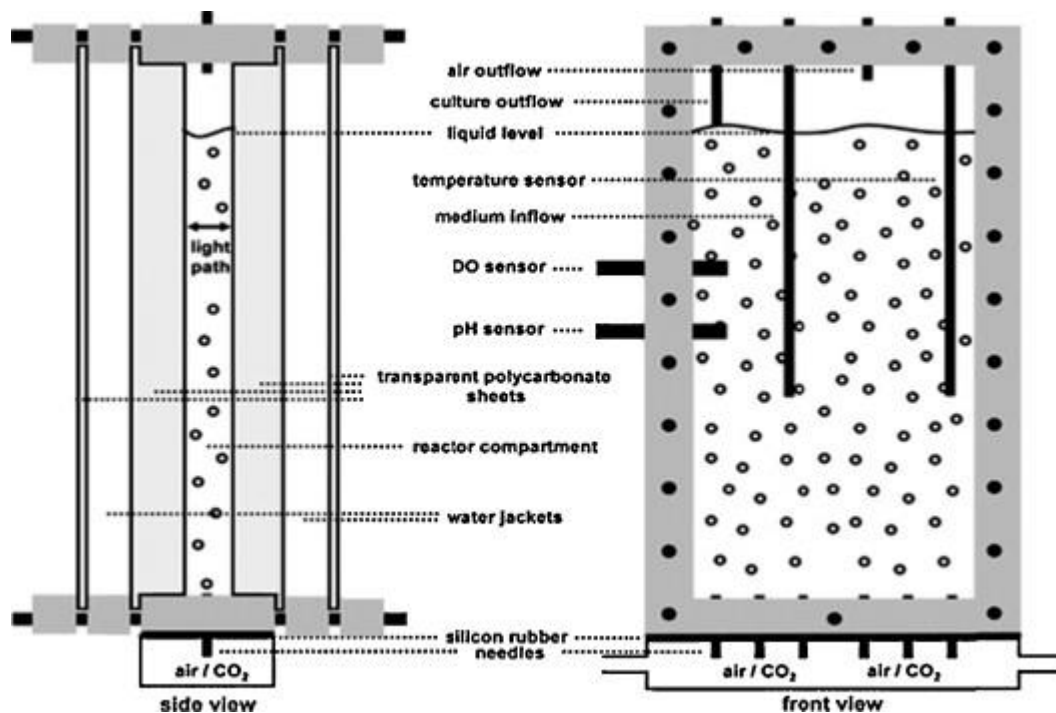


Figure 15 – Schematic of atypical flat plate photobioreactor used within a laboratory setting (Singh and Sharma, 2012).

2.1.4.3 Serpentine tubular photobioreactors

Serpentine tubular photobioreactors (PBR) of the type shown in Figure 16 are designed to enhance the growth conditions of an aquatic photoautotrophic organism by reducing limiting factors. Many designs exist and there is little consensus on the best design, with each having benefits and drawbacks. A tubular PBR allows control of the majority of abiotic variables that affect the growth of microalgae. These include but are not limited to temperature, turbidity, dilution rate, irradiance, and CO₂/O₂ concentrations. Each of these variables can be controlled at the cost of an increase in energy demand: temperature via a thermoregulator, turbidity by flow rate and dilution rate, dissolved CO₂ and O₂ by the pumping of air and other gases, and irradiance by artificial illumination. Controlling these variables is energy intensive and expensive, making the system poorly suited to biofuel production. For this reason it is economical to grow microalgae for high value products such as pharmaceuticals and nutraceuticals selling at prices in excess of \$500 kg⁻¹,

whereas biofuels in the long term need to be competitive with fossil fuels and to sell at between 25-50 US cents L^{-1} at the current market rate.

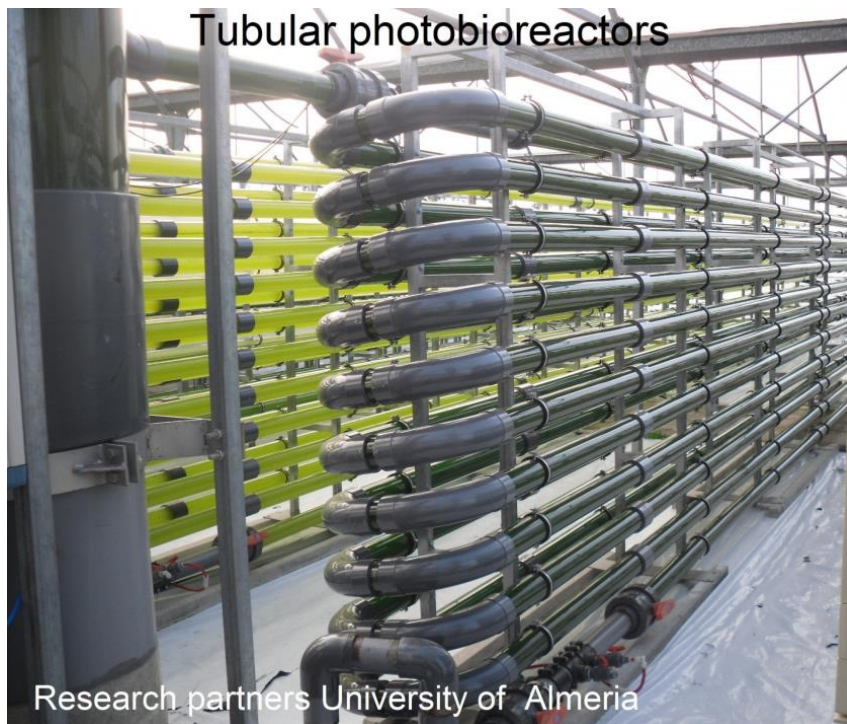
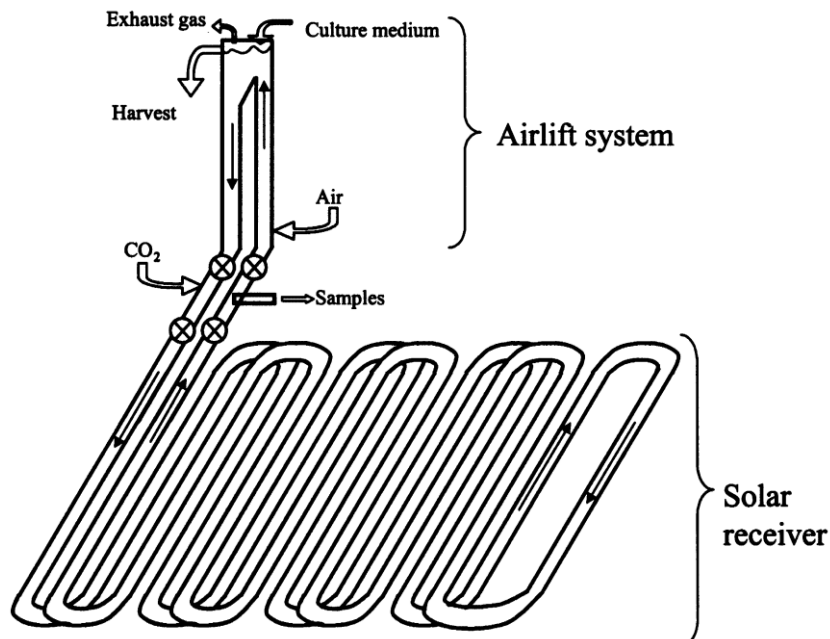


Figure 16 - Serpentine tubular reactor used at Almeria in southern Spain. The solar receiver returns on top of itself causing shaded regions from daylight (Fernandez et al., 2001)

The length of tubing determines the volume of O₂ gas build up, and the rate at which the culture media flows determines its rate of removal. If 300% saturation is deemed to be the maximum acceptable value and that the saturation at the inlet of the solar receiver is 100% the maximum length of tubing can be determined using the following Equation 2.3.

$$L_{\max} = jL ([O_2]_{\text{out}} - [O_2]_{\text{in}})/R_{\text{oxy}} \text{ (Stephenson et al., 2010) Equation 2.3}$$

L_{\max} is the maximum length of the tubing, jL is the supercritical velocity of the culture, O_2 in and out are the % saturation with regards to air and R_{oxy} is the volumetric rate of O₂ generation by photosynthesis.

The volumetric rate of oxygen generation is between 0.75 and 1.5 kg m⁻³ day⁻¹. If oxygen generation is equal to carbon fixation as shown in Equation 1.1 and the productivity is 20 g TS m⁻² of illuminated surface with up to 50% carbon content, then for every m⁻² there will be 10 g of O₂ gas produced per day (Acien Fernandez et al., 1998). If biomass productivity is between 0.75 and 1.5 kg TS m⁻³ day⁻¹ the volumetric rate of oxygen generation will be 0.375-0.75 kg m⁻³ day⁻¹. This gives maximum lengths of 80-171 m at an average velocity of 0.3 m s⁻¹, 115-53 m at 0.2 m s⁻¹, and 57-27 m at 0.1m s⁻¹ as shown in Table 2 (Stephenson et al., 2010), average velocities of 0.3 m s⁻¹ being typical in current serpentine photobioreactors. Sedimentation/ fouling will be of main concern at lower flow rates if length is not an issue.

Table 2 – Maximum distance between the exit of the airlift column and the entrance (m) based on Equations 2.1 and 2.3.

Flow rate m/s	Biomass production TS kg m ³ day ⁻¹														
	0.1	0.2	0.3	0.4	0.5	0.6	0.7	0.8	0.9	1	1.1	1.2	1.3	1.4	1.5
1	4000	2000	1333	1000	800	667	571	500	444	400	364	333	308	286	267
0.9	3600	1800	1200	900	720	600	514	450	400	360	327	300	277	257	240
0.8	3200	1600	1067	800	640	533	457	400	356	320	291	267	246	229	213
0.7	2800	1400	933	700	560	467	400	350	311	280	255	233	215	200	187
0.6	2400	1200	800	600	480	400	343	300	267	240	218	200	185	171	160
0.5	2000	1000	667	500	400	333	286	250	222	200	182	167	154	143	133
0.4	1600	800	533	400	320	267	229	200	178	160	145	133	123	114	107
0.3	1200	600	400	300	240	200	171	150	133	120	109	100	92	86	80
0.2	800	400	267	200	160	133	114	100	89	80	73	67	62	57	53
0.1	400	200	133	100	80	67	57	50	44	40	36	33	31	29	27

An oxygen removal and carbonation system commonly used in enclosed PBR is an airlift column, whereby the excess O₂ is removed and CO₂ increased by diffusion via the pumping of air into the base of a vertical column (Chisti and Mooyoung, 1993, Harker et al., 1996). An example can be seen on the left-hand side of Figure 16. This system can also be used for the mass transfer of the culture medium throughout the PBR (Rubio et al., 1999). Control of bubble size and addition of CO₂ into the air mix can increase the overall yield by increasing the surface area to volume ratio and concentration gradient, increasing the dissolved CO₂ concentration.

2.2 Algae and biofuels

Marine and fresh water algae contain no lignin and are primarily made of proteins, fats and simple sugars with some cellulose within the cell walls. Algae have been reported to produce up to 80% oil by dry weight and this can be converted into biodiesel using existing technology (Chisti, 2008). The absence of lignin could make algae easier to digest than terrestrial plant and wood materials which can require pre-treatments to break down the lignin and release cellulose and hemi-cellulose. It is the composition of algae

with a high protein and oil content coupled with a high productivity and photosynthetic efficiency that has raised interest in algae as a biofuel.

Numerous species of phytoplankton have been investigated for their feasibility as a biofuel source, particularly freshwater and brackish species such as *Chlorella*, *Scenedesmus*, *Dunaliella*, *Isochrysis*, *Nannochloropsis* and *Thalassiosira* (Converti et al., 2009, Chiu et al., 2009, Chisti, 2007). Marine cultures have a major potential advantage in relation to their fresh water counterparts, consisting in greater resistance to predation and invasive species; this is especially the case if they are grown in artificial terrestrial lakes or ponds away from any marine sources of contamination. This is because the culture medium itself is a hostile environment to fresh/ brackish organisms due to the high salt concentrations present. Some species, such as *Dunaliella* can thrive in salinities in excess of 40 g L⁻¹ total salt, where other marine micro algal species and predators would perish due to the high osmotic pressures; this enables a pure culture to be relatively easily maintained particularly if cultivated away from a natural marine environment. The high salinity may, however, pose potential problems with the future AD of the algal feedstock, and these are discussed in section 2.4.6.

Stress related growth has been found to increase the lipid fraction of the microalgal cell significantly, with studies showing a threefold increase from recorded values of 5% to 15%+ w/w (Converti et al., 2009). The stress is induced by altering abiotic factors: typically the nitrate concentration is reduced preventing the formation of proteins, limiting growth and causing starvation of the cell, resulting in the organism ceasing reproduction and storing fats instead. Gouveia and Oliveira (2009) found a 50% increase in lipid content with nitrogen starvation; they failed to report the growth yield of their experiments, however, only stating growth yields reported by other authors. Growth yields under nutrient restricted conditions may be substantially lower than the average in the literature. Other physical variables such as salinity have also been found to increase percentage lipid content. By increasing any environmental stress the microalgae are encouraged to cease growth and replication and begin storing lipids for survival. Takagi et al. (2006) found increasing salt concentration increased lipid percentage of the biomass, but reduced the overall yield.

2.2.1 Macro algae as a feedstock for biofuels

As with microalgae, use of macro algae as a feedstock for biofuel production is not a new concept, with research in the U.S Navy's Ocean Food and Energy Farm project in the 1970s (Bird and Benson, 1987). Over 100 species of macro algae are currently cultivated at a large scale for food, fertiliser, medicines and chemicals primarily in East Asia (Santelices, 2007, Ortiz et al., 2006). Currently macro algal culture is labour intensive and requires the altering of coastal environments. These areas are usually highly diverse and altering the environment for macro algal growth could negatively affect the ecology. Large-scale sea shelf macro algal farms could act like areas of protection from fishing in a similar way to oil rigs, however, increasing marine diversity by preventing fishing and mooring of boats, and maintaining habitats in a controlled manner. Unlike microalgae, macro algae can be relatively easy to harvest and maintain with little competition from other macro algal species once seeded.

2.2.1.1 Macro algae and anaerobic digestion

Macro algae have received a large amount of attention as a biofuel source due to its prolific growth rate in regions that are eutrophic. AD has been used successfully to dispose of the macro algal biomass that washes up on beaches causing coastal water fouling (Briand and Morand, 1997, Moen et al., 1997, Peu et al., 2011, Cecchi et al., 1996). AD is the easiest route for bioenergy from macro algae is (Cecchi et al., 1996, Hughes et al., 2012, Migliore et al., 2012, Vergara-Fernández et al., 2008). The high cellulose content and absence of lignin enables a higher proportion of organic material is available for fermentation and subsequent methanogenesis (Cecchi et al., 1996, Wise et al., 1979, Nkemka and Murto, 2010, Hughes et al., 2012, Vergara-Fernández et al., 2008). Despite the presence of readily hydrolysable sugars hydrolysis, however, remains the rate limiting step with regards to AD of macro algae (Raposo et al., 2012). Macro algae are constructed of highly recalcitrant material such as polyphenols and complex cellulosic fibres with lignin-type components which can reduce its biodegradability and potential methane yield. Current research has focussed on the pre-treatment of the feedstock to reduce its recalcitrance and increase the rate of hydrolysis (Obata et al., 2015, Karray et al., 2015, Nielsen and Heiske, 2011, Tedesco et al., 2013, Vivekanand et al., 2012).

Other potential problems exist involving the AD of marine macro algae. They contain a high proportion of sulphur which can produce H₂S as a by-product (Peu et al., 2011). Macro algae are seasonal, and there will be variability in the production and supply of the feedstock over the course of a year. Some of these potential problems are also evident with microalgae and are discussed further in section 2.4.9.

This report will focus on the use of microalgae as a feedstock for AD, macro algae will not be discussed further within the context of this report.

2.3 Algal species examined

Studies on the use of micro algae as a biofuel and on AD of algae have looked at a range of species to help identify suitable strains (Cecchi et al., 1996, Zamalloa et al., 2012b, Golueke et al., 1957, Mottet et al., 2014, J. Heerenklage et al., 2010, Ehimen et al., 2011, Lü et al., 2013, Brennan and Owende, 2010, Salerno et al., 2009, Asinari Di San Marzano et al., 1983). In the current work several common strains of microalgae were screened for their suitability for anaerobic digestion. A brief description of each species is given below. The function of each species as a biofuel is explored in greater detail in section 2.4.9.

2.3.1 *Chlorella vulgaris*

Chlorella is a spherical green freshwater microalga (Figure 17) commonly used in investigation of the use of waste water for biofuel production due to its association with algal waste water treatment ponds where it constitutes around 45% (raw sewage) to 65% (treated water) of the total phytoplankton present (Graham et al., 2009, Bhatnagar et al., 2010).

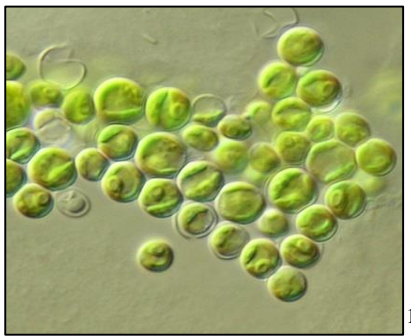


Figure 17 – Microscope image of *Chlorella sp.*

¹ botany.natur.cuni.cz/algo/images/CAUP/H1998_4.jpg

2.3.2 *Scenedesmus spp*

Scenedesmus sp. Is a non-motile freshwater/ brackish unicellular flat green microalgae consisting of colonies in 2,4,8 or 16 linearly arranged cells dependent on grazing threats, with predation increasing colony size shown in Figure 18 (Lee, 2008, Graham et al., 2009). Commonly found in wastewater streams it can grow rapidly and easily on wastewater nutrients.



Figure 18 – Microscope image of *Scenedesmus sp.*

² microscopy-uk.org.uk/mag/imgoct05/Scenedesmus-opoliensis.jpg,

2.3.3 *Nannochloropsis oculata*

Nannochloropsis oculata. is a common green marine and freshwater microalga 1-5 μm in diameter used in the aquaculture of marine molluscs shown in Figure 19 (fresh water species resembles *Chlorella* and lacks a pyrenoid). The algal biomass is occasionally used to supplement human and animal diets (Graham et al., 2009). *N. oculata* is high in the valuable molecules eicosapentaenoic acid (EPA) $\omega 3$ and 6 and in essential amino acids (Reboloso-Fuentes et al., 2001). It is the accumulation of triacylglycerols (TAG) under nutrient starvation that has driven interest in this species as a potential future biofuel source (Pal et al., 2011). The feasibility of using *Nannochloropsis sp* as a biofuel feedstock has been and is currently being investigated (Rocha et al., 2003, Cheng-Wu et al., 2001, Biller and Ross, 2011, Pal et al., 2011).

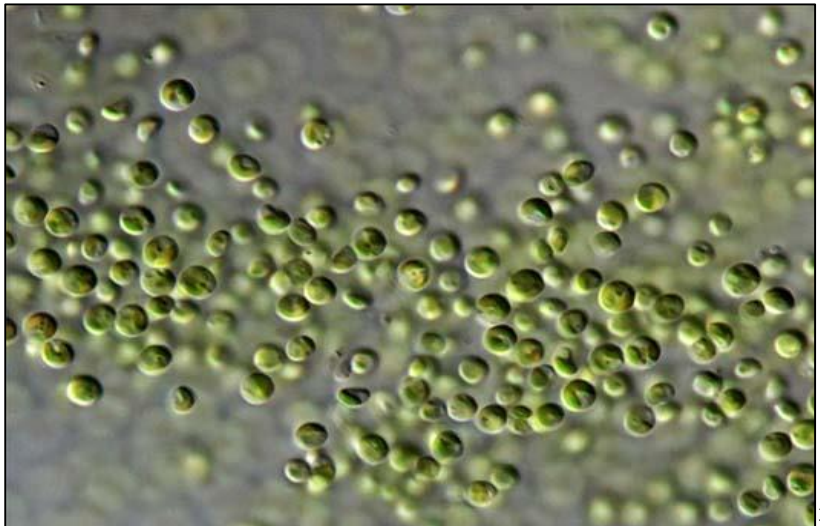


Figure 19 – Microscope image of *Nannochloropsis sp.*

2.3.4 *Isochrysis galbana*

Isochrysis galbana: is common yellow-brown marine microalga shown in Figure 20. It is found in coastal regions in the North Atlantic, is used frequently in the aquaculture of marine bivalves and can have a high oil content. The cell length is 5-6 μ m with two flagella approximately 7 μ m in length (Thronsen, 1997).

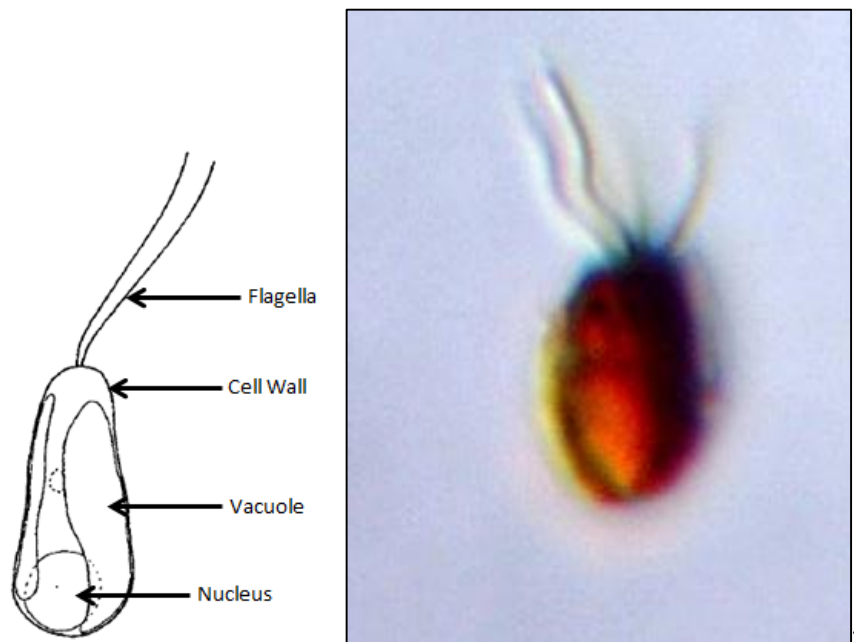


Figure 20 – *Isochrysis galbana* (Thronsen, 1997).

⁴ upload.wikimedia.org/wikipedia/commons/2/2f/Isochrysis_galbana.jpg,

2.3.5 *Dunaliella salina*

Dunaliella salina is a motile highly salt tolerant species that is found primarily in salt marshes and coastal waters in the Mediterranean and Atlantic. It comprises of two flagella and an elongated body as shown in Figure 21. Its ability to grow in hyper saline conditions makes it an ideal species to examine for the use of salt water aquifers and lakes for biomass production.

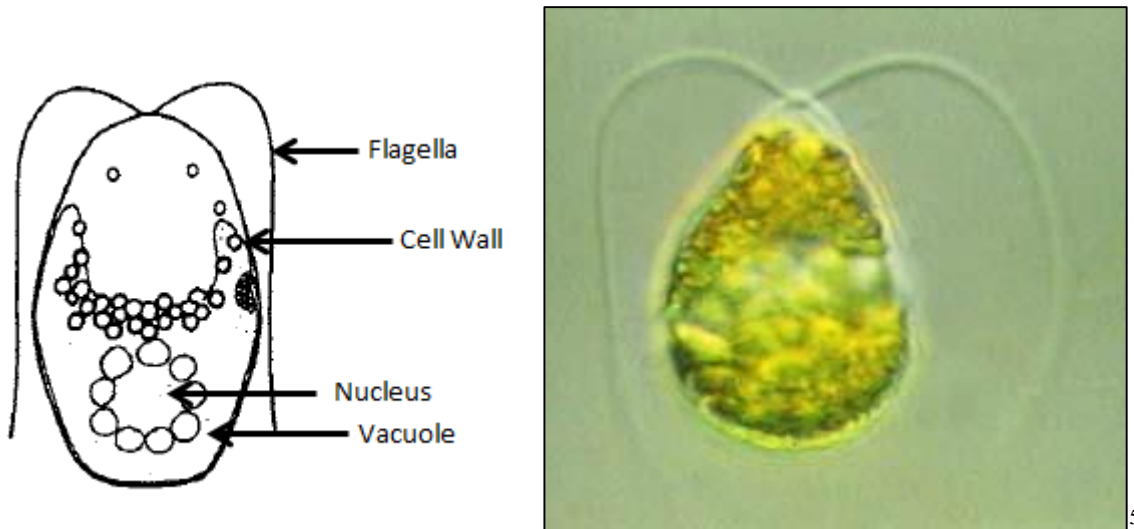


Figure 21 – *Dunaliella salina*

2.3.6 *Thalassiosira pseudonana*

Thalassiosira pseudonana is an extremely variable species of marine centric diatom found throughout the world's oceans shown in Figure 22 (Thronsen, 1997). Ranging in diameter from 2.5-15 μm and located in freshwater and coastal environments with an optimum growth range between 10-30°C, with growth rates typically increasing with temperature (Belcher and Swale, 1977). It is commonly used for aquaculture of molluscs (Graham et al., 2009).

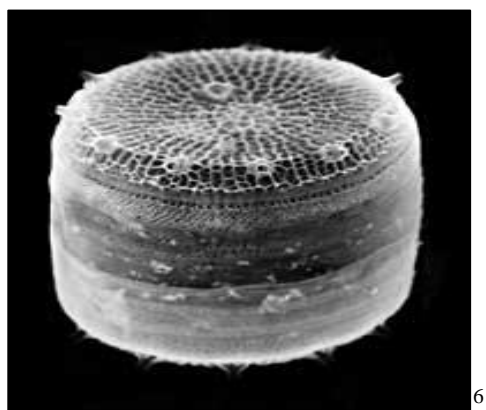


Figure 22 – SEM image of *Thalassiosira pseudonana*.

⁶ jgi.doe.gov/News/TpseuSEM.jpg.

2.3.7 *Rhodomonas spp*

Rhodomonas sp is a flagellate unicellular red/ brown marine microalga 14-30- μm in length, commonly used in aquaculture as a food source for copepods and other commercially important aquatic invertebrates (Lafarga-De la Cruz et al., 2006). It has two flagella and is a flattened cell as shown in Figure 23. It is found primarily in the North Atlantic coastal regions (Thronsen, 1997).

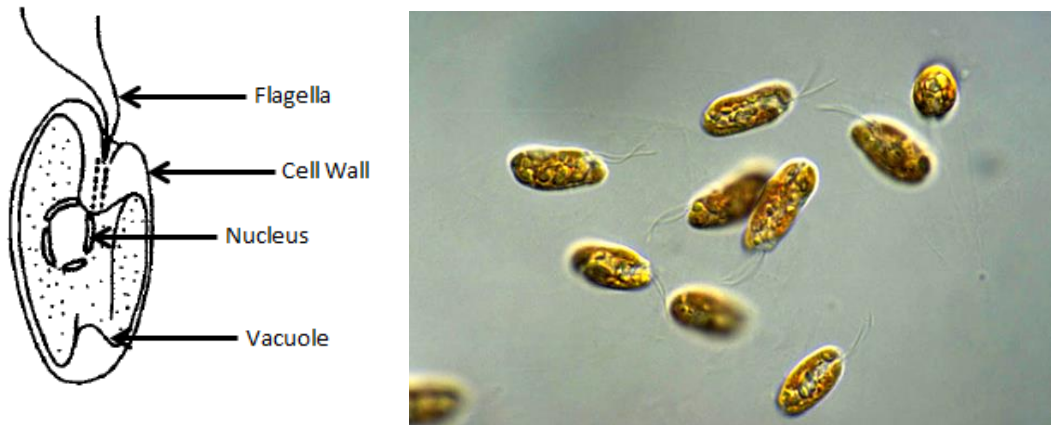


Figure 23 - *Rhodomonas sp* (Thronsen, 1997)

2.4 Anaerobic digestion

Anaerobic digestion is commonly used as an energy efficient and environmentally friendly way of remediating organic waste streams for energy recovery prior to disposal. This process involves the biological breakdown of complex organic matter in the absence of oxygen by a consortium of bacteria and archaea into biogas consisting primarily of CH_4 and CO_2 , with H_2 , H_2S and other trace gases. The bacteria and archaea exist in a delicate symbiotic relationship producing four main steps in AD: Hydrolysis, Acidogenesis, Acetogenesis and Methanogenesis, which occur in both series and parallel as shown in Figure 24. Fermentative bacteria hydrolyse particulate organic matter into simpler short chain molecules and methane producing archaea utilise these products for methane production (Figure 24). This relationship gives rise to a typical average biogas

⁷ http://cfb.unh.edu/phycokey/Choices/Cryptophyceae/RHODOMONAS/Rhodomonas_Image_page.htm

content of 55-65% CH₄ to 35-45% CO₂ within the AD of organic wastes; with proteins and lipids producing a higher percentage methane content of the biogas than carbohydrates. Several factors associated with the feedstock affect the consortium, primarily the presence/ absence of heavy/ light metals and substrate composition. As well as these, the design and operation can have a dramatic effect on the methane production and stability of the reactor, such as the organic loading rate (OLR), pH, temperature, rate of mixing, hydraulic retention time and dilution rate.

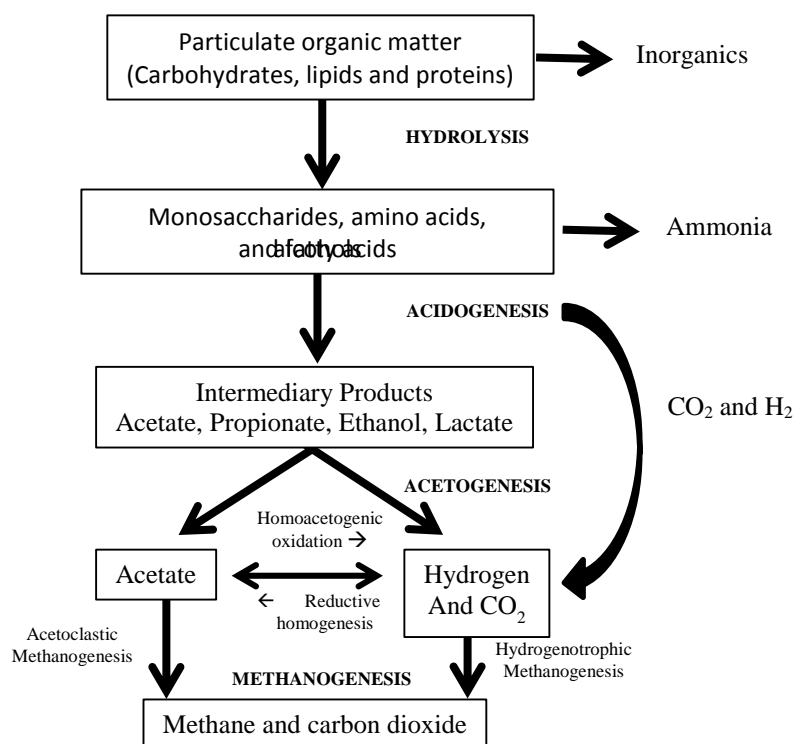
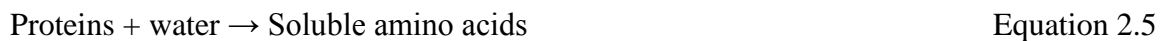


Figure 24 A schematic pathway of the anaerobic conversion of biomass to methane adapted from Demirel and Scherer (2008).

2.4.1 Hydrolysis

Hydrolysis is the first metabolic process in the conversion of complex particulate organic matter (POM) into short chain monomers by hydrolytic microorganisms (Gerardi, 2003). The hydrolysis process itself occurs outside of the cell by the use of exoenzymes (Chitinase, amylase, pectinase, cellulose, lipase, protease etc) (Chernicharo, 2007). As the acidogenic and acetogenic bacteria are unable to utilise the complex polymeric substances directly and lack the extracellular enzymes required to breakdown such material into its constituent monomers, mainly amino acids, sugars, and fatty acids, the

hydrolysis step is critical (Vavilin et al., 1996, Vavilin et al., 1997, Demirel and Scherer, 2008). This process is generally considered to be the rate limiting step within in the digestion of solid or particular matter, and if the hydraulic retention time (HRT) within a continuously stirred tank reactor (CSTR) is less than that of the rate of the solids hydrolysis rate, incomplete hydrolysis will occur reducing methane yields. The rate of hydrolysis can be significantly enhanced by increasing the temperature from the optimum mesophilic (35-37°C) range to thermophilic (55-70°C) increasing the hydrolysis coefficient from estimates of 0.1 - 0.2 day⁻¹ to 0.4 - 0.8 day⁻¹ (Ho et al., 2014, Siegrist et al., 2002, Ge et al., 2011). Pre-treatments can also increase the bioavailability of the POM. A simplified equation for the hydrolysis stage of anaerobic digestion can be written as:



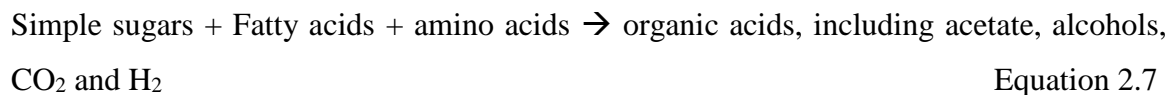
For cellulose the equation can be written as:



2.4.2 Acidogenesis

After the POM has been hydrolysed the resulting soluble monomers are fermented inside the cells of fermentative acidogen bacteria to produce several different simpler intermediate products, including but not limited to volatile fatty acids (VFA), long chain fatty acids (LCFA) hydrogen, carbon dioxide and ammonia (Figure 24) (Chernicharo, 2007). These intermediate products are used as substrates for both acetogens (amino acids, sugars, alcohols and fatty acids) and methanogens (H₂ and CO₂). This stage is generally considered to be the fastest within the AD process. Acidogenesis is the least susceptible stage to inhibition from heavy metals and high ammonia concentrations (Zayed and Winter, 2000, Koster and Lettinga, 1988). In toxicity tests using copper chloride, zinc chloride and nickel chloride Zayed and Winter (2000) observed complete inhibition of methanogens, but not acidogens. Under batch tests Fernandez and Forster (1994) found that the addition of 400 mg L⁻¹ of K⁺ to reactors fed on glucose or acetate as the only carbon source led to significant inhibition of the glucose reactors and not the

acetate fed reactors; suggesting that inhibition is occurring prior to methanogenesis, and the fermentative acidogens are inhibited by K^+ . The simplified reaction in the acidogenic stage of anaerobic digestion are as follows:



2.4.3 Acetogenesis

The intermediate products produced in acidogenesis are oxidised as a substrate by a consortium of acetogenic bacteria that produce acetate, carbon dioxide and hydrogen. Two main groups exist, the obligate hydrogen-producing acetogens (OHPA) which is the main acetogen group with regards to methanogenesis: and the homoacetogens which are often considered minor contributor to methanogenesis (Mara and Horan, 2003). The OHPA exist in a symbiotic relationship with methane producing Archaea whereby OHPA utilise VFA, LCFA and alcohols as substrates producing acetate, hydrogen and carbon dioxide and lowering the reactor pH shown in Equation 2.7; these products are subsequently metabolised by methanogens buffering the pH (Chernicharo, 2007, Gerardi, 2003). These microorganisms can only thrive in systems where their metabolic products are consumed, preventing accumulation of hydrogen which is inhibitory to OHPA, and fatty acids which is inhibitory to methanogens (Gerardi, 2003). When acetate is formed hydrogen is formed as a by-product, and if it accumulates will cause the termination of acetogenic activity shown in Equation 2.7. Koster and Lettinga (1988) found that acetogens are highly resistant to inhibition. Using UASB digesters they increased the ammonia concentrations to 5734 mg ammonia $-N L^{-1}$ and found there was little effect on acetogens but the methanogenic population activity reduced by 56.5%. the second group of acetogens referred to as the homoacetogens use a unique reductive pathway called the carbon monoxide dehydrogenase/acetyl-CoA synthase metabolic pathway, as the main pathway for energy conservation and for synthesis is from CO_2 (Müller, 2003). Equations 2.8 – 2.11 demonstrate the different pathways used by homoacetogens.





2.4.4 Methanogenesis

Methanogenesis is the final stage in the anaerobic digestion process whereby the fermentative products acetate, hydrogen and carbon dioxide are metabolised by methanogenic Archaea in the absence of oxygen to produce methane. Without methanogens the breakdown of organic material in anaerobic conditions would not occur due to the accumulation of the fermentative products increasing the acidity. This is often considered the slowest step in the AD process, primarily due to the low growth rate of methanogens, their low tolerance to environmental stress, the ease with which they are inhibited and the specificity of each substrate to the different groups of methanogens (Mara and Horan, 2003, Gerardi, 2003, Chen et al., 2008). Three main groups of methanogens exist: acetoclastic, hydrogenotrophic and methylotrophic methanogens, classified by the substrate utilised in the production of methane (Gerardi, 2003).

Acetoclastic methanogenic archaea utilise acetate by cleaving the substrate in two to produce methane and carbon dioxide, with the carbon dioxide produced available to hydrogenotrophic methanogens as a feedstock. Acetoclastic methanogens reproduce more slowly than the hydrogenotrophic methanogens: however often 70% of the methane produced is via the use of acetate. This is due to the limited supply of hydrogen within the reactor limiting the hydrogenotrophic methanogens. Hydrogenotrophic methanogens convert carbon dioxide to methane using hydrogen. The conversion of carbon dioxide and hydrogen to methane helps to maintain a low hydrogen partial pressure and regulate the acidity required for the acetogenic bacteria, and ultimately the acetoclastic methanogens to thrive (Gerardi, 2003, Mara and Horan, 2003). Reactors operating under a high hydrogen partial pressure and low pH observe a reduction in acetate and methane production (Gerardi, 2003, Mara and Horan, 2003). The methylotrophic methanogens consume substrates containing the methyl group (-CH₃): this group is minor in anaerobic digestion. The main chemical conversions occurring during methanogenesis can be written as follows:

Acetoclastic :



Hydrogenotrophic:



Methylotrophic:



No one species or group of methanogens can utilise all the substrates available for the production of methane, and therefore the successful operation of a reactor requires the presence of a large population and diversity of methanogenic archaea species (Gerardi, 2003, Stadtman and Barker, 1951).

2.4.5 Environmental factors that influence anaerobic digestion

Several factors influence the overall performance of an anaerobic reactor. These are both operation and substrate dependent, and are discussed below.

2.4.5.1 Temperature

Anaerobic digestion can occur at a range of temperatures with an optimum range above 15°C up to 100°C with extremophiles. Four main temperature ranges exist as shown in Table 3, each with its benefits and limitations, with lower temperatures having smaller operational costs for heating while higher temperatures may give an increased rate of reaction and reduce the required retention time within the system. Most methane-producing consortia exist in the temperature range of 30-60°C as mesophiles and thermophiles, with the majority of anaerobic digestion facilities operating within the mesophilic range of 25-45°C. With each decrease in temperature of 1°C from the optimum a 11% decrease in the rate of digestion occurs (Alaerts et al., 1993). The relative growth rate of methanogens increases within each temperature group, with the different temperature groups showing some overlap as seen in Figure 25 (Lettinga et al., 2001, Appels et al., 2008). For successful operation of an anaerobic digester the temperature must be maintained within one of these temperature ranges to prevent culture crashes.

Table 3 Optimum temperature ranges for the growth of methane producing archaea adapted from Gerardi (2003)

Bacterial Group	Temperature Range °C
Psychrophiles	5–25
Mesophiles	25–45
Thermophiles	50–60
Hyperthermophiles	>65

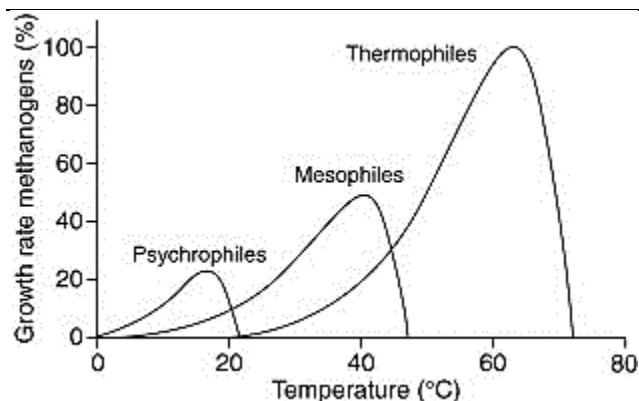


Figure 25 Relative growth rates of psychrophilic, mesophilic and thermophilic methanogens (Lettinga et al., 2001).

2.4.5.2 Alkalinity, pH and volatile acids

The buffering capacity of a digester is determined by the presence of a mixture of weak acids and their corresponding salts (Chernicharo, 2007). Carbonates formed by the production of carbon dioxide resulting in carbonic acid and the breakdown of protein releasing soluble ammonia which forms ammonia bicarbonate control the buffering capacity of the reactor (Georgacakis et al., 1982). Monitoring of the alkalinity is important in determining the stability of the digester, as alkalinity can be a simple indicator of VFA concentrations and can be used to indicate changes within the reactor, allowing corrective measures to be made to remediate them. It is generally accepted that an intermediate: partial alkalinity ratio for a reactor of below 0.5 is stable (Ripley et al., 1986, Ferrer et al., 2010)

Within the AD process the optimum pH is defined as a compromise between the optimum range for the growth rates and productivities of acidogenic bacteria (pH 5-7) and the

methanogenic archaea (pH 7-8), with a combined optimum between pH 6.5-8 (Chernicharo, 2007, Monnet, 2003). The operating parameters of anaerobic digesters are often defined by the limits of methanogenic growth to limit the domination of the acidogenic bacteria and the formation of excess VFA that can lead to microbial stress; the concentration of VFA (acetic acid, propionic acid, butyric acid and valeric acid) is often used as an indicator of reactor stability (Buyukkamaci and Filibeli, 2004, Rajeshwari et al., 2000, Khalid et al., 2011). If there is a change in pH beyond this range methanogens can be adversely affected, with the recovery of the reactor dependent on the scale and duration of the pH change and the VFA concentrations present when the pH changed (Chernicharo, 2007).

2.4.5.3 Macronutrients

Several macro-nutrients are required for AD, with the main ones being Carbon, Hydrogen, Nitrogen and Phosphorus (Parkin and Owen, 1986). The general ratio of the macronutrients C, N, P and S is 600:15:5:3, with a N/P ratio of between 5-10/1 depending on reactor operation (Fricke et al., 2007, Weiland, 2010). The overall stability of the reactor is determined by a balance of these macronutrients preventing the build-up of inhibitory products.

2.4.5.4 Carbon to nitrogen ratio

The C/N ratio is of interest in the digestion of micro algae due to the high nitrogen content of the biomass, as an excess of organic nitrogen can produce excess ammonia which can inhibit AD (Angelidaki and Sanders, 2004). For traditional AD a reported range of 20-30/1 of C/N has been found to produce a stable anaerobic digestion process with low ammonia and free ammonia concentrations (Zhang et al., 2007, Hills, 1979, Kayhanian, 1999).

The C/N ratio of between 5-11 in microalgae is considerably lower than that of terrestrial autotrophs which are at a ratio of roughly 36 (Elser et al., 2000). These values are below the C/N ratio of 20 and are generally considered to result in a gradual accumulation of the total ammonia nitrogen (TAN) and volatile fatty acids (VFAs) concentration which will reduce the methanogen activity and may lead to failure of the AD process (Parkin and Owen, 1986, Yen and Brune, 2007). The biodegradability of algae is low in comparison

to other traditional AD feedstocks, down to 24% in some instances compared to $\geq 80\%$ in food waste (Chynoweth et al., 2001). As less material is readily biodegradable the maximum potential effect of ammonia will be reduced. This will result in a reduced ammonia build up within an AD reactor, and as such the ammonia concentrations will not reach the maximum theoretical levels, as suggested by Heaven et al. (2011).

2.4.5.5 Micronutrients

Micronutrients are required in low concentrations for AD, whereas at high concentrations they can become inhibitory and toxic. They are primarily utilised in the formation and function of the enzymes required in the breakdown of the POM (Oleszkiewicz and Sharma, 1990, Zandvoort et al., 2006). Co, Mo, Ni, Se, W have been identified as essential for enzymatic activity within the anaerobic digestion process, with Fe, Cu, Ni and Zn essential for methanogens to produce their maximum methane yield (Zhang et al., 2003, Oleszkiewicz and Sharma, 1990, Worm et al., 2011). Deficiencies in any of these trace elements can cause reactor instability and a failure of the AD process. The addition of these trace elements can increase the degradation of the substrate improving methane yields. Excess trace elements, however, can cause inhibition and toxicity within the reactor. Other elements are also required in low doses such as Na, Mg, K Ca and S. These are discussed in more detail in section 2.4.6.2.

2.4.6 Potential inhibitors for the AD of marine microalgae

2.4.6.1 Inhibitors of anaerobic digestion

The bacteria and archaea within an anaerobic system exist in a finely balanced ecosystem, where temperature, pH, alkalinity, ammonia, heavy metals, light metals, organic loading rate (OLR) can have stimulating and inhibiting effects on the fermentative and methane producing microorganisms. The most likely inhibitors of anaerobic digestion of marine algae are discussed here.

2.4.6.2 Salt, anions and cations

Traditionally, high sodium and chloride concentrations have been considered to cause inhibition of methanogens in anaerobic wastewater treatment (Lefebvre and Moletta,

2006). Salt concentrations above 10 g L^{-1} have been shown to have an inhibitory effect, with an increase in osmotic stress on methanogens causing dehydration of the microorganisms and cell death (Hierholtzer and Akunna, 2012). Marine microalgae contain salts for osmoregulation and to prevent dehydration, resulting in a substrate elevated in salts, with the harvested biomass suspended in the salt water medium in which it was grown. This could cause methanogen cell death in a non-acclimatised AD system as high salt concentrations can dehydrate the archaea and bacteria (Kirst, 1990, de Baere et al., 1984). The main cations in seawater (Na^+ , K^+ , Mg^+ and Ca^+) are required in moderate concentrations for microbial growth and can have both inhibitory and stimulating effects (Chen et al., 2008). Data from McCarty (1964) on cation inhibition (Table 4) has been widely used for the last 50 years as a benchmark for the tolerances of methanogenic bacteria. This is becoming outdated as interest in halo tolerant species increases and produces conflicting data for these tolerances, with concentrations ranging from 4.4 g Na L^{-1} to 26.9 g Na L^{-1} for moderate inhibition of ~50% (Fang et al., 2011, Chen et al., 2003, Feijoo et al., 1995). Using molasses high in salt Fang et al. (2011) found a 50% inhibition of methane production with reactor concentrations between 11 and 28 g L^{-1} (Fang et al., 2011). The degree of inhibition may be dependent on inoculum source, with marine sediments having the greatest tolerance of Na of up to concentrations similar to seawater, whereas inoculum from non-halophilic sources such as municipal solids waste may have the lowest tolerance which is reflected in Table 5. Aspe et al. (1997) reported high salt tolerances with a lethal dose of 50% at 53 g Na L^{-1} (>140g total salt). This is interpolated from two data points between 20 g Na L^{-1} and 120 g Na L^{-1} , in a batch system, however, and may not be applicable to CSTR operation. Mottet et al. (2014) reported a 50% inhibition at 75 g Na L^{-1} when digesting the microalgal species *Dunaliella salina* using an acclimated inoculum from an industrial UASB reactor. They do report minimum differences between the maximum volume of methane produced per gram of VS at 15 g Na L^{-1} to the acclimated inoculum operating under 35 g Na L^{-1} , suggesting that acclimatisation may enable the successful digestion of marine substrates. Gradual exposure of non-halo tolerant methanogens to increasing salt concentrations leads to a build-up of tolerance (Feijoo et al., 1995). Feijoo et al. (1995) and de Baere et al. (1984) state that adaption to seawater salinity is required before full scale anaerobic digestion of marine material is considered, in order to improve methane production yields. Sulphates also present within marine waters, and unlike chlorides their presence is not necessarily

inhibitory, but the action of reduction and the products formed can cause a competitive reduction and inhibition of methanogenesis.

Table 4 – Observed effects of the light metal ions Na, Mg, Ca and K on methane production from large scale AD facilities (McCarty, 1964).

Cation	Concentration g L⁻¹		
	Stimulating	Mod inhibition	Strong inhibition
Ca	0.2	4.5	8.0
Mg	0.2	1.5	3.0
K	0.4	4.5	12.0
Na	0.2	5.5	8.0

Table 5 – Summary of anaerobic treatment of high salinity wastewater and substrates with successful <50% inhibited methanogens. Table adapted from Lefebvre and Moletta (2006) and Feijoo et al. (1995).

Innoculum	Halophilic inoculum	Total salt conc. g L ⁻¹	Reactor process	Reactor volume (L)	OLR g COD L ⁻¹	HRT (Days)	Reference
Inuline effluent	No	10	UASB ¹	1100000	23	0.3	(Kargi and Dincer, 1997)
Piggery manure	No	15	DFAFBR ²	1.4	0.5	4	(Rovirosa et al., 2004)
Fish Farm wastewater	No	35	CSTR ³	15	2.5	27.5	(Gebauer, 2004)
Fishery effluent	yes	14.6 – 17.9 (144)	CSTR ³	1.5	2	72	(Aspe et al., 1997)
SPWW ⁴	No	15	UAF ⁵	1.1	2	12	(Guerrero et al., 1997)
SPWW ⁴	No	7.7-26.3	UASB ¹	1	2.8	0.125	(Boardman et al., 1995)
SPWW ⁴	No	13.6-33.7	ACS ⁶	15000	13.6	10	(Omil et al., 1995)
SPWW ⁴	Yes		USBF ⁷	2.3	1-8	0.75	(Mosquera-Corral et al., 2001)
SPWW ⁴	Yes	30	Anaerobic filter	2.5	1.5-2	0.38	(Vidal et al., 1997)
Sludge SPWW ⁴	Yes	14-16	CSTR ³	15	1-3	30	(Gebauer, 2004)
Tannery wastewater	Yes	71	UASB ¹	5	14.3	5	(Lefebvre et al., 2006)
Standard ⁸	No	4.8 ^a	CSTR ³				(Kugelman and McCarty, 1965)
Marine sediment	Yes	18.4 ^a	Batch		n/a		(Sowers and Gunsalus, 1988)
Granular sludge	No	12-24	UASB ¹				(Rinzema et al., 1988)
Estuarine sediment and MSW digester	No	14.6	Batch				(Liu and Boone, 1991)
SPWW ⁴	Yes	12-30	UASB ¹				(Soto et al., 1993)
Municipal sewage sludge	No	18.8	ASBR ⁹	13	4	3	(Chen et al., 2003)
UASB	Yes	75	Batch				(Mottet et al., 2014)

Upflow anaerobic sludge blanket¹, down-flow anaerobic fixed bed reactor², completely stirred tank reactor³, Seafood processing waste water⁴, upflow anaerobic filter⁵, Anaerobic Contact system⁶, upflow sludge bed-filter⁷. 8 is the effluent of a lab scale anaerobic filter reactor in Feijoo et al. (1995), Anaerobic sequencing batch reactor⁹.

^a10% inhibition caused by sodium only

2.4.6.3 Strategies for overcoming salt inhibition

The most common method for overcoming salt inhibition is a gradual acclimatisation of the microorganisms to high salt, with the majority of studies shown in Table 5 utilising inoculum from industries where bacteria and archaea have adapted to high salinity, or combining estuarine and marine sediments with non-acclimatised inoculum. Osmoregulants glycine betaine, α -glutamate and β -glutamate can be used in the initial phase to reduce the effect of salinity and enable a gradual adaptation whilst maintaining a high methane yield (Vyrides and Stuckey, 2009).

Kimata-Kino et al. (2011) used an innovative method to acclimate a UASB by combining a shock increase in NaCl to 20 g L⁻¹ coupled with a gradual increase in total salinity, achieving 87% CH₄ production to that of the control group at a total NaCl concentration of 32 g L⁻¹. They suggest that the initial shock increase inhibited the methanogens as the fermentative products increased in concentration within the reactors. It is not known why the reactors were able to adapt rapidly when shocked to 20 g L⁻¹ NaCl, but it is likely that there is a population shift away from the acetoclastic methanogens, as these were inhibited at salt concentrations >32 g L⁻¹.

2.4.7 Sulphur and sulphate

Of concern when anaerobically digesting marine substrates is sulphate, which is the second most abundant anion in seawater with a concentration of around 2800 mg L⁻¹. Sulphate reducing bacteria (SRB) utilise sulphate as the electron acceptor for the respiration of fermentative products reducing the sulphate to hydrogen sulphide. Two distinct groups of SRB exist, heterotrophic SRB and autotrophic SRB. Heterotrophic SRB utilise a wide variety of compounds as substrates such as hydrogen, formate, methanol, ethanol, molasses, lactate, propionate/ butyrate, sugar and acetate competing with acetoclastic methanogens (Liamleam and Annachhatre, 2007, Lens and Kuenen, 2001). Autotrophic SRB utilise CO₂ as the carbon source and obtain electrons from the oxidation of hydrogen, competing with hydrogenotrophic methanogens (Liamleam and Annachhatre, 2007, Lens and Kuenen, 2001, Muyzer and Stams, 2008). Sulphur in varying states of oxidation can be utilised as a substrate through the process of disproportionation where thiosulphate, sulphite and sulphur are oxidised and reduced to form sulphate and hydrogen sulphide as shown in the stoichiometric equations 2.14 and 2.15 (Figure 26) (Bak and Pfennig, 1987, Böttcher et al., 2005). This enables SRB to consume a variety of feedstocks within the AD process.

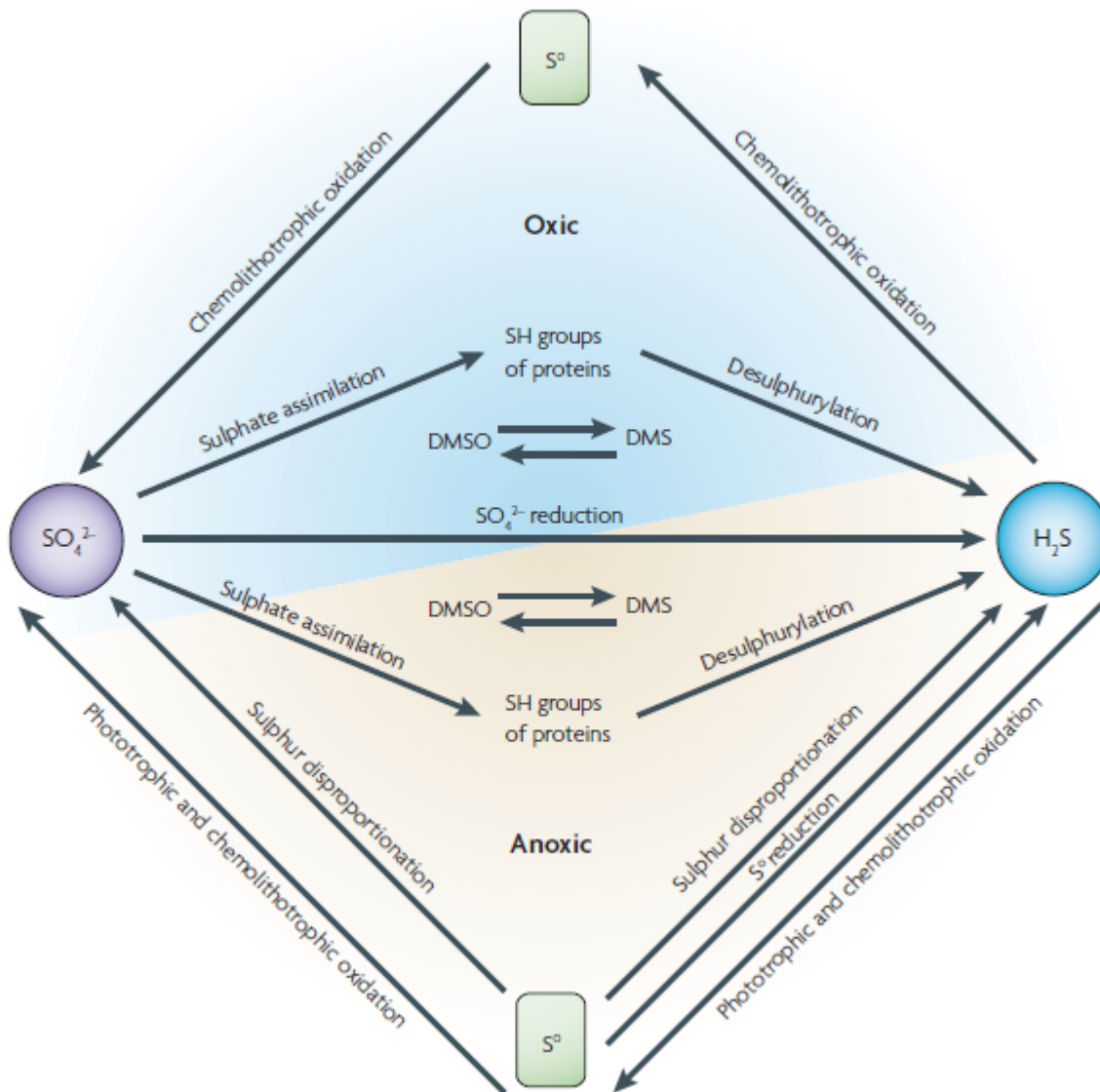


Figure 26 pathways for sulphur reduction and oxidation (Muyzer and Stams, 2008).



Currently there are 220 known species of SRB in 60 different genera (Barton and Fauque, 2009). Using the rRNA database and the 16S rRNA sequences Muyzer and Stams (2008) determined that there are seven phylogenetic lines of SRB, of which five are bacterial and two archaeal- showing that the term bacteria is used more for convenience than accuracy in this case. SRB exist in large numbers within the anaerobic environment, even when sulphate is limiting. This explains why in anaerobic digesters the introduction of sulphate can be met with a rapid production of hydrogen sulphide (Muyzer and Stams, 2008).

SRB have a syntrophic relationship with the fermentative bacteria within hydrolysis, acetogenesis and acidogenesis, utilising the same fermentative products as methanogens (Figure 27) (Hansen, 1993). However, sulphate reduction is more energetically favourable than methanogenesis (Table 6) and will outcompete methanogens and as they have a higher specific growth rate and a lower half saturation value, which gives them a kinetic advantage over methanogens (Archer and Kirsop, 1991). Of the groups mentioned above two major groups of SRB are of concern within the AD process: incomplete oxidisers that oxidise lactate to acetate (equation 2.17) and the acetoclastic SRB that completely oxidise acetate (equation 2.18) (Hilton and Oleszkiewicz, 1988).

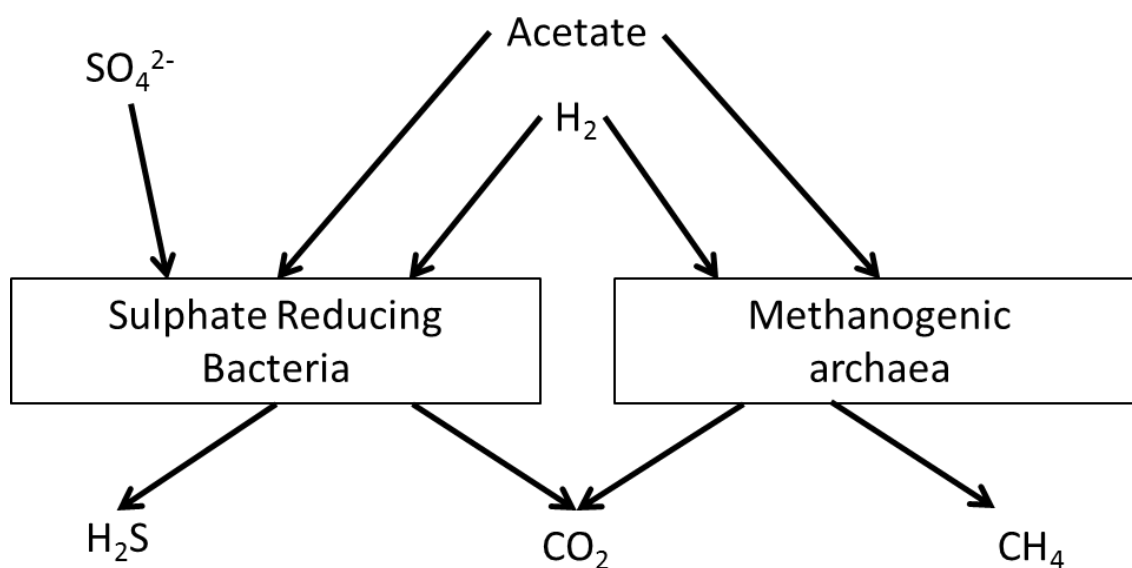


Figure 27 – Competition of the pathways between SRB and methanogenic archaea.



Table 6 – Free energy changes for remineralisation reactions (Morel and Hering, 1993).

Reaction	Free energy change (kJ mol ⁻¹ of CH ₂ O)
$\text{CH}_2\text{O} + \text{O}_2 \rightarrow \text{CO}_2 + \text{H}_2\text{O}$	-476
$2\text{CH}_2\text{O} + \text{SO}_4^{2-} \rightarrow \text{H}_2\text{S} + 2\text{HCO}_3^-$	-82
$2\text{CH}_2\text{O} \rightarrow \text{CO}_2 + \text{CH}_4$	-71

At higher sulphate concentrations competitive inhibition can occur (O'Flaherty et al., 1999). As the free energy of sulphate reduction is more favourable than that of methanogenesis competition can occur, thus between SRB and methanogens for the fermentation products reducing the methane potential (Liamleam and Annachhatre, 2007). The reduction of sulphate during AD is generally an undesirable process, with the production of H₂S causing toxicity/ inhibition to both methanogens and SRB. Precipitation of trace metals such as Ni, Co and Fe occurs by S²⁻, creating nutrient deficiency, malodour and damage to equipment as well as reducing methane yields. In extreme cases methanogen death can also occur due to production of potentially lethal concentrations of H₂S that readily permeate through cell membranes producing sulphide/ disulphide crosslinks between the polypeptide chains within the proteins (Koster et al., 1986, Vogels et al., 1988, Speece, 1983). Digesters at municipal wastewater treatment plants treating fresh water influent generally produce low concentrations of H₂S gas between 0 – 170ppmv (Rasi et al., 2007), with saline systems producing potentially much higher concentrations between 20000-80000 ppmv (Soto et al., 1991). H₂S is flammable and explosive, with gas mixtures of 4.5 to 45.5% v/v within air being explosive (Fletcher, 1998). When gas containing H₂S is combusted sulphur oxides are produced which are corrosive to metallic components within the combustion vessel and exhaust reducing the efficiency and lifespan of the equipment. The sulphur oxides are converted to sulphuric acid within the atmosphere adding to the environmental problem of acid rain.

Bacteria and archaea require sulphur for growth, with optimal concentrations reported in the range of 1-25 mg SO₄ L⁻¹ or a COD to sulphate ratio >10 being sufficient (Scherer and Sahm, 1981). Reported inhibitory concentrations of sulphate vary considerably between 50–1200 mg L⁻¹ depending on operating parameters (O'Flaherty et al., 1999, Scherer and Sahm, 1981, Hulshoff Pol et al., 1998). Concentrations between 200-1500 mg L⁻¹ of H₂S_{liq} have been reported to be inhibitory and toxic to both bacteria and archaea present within an anaerobic digester (Koster et al., 1986) (Parkin et al., 1990). This variation is primarily due to the inoculum's natural tolerance to sulphide, operational design, and COD to sulphur ratio determining the concentration of sulphide produced.

pH has the single greatest effect on toxicity by hydrogen sulphide, with sulphide primarily existing as the less toxic dissociated HS⁻ above a pH of 8-9 with the ionic equations 2.19, 2.20 and in Figure 28 (Garrels and Christ, 1965, Blunden and Aneja, 2008). However, Koster et al. (1986) and O'Flaherty et al. (1998a) both report that unionized / undissociated H₂S_{liq} is the main driver for sulphide inhibition at pH levels of 6.4 – 7.5, while at higher pH values of 7.8-8 inhibition is correlated with total sulphide. It is commonly reported that at pH 7-8 50% of sulphide exists as the

highly toxic $\text{H}_2\text{S}_{\text{liq}}$ which is the only form able to pass through the cell membrane (Chernicharo, 2007, Speece and Parkin, 1983).

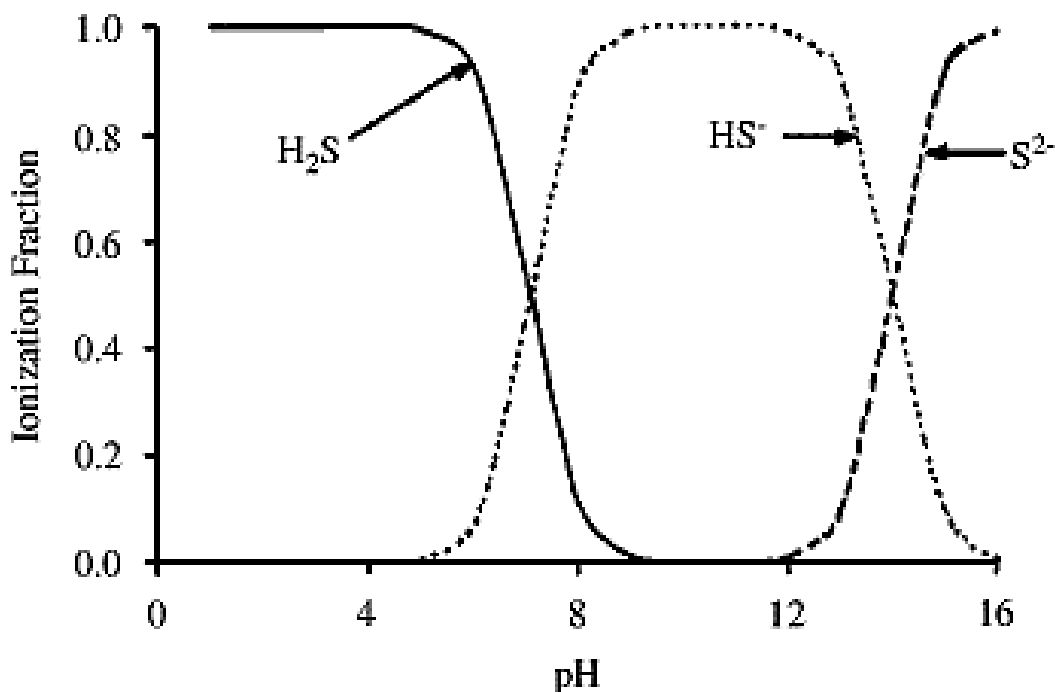


Figure 28 – Fractions of sulphide species present within an anaerobic digester in aqueous solution as a function of pH at 25°C, image adapted from Blunden and Aneja (2008).

2.4.7.1 Strategies for overcoming sulphur inhibition

Several established processes exist to promote the removal of sulphide from the digestate. A sulphate removal step can be incorporated whereby stripping, pH control, coagulation, oxidation or precipitation can occur or the gas produced upgraded (Chen et al., 2008). FeCl_3 dosing is a typical method for precipitating $\text{H}_2\text{S}_{\text{liq}}$ within the digester, whereby Fe(III) is reduced to Fe(II) producing FeSO_4 (Mamais et al., 1994). FeCl_3 dosing is a suitable method for high sulphur feedstocks, as it can prevent sulphate reduction enough to enable methanogenesis to resume/ occur (Wang and Banks, 2006). MoO_4^{2-} has been successfully used to selectively inhibit SRB, but it also inhibits methane producing archaea by being stereochemically similar to sulphate and competing in biochemical reactions such as membrane transport. Once loading of MoO_4^{2-} has ceased SRB function returns but

acetoclastic methane production has ceased completely, making this method unfeasible (Isa and Anderson, 2005, Ranade et al., 1999).

Co-digestion with substrates low in sulphate dilutes the sulphate present and may increase the COD to sulphate ratio. In the case of microalgae, however, the extraction and concentration step is currently energetically expensive and it is likely that the concentrations used would already be low with further dilution almost completely removing the algae as a feedstock (Milledge, 2010b).

Hydrogen sulphide can be removed from the headspace by the addition of small quantities of pure oxygen. Sulphide-oxidising bacteria under oxygen limited conditions can oxidise gaseous hydrogen sulphide into elemental sulphur (Steudel, 1996). The removal of hydrogen sulphide from within the headspace will cause an outgassing of dissolved H_2S from the digestate into the gas phase reducing the inhibitory effect. Gas injectors can be used to introduce low concentrations at less than 1% oxygen V/V into the reactor to stimulate the sulphide-oxidizing bacteria and remove H_2S (Kleinjan, 2005).

Only a limited amount of research has been undertaken to date on the effects of high sulphate conditions in AD of marine macro and micro algal species. Co-digestion of macro algae containing 6.4% sulphur with pig slurry produced biogas with up to 3.5% H_2S_{gas} , above UK legal limits for biogas use for bioenergy showing the inherent difficulties in digesting marine feedstocks (Peu et al., 2011, Muyzer and Stams, 2008). Migliore et al. (2012) used lake sediment as an inoculum and digested the overlying marine macroalgae *G. longissima* and *C. linum* in batch tests under mesophilic conditions. They found that the biogas produced contained 1.46% H_2S , which could increase if run under continuous conditions creating potential downstream problems.

2.4.8 C/N and algae digestion

It has been suggested that anaerobic digestion of the residual biomass after the extraction of lipids for biodiesel could reduce the biodiesel production costs by up to 40% (Harun et al., 2011). Extraction would act as a pre-treatment step rupturing the cell walls and facilitating breakdown of the cell contents. This could also prove problematic, however, due to an increase in the %N content of the biomass. Removal of the carbon in the lipid fraction would decrease the C:N ratio further, which could prevent successful AD of the remaining substrate due to an increased ammonia toxicity. In principle it would be more energetically favourable to digest the whole organism, as lipids have higher specific biogas and methane yields than carbohydrates and proteins, and no energy-

consuming step is required. Co-digestion with substrates with a high C:N, such as waste paper, could alleviate the problem (Heaven et al., 2011, Syrett and Thomas, 1973, Yen and Brune, 2007). Ehimen et al. (2011) investigated the use of microalgae residues resulting from the biodiesel production process. Using *Chlorella* subjected to an acid catalysed transesterification process with the remaining biomass frozen at -24°C they fed CSTR at a range of OLR, HRT, and temperatures and with additional glycerol to determine the effect on the specific methane production (SMP). It was found that the HRT and C:N greater than 12.44 ratio had the greatest effects on the SMP, with the addition of glycerol increasing the SMP by $>50\%$ compared to that of reactors fed only on the algal residues. The authors stated that the methane recovery from post transesterified microalgae residues with an optimised growth and extraction regime could potentially improve the future commercial viability of microalgae biodiesel production. Yen and Brune (2007) co-digested algal sludge containing *Scenedesmus* and *Chlorella* spp with waste paper from laser printing. They also found improved methane yields with co-digestion, but at a higher C/N of between 20-25/ 1 with 40% of the VS from microalgae. The authors reported an increase in cellulose degradation due to the presence of extra nutrients from the microalgae, which may increase the biodegradation of the algal substrate. At C/N above 25 a reduction in the SMP was observed producing TAN concentrations of 65 mg L^{-1} with low nitrogen concentrations potentially limiting fermentation.

González-Fernández et al. (2011) examined the use of the algal biomass grown in a photobioreactor cultured on swine wastes to improve the digestibility of swine manure. The algal biomass was harvested from the photobioreactor wall and co-digested with the swine manure under batch conditions at different substrate/inoculum VS ratio with varying proportions of VS from algae and swine manure. They found that SMP reduced with an increasing proportion of algae to swine manure and stated that the recalcitrant nature of the algae was the main driver for this. Conversely Zhong et al. (2012) reported an increase in SMP of 61% from co-digesting the cyanobacteria Taihu blue algae with corn straw at a C/N of 20/1 under batch conditions compared to the mono-digestion of corn straw. Samson and LeDuy (1983a) digested *Spirulina maxima* cultured within a photobioreactor and harvested by centrifugation then frozen until use with three different high carbon waste streams: primary domestic waste sewage sludge, peathydrolyzate and spent sulphite liquor. Using 2 L Erlenmeyer flasks with a 1.5 L working volume under mesophilic conditions, they fed reactors with a mixture of algae and the high carbon substrate to achieve a HRT of 20 days. They reported a two-fold increase in SMP from the digestion of algal biomass with sewage sludge, with slight improvements in SMP with the other substrates compared to sewage sludge alone. The authors

suggest that the C/N ratio is one of the greatest drivers in SMP with the addition of high carbon sources improving digestibility considerably.

2.4.9 Anaerobic digestion of algae

Limited research has been conducted on the anaerobic digestion of whole microalgae without pre-treatment under continuous digestion conditions. The majority of research has focused on BMP analysis of the biomass, as shown in Table 7 summarises reported values for the SMP for fresh water and marine microalgae under different operational conditions, including the species, inoculum source, pre-treatment type and maximum SMP for both the pre-treated sample and algae without any pre-treatments. Any comments on inhibition and its potential causes are also noted. Continuous digestion findings are reported at the bottom of the table. Both fresh water and marine species have a range of SMP for similar species under operational conditions. Different species of *Chlorella* digested with different inoculum sources as a BMP under mesophilic conditions had a range of SMP between 0.098 – 0.361 L CH₄ g⁻¹ VS added showing the variability that can occur within genus types (Frigon et al., 2013, Polakovičová et al., 2012). The same species of *Chlorella vulgaris* produced SMP of between 0.129 and 0.361 L CH₄ g⁻¹ VS added using different inoculum sources (Frigon et al., 2013, González-Fernández et al., 2011). This shows the variability in biodegradation that can occur under different operating conditions for the same species of algae. The lowest SMP reported was for *Dunaliella tertiolecta* with an SMP of 0.024 L CH₄ g⁻¹ VS added; less than 9% of the theoretical methane potential (TMP); which was attributed to the high salt content and the presence of NaOH used as a flocculant in the harvesting process of the algae, showing the potential effects of inhibition on a non-acclimatised inoculum (Lakaniemi et al., 2011b). The highest SMP was reported by De Schampelaire and Verstraete (2009) for a mixed algal species with a thermal pre-treatment producing 0.6 L CH₄ g⁻¹ VS.

The methane potential of microalgae falls within reported yields for second generation biofuels, with average methane productions for maize crop waste at 0.338 l CH₄ g⁻¹ VS, Wheat straw at 0.290 l CH₄ g⁻¹ VS, rice straw at 0.302 l CH₄ g⁻¹ VS and sugarcane bagasse at 0.278 l CH₄ g⁻¹ VS (Chandra et al., 2012). These similarities in methane potential and the possibility to exceed these values have fuelled the interest in the use of marine microalgae as a feedstock for AD.

2.4.9.1 Continuous digestion vs BMP assays

BMP assays are useful indicators of the maximum methane potential of a feedstock. The high ratio of digestate to substrate can prevent any inhibitory effects of the substrate occurring by dilution enabling a maximum biological methane production to be established. This, however, does prevent any effects that can occur during continuous operation to be established. This is particularly true with regards to marine microalgae which have been reported to have a high nitrogen, salt, and sulphate content and can be highly recalcitrant. All of these can present potential problems when digested under continuous operation, which may not be apparent under batch analysis. Under batch conditions there is minimal adaption by the microbial community to the feedstock, so the ability for the methanogenic consortium to adapt cannot be determined unless continuous analysis has occurred. The low concentrations of sulphate within the substrate sample and low initial populations of SRB will produce lower concentrations of hydrogen sulphide than within a continuous system. Due to the recalcitrant nature of microalgae, BMP assays of long durations can create a misrepresentation of the potential energy recovery to those achievable from continuous operation that usually operate with shorter hydraulic retention times. This presents problems with regards to calculating energy balances with BMP assays only, as these will produce a false maximum. The methane production kinetics along with the maximum SMP would help to indicate a suitable operational HRT of a continuously run system more than just the SMP alone. It is important to ensure that a suitable inoculum is selected and potential pre-treatments considered and conducted on each species of algae. Alternative systems such as the fuel cell have been reported as a potential method for successful energy recovery from microalgae. The microbial fuel cell with thermal pre-treatments reports the greatest SMP under continuous operation (De Schamphelaire and Verstraete, 2009). AD under continuous operation, however, has not been fully examined and still requires further investigation into its potential.

The majority of analysis has focussed on the BMP of algae, with currently ten reports examining the continuous digestion of microalgae (Table 7). All reported methane yields shown in Table 7, with the exception of the freshwater genus *Chlorella* at or below the minimum reported BMP methane potential. For *Nannochloropsis*, continuous digestion studies show a range of SMP values that are up to 50% of reported BMP for a similar genera, as low as $0.130 \text{ L CH}_4 \text{ g}^{-1} \text{ VS}$, (Park and Li, 2012).

The coupling of the growth of microalgae and anaerobic digestion has been suggested for the recycling of nutrients within a wastewater treatment works, potentially reducing energy inputs. The European Union is currently funding a variety of projects on algal biomass (FP7, 2015), including

one in this area. Rogalla (2014) reported a positive energy balance when algae cultivated on waste water within an optimised raceway pond were co-digested with waste water biosolids. The reported energy gain was sufficient to convert a waste water treatment plant from being an energy consumer to an energy producer. At present, however, there is limited information on this project other than what was presented at conference. Further research is therefore required into the continuous digestion of microalgae to add to the current literature to address the issues mentioned above.

Chapter 2

Table 7 Methane production and operational conditions for the anaerobic digestion of microalgae. All results reported are the maximum SMP reported and the conditions to which they were reached.

Algal Substrate	Inoculum source	Pre treatment/co digestion	Reactor Process	Operating conditions	OLR (g VS L ⁻¹)	HRT (days)	Reactor size (l)	SMP (l CH ₄ g ⁻¹ VS added)		C/N	Inhibition	Reference
								Algae only	pre-treated / co digestion			
40% <i>Chlamydomonas</i> , 20% <i>Scenedesmus</i> and 40% <i>Nannocloropsis</i>	-	Thermal hydrolysis	BMP	Mesophilic	-	-	-	0.188	0.395	-	-	(Alzate et al., 2012)
Algal biomass	Municipal sewage sludge	Microwave	BMP	Mesophilic	-	-	-	0.117	0.208	-	-	(Passos et al., 2013)
<i>Arthrospira platensis</i>	Sewage sludge	-	BMP	Mesophilic	-	-	-	0.481			-	(Mussgnug et al., 2010)
Blue green algae	-	-	BMP	Psychrophilic	-	-	-	0.366	-	-	-	(Rui et al., 2009)
<i>Botryococcus braunii</i>	Apple digestate	-	BMP	Mesophilic	-	-	-	0.343				(Frigon et al., 2013)
<i>Botryococcus braunii</i>	Apple digestate	-	BMP	Mesophilic	-	-	-	0.370				(Frigon et al., 2013)
<i>Chlamydomonas debaryana</i>	Apple digestate	-	BMP	Mesophilic	-	-	-	0.302				(Frigon et al., 2013)
<i>Chlamydomonas reinhardtii</i>	Sewage sludge	-	BMP	Mesophilic	-	-	-	0.587			-	(Mussgnug et al., 2010)
<i>Chlamydomonas reinhardtii</i> and <i>Pseudokirchneriella subcapitata</i>	-	Thermal	BMP	Mesophilic	-	-	-	0.35-0.6	0.28-0.36	-	-	(De Schamphelaire and Verstraete, 2009)

<i>Chlamydomonas sp</i>	Apple digestate	-	BMP	Mesophilic	-	-	-	0.333					(Frigon et al., 2013)
<i>Chlorella kessleri</i>	Sewage sludge	-	BMP	Mesophilic	-	-	-	0.335			-		(Mussgnug et al., 2010)
<i>Chlorella sorokiniana</i>	Maize fed digestate	Dried and milled	BMP	Mesophilic	-	-	-	0.098	0.212		-	-	(Polakovičová et al., 2012)
<i>Chlorella sorokiniana</i>	Apple digestate	-	BMP	Mesophilic	-	-	-	0.283					(Frigon et al., 2013)
<i>Chlorella sorokiniana</i>	Apple digestate	-	BMP	Mesophilic	-	-	-	0.331					(Frigon et al., 2013)
<i>Chlorella vulgaris</i>	sewage sludge		BMP	Mesophilic	-	-	-	0.40-0.45 COD removed			n/a		(Sánchez Hernández and Travieso Córdoba, 1993)
<i>Chlorella vulgaris</i>	Granular sludge	Bacterial bioaugmentation	BMP	Mesophilic	-	-	-	0.317	0.402		-	-	(Lü et al., 2013)
<i>Chlorella vulgaris</i>	Municipal wastewater sludge	-	BMP	Mesophilic	-	-	-	0.286	-		-	-	(Lakaniemi et al., 2011a)
<i>Chlorella vulgaris</i>	Apple digestate	-	BMP	Mesophilic	-	-	-	0.361					(Frigon et al., 2013)
<i>Chlorella vulgaris</i>	Apple digestate	-	BMP	Mesophilic	-	-	-	0.263					(Frigon et al., 2013)
<i>Chlorella vulgaris</i> and <i>Scenedesmus obliquus</i>	Waste water sludge	Co digestion with swine manure	BMP	mesophilic	-	-	0.5	0.129	238		8.3-10.4	n/a	(González-Fernández et al., 2011)
<i>Chlorella sp</i>	Apple digestate	-	BMP	Mesophilic	-	-	-	0.309					(Frigon et al., 2013)
<i>Chlorella sp.</i>	Apple digestate	-	BMP	Mesophilic	-	-	-	0.302					(Frigon et al., 2013)
<i>Chlorella sp., Scenedesmus</i>	Sewage sludge			Mesophilic	1.44-2.89	11	-	0.170-0.320	-		-	-	(Lakaniemi et al., 2011b)

Chapter 2

<i>Dunaliella salina</i>	Sewage sludge	-	BMP	Mesophilic	-	-	-	0.505			-	(Mussgnug et al., 2010)
<i>Dunaliella salina</i>	Sediment, Industrial UASB treating sugar syrup and sewage sludge digester	-	BMP	Mesophilic	-	-	-	0.345	-	-	Inhibited at salinity greater than 35g L ⁻¹	(Mottet et al., 2014)
<i>Dunaliella tertiolecta</i>	Municipal wastewater sludge	-	BMP	Mesophilic	-	-	-	0.024	-	-	Inhibited by salinity, SO ₄ and NaOH used as a flocculant	(Lakaniemi et al., 2011a)
<i>Euglena gracilis</i>	Sewage sludge	-	BMP	Mesophilic	-	-	-	0.485			-	(Mussgnug et al., 2010)
<i>Glossomastix chrysoplata</i>	Apple digestate	-	BMP	Mesophilic	-	-	-	0.227				(Frigon et al., 2013)
<i>Isochrysis spp</i>	Apple digestate	-	BMP	Mesophilic	-	-	-	0.408				(Frigon et al., 2013)
<i>Micractinium sp</i>	Apple digestate	-	BMP	Mesophilic	-	-	-	0.360				(Frigon et al., 2013)
<i>Microcystis spp</i>	Adapted inoculum to algae and straw	Co digested with straw	BMP	mesophilic	-	-	0.15	0.201	0.325	6-20	Reduced yields at low C/N and High C/N	(Zhong et al., 2012)
<i>Microcystis spp</i>	Cattle manure digestate	-	BMP	Mesophilic	-	-	-	0.140	-	-	Decrease in SMP at low innoc/substrate	(Zeng et al., 2010)
<i>Nannochloropsis gaditana</i>	Apple digestate	-	BMP	Mesophilic	-	-	-	0.228				(Frigon et al., 2013)
<i>Nannochloropsis salina</i>	Digestate treating <i>Nannochloropsis salina</i>	Thermal pretreatment	BMP	Mesophilic	-	-	-	0.2 COD added	0.57 COD added	12.2	-	(Schwede et al., 2013)

<i>Neochloris oleoabundans</i>	Apple digestate	-	BMP	Mesophilic	-	-	-	0.308				(Frigon et al., 2013)
<i>Phaeodactylum. tricorutum</i>	Potato processing digestate	-	BMP	Mesophilic	-	-	-	0.24				(Zamalloa et al., 2012a)
<i>Porphyridium aeruginosa</i>	Apple digestate	-	BMP	Mesophilic	-	-	-	0.352				(Frigon et al., 2013)
<i>Scenedesmus. obliquus</i>	Potato processing digestate	-	BMP	Mesophilic	-	-	-	0.36				(Zamalloa et al., 2012a)
<i>Scenedesmus dimorphus</i>	Apple digestate	-	BMP	Mesophilic	-	-	-	0.397				(Frigon et al., 2013)
<i>Scenedesmus obliquus</i>	Sewage sludge	-	BMP	Mesophilic	-	-	-	0.287			-	(Mussnug et al., 2010)
<i>Scenedesmus sp</i>	Granular sludge treating sugar wastes	Ultrasonic and thermal	BMP	Mesophilic	-	-	-	0.081 COD added	0.153(ultrasound) 0.128(Thermal) COD added	-	Reduced yield at low ultrasound	(González-Fernández et al., 2012b)
<i>Scenedesmus sp</i>	Apple digestate	-	BMP	Mesophilic	-	-	-	0.258				(Frigon et al., 2013)
<i>Scenedesmus sp</i>	Apple digestate	-	BMP	Mesophilic	-	-	-	0.306				(Frigon et al., 2013)
<i>Scenedesmus sp</i>	Apple digestate	-	BMP	Mesophilic	-	-	-	0.410				(Frigon et al., 2013)
<i>Thalassiosira weissflogii</i>	Apple digestate	-	BMP	Mesophilic	-	-	-	0.265				(Frigon et al., 2013)

<i>Chlorella</i>	High nitrogen adapted	Lipid extraction	CSTR	Mesophilic	5	15	4	0.302		8.53	-	(Ehimen et al., 2011)
<i>Chlorella vulgaris</i>	Sewage sludge	-	CSTR	Mesophilic	6 COD ^{ug}	28	1	0.240			-	(Ras et al., 2011a)

Chapter 2

<i>Nannochloropsis salina</i>	Sludge treating maize and cattle dung	Thermal pretreatment	CSTR	Mesophilic	2	120	22	0.13	0.27	12.2	-	(Schwede et al., 2013)
<i>Nannochloropsis salina</i>	Waste water effluent	Co digested with lipids	CSTR	Mesophilic	2-6	13-40	1	0.13	0.54		Digester failure at OLR >2g VS L ⁻¹	(Park and Li, 2012)
<i>Scenedesmus spp</i>	Digestate treating algae	-	CSTR	Mesophilic	2-3.5	20-30	1.5	0.139	-	-	-	(Tran et al., 2014)
<i>Scenedesmus spp.</i> and <i>Chlorella spp</i>	-	Co digestion with waste paper	CSTR	Mesophilic	5	10	4	0.143	0.321	22.6	Reduced yields at low C/N and High C/N	(Yen and Brune, 2007)
<i>Spirulina maxima</i>	-	-	CSTR	Mesophilic	20-100	5-40	1.5	0.35			High loadings ammonia inhibition occurred	(Samson and Leduyt, 1986)
<i>Spirulina maxima</i>	-	Co digested with sewage sludge	CSTR	Mesophilic	3	20	1.5	0.160	0.36	6.2	High C/N produced greatest methane yields	(Samson and LeDuy, 1983a)
<i>Chlamydomonas reinhardtii</i> and <i>Pseudokirchneriella subcapitata</i>	-	Thermal	Microbial fuel cell	Mesophilic	-	0.01-0.015	-	0.3	0.6	-		(De Schamphelaire and Verstraete, 2009)
<i>Phaeodactylum tricornutum</i>	Potato processing digestate		ANMBR	Mesophilic	1gCOD	2.6	8	0.350 COD added	-	-	-	(Zamalloa et al., 2012b)

2.4.9.2 Algal cell wall structure

Within the AD of terrestrial biomass the hydrolysis step is often rate limiting, whereby terrestrial autotrophs often require physical, chemical or biological pre-treatments due to the resistance of lignocellulose to hydrolysis (Liu et al., 2012). This has proven successful at improving the digestibility of the feedstock but adds to the cost of processing. It has been suggested that the lack of lignocellulose in microalgae would make it a suitable substrate for AD (Sialve et al., 2009, Heaven et al., 2011), however microalgal cell walls are resistant to bacterial breakdown and as such cell disruption may be beneficial required (Markou et al., 2012). Cell wall disruption may be the main driver in improving the biodegradability of the microalgal substrate. This is likely to be difficult due to the high cell wall volume to size of the organism and its complex composition (Roberts, 1974, Klemm et al., 2005, González-Fernández et al., 2012a).

Cell walls consist of several layers of highly ordered glycoproteins, pectin, cellulose and hemicellulose, with the cellulose within algae being highly polymerised and the diameter of fibres greater than in terrestrial plants (Roberts, 1974, Klemm et al., 2005, González-Fernández et al., 2012a). This polymerisation could result in difficulties in the hydrolysis of the cellulose, as well as the breakdown of the cell wall material, reducing the methane yield. Recalcitrant compounds found in pollen primarily silica, uronic acid lignine polyaromatics, heteropolysaccharides, sporopollenin and algaenan are often associated with a high resistance to biodegradation, and are particularly effective against extracellular enzymes: these are present in *Chlorella spp*, *Dunaliella spp* and *Scenedesmus spp* with the polymers resulting in AD inhibition regardless of cell wall disintegration (Leeuw et al., 2006, Syrett and Thomas, 1973, González-Fernández et al., 2012a, Gunnison and Alexander, 1975a, Gunnison and Alexander, 1975b). Mussgnug et al. (2010) noted that *Scenedesmus obliquus* and *Chlorella kessleri* have hemicellulose containing carbohydrate based-walls which make them tougher to digest: *S. obliquus* especially so as it contains sporopollenin-like biopolymer (Mussgnug et al., 2010). They report that the degree of cell degradation is crucial for the successful conversion of biomass into biogas with species that had the greatest cell disruption and disintegration producing higher biogas yields (Mussgnug et al., 2010). Gerken et al. (2013) also found that microalgae particularly *C. vulgaris* and *Nannochloropsis spp* have a recalcitrant cell wall composed of a complex matrix of polysaccharides and glycoproteins (Gerken et al., 2013).

Chapter 2

Cell walls of fresh water micro algae are typically thinner than those of their marine counterparts due to the need to osmoregulate and maintain turgor pressure at high salinities causing a thickening and increasing complexity of the cell wall (Kirst, 1990). Increasing salinity may therefore decrease the ease with which intercellular products are accessible to methanogens for fermentation and conversion to biogas. It has been reported, however, that the saline microalgal species *Nannochloropsis* and *Dunaliella* which have a highly proteinacious cell wall were relatively more easily digested than the fresh water species *Chlorella* and *Scenedesmus* with a highly carbohydrate based cell wall, suggesting that cell wall composition is potentially the main driver in digestibility, followed by the thickness of the cell wall (Ras et al., 2011b, González-Fernández et al., 2012a).

Once the cells are ruptured and hydrolysis of the organics within has occurred, acetogenic bacteria oxidise the products from the acetogenic phase into substrates that are suitable for methanogens. Once these products are formed methane production can occur. Despite the cell wall material being ruptured, however, it is often not broken down and passes through the system undigested reducing the potential methane yield. It would therefore be pertinent if species selection is possible to select microalgae that possess simple cell walls that are easily ruptured and easily digestible under anaerobic conditions.

2.4.9.3 Pre-treatments for the AD of Algae

Pre-treatment of feedstocks for AD can be undertaken to improve the digestability of the substrate. This can increase the net energy production, improve the quality of the digestate by sterilisation and/or potentially release nutrients that can be recovered downstream. Several conventional methods exist for the pre-treatment of wastewater biosolids, biological, thermal hydrolysis, mechanical and chemical (Carrère et al., 2010).

One of the simplest pre-treatments is freezing the organic material. This acts as a mechanical pre-treatment that leads to the formation of ice crystals within the cells of organic material rupturing them to release the organics inside and thus increasing the concentration of soluble organic products (Liu et al., 2008). Samson and Leduy (1983c) reported an increase of 26% of the soluble products present after freeze/thawing of the

algal biomass *Spirulina maxima*. This would initially increase the rate of hydrolysis, as feedstock is more readily available to hydrolytic bacteria, and potentially the overall SMY if the quantity of accessible feedstock is increased.

There are presently few studies on the pre-treatment of microalgae for subsequent anaerobic digestion. Chen and Oswald (1998) investigated the effects of thermochemical pre-treatment on the fermentation of an algal biomass from a high rate sewage stabilisation pond harvested by settling and centrifugation. The algal biomass was pre-treated at a temperature range of 60-100°C and with a NaOH chemical treatment of 0-200g kg⁻¹. The results showed that a pre-treatment of 100°C with no NaOH for eight hours at a solids concentration of 3.7% increased the SMP by 33% compared to the control under mesophilic conditions (35°C). They reported inhibition of methanogenesis due to the NaOH present. Similarly Schwede et al. (2013) reported an increase in gas production from 0.2 to 0.57 m³ biogas kg VS⁻¹ under batch conditions and from 0.13 to 0.27 m³ biogas kg VS⁻¹ in semi-continuous digestion of *Nannochloropsis salina* harvested by centrifugation and undergoing thermal pre-treatment at 120°C with pressure compensation. The reported reduction in yield for continuous operation is attributed to an increase in VFA concentration caused by elevated ammonia and salt concentrations within the feedstock highlighting the importance of adapting the inoculum (Schwede et al., 2013). González-Fernández et al. (2012b) found that pre-treatment at 80°C of a laboratory-grown culture of *Scenedesmus* harvested by gravitational settling improved gas production by 60% compared to the control. They also investigated the effect of sonication which caused an increase in SMP of 90% at an energy of 130 MJ kg⁻¹, which could be jointly due to sonication and an increase in temperature to 85°C during the process. In both cases pre-treatments reduced the size of the particulate organic matter (POM) and increased the soluble organic matter present. Alzate et al. (2012) found similar increases in SMP of up to 62% from thermal pre-treatment of mixed algal species harvested by centrifugation at a temperature of 170°C. At 110°C they observed a 20% increase, similar to that found by Chen and Oswald (1998), with the difference possibly due to the use of mixed algal species and of harvesting methods potentially capable of rupturing the cell wall. At lower sonication energies of 10 MJ kg⁻¹ Alzate et al. (2012) observed an increase in SMP of 6-24%, which is substantially better than the decrease of 10% observed by

Chapter 2

González-Fernández et al. (2012b) at 35 MJ kg⁻¹ compared to that of the untreated control.

Passos et al. (2013) used a microwave pre-treatment on microalgae harvested from a high rate algal pond by gravitational settling. Under mesophilic batch conditions they found a 78% increase in the final SMP of the algal biomass after 45 days, with an initial increase of 75% compared to the control at a applied specific energy of 65400 kJ kg⁻¹ TS. Despite the increase in SMP the authors suggested that because of the high energy utilisation in microwave pre-treatment alternative lower energy pre-treatment methods should be investigated.

It is clear that thermal pre-treatment can produce similar improvements in digestibility for different algal feedstocks grown on different culture media and harvested by different techniques, while the improvements due to other techniques can vary considerably. All microalgal species examined showed substantial improvements in the rate of biodegradability and in final methane yields, supporting the value of a pre-treatment step; the different cell compositions and structures of the different species analysed mean, however, that it is necessary to investigate each algal feedstock individually to determine a suitable pre-treatment protocol. Energy balances must also be calculated to ensure there is a net gain in energy recovered, as several authors have reported improved methane yields using various pre-treatments, but either at a net energy loss or no significant gain (Lee et al., 2013, Lü et al., 2013, Yen and Brune, 2007, Lee et al., 2012).

Currently research has focussed on the mesophilic digestion of microalgae under both batch and continuous studies (Table 7), primarily due to the inherent stability of the methanogenic consortium, the sensitivity of thermophiles to high ammonia concentrations that could occur under continuous algal digestion, and the increased operational costs of running digesters at higher temperatures. Due to the limited current research of continuous studies of algal digestion coupled with the majority of existing research into batch analysis under mesophilic conditions, this report will focus on the mesophilic digestion of marine substrates.

2.4.10 Conclusions from the literature review

The use of algae for biofuel production requires further research into reducing the energy inputs and start-up costs involved with the growth and harvesting of the biomass. The use of freshwater is not feasible in regions with high irradiance due to the need for agriculture and consumption, however the use of salt water aquifers that cannot be used for irrigation or drinking could be considered.

Currently the use of algae as a biofuel is not economically viable, with the relatively low cost of fossil fuel and reliance on intermittent government subsidies. Microalgal biomass does have a potential role, however, in the development of biofuels, with potentially a combined approach utilising the entire algal cell from high value products for the nutraceutical/ pharmaceutical industries to reduce costs. Research has focussed on the extraction of lipids for biodiesel production with little success. Anaerobic digestion of the whole organism, however, offers a promising alternative to the extraction of oil or sugars, allowing the whole organism to be converted to biogas.

Anaerobic digestion of microalgae is still, however, in its infancy. The current knowledge of marine micro algae as a feedstock for AD is limited, with research to date focussing on batch analysis rather than continuous digestion experiments leaving the feasibility of marine microalgae as a feedstock open to speculation. It is clear that reported BMP values often give currently unfeasible upper estimates of the SMP of microalgae.

Saline substrates can have an inhibitory effect upon the methanogenic consortium with the anaerobic digestion process. The addition of chloride salts to non-acclimatised inoculum can cause instability, with the consumption of sulphate causing a reduction in methane yield due to initially competition for fermentative products and inhibition by the sulphide produced. A wide range of values have been reported to be stimulating, inhibitory or toxic for both chloride and sulphate salts, with no general agreement between them. It has been often suggested that adaption to high salinities must occur prior to digestion of saline feedstocks, but to date no protocol has been developed to address this.

Within this literature review several factors that could inhibit the anaerobic digestion process when digesting marine algae or saline substrates have been identified that as of

Chapter 2

yet have not been investigated fully. This is primarily due to the prevalence of BMP assays that typically eliminate inhibitory effects, and very few studies into continuous digestion. The specific research needs identified within the literature review that will be addressed in the following chapters are:

- The effects of increasing chloride salt concentrations on non-acclimatised readily available biosolids that could be easily sourced for potential future pilot scale experiments. There is currently limited and varied data for the inhibition of the methanogenic consortium to chloride salts, this report attempts to address this issue.
- The adaption of the methanogenic consortium to increasing chloride salts to overcome the inhibitory effects of the salt. Currently little data is available for successful regimes to adapt a non-acclimatised methanogenic consortium to chloride salts at marine concentrations. This report aimed to successfully adapt a readily available inoculum source for the subsequent AD of marine feedstocks.
- Determine tolerances for sulphate at and above marine concentrations under anaerobic conditions on the methanogenic consortium and its effects on methane yield as a precursor to digesting marine algae. This aimed to determine the ability for the methanogenic consortium to adapt to the hydrogen sulphide produced.
- Compare the digestibility of different marine species cultivated and harvested under identical circumstances using batch analysis, with selected strains continuously digested under marine concentrations of chloride and sulphate salts. This will be used to highlight the differences between batch and continuous analysis.

This research therefore aimed to investigate the salt tolerances of methanogens from municipal biosolids digestion and their gradual adaption to higher salinities within a CSTR under mesophilic conditions in order to successfully digest marine feedstocks.

CHAPTER 3

3. Methodology

This section contains the methods used on multiple occasions during the current research. Specific experimental designs and methods are described before each results section when required.

3.1 General

Laboratory practice. All analysis and general practice within the laboratory was undertaken using good laboratory practice, with the appropriate risk assessments and when necessary COSHH assessments carried out prior to working. All equipment within the laboratory was used in accordance with the manufacturer's guidelines and was regularly inspected and maintained by laboratory technicians.

All reagents unless otherwise stated were prepared from laboratory grade chemicals obtained from Fisher Scientific (Loughborough, UK)

All solutions were prepared using ultra pure deionised (DI) water obtained by filtering through a Barnstead Nanopure ultrapure water purification system with a conductivity of 18 M Ω – cm resistivity (Thermo Scientific, UK).

Algal laboratory cultures were prepared using DI. Larger outdoor cultures and synthetic sewage were prepared with tap water.

3.2 Culture media and feedstocks

As a basic growth medium Jaworski's Medium (JM) was used throughout, with the exception of samples cultivated at Almeria, which were cultivated on commercial fertilisers. Fresh water and salt water media was prepared using Milli-Q ultra-pure water as specified by the Culture Collection of Algae and Protozoa Scotland and by ASTM (1992). Each medium was prepared as a stock solution at 1000x concentration, filtered

with 0.2µm Whatmann glass fibre filters and stored within a glass container at 4°C until use, with new solutions made every four weeks. Artificial seawater was produced by dissolving 18 g of salts (Ultramarine Synthetic Sea Salts, USSS, Waterlife research Industries LTs, UK, Bristol) for brackish conditions and 33.6 g of USSS salts for marine conditions into 1 L of Milli-Q water for laboratory experiments as directed by CCAP. The culture medium was then prepared by adding Milli-Q water/ saline water to the required volume of stock solution and autoclaving at 120°C for 15 minutes in a container, with a porous foam bung capped with aluminium foil.

3.2.1 Jaworski's Medium (JM)

Jaworski's Medium was selected for study as this medium was previously successfully used for the growth and maintenance of several freshwater species by Whalley (2008) within the research group. The medium also contained all the main micronutrients, trace metals and vitamins outlined in the literature review for successful cultivation of microalgae. Each constituent was kept in a fridge at 2-4°C in separate glass containers labeled as Stock 1-9, as shown in Table 8.

Table 8 – Jaworski's medium (JM).

Stock	Chemical Component	Concentration (mg L ⁻¹)
1	Ca(NO ₃) ₂ ·4H ₂ O	20.00
2	KH ₂ PO ₄	12.40
3	MgSO ₄ ·7H ₂ O	50.00
4	NaHCO ₃	15.90
5	EDTA FeNa	2.25
	EDTANa ₂	2.25
6	H ₃ BO ₃	2.48
	MnCl ₂ ·4H ₂ O	1.39
	(NH ₄) ₆ Mo ₇ O ₂₄ ·4H ₂ O	1.00
7	Cyanocobalamin	0.04
	Thiamine HCl	0.04
	Biotin	0.04
8	NaNO ₃	80.00
9	Na ₂ HPO ₄ ·12H ₂ O	36.00

3.2.2 Almeria Culture medium

This culture medium was formulated from industrial fertilizers used for the strains of *Chlorella* and *Scenedesmus* kindly grown at the Las Palmerillas agricultural research facility of Fundacion Cajamar in El Ejido, Almeria, Spain by Jose Louis Mendoza Martin in a pilot-scale raceway pond and photobioreactor.

Table 9 – Composition of culture medium used in raceway ponds in Almeria Spain (information provided by Jose Louis Mendoza Martin).

Stock	Concentration		
	(mmol ⁻¹)	Molar mass	g ⁻¹
NO ₃	9.02	62	0.559
NH ₄	0.82	18	0.015
H ₂ PO ₄	2	97	0.194
K	2.6	39	0.101
Ca	6.15	40	0.246
Mg	3.5	24	0.084
SO ₄	1.45	96	0.139
HCO ₃	2.8	61	0.170
Na	5.2	23	0.120
Cl	11.1	35.5	0.394
Fe	2.66	56	0.149
Mn	1.12	55	0.0616
Zn	0.75	65	0.0488
B	0.63	11	0.007
Cu	0.1	63.5	0.006

3.2.3 Low Sulphate medium

A low sulphate medium was used to investigate the effects of reducing the sulphate concentration on the growth of microalgae. The low sulphate media consisted of all the constituents of JM with varying sulphate concentrations of 100%, 20% 10% and 1% of the original component shown in Table 10. The equivalent magnesium was added as MgCl to the reduced sulphate maintaining the Mg concentration.

Table 10 – Sulphate concentration of low sulphur growth culture media experiments for marine algae.

% sulphate of JM recipe	Sulphate Concentration (mg L ⁻¹)
1	0.195
10	1.95
20	3.9
100	19.5

Feedstock's used for continuous anaerobic digestion studies

Several feedstocks were used throughout this research consisting of a synthetic sewage medium, artificial salt solutions and microalgae.

It was decided that a synthetic sewage/ wastewater should be used for the adaption of an inoculum to high chloride and sulphate salts. This decision was made based on the fact that the strength and composition of wastewater can vary depending on a number of factors such as, water availability, climatic conditions, economic status and social customs. The artificial wastewater used within this report is a substrate widely used within the research group, and for this reason its behaviour is well understood, its methane potential well known and as such is very applicable for novel, lab scale experimentation when control of variables is critical (Ali, 2014, Whalley et al., Pacheco-Ruiz et al., 2015)

The artificial Synthetic wastewater used within this research was designed to simulate the properties of real sewage (Whalley et al.). Table 11 and Table 12 show the

Chapter 3

constituent parts of the Synthetic wastewater. It was decided to use the synthetic waste water at full strength as this has greater volatile solids content, similar to that of municipal biosolids digestate. When made up to full strength it has a chemical oxygen demand of 54g L^{-1} and volatile solids concentration of 33g VS L^{-1} .

Table 11 – Synthetic wastewater composition as described by Whalley et al. (2013) and Ali (2014).

Component	Units	Quantity
Trace element solution (Table 2)	ml	1
Yeast (block bakers form)	g	23
Urea	g	2.14
Full cream milk (UHT sterilised)	ml	144
Sugar (granulated white)	g	11.5
Blood (freeze dried)	g	5.75
Ammonia phosphate	g	3.4
Tap water		to make up to 1 litre

Table 12 – Trace element solution

Component	Quantity	
HCl	5.1	ml
FeCl ₂ .4H ₂ O	1.5	g
H ₃ BO ₃	60	mg
MnCl ₂ .6H ₂ O	100	mg
CoCl ₂ .6H ₂ O	120	mg
ZnCl ₂	70	mg
NiCl ₂ .6H ₂ O	25	mg
CuCl ₂ .2H ₂ O	15	mg
Na ₂ MoO ₄ .2H ₂ O	25	mg
		to make up to 1 litre
DI water		litre

The bulk chemical artificial sea salt recommended by CCAP (Ultramarine Synthetic Sea Salt) contained all the marine salts at an average seawater composition. As this bulk chemical also contained sulphate an alternative artificial salt water media was formulated in order to determine the effects of sulphate on both the microalgae and its

subsequent effect on anaerobic digestion. From here on in artificial salt will refer to the salt medium formulated from laboratory chemicals (Fisher Scientific, Sigma Aldrich) NaCl, MgSO₄.7H₂O, MgCl₂.6H₂O, CaCl₂ and KCl. This artificial salt solution was formulated to represent mean ocean concentrations of the main ions. The salt solution was made to ten times the concentration with Cl, Na, Mg, Ca and K at molar ratios of 1:0.87:0.03:0.03:0.02, similar to mean ocean values Table 13 to enable marine levels of salt to be reached without a high dilution. The concentration of magnesium was maintained in each by reducing magnesium chloride concentrations with increasing magnesium sulphate concentrations, with the concentrations of SO₄ shown in Table 10.

Table 13 – artificial seawater consisting of the 6 main ions found in seawater, used within the sulphate growth experiments and continuous cultivation of marine microalgae for continuous digestion (Brown et al., 2005).

Element	g L ⁻¹	Moles	Mass of compound	
			(g)	
Cl	19.5	0.6		
Na	10.8	0.5	27.4	NaCl
Mg	1.3	0.1	3.2	MgCl ₂ .6H ₂ O
Ca	0.4	0.0	1.51	CaCl ₂ .2H ₂ O
K	0.4	0.0	0.7	KCl

Table 14 – Sulphate concentrations and additions.

Flask number	mg SO ₄ L ⁻¹
F1	0
F2	160
F3	790
F4	1580
F5	2360
F6	3150
F7	3940
F8	4730

3.3 Culturing algae

Agar plates and tubes were prepared by adding 15 g of agar to 1 L of prepared culture media, decanting the liquid into agar plates/ tubes whilst warm and leaving to cool under aseptic conditions. All inoculation steps were undertaken using clean microbiological practice in an aseptic environment to minimise contamination. Agar plates were used to maintain cultures in case of culture death. Various culture media used are listed below. Jaworski's Media was used throughout the experiment as this gave adequate results in growth cultures compared to the other media analysed. Silicate was added for the marine species *T. pseudonana*.

250 ml Erlenmeyer flasks were used as starter cultures (Figure 29) with 100 ml of culture media added and autoclaved as described above. Algae were initially transferred to each flask using a 1 ml pipette under aseptic conditions from the starter cultures provided by CCAP and the National Oceanography Centre Southampton. These cultures were cultivated under an irradiance of $120 \mu\text{mol m}^{-2} \text{s}^{-1}$ on a shaking plate at 100 rpm to prevent settling. After two weeks the starter cultures had reached their maximum density and began to enter their lag phase; at this point they were decanted into a 2 L Erlenmeyer flask containing 900 ml of fresh autoclaved culture media under aseptic conditions and allowed to grow for one week to enter the log phase of growth.



Figure 29 Algal starter cultures growing in the laboratory.

When the starter culture had entered its log phase it was decanted into a 25 L culture vessel containing 19 L of fresh culture media for large-scale laboratory cultivation. Algae were grown in JM and artificial seawater, and adapted for silica and high carbonate organisms in 4 x 25 L pyrex glass bottles as shown in Figure 30. These containers were continuously illuminated by nine 30W 3500k fluorescent tubes at $80 \mu \text{mol m}^{-2} \text{s}^{-1}$ and mixed by aeration at 10L min^{-1} from a stainless steel sparger located at the bottom of the container. The air used was initially filtered through a $0.2 \mu \text{m}$ glass fibre filter. To increase the air's humidity, air was passed through MQ ultra-pure water which was changed daily before being filtered again and entering the culture vessel (Figure 31). This was to prevent and reduce the rate of evaporative loss. A u-bend exit was provided in the exhaust to prevent external contamination if the pump failed. The cultures were allowed to grow for two weeks to enter their lag phase before being harvested.



Figure 30 – 25 L culturing vessels.

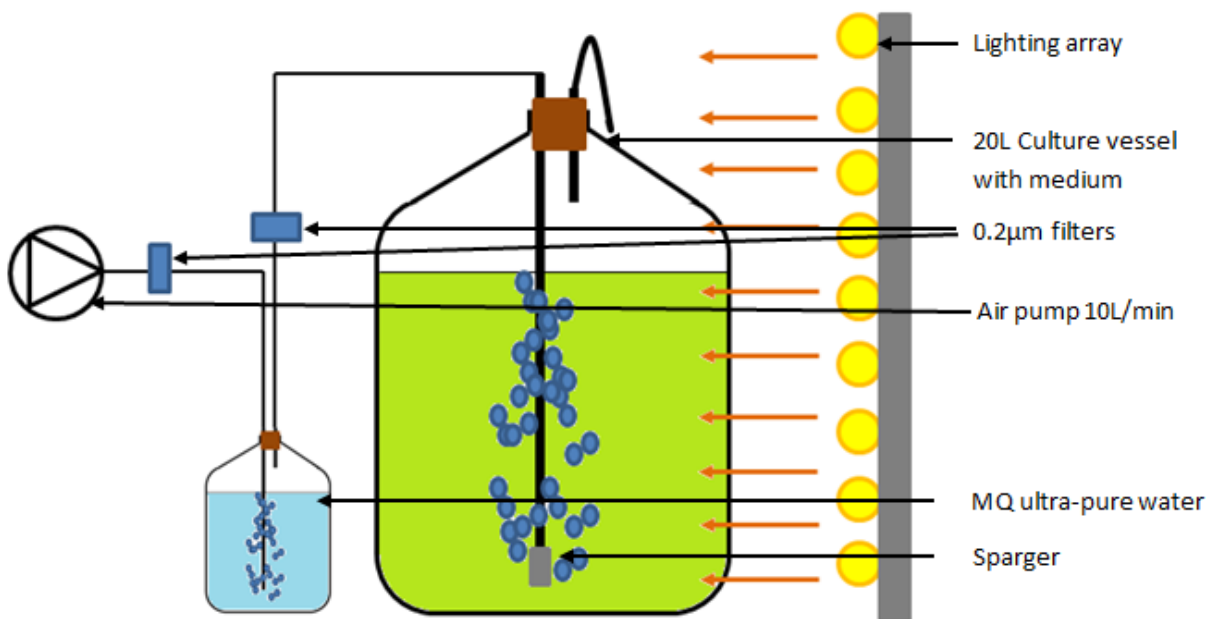


Figure 31 – Schematic of bubble column used to grow algae for BMP examination.

3.3.1 Photobioreactor Design

Larger-scale culturing of marine microalgae was undertaken within a serpentine tubular photobioreactor as shown in Figure 32. Each Perspex tube has an internal diameter of 100 mm creating an overall volume of ~300 L including the header tank (

Table 15). The flow is driven by an airlift located at the base of the photobioreactor with a riser of 2.5 m (variable to adjust head height) with a sparger and compressor supplying 80 L min⁻¹ of filtered air. The flow rate of water was determined to be sufficient to prevent settling, but not too turbulent as to harm the algae shown in Table 16 and Table 17. Neutrally buoyant and denser beads are included in the culture medium to help prevent the sedimentation and accumulation/ fouling of algae on the clear tubes by scouring the surface of the tubes.

The photobioreactor was located in Southampton, UK at 50°54'N 1°23'W and was constructed within a south-facing greenhouse to provide natural illumination. The reactor is also artificially illuminated with 480W of 3500K cool white fluorescent tubes on each culture tube providing 694 W m⁻². Temperature within the culture media was regulated with a thermoregulator connected to the riser and the internal fluorescent lighting maintained a minimum temperature within the culture media of 25°C (±1°C).

The culture medium was prepared using tap water within a 210 L stainless steel drum. To fill the reactor valves at the base of the reactor on both sides were opened and the culture medium was pumped into the PBR via a rotary vane pump at a flow rate of 40 L min⁻¹. The reactor was emptied by opening the valves and pumping into a 300 L storage container ready for centrifugation/disposal. Starter cultures were grown in four 20l containers as described above and at the end of log phase were used as an inoculum pumped into the top of the reactor.

Under continuous operation 210 L of culture media was prepared every three days and gradually pumped into the return down flow from the header tank via a peristaltic pump at a flow rate of 70 L day⁻¹, with the excess culture medium exiting via an overflow channel in the header tank to a 300l collection drum. Daily centrifugation occurred as described below.

Between runs the reactor was emptied and filled with tap water and cleaned with Biochlor effervescent chlorine tablets (Fisher Scientific, UK) at a maximum

Chapter 3

concentration of 1 tablet per 10 L of water. The reactor was mixed for 30 minutes then the air compressor was turned off to prevent degassing of the chlorine, and the reactor left for 24 hours. After 24 hours beads were added to the reactor and the air lift turned back on for 24 hours to scour off any biofouling that had occurred and to degas the residual chlorine. The reactor was then emptied and any tubes with persistent biofouling were removed and cleaned manually. The reactor was reassembled and rinsed with tap water to remove any excess chlorine immediately before re-inoculation.

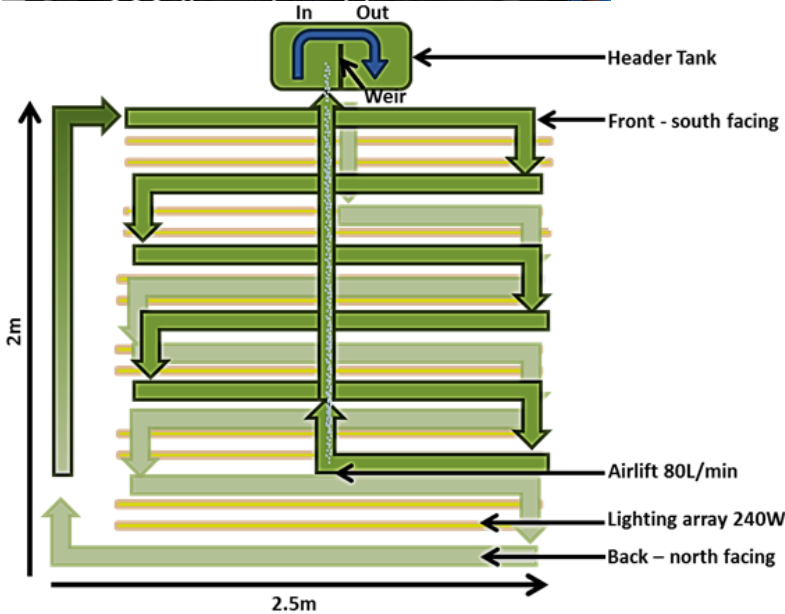


Figure 32 – Above, photo of constructed photobioreactor, and below schematic of the serpentine tubular photobioreactor used for the continuous growth of marine microalgae.

Table 15 – Overall hydraulic design of the photobioreactor. The total volume has been estimated with a header tank volume of approximately 20L.

Hydraulic Design - Photobioreactor			
Tube OD	110	mm	
Tube ID	100	mm	
X-sectional Area	0.008	m ²	
Horizontal Length	1.8	m	
no. of lengths	12		
Total horizontal length	21.6	m	
Vertical gap	0.4	m	
Total pipe length	28.51	m	
Solar receiver surface area	6.8	m ²	
Solar receiver Volume	0.223	m ³	
Total volume or reactor	0.319	m ³	

Table 16 Determination of flow type using the Reynolds Equation. Turbulent flow should help prevent sedimentation and increase mixing enabling movement between light and dark areas.

Medium properties			
Dynamic			
viscosity	0.001	kg m ⁻¹ s ⁻¹	vary with algae type
medium density	1000	kg m ⁻³	vary with algae type
gravitational constant	9.806	m s ⁻²	Assumed algae medium to be fully mixed with water
Velocity	0.3	m s ⁻¹	
Flow rate	0.14	m ³ min ⁻¹	
	141.4	L min ⁻¹	
Reynold's			
number, Re	29940		
Flow type:	TURBULENT		

Table 17 – Determination of the size of micro-eddies using equations from Fernández et al. (2001).

Dimension	of		
algal cell	0.00005	m	
Velocity	0.3	m s^{-1}	
tube diameter	0.1	m	
μL	0.001	kg m^{-2}	
ρ	1000	kg m^{-3}	
Re	29940.12		
Cf	0.006		Fanning's coefficient
ξ	0.0032	$\text{m}^2 \text{s}^{-3}$	Energy dissipation per unit mass scale of micro eddies (different to friction factor)
λ	0.0001	m	
VELOCITY			
OK			

3.3.2 Growth rate

3.3.2.1 Optical density

Optical density (OD_{680}) of algal cultures was measured in cylindrical glass cuvettes with a 1 cm light path using a Cecil (1000 series) Scanning Spectrophotometer at a λ of 680 nm which detects the chlorophyll *a* pigment.

3.3.2.2 Growth rate determination

The growth rate for each of the laboratory-grown micro-algal species was determined in 250 ml working volume Erlenmeyer flasks (Figure 33). Each flask had an optical glass side-arm tube of 10 mm path length, allowing direct readings of the culture optical density (OD) at $\lambda = 678$ nm to be taken using a spectrophotometer (Cecil 3000 series, Cecil Instruments, UK) without opening the flasks. 50 ml of culture medium was prepared in each flask with 1 ml of algal culture in the log phase of growth with data recorded twice daily for 10 days.



Figure 33 Algal cultures in side arm flasks for growth rate determination

Continuous growth experiments used a side arm flask for the in situ analyses of OD₆₈₀ to prevent contamination and depletion of the algal culture.

Equations 3.1 and 3.2 were used to determine the growth rates of all the micro algal species examined (Richmond, 2004). Values were determined during the exponential phase of growth, which was identified by taking the log₂ + 10 of the optical density.

Proportional rate of change (growth rate μ (day⁻¹))

$$\mu = \frac{\ln\left(\frac{N_t}{N_0}\right)}{\Delta t} \quad \text{Equation 3.1}$$

Doublings per day

$$k = \frac{\mu}{\ln(2)} \quad \text{Equation 3.2}$$

where N_t and N_0 are the TSS concentrations based on OD at the start and end of the exponential growth phase, and Δt is the time elapsed.

Growth yield in g volatile solids (VS) L⁻¹ day⁻¹ was calculated from the TSS content at the start and end of the exponential growth phase, divided by the number of days elapsed and the ratio of measured VS/total solids (TS).

Using the growth rate results from the batch analysis, an estimated maximum growth yield was theorised for the potential operation of a continuous growth system run at a

Chapter 3

volatile solids concentration of algae at 0.5 g VS L^{-1} . This value was divided by the inverse of the doubling rate to determine a maximum dilution rate of fresh media per unit volume of growth system, to determine a theoretical harvested biomass per unit volume of reactor as $\text{g VS L}^{-1} \text{ d}^{-1}$. This value can then be used to determine the effects of maximum growth rate and biochemical methane production.

The Monod equation and model shown in Figure 34 was used to determine the effect of a limiting nutrient or abiotic factor such as sulphate and temperature on the specific growth rate (Monod, 1949).

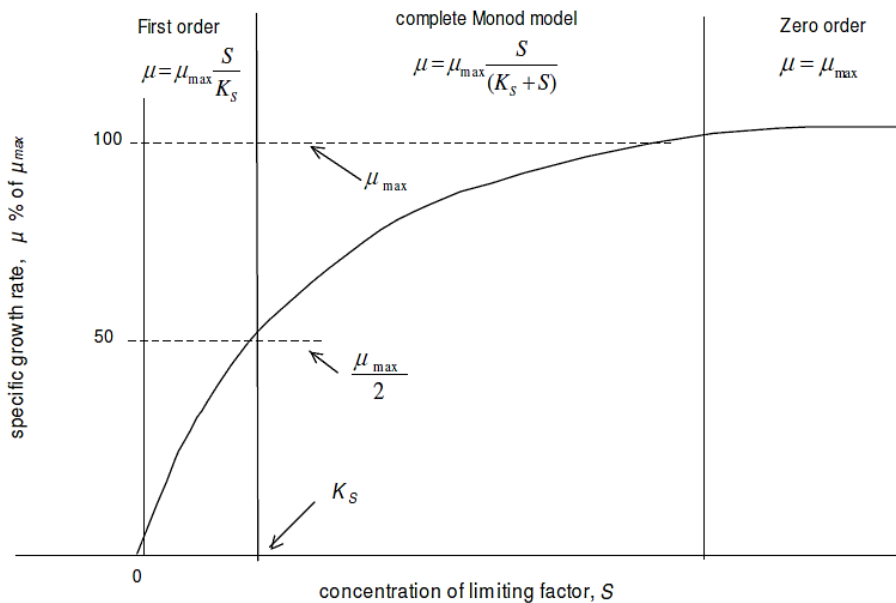


Figure 34 – Relationship between the growth limiting factor (s) and the specific growth rate as a % of the maximum growth rate under ideal conditions for the Monod equation model (Monod, 1949).

3.3.3 Algae examined

Algae were obtained from the Culture Collection of Algae and Protozoa (CCAP) and the National Oceanography Centre Southampton.

Species = *Chlorella vulgaris*

Nannochloropsis oculata

*Isochrysis galbana*⁸

*Dunaliella salina*⁸

*Thalassiosira pseudonana*⁸

*Scenedesmus spp*⁹

3.3.4 Large-scale algal harvesting

For the algal biomass characterisation experiments and the continuous growth of *Isochrysis* within the PBR harvesting was conducted with a continuous centrifuge thermoregulated to 20°C (Powerfuge pilot (CARR) USA) (Figure 35) at a rate of 1L min⁻¹ at 14000RPM or 17000 G. The algal paste was collected from the centrifuge, homogenised by stirring and frozen at -17°C until use. For the *Dunaliella* species grown under continuous conditions in the 300 L PBR an air cooled disk stack centrifuge Ukrainian milk separator creamer (Figure 36) was used at a flow rate of 1 l min⁻¹ (Heasman et al., 2001).



Figure 35 – Powerfuge pilot centrifuge setup to centrifuge lab grown microalgae.

⁸ Species kindly provided by Dr John Gittins NOC Southampton.

⁹ Kindly provided by Lisha Gan and Jose Louis Mendoza of the Faculty of engineering and the Environment, Southampton, UK.



Figure 36 – Ukrainian milk creamer.

3.3.4.1 Race-way grown algae

Scenedesmus sp. was grown in large scale algal raceway ponds by Jose Louis Mendoza Martin as outlined in Mendoza et al. (2013). All algae were centrifuged and either frozen and freeze dried or frozen before transportation to Southampton UK.

3.4 Basic analysis

3.4.1 pH

Innoculum and digestate pH was measured immediately after sampling to minimise pH fluctuations due to outgassing of dissolved CO₂ from the liquid. The pH was measured using a Mettler Toledo FE20/EL20 pH metre with a glass electrode. The probe was calibrated using pH 7.0 and 9.2 buffers prepared from Fisher Scientific buffer tablets.

3.4.2 Alkalinity

Digestate alkalinity was determined by titration with sulphuric acid. 5-10g of sample was made up to 40 ml with deionised water and titrated against 0.25 N H₂SO₄ to a pH of 9.0

4.0 to determine total alkalinity. During titration the substrate was continuously stirred with a magnetic stirrer. To determine partial alkalinity (PA) and intermediate alkalinity the titration was recorded at a pH of 5.7 and 4.3.

Alkalinity was determined using an amended Standard Method 2320B (APHA, 2005, Ripley et al., 1986).

Alkalinity in mg CaCO₃ L⁻¹ was calculated using the following equation:

$$ALK = \frac{A \times N \times 50000}{V_s} \quad \text{Equation 2.13}$$

Where A is the amount of acid used to titrate the sample, in mL;

N is the normality of titrant;

50,000 is the conversion factor of L to mL and 50 mg CaCO₃ to 1 milliequivalent alkalinity;

V_s is the volume of the sample, in mL.

3.4.3 Volatile fatty acids (VFA)

Volatile fatty acids were analysed by a gas chromatograph (GC). Samples were prepared by freezing at -20°C in 2 ml centrifuge tubes. Before analysis the samples are removed from the freezer and placed within a fridge at 4°C to defrost for 12 hours. After the samples have thawed out they are centrifuged at 17900g (VWR micro 2416 USA) for 10-20 minutes depending on TS content and 0.9 ml of supernatant added to a separate 2 ml centrifuge tube with 0.1ml of concentrated formic acid. This solution is centrifuged again for 10 minutes. The subsequent supernatant is then analysed using a Shimadzu GC-2010 gas chromatograph, using a flame ionisation detector with a FFAP capillary column with a 0.25 mm internal diameter, 0.25µm thickness and 30 m length. Hydrogen gas was used as the carrier gas, produced using a hydrogen generator. The residence time of the sample was 28 minutes. Standards containing 50, 250 and 500 mg L⁻¹ of mixed acetic, propionic, iso-butyric, n-butyric, iso-valeric, valeric, hexanoic and heptanoic acids were used for calibration.

3.4.4 Total Kjeldahl Nitrogen (TKN) and total ammonia nitrogen (TAN)

TKN determines the total organic and ammonia nitrogen within the sample. Between 0.5-1.5g of sample is added to a glass digestion tube with 12 ml concentrated H₂SO₄ and one Kjeltab Cu 3.5 catalyst tablet. The glass digestion tube is placed into a heating block and connected to an exhaust system within a fume cupboard. The substrate undergoes acid digestion at 420°C±10°C for at least two hours or until all tubes show a clear blue colour. After cooling, 50 ml of distilled water is added before the distillation step.

For distillation a Tecator Kjeltac System 1002 distillation unit was used. 10 M NaOH is added to each solution to raise the pH above 9.5, facilitating the volatilisation of ammonia. Each sample is distilled using high temperature distilled water for four minutes and the distillate collected in a 250 ml Erlenmeyer flask containing 25 ml boric acid solution.

The distillate is then titrated with H₂SO₄ (0.25 N), until a colour change from green to pink is obtained. The titre value and mass of sample are then used in the following equation to determine TKN:

$$NH_4N, mgL^{-1} = \frac{(A-B) \times 14.0 \times 0.25 \times 100}{V_{sample}} \quad \text{Equation 2.14}$$

Where *A* is the volume of 0.25 N H₂SO₄ used to titrate the sample, in ml;

B is the volume of 0.25 N H₂SO₄ used to titrate the blank, in ml;

V_{sample} is the volume of the original sample, in ml.

TAN is determined by adding 0.5-1.5 g of substrate into a glass digestion tube, adding 50 ml of deionized water and following the above steps from the distillation process.

3.4.5 Total solids and volatile solids

TS and VS determination was based on Standard Method 2540 G (APHA, 2005). After thorough agitation, approximately 10 g of sample was transferred into a weighed crucible. Samples were weighed to the range of 10 ± 0.0001 g (Sartorius BP210S

balance, Sartorius AG, Gottingen Germany) and placed in an oven (LTE Scientific Ltd., Oldham UK) for drying overnight at $105^{\circ}\text{C} \pm 1^{\circ}\text{C}$. After drying the samples were transferred to a desiccator to cool for at least 40 minutes. Samples were then weighed again with the same balance, transferred to a muffle furnace (Carbolite 201, Carbolite, UK) and heated to $550 \pm 10^{\circ}\text{C}$ for two hours. After this ashing step, samples were again cooled in a desiccator for at least one hour before weighing a third time.

After all analyses, crucibles were washed with detergent, rinsed with DI water, and dried in an oven at least an hour and then transferred from the oven to a desiccator for cooling to room temperature and stored there for the next analysis. Total and volatile solids were calculated according to the following formulae:

$$\%TS = \frac{W_3 - W_1}{W_2 - W_1} \times 100 \quad \text{Equation 2.4}$$

$$\%VS \text{ of TS} = \frac{W_3 - W_4}{W_3 - W_1} \times 100 \quad \text{Equation 2.5}$$

Where

W_1 is the weight of the empty crucible, g;

W_2 is the weight of the crucible containing the fresh sample, g;

W_3 is the weight of the crucible and sample after drying at 105°C , g;

W_4 is the weight of the crucible and sample after heating to 550°C , g;

3.4.6 Total Suspended Solids

Total suspended solids (TSS) were analysed using the method 2540 G in Standard Methods for the Examination of Water and Wastewater (APHA, 2005). 47 mm 0.2 μm pore size Whatman glass fibre filters were dried at $103\text{-}105^{\circ}\text{C}$ to remove all moisture and pre weighed before filtering. A known volume of sample was filtered through the dried glass fibre filter using a vacuum pump and the filters were placed in an oven at $103\text{-}105^{\circ}\text{C}$ before weighing. The initial weight of the filter is then subtracted from the final weight to give the total weight of the suspended solids. The calculation is as follows:

mg total suspended solids/ ml = ((weight of filter before- weight of filter after in mg) x 1000)/ sample volume ml

3.4.7 VS destruction

VS destruction was calculated by comparing the %VS of the influent and the %VS of the effluent as described in the following equation:

$$VS\ destruction = \frac{VS\ sbp\ in\ X\ MASS\ sbp\ in - VS\ digestate\ out\ X\ (Mass\ sbp\ out)}{VS\ sbp\ in\ X\ MASS\ sbp\ in} \times 100 \quad \text{Equation}$$

3.3

Where,

VS SBP in is SBP added to the digester (g VS kg⁻¹ WW)

VS SBP out is digestate removed from digester (g VS kg⁻¹ WW)

VS Biogas out is biogas removed from digester (g VS kg⁻¹ WW)

3.4.8 Determination of solids loss

Solids losses from the high salt reactors were determined using the difference between the control reactors TS and the salt spiked reactors TS, against the expected TS content from the addition of salt.

Under the assumption that all the chloride salts added were conservative and could only be removed via the digestate from the reactor, the difference between the cumulative excess TS within the salt spiked reactors and that of the controls was subtracted from the cumulative added salt content. This difference determined the losses in salt content from the reactor via precipitation.

3.4.9 Cell number

Cell numbers were calculated using the cell counting method outlined in Standard Methods for the Examination of Water and Wastewater (APHA, 2005) and Algal Culturing Techniques (Anderson, 2005, Spicer, 1988). A homogeneous sample of the culture is placed onto a haemocytometer and the cells counted in 80 squares using a

light microscope at 40x magnification in phase 2 and the average amount of cells was estimated using the following equations:

$$1 \text{ mm}^3 = \text{total cells counted} \times 4000/80 \quad \text{Equation 3.5}$$

$$1 \text{ ml} = (\text{total cells counted} \times 4000/80) \times 1000 \quad \text{Equation 3.6}$$

3.4.10 Light metal cations by Flame Absorption Spectrometry

Light metal cations were measured using a Flame Atomic Absorption Spectrometer (Perkin Elmer) operated according to manufacturer's instructions using a hollow cathode lamp. The conditions used are shown in Table 18, including interference suppressors and check standard concentrations. Calibration solutions were prepared from a stock solution of K, Mg, Na and Ca (Fisher Scientific Standard solution, 1000 mg l⁻¹ in nitric acid (HNO₃) for atomic spectroscopy) by dilution to the required concentration range using 12.5% HNO₃. Samples were diluted to below 1000 mg L⁻¹ of each cation with 0.1g L⁻¹ of KCl and LaCl and 10 ml L⁻¹ of HNO₃ added. Samples were then analysed for K, Na, Mg and Ca as described above.

Table 18 Parameters used to identify metal cations using the AA

Element	Wave length (nm) / Slit setting (nm)	Fuel / Support	Interference elimination
K	766.5/1.0	Acetylene /Air	Lanthanum Chloride
Na	589/0.5	Acetylene /Air	Lanthanum Chloride
Mg	285.2/0.5	Acetylene /Air	Lanthanum Chloride/ Potassium chloride
Ca	422.7/0.5	Nitrous oxide / Acetylene	Lanthanum Chloride/ Potassium chloride

3.4.11 Elemental composition

Carbon, hydrogen and nitrogen contents of samples were determined using a FlashEA 1112 Elemental Analyser (Thermo Finnigan, Italy). Air dried material was milled to obtain a homogenous sample. Sub-samples of approximately 3-4 mg were weighed into standard weight tin disks using a five decimal place analytical scale (Radwig, XA110/X, Poland). These were placed in a combustion/reduction reactor held at 900 °C then flash combusted in a gas flow temporarily enriched with oxygen resulting in a temperature greater than 1700°C and the release of N_xO_x, CO₂, H₂O and SO₂ (depending on the composition of the sample). The gas mixture was then analysed by GC with the

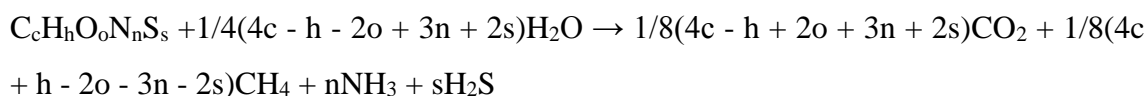
different components are measured by appropriate detectors. The working conditions of the elemental analyser were as described in the manufacturer's technical literature and method sheets. Standards used in this analysis were atropine, methionine, l-cystine, pasta, basil leaf, sulphanilamide, nicotinamide and birch leaf 10 mg of vanadium pentoxide was added to the substrate to determine total sulphur as this acts as a catalyst to release sulphur bonds. The TS and VS of dried and milled samples were also analysed to obtain accurate values. The results of the elemental composition (CHON) were also used for calculation the theoretical biogas production by (modified) Buswell equation (Buswell and Mueller, 1952) equation and the Dulong equation according to the method in Combustion file 24 (IFRF, 2013).

3.4.12 Calorific value

CV was measured using a ballistic bomb calorimeter (CAL2k, Digital Data Systems Ltd, South Africa) according to the manufacturer's instructions. Benzoic acid was used as standard, with a higher heating value (HHV) of 26.454 kJ g⁻¹. Samples of around 1 g were weighed to an accuracy of 0.1 mg and then placed in the vessel.

3.4.13 Theoretical methane potential, Buswell equation

The maximum methane potential of a substrate can be calculated using the Buswell Equation and the chemical composition of the substrate C_nH_aO_bN_dS_s. This gives an estimate for the biogas composition and an over estimate of the volume produced as it assumes 100% breakdown of the substrate. As such this gives a maximum theoretical value to which gas production for that substrate cannot exceed (Symons and Buswell, 1933).



3.4.14 Gas volume and composition

Biogas composition was measured using a Varian CP – 3800 GC (Varian, Oxford, UK) with a gas sampling loop and thermal conductivity detector with argon as a carrier gas

at a flow rate of 50 ml min⁻¹ with a run time of 1.4 minutes per sample. The GC was fitted with a Haysep C column with a molecular sieve 13 x (80-100 mesh) at an operating temperature of 50°C. A standard gas of 35% CO₂ and 65% CH₄ was used to calibrate the GC. A sample of 10 ml was taken from the gas-impermeable sampling bags used for sample collection and injected into the gas sampling loop. Air that may have entered during the feeding of reactors was excluded from the total sample volume using Equation 3.7, with the remaining gas inferred to be CO₂.

$$\text{Corrected CH}_4\% = \text{CH}_4\% / (1 - \text{Air}\%) \quad \text{Equation 3.7}$$

Gas volume during the salt acclimatisation experiment using 2-L CSTR digesters was determined using tipping-bucket gas counters with continuous data logging calibrated weekly by collecting the gas from the outlet of the gas counter in a gas-impermeable Tedlar bag (SKC Ltd, Blanford Forum, UK). The gas volume was then calculated using a water displacement weight type gasometer (Walker et al., 2009). The initial height of the solution within the gasometer recorded (h_1) before the introduction of biogas from the gas bag into the gasometer through the top valve. The gas bag opened enabling the gas to vent into the gasometer where the mass of solution (m) was recorded in the collection vessel below the gasometer and the final height (h_2) were recorded along with the temperature (K) and pressure (p) in the room. All gas volumes reported are corrected to standard temperature and pressure of 0 °C, 101.325 kPa as described by Walker et al. (2009) (Walker et al., 2009). All other anaerobic digestion experiments involving the collection of biogas determined the biogas volume directly from the gas-impermeable sampling bags only. Equations 3.8 and 3.9 were used to determine the gas volume:

Height gasometer Equation 3.8

$$V_{stp} = \frac{T_{stp} A}{T_{atm} P_{stp}} \left((p_{atm} - p_{H_2O}(T_{atm}) - \rho_b g (h_{t2} - h_{c2})) h_{c2} - (p_{atm} - p_{H_2O}(T_{atm}) - \rho_b g (h_{t1} - h_{c1})) h_{c1} \right)$$

Weight gasometer Equation 3.9

$$V_{stp} = \frac{T_{stp} A}{T_{atm} P_{stp}} \left[\left((p_{atm} - p_{H_2O}(T_{atm}) + \rho_b g \left(H - h_1 - \frac{m_b}{A \rho_b} \right)) \left(h_1 + \frac{m_b}{A \rho_b} \right) \right) - (p_{atm} - p_{H_2O}(T_{atm}) + \rho_b g (H - h_1)) h_1 \right]$$

Where:

V = gas volume (m³)

Chapter 3

P = pressure (Pa)

T = Temperature (K)

H = total height of column (m)

h = distance to liquid surface to datum (m)

A = cross-sectional area of gasometer (m²)

m_b = mass of barrier solution (kg)

p = density of barrier solution (kg m⁻³)

g = gravitational acceleration (m s⁻²)

1, 2, stp, atm, b, t, c subscripts refer to condition 1 (before addition of gas to column), condition 2 (after gas addition to column), standard temperature and pressure, atmosphere, barrier solution, collection trough and column respectively. The volume of methane and carbon dioxide content was calculated assuming these gases made up 100 % of the biogas after correction for moisture content, i.e. For measuring CH₄ a % and CO₂ b % the corrected values were obtained from

$$V_{\text{CH}_4} = Va/(a+b)$$

$$V_{\text{CO}_2} = Vb/(a+b)$$

Where :

V = measured gas volume as stp after correction for water vapour content (litres)

a = measured CH₄ content (%)

b = measured CO₂ content (%)

3.4.14.1 Residual biogas production

Residual biogas was measured after the continuous operation of the reactors had ceased.

Gas was collected using the same gas-impermeable sampling bags used within the continuous studies with biogas volume measured as outlined above.

3.4.15 Sulphide analysis

3.4.15.1 Hydrogen sulphide gas

H₂S gas was analysed using a H₂S-AE sensor supplied by Alphasense Ltd (Essex, UK) running on an Alphasense digital transmitter board with signal conditioning using the Alphasense Digital Transmitter Interface v.1.0.2 and associated software. The gas flow over the sensor was maintained at 500 ml min⁻¹ during calibration and normal operation. Calibration was performed at a zero cal point using clean air and a span cal point using the calibration gas, which was a mixture of H₂S and CO₂ made by SIP Analytical Ltd (Composition: 404 ppm H₂S, 35.19 % CO₂, Balance – Methane). Samples were run from gas samples collected in gas sampling bags, with gas passed over the sensor until a stable reading was obtained. The output was recorded and compared to the standard curve to give a direct reading in ppm H₂S.

3.4.15.2 Soluble H₂S

Soluble sulphide was determined using Henry's law (equation) and the headspace concentration of H₂S gaseous from the gas determination. The unionised fraction of hydrogen sulphide was determined using the following equations, with the total soluble sulphide fraction presumed to consist of H₂S and HS⁻ due to the operational pH range within the reactors (Millero, 1986, APHA, 2005).

$$P = Hx \quad \text{Equation 3.13}$$

Where P is the partial pressure of the solute in the gas phase (atm)

H is Henry's proportionality constant (atm mol fraction⁻¹)

x is the concentration of solute in the liquid phase (mol mol⁻¹)

The value of H for H₂S was taken as 4.32 x 10⁻² atm mol fraction⁻¹ at 35^oC (Perry Robert et al., 1997).

3.4.16 Total soluble sulphide - calculated

The following equations were used to determine the ratio of H₂S to HS⁻ to calculate total soluble sulphide (Millero, 1986, APHA, 2005).

$$pK^1 = 32.55 + 1519.44/T - 15.672 \log T + 0.02722T$$

Chapter 3

$$A = -0.2391 + 35.685/T$$

$$B = 0.0109 - 0.3776/T$$

$$pK_{sw} = pK^1 + AS^{1/2} + BS$$

$$a = pH - pK_{sw}$$

$$b = 10^a$$

$$\alpha_{H_2S} = \frac{1}{1+b}$$

$$\text{Total Sulphide} = \frac{1}{\alpha_{H_2S}} \times H_2S(aq)$$

Where:

pK is the negative logarithm of the acidic dissociation constant of H_2S

S is salinity

T is temperature in $^{\circ}K$

VBP is volumetric biogas production $L L^{-1} day^{-1}$.

3.4.17 Soluble sulphide – ion selective electrode

Total soluble sulphide was measured using a sulphide ion selective electrode following the manufacturer's instructions for the use of the electrode (JENWAY 3345 ion metre, Double Junction Reference Electrode and 1225 Sulphide instructions).

A full strength sulphide stock solution was prepared by diluting 100 mg $Na_2S \cdot 9H_2O$ within a 100 ml volumetric flask with degassed ultra-pure water. Standards were prepared daily by diluting the sulphide stock solution in an Alkaline Anti-oxidant Reagent (AAR) as shown in Table 19 prepared in 1 l of ultra-pure water degassed with N_2 . 80g of NaOH, 35g ascorbic acid and 67g of EDTA- Na_2 added directly. The AAR solution is stored at room temperature in an airtight brown glassed flask to prevent the breakdown of the solution. Samples were prepared by centrifuging 50 ml of sample at 1500g for 10 minutes filtering the supernatant and filtering through a 0.2 μm Whatmann GFF. The sulphide was fixed within the sample by adding 40 ml of AAR and 75 μl of zinc acetate to the 50 ml sample within a 100 ml volumetric flask adding MQ water up to 100 ml agitating the solution to prevent precipitation.

Table 19 Soluble sulphide standards.

Cal ID	Dilution	Sulphide sol. ID	final concentration mg L ⁻¹
Cal. 4	1:10	Stock sol. (133 mg L ⁻¹)	13
Cal. 3	1:100	Stock sol. (133 mg L ⁻¹)	1.3
Cal. 2	1:1000	Cal. 3 (1.3 mg L ⁻¹)	0.13
Cal. 1	1:10000	Cal. 3 (1.3 mg L ⁻¹)	0.013

The stock solution of sulphide was standardised by titration with iodine, sodium thiosulphate and starch. The Na₂S.9H₂O was kept in an airtight container within a desiccator to prevent absorption of moisture. The titration occurred as follows To 10 mL of Iodine 0.1N (0.05 M) add 100 mL of water, add 1 mL of HCl conc and 4 mL of stock solution tip under surface of iodine. Titrate with Sodium Thiosulphate using few drops of starch solution to nearly the end of the titration until blue colour disappears. 1 mL of 0.025N I₂ react with 0.4 mg of S²⁻. (Titre aprox. 3-10 mL for stock solution).

The concentration of sulphide is determined using the following equation:

$$(((I_{vol} \times I_{mol}) - (S_2O_3Na_{2vol} \times S_2O_3Na_{2mol})) \times 0.8 \times 1000) / vol_{stock}$$

Where:

I_{vol} is the volume of iodine (ml)

I_{mol} is the molarity of iodine (N)

S₂O₃Na_{2vol} is the volume of sodium thiosulphate (ml)

S₂O₃Na_{2mol} is the molarity of sodium thiosulphate (N)

vol_{stock} is the volume of the stock solution

3.4.18 Soluble sulphate

Sulphate was analysed using a Metrohm ion chromatograph 882 with autosampler and 6.1006.100 Metrosep Anion Dual 2 column. 2 mmol L⁻¹ NaHCO₃ 1.5 mmol L⁻¹ NaCO₃ with 2% v/v acetonitrile eluent for cleaning and the mobile phase of operation, this was filtered through 0.45µm filter and sonicated for 30 minutes before use to remove particulates and CO₂. Each run was conducted with a residence time of 17 minutes and

Chapter 3

the ions nitrate, nitrite, phosphate and sulphate determined. 0.1 M Sulphuric acid was used to clean the suppressor apparatus after each injection maintaining the baseline. Milli-Q water was replenished each day of use, and new reagents used for each run. 20 standards were used between 10ppm to 0.01ppm of each ion. Algal culture samples were first filtered through a 0.2 μm Whatmann GFF before analysis. Samples containing high salt concentrations were diluted by a factor of 100 to prevent saturation and fouling from the chloride and metal ions. For digestate samples containing high salt a 2 ml sample was centrifuged for 15 minutes at 1500g, the supernatant removed and filtered through a 0.2 μm Whatmann GFF and diluted by 100.

3.4.18.1 Sulphur mass balance

A sulphur mass balance was implemented to determine % removal of sulphate from within the reactors using the following assumptions and equations.

There are a few limitations with this mass balance approach. This is due to the difficulties in determining soluble sulphate post digestion and the inherent difficulty in measuring the precipitated sulphur within the reactor, any fluctuations in percentage removal are expected to contain non digested sulphur as sulphate and organic sulphur, and inorganic sulphur precipitated within the reactor. The following equation gives a rough estimate of the percentage sulphur consumed and removed from within the digester.

$$\% \text{ removal} = 100 / \text{Sulphur}_{in} \times \text{Sulphur}_{out}$$

The main assumption was that in a steady state system the sulphur added to the reactor should equal the sulphur removed as a gas, within the digestate effluent or precipitated within the reactor.

Under steady state the Sulphur entering the system should equal the sulphur exiting the system so that: $\text{Sulphur}_{in} = \text{Sulphur}_{out}$.

$\text{Sulphur}_{in} = \sum \text{Mass of sulphur added as } \text{g day}^{-1} \text{ from sulphate and mass of sulphur within VS content of substrate added as } \text{g day}^{-1}$.

$\text{Sulphur}_{out} = \sum \text{Mass of sulphur produced as } \text{g day}^{-1} \text{ from } \text{H}_2\text{S} \text{ gas and removed as soluble sulphide as } \text{g day}^{-1}$.

$$\% \text{ of undetermined sulphur} = 100 - 100 / \text{Sulphur}_{in} \times \text{Sulphur}_{out}$$

3.5 Anaerobic digestion

Continuously stirred tank reactors (CSTR) were used for the continuous anaerobic digestion studies each with a two litre capacity and 1.5-litre working volume (Figure 37 and 37). Each reactor was constructed out of PVC tubing with a gas tight lid and base. Feeding occurred through a port at the top, which was sealed during operation, and digestate removal through an outlet at the base. A draught tube liquid seal in the top of the reactor with an asymmetric bar stirrer connected to a 40 rpm motor mounted to the digester mixed the digestate. Temperature was maintained at $35^{\circ}\text{C} \pm 1^{\circ}\text{C}$ by circulating water from a thermocirculator through copper coils around the digester. Feeding was done on a daily basis with digestate removed daily to maintain the working volume.

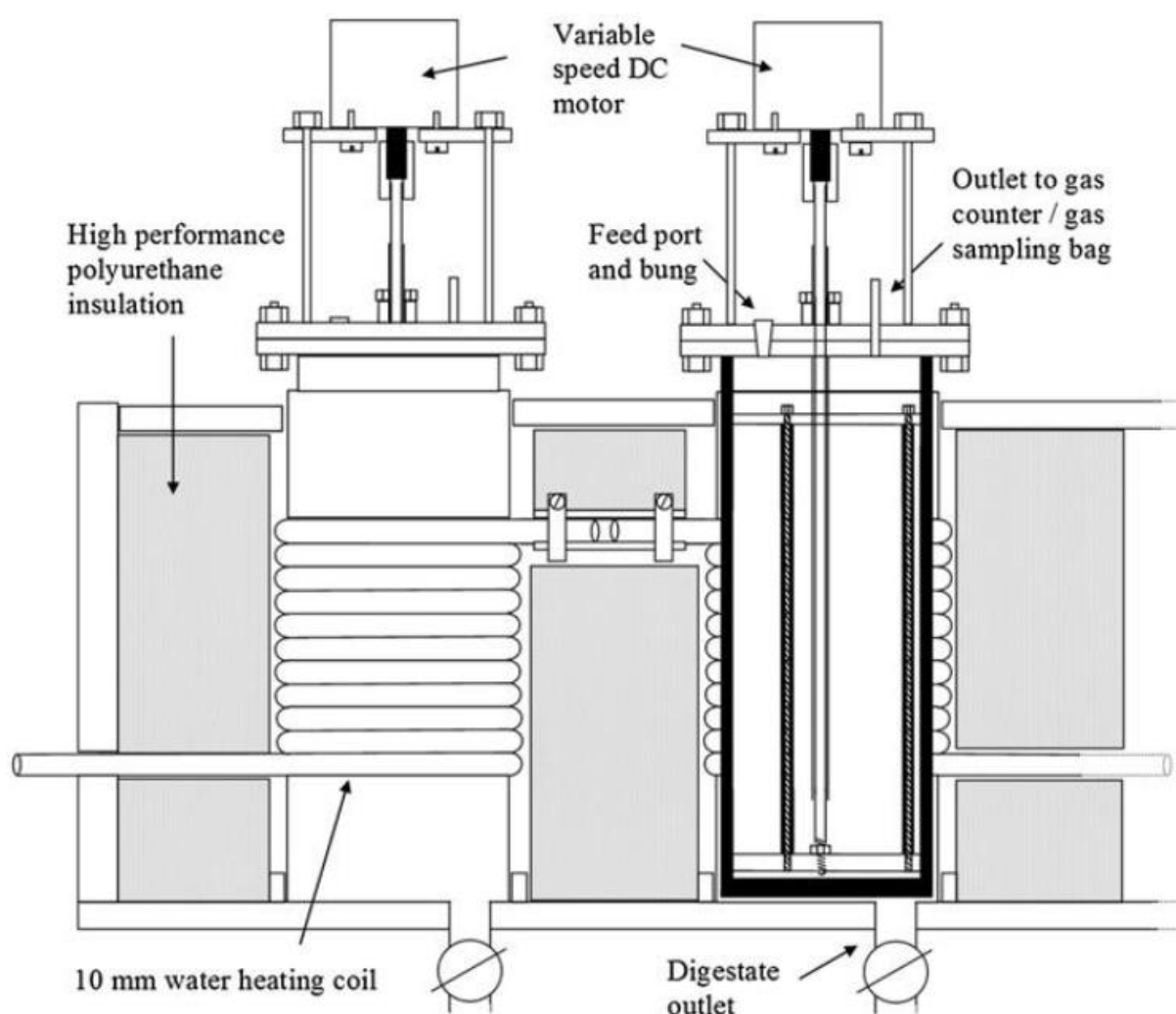


Figure 37 – CSTR design for semi continuous anaerobic digestion studies (Jiang et al., 2012).



Figure 38 2 litre CSTR

3.5.1 Biochemical methane potential assay

The biochemical methane potential assay is a method for determining the maximum methane yield of an organic substrate by anaerobic digestion within a defined medium of mixed flora. In all tests a sample of substrate is incubated with a suitable inoculum for a predetermined time, or until the gas production is equal to that of the control according to the method outlined in ASTM (1992).

Each test was set up in triplicate with three controls of inoculum without added substrate alongside positive controls (cellulose powder from Sigma-Aldrich, Dorset-UK), all in triplicate. Municipal biosolids digestate (Wastewater Treatment Works, Millbrook, Southampton) was used as an inoculum for the BMP test. Before use the inoculum was sieved to remove coarse and fine particles of grits and sand. The TS and VS of the inoculum was determined and from this the volume required for the reactor.

Each static reactor with a working volume of 300 cm^3 was filled to $\sim 300 \text{ ml}$ of

inoculum. The quantity of volatile solids within each reactor was calculated using Equation 2.10.

$$\text{Total VS}_{\text{inoculum}} (\text{g}) = (\text{mass of inoculum added (g)} \times \text{VS}_{\text{inoculum}} (\%))/100 \quad (2.10)$$

A ratio of VS_{inoculum} (VS_i) to VS_{substrate} (VS_s) of 4:1 with the mass of substrate added shown in Equation 2.11 was used.

$$\text{Mass of substrate (g)} = (\text{VS}_{\text{inoculum}} (\text{g})/4 \times 100/\text{VS}_{\text{substrate}} (\%)) \quad (\text{Equation 2.11})$$

The inoculum was collected one day prior to analyses and allowed to degas over a 24 hour period and maintained at 35°C using a water bath. The substrate is decanted into the inoculum and sealed with a rubber bung with a gas outlet connected to the gasometer. The water level within the gas collectors was recorded before adding the substrate to the inoculum and connecting to the gasometer. Biogas was collected in glass cylinders by displacement of a 75% saturated sodium chloride solution acidified to pH 2, in order to reduced losses of methane by dissolution. The height of the solution in the collection cylinder was recorded manually. Vapour pressure and salt solution density were taken into account in correction of gas volumes to a standard temperature and pressure (STP) of 0°C and 101.325 kPa (Walker et al., 2009). Samples for gas composition analysis were taken from the cylinders each time they were refilled, at intervals of no more than 7 days to avoid the risk of overfilling or losses of methane.

3.5.2 Simulated SMY

Biodegradability of the micro-algal samples was assessed from BMP kinetic data using the pseudo-parallel first order model shown in equation 2.12, where Y (L CH₄ g⁻¹ VS) is the specific methane production at time t (day), Y_{max} is the measured or estimated ultimate methane yield (L CH₄ g⁻¹ VS), k_1 is the first order rate constant (day⁻¹) for readily biodegradable material, k_2 is the first order rate constant (day⁻¹) for less readily biodegradable material and P is the proportion of readily biodegradable material (Rao et al., 2000).

$$Y = Y_{max}(1 - Pe^{-k_1t} - (1 - P)e^{-k_2t}) \quad \text{Equation 2.12}$$

3.6 Statistical analysis

Statistical analysis was undertaken using the software package R, (Bristol University) on the BMP assays and continuous digestion data.

One way ANOVA and F test was conducted on the BMP assays with a sample size of 8 comparing both individual species and marine and fresh water.

Kruskal –Wallis one-way ANOVA on the continuous digestion specific methane production.

P values < 0.05 were deemed to be significant.

CHAPTER 4

4. Experimental Results

4.1 Algal characterisation

4.1.1 Introduction

The focus of this part of the research was to characterise and determine the methane potential of pure cultures of various microalgae for future continuous cultivation and anaerobic digestion. Cultures were cultivated on suitable media before harvesting and characterisation occurred. Different concentrations of Jaworski's Medium (JM) were also tested to determine a suitable concentration for maximum algal production.

Sulphate was identified in the literature review as a potential inhibitor of methane production within AD as its use as a substrate for SRB cause competition between SRB and methanogens, with the subsequent production of toxic H_2S . The sulphate concentration of 20 mg $SO_4 L^{-1}$ in JM is below the lower threshold of reported potentially inhibitory concentrations for AD (O'Flaherty et al., 1999, Scherer and Sahn, 1981, Hulshoff Pol et al., 1998). Marine concentrations of SO_4 are two orders of magnitude above reported inhibitory concentrations, however, at an average 2800 mg $SO_4 L^{-1}$. In order to compare the biochemical methane production (BMP) of marine algae grown on culture media containing marine concentrations of sulphate with those grown at micro nutrient concentrations in JM, it was first necessary to determine if cultures of marine species that exist in high sulphate conditions could thrive in low sulphate conditions.

The purpose of the experiments in this part of the work was to establish the effect of various types of media and conditions on growth rates and yields for selected microalgae and on their potential for methane production.

4.1.2 Growth rates and growth yields

Objective: to determine the growth yield and growth rate of various microalgae grown on JM with varying concentrations of sulphate with an artificial marine medium made with USSS and freshwater medium.

Methodology: The freshwater species *Scenedesmus* sp, *C. vulgaris* and the marine species *I. galbana*, *T. pseudonana*, *N. oculata*, *Rhododomas* sp and *D. salina* were grown on JM. Initial screenings were conducted to determine the growth rate and yield as described in section 3.3.2. TSS were determined using the optical density (OD) of the culture medium based on calibration curves for measured TSS and OD obtained for each species shown in Figure 39.

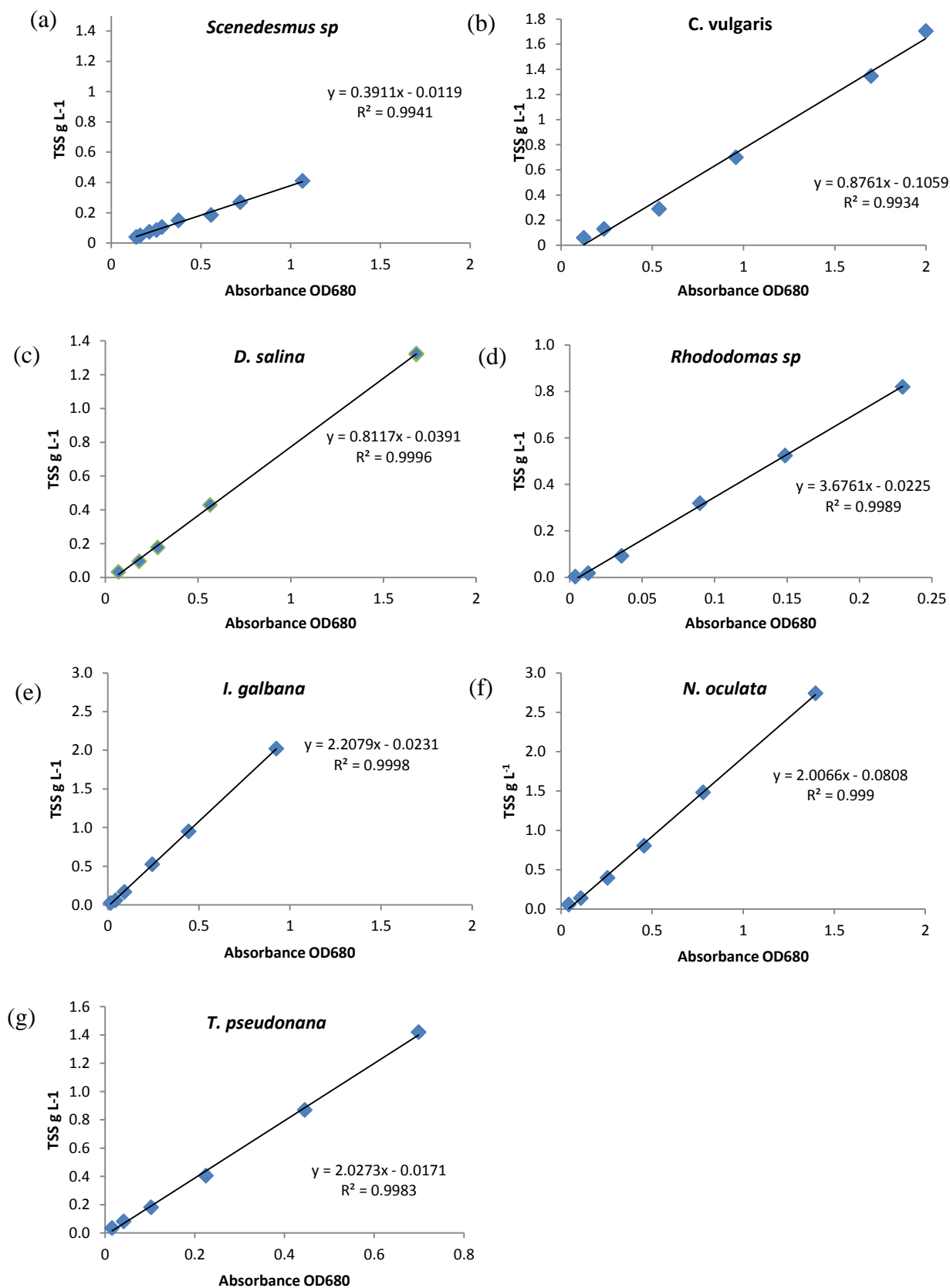


Figure 39 Calibration curves for TSS g L⁻¹ and absorbance at an optical density of 680 for each species grown on JM. (a) *Scenedesmus sp*, (b) *C. vulgaris*, (c) *D. salina*, (d) *Rhododomas sp*, (e) *I. galbana*, (f) *N. oculata*, (g) *T. pseudonana*.

4.1.2.1 Results

Figure 40 and Table 20 show the growth data, rates and yields obtained for the freshwater algal species *Scenedesmus*, *C. vulgaris* and the marine species *I. galbana*, *T. pseudonana*, *N. oculata*, and *D. salina* under the conditions applied.

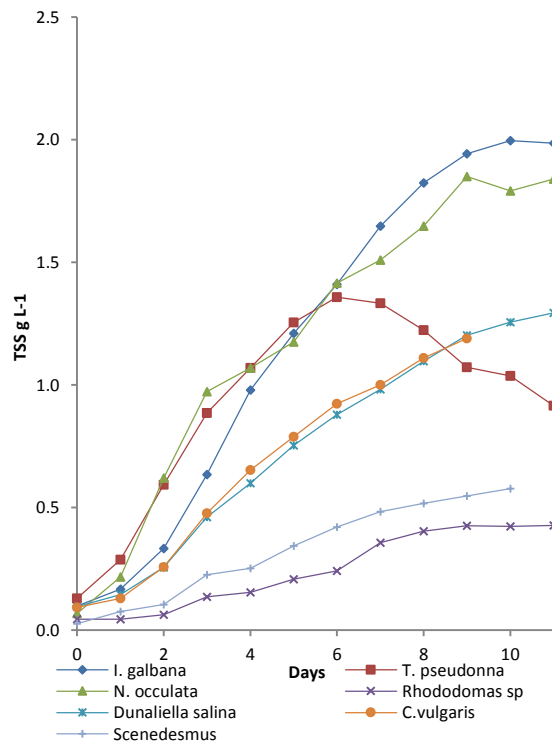


Figure 40 Results for growth of freshwater microalgae cultivated on JM and marine microalgae cultivated on JM under both fresh water and marine media with USSS in g TSS L⁻¹.

Table 20 growth rates and yields of six microalgae cultivated on JM in deionised water only for fresh water species and deionised water and USSS for marine species.

Species	VS (%TS)	Duration of log phase of growth (d)	Media type, saline or fresh water	Initial TSS g L ⁻¹ (a)	Final TSS g L ⁻¹ (a)	Doubling rate (a) day ⁻¹	^b Estimated growth yield under continuous operation g VS L ⁻¹ day ⁻¹
<i>I. galbana</i>	67.2%	3	Saline	0.098	1.990	0.610	0.31
<i>T. pseudonana</i>	59.8%	2	Saline	0.130	1.357 ¹	0.710	0.36
<i>D. salina</i>	50.4%	3	Saline	0.100	1.100	0.590	0.30
<i>N. oculata</i>	80.3%	2	Saline	0.069	1.850	0.770	0.39
<i>C. vulgaris</i>	94.7%	3	Fresh water	0.09	1.10	0.750	0.38
<i>Scenedesmus</i> sp.	83.9%	3	Fresh water	0.030	0.58	0.760	0.38
<i>Rhododomas</i> sp. ²	N/D	3	Saline	0.098	0.426	0.470	0.24

^a Measured by OD and calculated on a total suspended solids and volatile solids basis.

^b Estimated from the maximum dilution rate and an expected initial biomass concentration of 0.5 g VS L⁻¹

¹Maximum solids concentration before flocculation occurred.

² Data based on one successful replicate.

Growth data were determined on a TSS basis as *T. pseudonana* is a diatom with an inorganic silica cell wall; for conversion of TSS to VS or VSS the VS/TS ratio at the end of the run was used (Table 20). Growth yields for the laboratory-grown cultures were between 0.08-0.22 g VS L⁻¹ day⁻¹, with growth rates from 0.47-0.77 day⁻¹. The marine species *N. oculata* had the highest growth rate and yield, followed by the fresh water (FW) species *C. vulgaris*. The greatest yields were from the marine species, with final TSS between 1.2 - 2.5 g L⁻¹, higher than those of the FW species.

The growth rates measured here were in most cases equal to or lower than typical maximum growth rates reported in the literature, which range e.g. from 0.55-0.80 day⁻¹ for *I. galbana*, 1.33-2.52 day⁻¹ for *T. pseudonana*, 0.77-1.00 day⁻¹ for *Dunaliella tertiolecta*, 1.59-2.90 day⁻¹ for *C. vulgaris* and 1.34-2.2 day⁻¹ for *Scenedesmus* sp. (Cole and Wells, 2008). Factors

causing the lower growth rates observed include differences in growth media composition with up to an order of magnitude lower nitrogen and phosphorus content in the media used, the use of artificial light and different culturing vessels (Renaud et al., 2002, Berges et al., 2002, Thompson, 1999, Jitts et al., 1964, Sandnes et al., 2005, Goldman and Graham, 1981, Hoogenhout and Amesz, 1965, Cole and Wells, 2008). The higher growth yields and growth rate of the marine species over the FW species examined within this study suggests a potential advantage in areal productivity for marine microalgal biomass production over FW. However, this may not be necessarily true under different culture conditions with freshwater species in other studies producing similar and greater growth yields and growth rates.

Throughout the algal screening it was noted that several species would fail to culture, continuously experience culture crashes or become readily contaminated with other algae. These were mainly *I. galbana*, *Rhodomonas sp.* and *T. pseudonana*. The most resilient and easily cultured species observed were the fresh water species *Chlorella vulgaris* and the salt water species *N. oculata* and *D. salina*.

Rhodomonas sp. failed to culture successfully in one of the replicates, with the successful cultures showing very slow growth indicative of this species. As such this species was not investigated further.

The commercially bought bulk artificial sea salt USSS was only used during this initial growth study. As the composition of the sea salt was unknown and potential commercial sensitivity around determining this it was deemed necessary to use individual components to manufacture a mean ocean concentration of sea salt. For this a salt medium consisting of NaCl, MgCl, CaCl₂ and KCl was formulated as described in section 3.2.3 for subsequent use in algal growth studies.

4.1.3 Sulphate and growth rate/ yield for marine microalgae

Objective: To determine the minimum concentration of SO₄ required to maintain a continuous algal biomass yield of *D. salina*, *N. oculata* and *I. galbana* under semi continuous cultivation for the large-scale growth trials.

Methodology: Four separate JM stock solutions were prepared as described in section 3.2 with concentrations of sulphate at 19.5, 3.9, 1.95 and 0.2 mg SO₄ L⁻¹, corresponding to 100%,

20%, 10% and 1% of the total sulphate within the original JM, as shown in Table 12 (section 3.3). Each solution was made with an artificial salt medium consisting of NaCl, MgCl, CaCl₂ and KCl as described in section 3.2.3. 50 ml of each solution was added to 9 Erlenmeyer flasks, (total 36 flasks), which were sealed with a porous foam bung and aluminium foil and autoclaved at 120°C for 15 minutes.

Algal starter cultures maintained on JM with USSS were used as inoculum within their log phase of growth as described in section 3.3. Triplicate flasks of JM at each concentration of SO₄ were inoculated with 1 ml of each species *D. salina*, *N. oculata* and *I. galbana* under aseptic conditions. All flasks were placed within an illuminated orbital incubator at 120 rpm, 25°C, and an illumination of 120 μ mol m⁻². After 14 days all cultures were removed from the incubator and the cell number and TSS measured as described in section 3.4.6 and 3.4.8. 1 ml of each culture was inoculated into an Erlenmeyer flask containing JM at the same initial concentration of SO₄ as in the previous stage, using the stock solutions and method described above, and cultured for 14 days. This practice was repeated for three more generations, with the final generation cultured into Erlenmeyer flasks with side-arms for daily in-situ analysis of the OD. The steps in the procedure are illustrated in Figure 41.

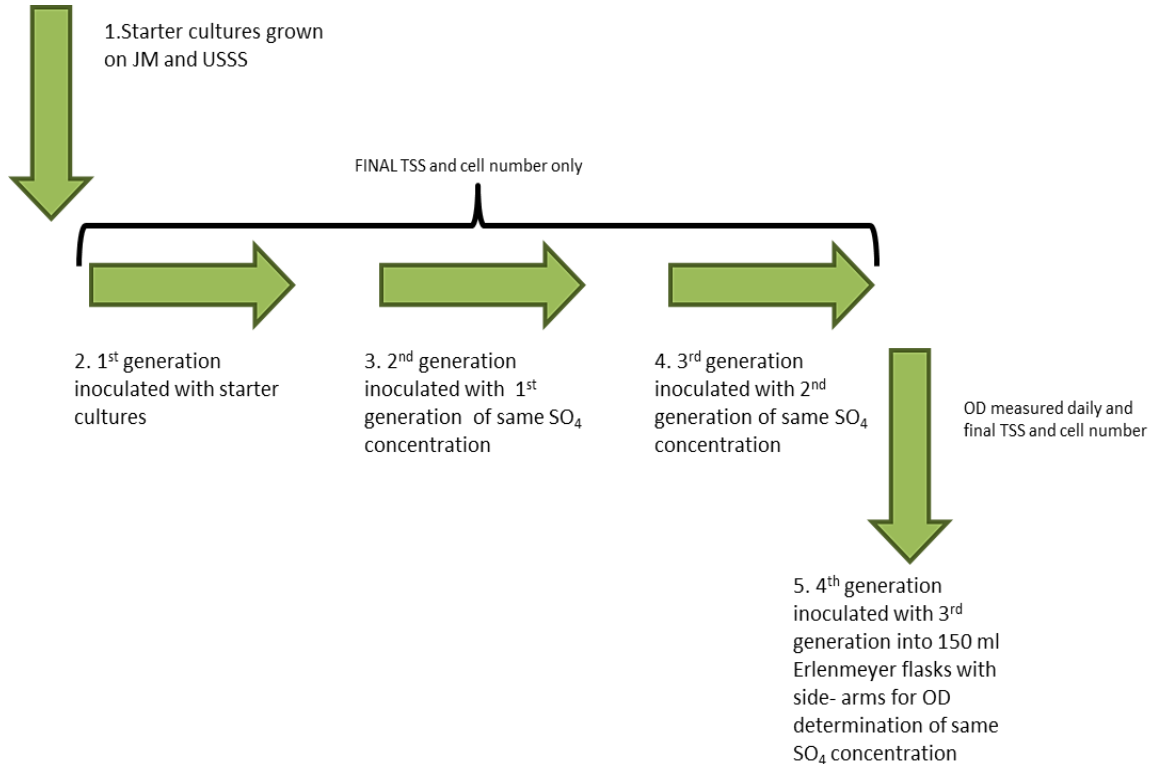


Figure 41 Flow diagram of the SO₄ analysis experiment for each sulphate concentration.

Chapter 4

Growth yields and cell numbers for the four-generation low sulphate experiments are shown in Figure 42 and Table 21. The results showed that *I. galbana*, *D. salina* and *N. oculata* could all be successfully cultured at sulphate concentrations of $19.5 \text{ mg SO}_4 \text{ L}^{-1}$, with *D. salina* producing the greatest growth yield of up to 1.6 g L^{-1} TSS at the end of the fourth run, whereas *I. galbana* produced 1.2 g L^{-1} in their final culture. *T. pseudonana* failed to culture successfully and was not investigated further.

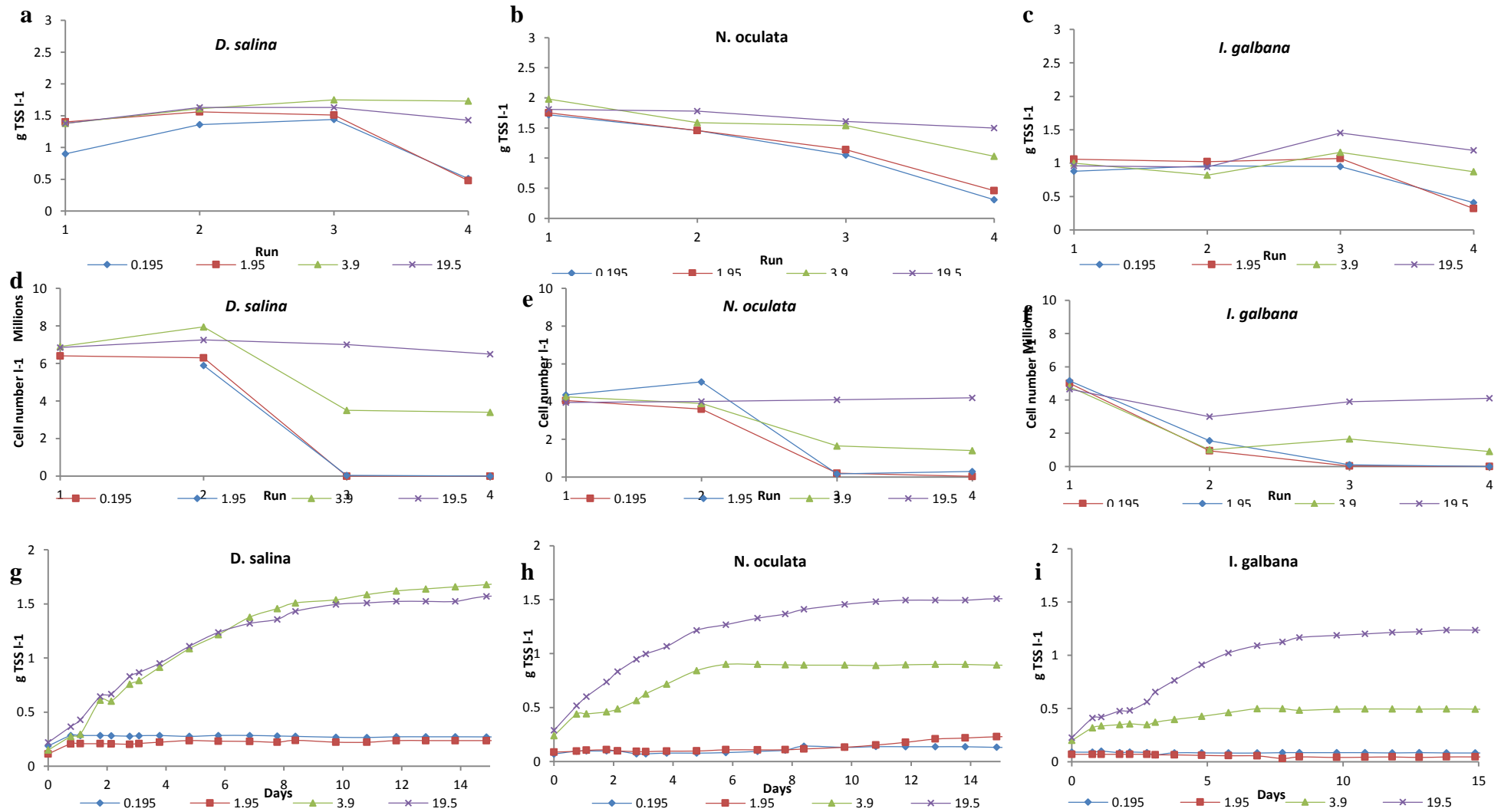


Figure 42 Final growth yields (a-c) and cell numbers (d-f) for the four generation runs with *D. salina*, *N. oculata* and *I. galbana* grown on JM and artificial salt with different concentrations of SO₄. Kinetic growth rate for the fourth generation run determined by OD in figures g-i.

Table 21 Final TSS g L⁻¹ and cell number for the species *N. oculata*, *D. salina* and *I. galbana* at the SO₄ concentrations of 0.195, 1.95, 3.9 and 19.5 mg SO₄ L⁻¹ for each generational run.

<i>D. salina</i>								
Generation	mg SO ₄ L ⁻¹							
	0.195		1.95		3.9		19.5	
	TSS g L ⁻¹	Cell number	TSS g L ⁻¹	Cell number	TSS g L ⁻¹	Cell number	TSS g L ⁻¹	Cell number ml ⁻¹
1	0.9	6400000	1.4	-	1.38	7500000	1.38	8000000
2	1.36	6300000	1.56	5900000	1.61	8500000	1.63	7250000
3	1.44	0	1.51	33333	1.75	4200000	1.63	7000000
4	0.51	0	0.48	0	1.73	3400000	1.43	6500000

<i>N. oculata</i>								
Generation	mg SO ₄ L ⁻¹							
	0.195		1.95		3.9		19.5	
	TSS g L ⁻¹	Cell number	TSS g L ⁻¹	Cell number	TSS g L ⁻¹	Cell number	TSS g L ⁻¹	Cell number ml ⁻¹
1	1.72	4000000	1.75	4000000	1.98	4000000	1.81	3950000
2	1.46	3600000	1.46	5050000	1.59	3900000	1.78	4000000
3	1.051	200000	1.142	166667	1.54	1650000	1.61	4100000
4	0.31	33333	0.46	300000	1.03	1400000	1.5	4200000

<i>I. galbana</i>								
Generation	mg SO ₄ L ⁻¹							
	0.195		1.95		3.9		19.5	
	TSS g L ⁻¹	Cell number	TSS g L ⁻¹	Cell number	TSS g L ⁻¹	Cell number	TSS g L ⁻¹	Cell number ml ⁻¹
1	0.88	4500000	1.06	4750000	1	5000000	0.96	4650000
2	0.96	950000	1.02	1550000	0.82	1000000	0.94	3000000
3	0.95	33333	1.07	100000	1.16	1650000	1.45	3900000
4	0.41	0	0.32	0	0.87	900000	1.19	4100000

At 19.5 mg SO₄ L⁻¹ *I. galbana* and *D. salina* had relatively stable final TSS and cell numbers for each generational run, of between 1.38 – 1.46 and 0.96 – 1.19 g TSS L⁻¹ respectively; *N. oculata* showed a slight decline in final TSS from 1.81 to 1.50 g TSS L⁻¹ through successive generations. Cell numbers at 19.5 mg SO₄ L⁻¹ were stable for all species, with 6.0 to 6.5 x 10⁶, 4.0 – 4.2 x 10⁶, and 4.1 – 4.6 x 10⁶ cells ml⁻¹ for *D. salina*, *N. oculata* and *I. galbana* respectively (Figure 42d-f). At sulphate concentrations above 3.9 mg SO₄ L⁻¹ all three species tested showed an exponential growth phase, which lasted two days for *D. salina* and *N.*

oculata, and four days in the case of *I. galbana*. All three species showed no noticeable growth for the concentrations 1.95 and 0.195 mg SO₄ L⁻¹ (Figure 42 g-i).

For the first two generations all cultures showed similar behaviour at all concentrations of SO₄ (Figure 42 a – f). After three generations, however, corresponding to a x 1000 dilution of the original inoculum and culture media, there was a decline in final TSS and cell number at SO₄ concentrations of 0.195 and 1.95 mg L⁻¹.

After the third generation large amounts of cellular debris was seen in all cultures after 14 days at concentrations below 3.9 mg SO₄ L⁻¹, with no apparently healthy whole cells observed (Figure 42 d – f and Figure 44). Clumping of dead cells occurred, with reduced carry-over of algae into subsequent cultures (Figure 44b and c). The number of apparently healthy cells for successive cultures declined with the lower sulphate concentrations of 0.195 and 1.95 mg SO₄ L⁻¹, for all species, remaining constant at the higher concentration. This suggests that sulphate is becoming limiting for replication and the cells are entering a stationary or possibly a decay phase of growth, with cell division declining. These results support the findings of Giordano et al. (2000) who reported a decline in growth rate for *D. salina* below a concentration of 9.6 mg SO₄ L⁻¹.

Measured final sulphate concentrations within the culture medium after growth decreased through successive generations were towards 0.1 mg L⁻¹ sulphate (Figure 43), indicating that the majority of sulphate available had been consumed by the microalgae and retained within the cells, which were removed prior to SO₄ analysis. The high SO₄ concentration at the end of generational run one is caused by carry-over from the starter culture.

Discrepancies between the final TSS concentrations of Figure 42a and g, and c and i are likely due to the use of OD to determine the in-situ TSS not being reliable enough at the lower TSS concentrations observed in these final assays. The difference in TSS in the third generational run and the low cell count is due to the absence of readily identifiable viable whole cells, but the presence of cellular debris.

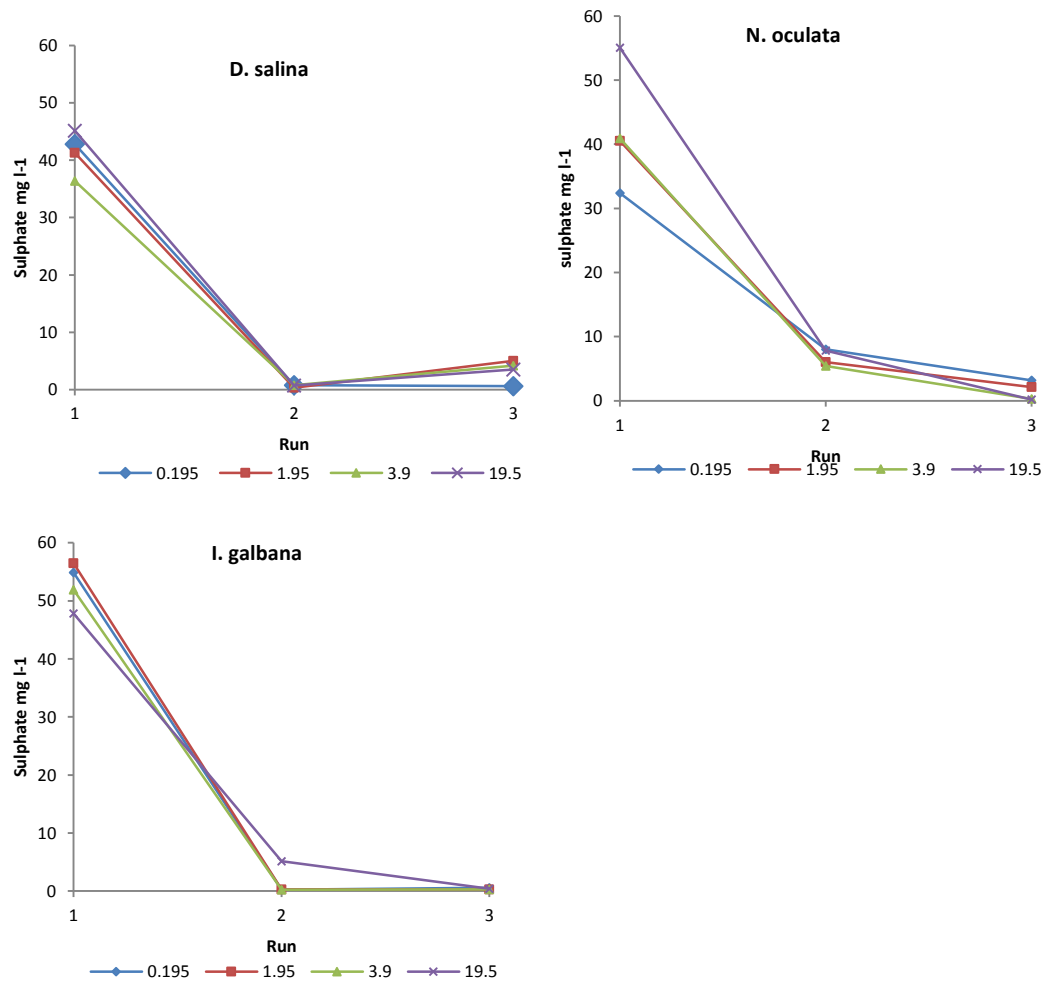


Figure 43 Sulphate concentration in mg L⁻¹ for the end of each generational run.

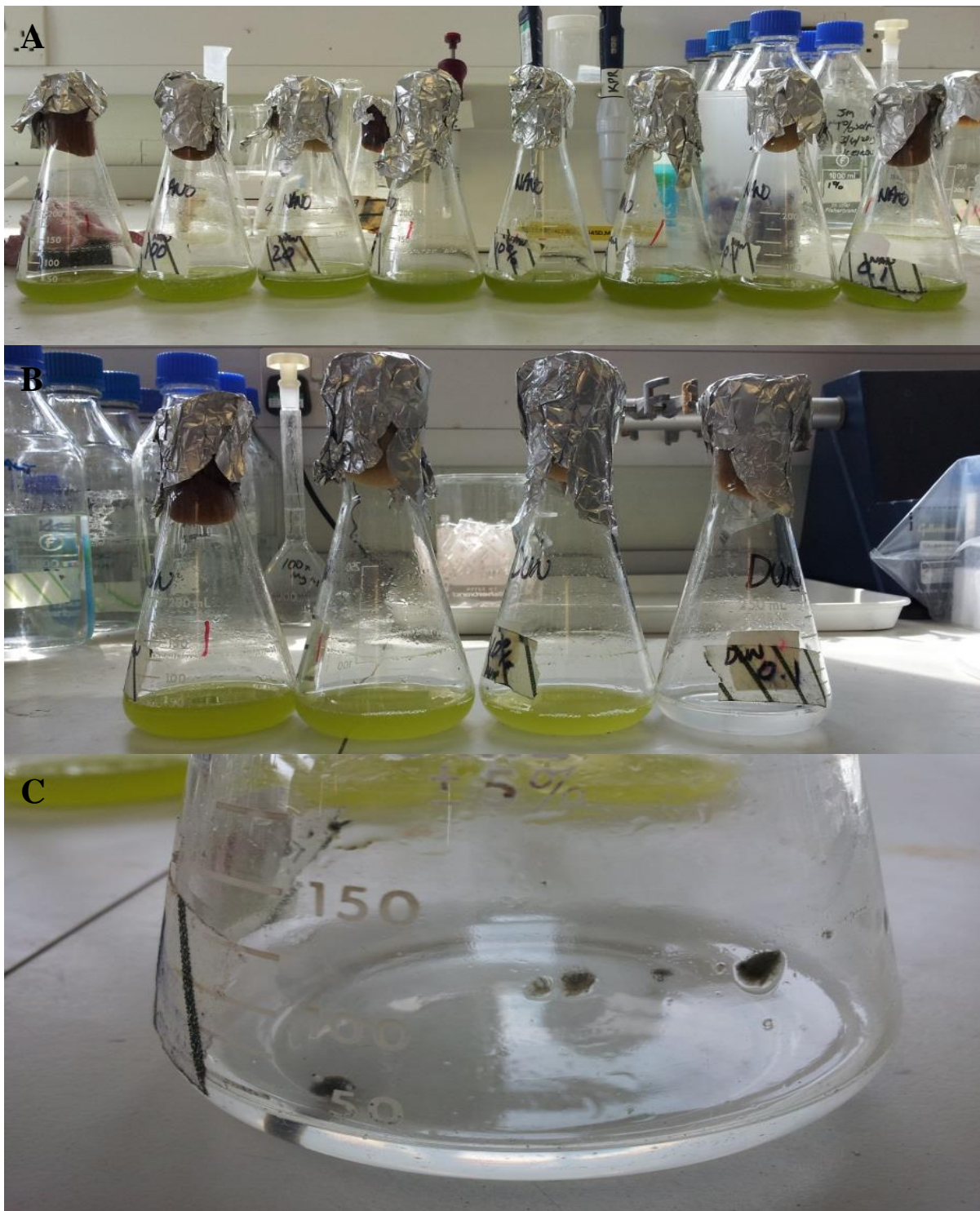


Figure 44 Cultures post growth for *D. salina* under batch conditions for the SO_4 concentration study. (a) first generation of *D. salina* with decreasing sulphate concentration from left to right, (b) final generation of *D. salina* with decreasing sulphate concentration from left to right, (c) clumped organic matter in failed final culture of *D. salina* at 0.1% sulphate.

The final generation results show that a low sulphur medium of 19.5 mg SO₄ L⁻¹ will not adversely affect the algal yield of *D. salina*, although it may have impeded that of *I. galbana* and *N. oculata*, where TSS was lower than previous experiments utilising Ultramarine synthetic sea salt with a difference of up to 0.8g L⁻¹ TSS, suggesting these species are possibly more sensitive to lower sulphate concentrations (Figure 40). The growth rates for *D.salina* and *N. oculata* were similar at 0.484 and 0.469 day⁻¹ respectively at SO₄ concentration of 19.5 mg SO₄ L⁻¹, whereas *I. galbana* was slightly lower at 0.385 day⁻¹. *D. salina* growth rate was unaffected at the lower SO₄ concentration of 3.9 mg SO₄L⁻¹ at 0.489 day⁻¹ whereas *N. oculata* and *I. galbana* reduced by up to 50% shown in Figure 43.

Table 22 growth rates of *D. salina*, *N. oculata* and *I. galbana* for the four sulphate concentrations 19.5, 3.9, 1.95 and 0.195 mg SO₄ L⁻¹ determined from the fourth generation run.

	<i>D. salina</i>				<i>N. oculata</i>				<i>I. galbana</i>			
mg SO ₄ L ⁻¹	0.195	1.95	3.9	19.5	0.195	1.95	3.9	19.5	0.195	1.95	3.9	19.5
Doubling rate (day ⁻¹)	0	0	0.489	0.484	0.219	0.221	0.366	0.469	0	0	0.200	0.385

4.1.3.1 Concluding remarks

Decreasing sulphate concentrations below that recommended within the JM can give rise to culture crashes in successive cultures. It is therefore recommended that all future experimentation uses as a minimum 20 mg l⁻¹ of SO₄, particularly if continuous culturing is to occur.

4.1.4 Optimum concentration of JM

Objective: To determine the optimum concentration of JM for use in larger-scale continuous culture experiments.

Methodology: microalgae were cultivated in different concentrations of JM from 0 to 10 times the normal strength. Maximum growth rate was determined by OD and growth yield based on TSS was assessed after fourteen days. The Monod equation given in section 3.3.2 was used to model the growth of the microalgae under the different nutrient concentrations.

NaCl, MgCl₂ 6H₂O, CaCl₂ 2H₂O and KCl were combined with JM at the same concentrations described in section 3.2.3 for an initial screening of the maximum growth yield and growth of starter cultures of *D. salina*, *N. oculata* and *I. galbana*.

Results

Increasing the concentration of JM increases both the maximum growth rate and final growth yield after two weeks of cultivation (Figure 44 and Table 23). The growth rate increases for JM concentrations of up to 2x the recommended value, reaching a plateau between 2x and 3x the JM concentration, as shown in Figure 45. This doubling in media concentration, however, does not double the growth rate but increases it by 11%, with a growth yield difference of 10%. Above this concentration there is a decline in the maximum growth rate, with a 10x concentration showing a reduction in growth rate possibly due to inhibition from the high concentration of trace nutrients.

The maximum growth yield at the end of the two-week cultivation increased up to a 5x concentration of JM, to a maximum yield of 1.83 g TSS L⁻¹. When the concentration of JM is compared to the growth yield, however, the greatest percentage return as g L⁻¹ algae as a % of JM added, was observed for the 100% strength, with greater concentrations giving diminishing returns for the increase in nutrients (Table 23). These results suggest that under continuous operation the normal concentration of JM is satisfactory.

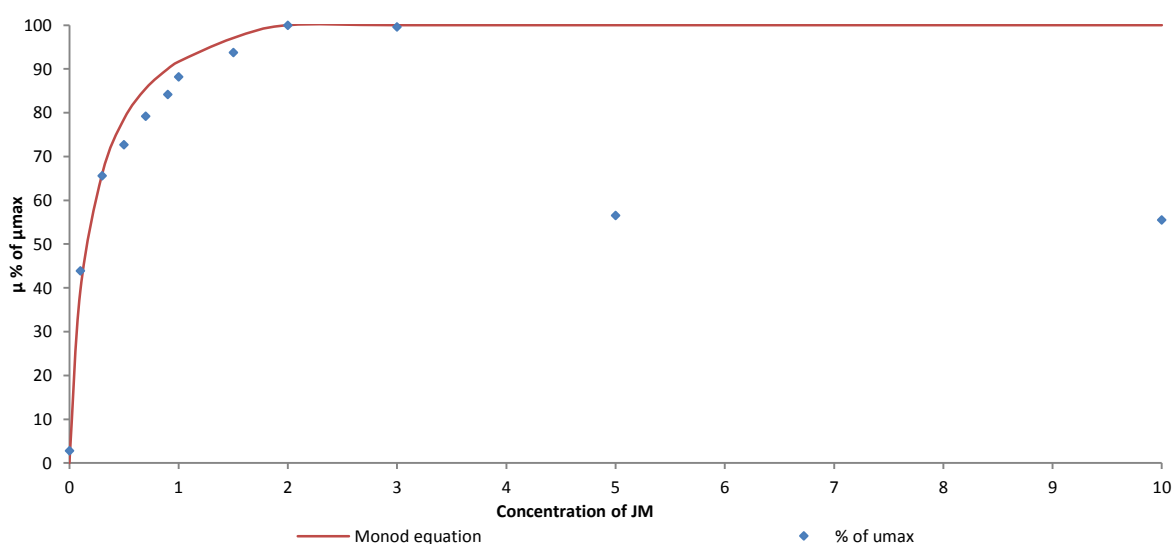


Figure 45 Growth rates of *D. salina* grown on salt formulation as described in section 3.2.3 and differing total concentrations of JM.

Table 23 Growth yields of *D. salina* after 14 days growing on various strengths of JM.

	Proportion of JM											
	0	0.1	0.3	0.5	0.7	0.9	1	1.5	2	3	5	10
TSS g L ⁻¹	0.05	0.15	0.31	0.40	0.58	0.60	1.25	1.25	1.38	1.83	1.91	1.76
g L ⁻¹ % of JM		1.48	1.04	0.79	0.85	0.32	1.25	0.83	0.69	0.61	0.38	0.18

4.1.4.1 Concluding remarks

Increasing the concentration of JM did increase the growth rate and final growth yield. There was, however, diminishing returns in the growth yield above the recommended concentration within the recipe and doubling the concentration only gave a 10% increase in growth rate. It is therefore recommended that all experimentation is undertaken with the original recommended concentration of JM.

4.1.5 Characterisation of freshwater and marine microalgae

Objective: the objective of this work was to cultivate and determine the characteristics of several fresh water and marine microalgae grown on JM for their suitability as a potential feedstock for methane production via AD.

Methodology: Six samples were grown within the laboratory using JM media and DI water, with Ultramarine Synthetic Sea Salt added to the marine species. The fresh water micro algal species *Scenedesmus sp*, *C. vulgaris* and the marine species *I. galbana*, *T. pseudonana*, *N. oculata*, and *D. salina* were cultivated within 20 L containers as outlined in Section 3.3 with biomass harvested as outlined in Section 3.3.4.

Two samples which had been grown on agricultural fertilisers added to reservoir water within a raceway pond and within a photobioreactor (PBR), respectively, were obtained from Almeria, Spain.

Results

Table 24 shows the results of characterisation of the different micro-algal samples. VS content as a proportion of TS ranged widely for the laboratory-grown cultures, from around 50.4% for *D. salina* to 94.7% for *C. vulgaris*. After centrifugation the laboratory-grown

samples had moisture contents from 68.1-78.8 %. If the VS content is corrected to allow for the quantity of sea salt assumed to be present within this moisture fraction in each sample, the revised VS content of the marine samples was 73.4, 68.2, 54.7 and 86.4 % of TS for *I. galbana*, *T. pseudonana*, *D. salina* and *N. oculata* respectively, with the values for all but *N. oculata* still below those for the two laboratory-grown freshwater species. Low VS/TS ratios for marine and diatom species have been reported elsewhere (Zhao et al., 2014, Bohutskyi et al., 2014, Buxy et al., 2012, Santos et al., 2014, Mottet et al., 2014), but Zhu and Lee (Zhu and Lee, 1997) also showed that the TS content of unwashed samples may be as much as 20% higher than washed cells. The value for *N. oculata* was similar to that reported in other studies (Zhao et al., 2014). The difference in values for the two large-scale samples may reflect the different cultivation systems, with the open raceway subject to both ingress of wind-blown grit and increases in salt concentration due to evaporation.

Carbon content ranged from 43.7-54.2% on a VS basis. The nitrogen content as determined by elemental analysis showed reasonably good agreement with TKN concentrations, which were between 4.7-9.6% VS. As expected, the resulting C/N ratios were all well below the recommended range of 20-30 for anaerobic digestion, and similar to those reported in the literature (Ward et al., 2014). Sulphur concentrations were higher in marine than in freshwater species. Calorific values ranged from 8.4-23.6 kJ g⁻¹ TS, reflecting the different proportions of inorganic material present in the samples. On a VS basis the CV was more uniform at 20.0-25.0 kJ g⁻¹ VS, reflecting the similar elemental composition of the organic fractions. C, H, and N in the ashed components of the marine species were negligible (< 0.25% TS).

Table 24 Characteristics of 8 micro-algal samples

Species	VS	TKN	CV	Elemental composition (% of VS)					C/N ^b
	(%TS)	%N of VS	MJ kg ⁻¹ VS	C	H	O ^a	N	S	
<i>I. galbana</i>	67.2±0.61	6.61±0.01	23.4	52.94±0.65	7.93±0.16	28.49	6.71±0.06	4.02±0.04	8.0
<i>T. pseudonana</i>	59.8±1.24	6.29±0.01	21.9	47.68±0.34	7.67±0.02	34.44	5.49±0.04	3.91±0.13	7.6
<i>D. salina</i>	50.4±0.65	6.10±0.01	20.0	43.71±0.62	7.99±0.08	36.75	6.90±0.04	5.45±0.68	7.2
<i>N. oculata</i>	80.3±0.48	4.66±0.01	21.6	50.66±0.54	7.18±0.07	35.66	4.67±0.04	1.85±0.06	10.9
<i>C. vulgaris</i>	94.7±0.32	5.15±0.02	25.0	52.97±0.51	7.91±0.08	33.13	4.68±0.03	0.84±0.02	10.3
<i>Scenedesmus</i> sp.	83.9±0.05	7.36±0.00	21.5	46.51±0.29	6.89±0.07	38.82	6.32±0.03	0.42±0.02	6.3
PBR (Freeze dried)	82.0±0.03	8.40±0.00	24.4	54.18±0.65	6.77±0.11	29.86	9.63±0.10	0.79±0.02	6.4
Raceway	39.4±0.17	9.95±0.00	21.3	45.51±0.87	8.98±0.09	34.60	8.66±0.13	0.96±0.10	4.6

^a Oxygen calculated by difference based on determination of C, H and S by elemental analysis and N by TKN.

^b C/N ratio calculated using TKN on a VS basis

4.1.5.1 Concluding remarks

The characteristics of the eight samples analysed are relatively typical of other algal species reported within the literature. This research highlights the differences in the range of compositions that can occur when different micro-algal species are grown under identical conditions. When the same species, such as *Scenedesmus* is grown under laboratory conditions, within an open raceway, and within a PBR there are large differences in their compositions. This highlights the importance of not relying on laboratory grown species for characterisation in different systems.

4.1.6 BMP and theoretical energy values

The objective of this part of research was to determine the methane potential of the microalgae cultivated in section 4.1.4.

Methodology: Two BMP assays were conducted as outlined in Section 3.5.1, with an initial 28 day screening for the species *I. galbana*, *T. pseudonana*, *N. oculata*, *D. salina*, *C. vulgaris* and a PBR and raceway sample cultivated in Almeria, Spain. Analysis of the methane production kinetics revealed that the species *N. oculata*, *C. vulgaris*, and the PBR and raceway samples cultivated in Almeria, Spain, had not completely digested and an 88 day BMP was conducted for these species and for a sample of *Scenedesmus* cultivated as outlined in Section 3.3.

The two BMP assays were run consecutively, in each case using fresh inoculum taken from Millbrook wastewater treatment works within a one-month period.

Results

The BMP value for the cellulose controls in the 28-day and 90-day tests were 0.412 ± 0.007 and 0.415 ± 0.004 L CH₄ g⁻¹ VS respectively, with the difference of <0.5% giving confidence in the comparability of results from the two assays.

The results of the 28-day test are shown in Figure 46: it can be seen that the cumulative specific methane yield of some samples was still increasing by the end of the test, whilst other appeared to have reached their maximum. For this reason the second test was carried out on selected samples over a more extended period. Of the samples for which it appeared

possible to determine a BMP in the 28-day test, the two marine species *T. pseudonana* and *I. galbana* had the highest values at 0.435 and 0.349 L CH₄ g⁻¹ VS, respectively. This was considerably higher than the BMP of 0.276 L CH₄ g⁻¹ VS for *D. salina*, while *N. oculata* had not achieved its maximum potential in this period. The freshwater samples of *C. vulgaris* and the large-scale raceway and PBR materials did not reach their final BMP values but their specific methane yields after 28-days were 0.300, 0.216 and 0.130 L CH₄ g⁻¹ VS, respectively.

Figure 47 shows the results for cumulative specific methane yield in the 90-day BMP test. *N. oculata* showed an increase of ~22% above the 28-day value, with a cumulative specific methane production of 0.231 L g⁻¹ VS day⁻¹ which was taken as the BMP value. The difference for the freshwater species *C. vulgaris* was within the standard deviations of the two tests, and the final BMP was therefore taken as 0.307 L CH₄ g⁻¹ VS based on the 90-day test results. A laboratory-grown culture of *Scenedesmus* sp. was also tested and had a BMP of 0.261 L CH₄ g⁻¹ VS.

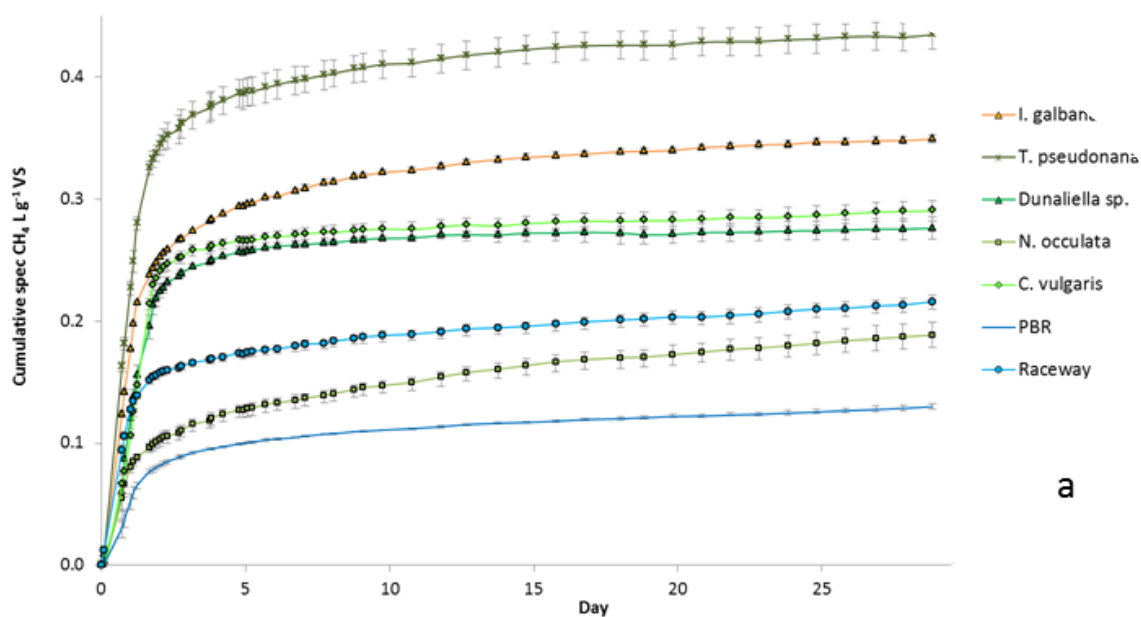


Figure 46 28-day BMP cumulative net specific methane yield of marine and freshwater microalgae, (a) and (b) 90-day BMP test

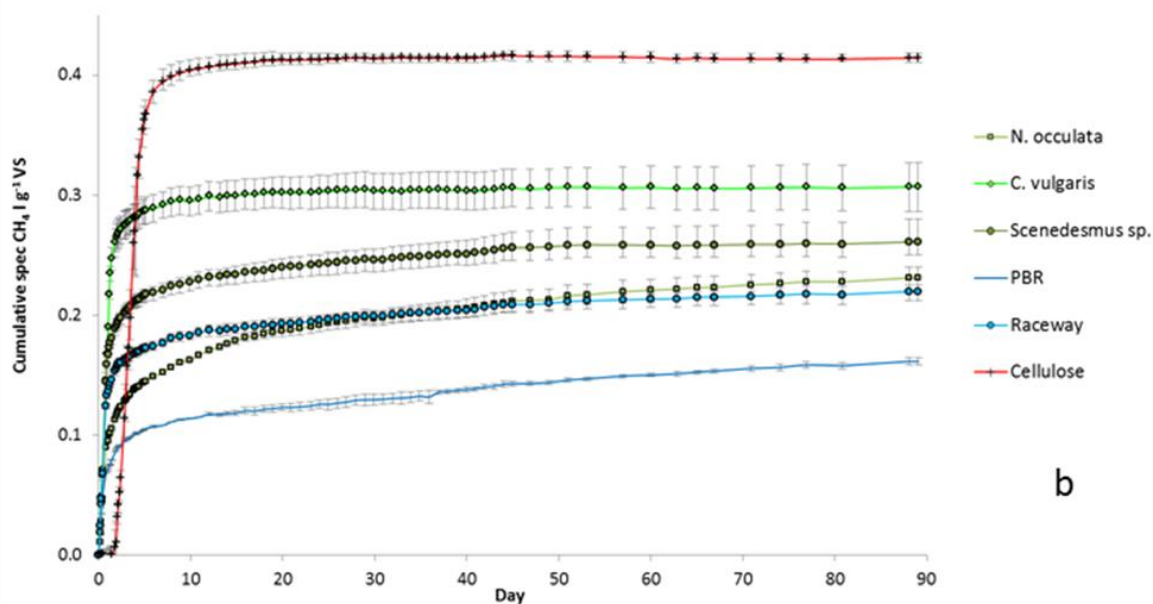


Figure 47 88 - day BMP cumulative net specific methane yield of marine and freshwater microalgae

The freeze-dried sample from the PBR and the fresh frozen raceway sample had measured BMP values of 0.161 and 0.220 L CH₄ g⁻¹ VS respectively, considerably below that of the laboratory-cultured *Scenedesmus*. The BMP of the raceway sample was also lower than might be expected based on the individual BMPs for the laboratory-grown samples of *Chlorella* and *Scenedesmus*, the two species comprising the main fractions of the raceway population. The extended test gave an increase of ~24% in the specific methane yield of the PBR sample, which appeared to be still rising slightly even after 90 days; but the raceway sample showed no significant change from the 28-day result and the 90-day value was therefore taken as the measured BMP.

The predicted theoretical methane production (TMP) values based on the Buswell equation were between 0.45-0.57 L CH₄ g⁻¹ VS. The greatest TMP was from the marine species, with *Scenedesmus* producing the lowest TMP at 0.445 L CH₄ g⁻¹ VS. The measured BMP values ranged from 30.0-88.2% of the TMP, indicating widely different degrees of VS breakdown. Measured CV expressed on a VS basis showed reasonable agreement with the theoretical CV values, giving some confidence in the elemental analysis results. The marine species *I. galbana* and *T. pseudonana* had the greatest apparent conversion efficiency of measured CV into methane, at 59.5% and 79.2% respectively, whereas the conversion efficiencies for *N. oculata* and the freshwater species were lower at 26.4% to 49.0% (Table 25).

Table 25 BMP, TMP and calorific values

Species	Measured BMP			TMP	Theoretical CV	BMP as % of TMP	Energy value of CH ₄ from BMP	% of CV converted to CH ₄ ^c
	L CH ₄ g ⁻¹ VS	±	0.004	L CH ₄ g ⁻¹ VS	kJ g ⁻¹ VS	%	kJ g ⁻¹ VS	
<i>I. galbana</i>	0.349	±	0.004	0.568	24.5	61.5	13.9	59.5
<i>T. pseudonana</i>	0.435	±	0.017	0.493	21.8	88.2	17.3	79.2
<i>D. salina</i>	0.276	±	0.011	0.455	20.9	60.7	11.0	55.1
<i>N. oculata</i> ^b	0.231	±	0.010	0.516	21.7	44.7	9.2	42.6
<i>C. vulgaris</i> ^b	0.307	±	0.029	0.566	23.4	54.2	12.2	49.0
<i>Scenedesmus</i> sp. ^b	0.261	±	0.017	0.445	19.6	58.7	10.4	48.3
PBR (FD) ^b	0.161	±	0.017	0.537	23.1	30.0	6.4	26.4
Raceway ^b	0.220	±	0.007	0.492	22.1	44.7	8.8	41.0

^a 28-day test; ^b 90-day test value; ^c based on measured CV

The BMP values for freshwater *C. vulgaris* and *Scenedesmus* sp. obtained in the current work are typical of median values found in the literature (Ward et al., 2014, Mussgnug et al., 2010, Frigon et al., 2013, Lakaniemi et al., 2013). Fewer results are available for marine species, but for the genera above the values of 0.408 L CH₄ g⁻¹ VS have been reported for *Isochrysis* sp. (Frigon et al., 2013), 0.38 and 0.265 L CH₄ g⁻¹ VS for *Thalassiosira weissflogii* (Frigon et al., 2013, Bohutskyi et al., 2014), 0.204 and 0.323 L CH₄ g⁻¹ VS for *Dunaliella salina* (Mussgnug et al., 2010, Mottet et al., 2014), and 0.204 L CH₄ g⁻¹ VS for *N. oculata* (Buxy et al., 2012).

4.1.7 Methane production kinetics

The kinetic coefficients were calculated using the BMP data from Section 4.1.5 and the method described in Section 3.5.2. The kinetic coefficients obtained from the methane potential tests are shown in Table 25. As these are from batch testing they cannot be used directly for continuous or semi-continuous digestion, but they do indicate the amenability of the material to digestion and the type of reactor and retention time likely to be required in a full-scale system. Several species showed a small delay in the onset of rapid gas production, especially in the first test, and the fit of the kinetic models for *I. galbana* and *D. salina* was considerably improved by imposing a lag phase of 0.3 and 0.5 days, respectively (Figure 48). Both BMP assays give similar kinetics for the same species suggesting a good agreement between analyses.

Table 26 Methane yields and kinetic constants obtained from modelling

	Y_{\max} (L CH ₄ g ⁻¹ VS)	P	k₁ day ⁻¹	k₂ day ⁻¹	R²^a	Lag day	Comment
<i>28-day values</i>							
<i>I. galbana</i>	0.350	0.71	1.93	0.15	0.9989	0.3	Almost at max in 28-day BMP
<i>T. pseudonana</i>	0.445	0.83	1.08	0.07	0.9937	0.1	Almost at max in 28-day BMP
<i>D. salina</i>	0.276	0.89	1.36	0.13	0.9980	0.5	At max in 28-day test
<i>N. oculata</i>	0.220	0.47	1.26	0.05	0.9977	0.1	Still rising in 28-day test
<i>C. vulgaris</i>	0.300	0.86	1.38	0.04	0.9882	0.5	Still rising in 28-day test
PBR (FD)	0.175	0.53	1.08	0.02	0.9942	0.3	Still rising in 28-day test
Raceway	0.220	0.70	1.55	0.06	0.9972	≤ 0.1	Still rising in 28-day test
<i>90-day values</i>							
<i>N. oculata</i>	0.231	0.55	1.20	0.04	0.9955	≤ 0.1	Possibly still rising slightly
<i>C. vulgaris</i>	0.307	0.92	1.22	0.07	0.9905	-	-
<i>Scenedesmus</i> sp.	0.261	0.77	1.70	0.05	0.9951	≤ 0.1	-
PBR (FD)	0.175	0.54	1.21	0.02	0.9945	-	Still rising slightly at end of test
Raceway	0.220	0.75	1.66	0.04	0.9956	≤ 0.1	-

^a R² values indicate correlation between experimental and modelled data

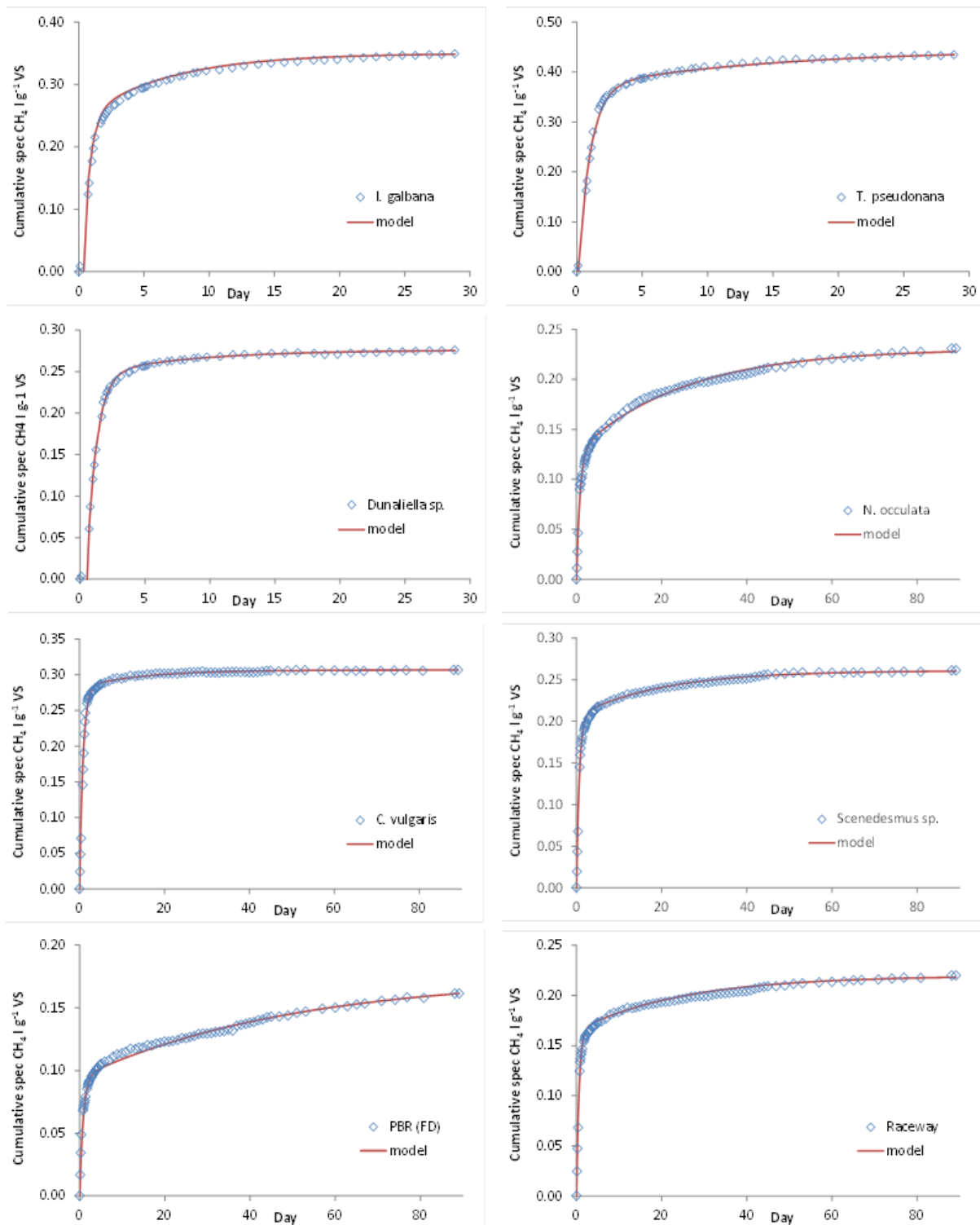


Figure 48 Cumulative net specific methane yield of marine and freshwater microalgae (average of experimental data points for replicates) with kinetic models

The proportion of anaerobically biodegradable material that was readily degradable was over 80% for *T. pseudonana*, *D. salina* and *C. vulgaris*, and over 70% for *I. galbana*, *Scenedesmus* sp. and the raceway sample; while for *N. oculata* and the PBR sample it was much lower.

Values for k_1 ranged from 1.08-1.93 day⁻¹ with the majority lying between 1.2-1.5 day⁻¹, indicating that the properties of the readily degradable fraction were similar in these cases. Values of k_2 showed more variability, ranging from 0.02-0.15 day⁻¹. The PBR sample had the lowest values for k_1 and k_2 . Samples tested for both 28 and 90 days showed similar kinetic coefficients in each case, giving some confidence in the results: final BMP values from the two tests were also similar apart from for *N. oculata*. The modelled BMP values were mainly similar to the experimental results, but modelling gave slightly higher BMPs for *I. galbana*, *T. pseudonana* and the PBR sample, indicating the need for a longer test duration in these cases.

4.1.8 Growth yield and effect on overall methane productivity

Growth yields for the laboratory-grown cultures were between 0.08-0.22 g VS L⁻¹ day⁻¹, with growth rates from 0.59 - 0.77 day⁻¹, as shown in Table 20 (section 4.1.2). The theoretical growth yields were much higher, and more consistent between the species from 0.295 – 0.38 g VS L⁻¹ d⁻¹. This is likely due to the inferred starting biomass concentration being much higher. Methane productivity per unit of culture volume was calculated using the modelled BMP values and the theoretical growth yield in g VS L⁻¹ day⁻¹ shown in Table 27. The highest value was for *T. pseudonana* at 0.16 L CH₄ L⁻¹ day⁻¹ and the lowest for *D. salina* at 0.08 L CH₄ L⁻¹ day⁻¹, both of which are marine species. *N. oculata* and *C. vulgaris* had similar methane productivities, with the lower methane potential of *N. oculata* being compensated for by its higher growth yield (Table 27). The two freshwater species had similar growth rates, but methane productivity was affected by both the growth yield and the BMP value: *Scenedesmus* sp. was not only poorly degradable, which has also been reported by other researchers (Ward et al., 2014, Frigon et al., 2013, Lakaniemi et al., 2013), but also had a lower VS/TS ratio in the harvested biomass. The same was true for the marine species *I. galbana* and *D. salina*, where the growth rates were similar but the growth yield of *D. salina* was half that of *I. galbana* due to the low VS content of the harvested biomass, while the VS itself proved recalcitrant to conversion in the BMP test. Reported data for the raceway sample (Tran et al., 2014) indicates a growth yield of around 0.04 g VS L⁻¹ day⁻¹, giving a methane productivity of only around 0.01 L CH₄ L⁻¹ day⁻¹ for the period considered.

Table 27 Growth rates and growth yields (from section 4.1.2) with potential methane production per litre of culture per day for selected samples of freshwater and marine microalgae.

Species	Modelled BMP	Doubling rate	Maximum dilution rate ^(b)	Growth yield	
	L CH ₄ g ⁻¹ VS	day ^{-1(a)}		g VS L ⁻¹ day ^{-1(c)}	L CH ₄ L ⁻¹ day ⁻¹
<i>I. galbana</i>	0.35	0.61	1.64	0.305	0.11
<i>T. pseudonana</i>	0.445	0.71	1.41	0.355	0.16
<i>D. salina</i>	0.276	0.59	1.69	0.295	0.08
<i>N. oculata</i>	0.231	0.77	1.30	0.385	0.09
<i>C. vulgaris</i>	0.307	0.75	1.33	0.375	0.12
<i>Scenedesmus sp.</i>	0.261	0.76	1.32	0.38	0.10

^a Measured by OD and calculated on a total suspended solids and volatile solids basis.

^b Maximum dilution rate calculated from the doubling rate.

^c Theoretical growth yield under continuous dilution per unit volume of reactor with an initial volatile solids content of 0.5 g VS L⁻¹.

4.1.9 Discussion of algal screening

There is as yet no single widely-accepted protocol or duration for a BMP assay for biomass samples, although the International Water Association's Task Group on Anaerobic Biodegradation, Activity and Inhibition (ABAI) has provided guidelines on key requirements for a test protocol (Angelidaki et al., 2009). In most cases the 28-day BMP test used here gave a reasonable approximation of the final values obtained from the 90-day test and from modelling, providing some confidence in the method used and in the validity of the results. When using this approach, however, it is essential to comment on whether the cumulative methane yield has reached its maximum by the end of the test period: otherwise the result should not be considered as the final BMP value. BMP assays carried out over a fixed or short period do not necessarily provide reliable comparative values, especially for micro-algal material which may continue to be degraded for 90 days or more.

The range of BMP values found in the present work was wide, even when reported on a VS basis, indicating that a proportion of the organic matter is either non-biodegradable or protected from biodegradation by incorporation into structural cell material: this is analogous to the situation in terrestrial plants, in which the cellulose in woody biomass is protected by a

non-degradable lignin fraction. Although lignin is not a component of algal cells, similar cross-linked macromolecular structures exist in the cell walls offering protection to the cell contents or simply making the cell wall carbon non-digestible (Roberts, 1974, Gerken et al., 2013). Mussgnug et al. (Mussgnug et al.) noted that *Scenedesmus obliquus* and *Chlorella kessleri* have hemicellulose-containing carbohydrate-based walls which make them tougher to digest, *S. obliquus* especially so as it contains a sporopollenin-like biopolymer. Gerken et al. (Gerken et al., 2013) in a detailed study of the susceptibility of *C. vulgaris* and other microalgae to enzymatic degradation noted that major changes in cell wall composition might depend on very small differences in growth conditions, as well as on culture age. To draw firm conclusions on the significance of these factors for anaerobic digestion of micro-algal biomass, and on the optimum strategies to enhance degradation, further fundamental work is required looking at the composition and molecular structure of micro-algal cells, possibly coupled with cell fractionation to ascertain where the recalcitrant fractions lie.

The laboratory-grown species tested showed a range of growth rates and yields under the conditions used, both of which influenced the overall methane productivity. Although BMP values are often quoted with the aim of providing an indication of the energy potential of a biomass crop, it is equally or even more important to consider the overall biomass productivity per unit of production capacity. This concept is commonly applied when looking at terrestrial energy crops, where net energy production is considered in GJ per hectare-year (Salter and Banks, 2009). The combination of growth rates and methane yields obtained under standard conditions used in the present work provides a possible approach to providing equivalent information on algal biomass crops; but further data on the energy inputs to algal cultivation systems are needed for determination of overall energy balances (Chisti, 2007, Benemann, 2008).

In most cases the growth rates obtained in the conditions used were lower than literature values for maximum growth rates, for the reasons already noted above (Renaud et al., 2002, Berges et al., 2002, Thompson, 1999, Jitts et al., 1964, Sandnes et al., 2005, Goldman and Graham, 1981, Hoogenhout and Amesz, 1965, Cole and Wells, 2008). When considered on the basis of growth yields, however, the values obtained are similar to those that might be expected from larger-scale open systems. Algal growth yields in raceway systems are normally quoted on an areal rather than a volumetric basis. If the volumetric growth yields achieved are converted to areal values by assuming a typical water depth of 0.2 m, the results

would range from 27-55 g VS m² day⁻¹, in the mid-to-upper range of reported values for open raceway systems (Tran et al., 2014, Banks et al., 2011). For the purposes of offering a practical testing protocol, the growth conditions used may therefore be considered an appropriate choice, as the micro-algal yields achieved are representative of those in large-scale systems that are operating very effectively.

Growth yields for the laboratory-grown *C. vulgaris* and *Scenedesmus* sp. were much higher than those estimated for the raceway culture. In large-scale systems there are likely to be limitations due to factors such as light, temperature, dissolved oxygen concentration and the applied dilution rate. It is not known how or to what extent these factors may also affect the degradability of the micro-algal biomass, and hence its BMP. The BMP value of the freeze-dried PBR sample was much lower than either the laboratory culture of *Scenedesmus* sp. or the raceway sample, however, with one possible explanation being the loss of more readily-degradable volatile organic compounds through sublimation during the freeze-drying process. The low values found for the kinetic constants P and k_I in modelling the PBR sample may give support to this view. Reductions in BMP values have also been reported after oven drying of *Chlorella kessleri* and *Chlamydomonas reinhardtii* (Mussnug et al., 2010). Further work is clearly needed on the likely impact of growth conditions and of post-harvest storage and processing on digestibility.

The marine species *T. pseudonana* appeared to be the first choice for methane production, with an overall energy conversion of 79.2% of its calorific value and a good growth yield. It should be remembered, however, that good performance in laboratory conditions may not translate to large-scale systems where ease of cultivation, sustainable high productivity and resistance to predation are also key factors. This species, however, was subject to sudden or continuous culture crashes. The next best performances were from the marine *I. galbana*, closely followed by the marine *N. oculata* and freshwater *C. vulgaris*. While *C. vulgaris* achieved 90% of its BMP value within the first 3 days of the test, however, *N. oculata* required 77 days (Figure 2): the difference is clearly visible in the respective values of the kinetic coefficients P and k_I . This difference in degradation behaviour may have significant implications for the required retention time, reactor volume and operating costs in large-scale continuous digestion systems. It is also notable that the BMP value for *N. oculata* was much lower than for *C. vulgaris*, while the value for *C. vulgaris* was only 70% that of *T. pseudonana*: the three species achieved respectively 44.7, 54.2 and 88.2% of their TMP values (Table 2). The development of effective pre-treatments to enhance degradability is

thus likely to have a major influence on the choice of species, especially given the variability of reported BMP values even for a single species (Ward et al., 2014, Frigon et al., 2013, Lakaniemi et al., 2013). Harvesting and storage methods may themselves act as pre-treatments (Samson and Leduy, 1983b, Gerken et al., 2013), with both freezing and centrifugation potentially capable of rupturing cells and thus leading to increased methane yields or improved production kinetics. *T. pseudonana* has a solid silica cell wall consisting of two frustules, which can open during centrifugation: this may have contributed to the high values for BMP and for TMP conversion on a VS basis compared to those for the microalgae with organic cell walls in the current study. The differing BMP values of 0.265 and 0.38 L CH₄ g⁻¹ VS reported for the diatom *Thalassiosira weissflogii* (Bohutskyi et al., 2014) could thus reflect whether the harvesting technique was able to cause frustule separation.

There is a significant difference between the species BMP analysed of 0.031, however between the fresh water and marine groups there is no significant difference with P values at 0.1. This suggests that if mixed species were cultivated there would be potentially be no significant difference between marine and freshwater methane potentials, however, if grown as a mono culture the methane potential variation would be significant.

Ammonia is known to be inhibitory to methanogenesis, though there is some debate about toxicity thresholds, in part because microbial populations can acclimatise to high concentrations to some extent (Chen and Oswald, 1998). The Buswell equation allows estimation of the theoretical maximum amount of ammonia that could be produced from degradation of the micro-algal biomass. For the samples tested, assuming a feedstock VS concentration of 5% the maximum theoretical ammonia concentration would range from 2.3 g N L⁻¹ for *N. oculata* to 5.0 g N L⁻¹ for the raceway sample. These values are below the toxic range for mesophilic digestion, but would be problematic in thermophilic digestion, where inhibition can occur at concentrations > 1.7 g N L⁻¹ (Yenigün and Demirel, 2013). At a feedstock VS content of 10% the maximum ammonia concentrations would double, and could cause the onset of inhibition in mesophilic conditions. Alternatively, a crude estimate could be made of the maximum solids concentration at which the micro-algal material could be digested without exceeding a limiting ammonia concentration, based on the total N or TKN content and the degree of breakdown of the biomass as indicated by the proportion of CV recovered as methane in the BMP test. For the samples tested, based on measured TKN and BMP values and assuming limiting TAN concentrations of 6.0 and 2.5 g N kg⁻¹ WW for

stable mesophilic and thermophilic digestion respectively, the maximum feedstock VS content would range from 12.0 % VS for *T. pseudonana* to 30.2 % VS for *N. oculata* in mesophilic conditions, and from 5.0 to 12.6% VS in thermophilic conditions, respectively. These values do not take into account the reduction in the mass of digestate produced compared to that of feedstock added. This has the effect of increasing the digestate TAN concentration: a correction for this can also be estimated, based on the mass of biogas produced in the BMP test. In practice, however, this method of estimation of maximum feedstock concentrations is conservative, as some of the ammonia released is taken up to meet the growth needs of the anaerobic microbial consortium. The quantity of anaerobic microbial biomass and the digestate ammonia concentration in a digester are functions of the organic loading rate (OLR), the hydraulic retention time (HRT) and the type of substrate (Lindorfer et al., 2012), but relationships between these factors are not sufficiently well understood to allow more accurate predictions. It should be noted, however, that improving the degree of biomass degradation may lead to higher TKN conversion, and thus to lower optimum post-harvest concentrations (Heaven et al., 2011). The low C/N ratio for all the algal species suggests that ammonia toxicity/inhibition may be a risk in non-acclimatised systems at the moderate to high algal biomass feedstock concentrations required to reach high OLR (Yen and Brune, 2007). This could be avoided by co-digestion with another waste stream with lower TKN content or, for readily degradable algal species, by using a more dilute feedstock to enable a short HRT (Yen and Brune, 2007). The latter option would reduce harvesting costs, but would increase the digester and feedstock heating requirement per unit of biomass and thus affect the overall energy balance.

Although three of the marine species appeared to be good candidates for methane production in continuous culture the micro-algal cells can accumulate sulphur. This is, however, insignificant compared to the culture medium values of SO_4 with less than $50 \text{ mg SO}_4 \text{ g}^{-1} \text{ VS}$ of the highest marine species compared to the concentrations of sulphate in the seawater with, on average 2800 mg L^{-1} as SO_4 (Sarmiento and Gruber., 2006). In anaerobic digestion sulphate will be converted to hydrogen sulphide if sulphate-reducing bacteria (SRB) are present, and at lower concentrations the competition for fermentative substrate between SRB and methanogens will reduce the maximum methane productivity. At higher concentrations sulphides are inhibitory and toxic to methanogenesis (Chen and Oswald, 1998). The speciation and partitioning of sulphur compounds is dependent on pH and redox conditions, but the amount present in both the biomass and the growth medium may affect the optimum

solids concentration for harvesting and digestion. The greatest source of available sulphur is likely to be from the culture medium in which the biomass is suspended, as this can contain up to 1000 times more sulphur than in the biomass. Based purely on the Buswell equation, however, the maximum possible H₂S concentrations would range from 3400 ppmv for the laboratory-grown fresh water *Scenedesmus* sp. suspended in its original culture media to 44600 ppmv for the marine *D. salina*, with values above 10000 ppmv for all of the marine species within the saline culture media. All of these are problematic in downstream biogas use.

Salinity is a further issue for marine species, due to toxicity from light metal cations and particularly sodium: in this case, however, the solids concentration of the micro-algal feedstock and the reactor retention time are likely to have relatively little effect as the operating concentration of these ions is likely to be close to that in the growth medium. Excluding outliers, such as the value of 60 g Na L⁻¹ based on interpolation between 20.8 and 120 g Na L⁻¹ under batch conditions (Aspe et al., 1997), reported tolerances for sodium in non-acclimated mesophilic consortia are generally < 12.0 g Na⁺ L⁻¹ (Chen and Oswald, 1998), which is considerably below the average concentration found in seawater. The main ions in sea water (Na⁺, K⁺, Mg⁺ and Ca²⁺) are required in moderate concentrations for microbial growth and can have both an inhibitory and stimulating effect (Chen et al., 2008), but at sea water salinity adaption may be required before full-scale anaerobic digestion of marine material is considered (Feijoo et al., 1995, de Baere et al., 1984). Thus it is likely that simple acclimatisation protocols will have to be developed to generate inoculum for large-scale commercial operation, in order to avoid the need for expensive washing procedures.

4.1.10 Conclusions from algal screening

The study indicated that some species are easier to cultivate and more resilient than others, with *D. salina* and *N. oculata* providing consistent mono cultures. Reducing the sulphate content of the culture media below 20 mg L⁻¹ can cause culture crashes, while increases in the concentration of total JM above double the recommended concentration give diminishing returns. It was decided that subsequent cultures are grown on full strength JM to ensure all nutrients are adequately present for growth.

The work confirmed other studies that have shown wide variability between different micro-algal species, especially when grown under different conditions, with respect to their potential as substrates for methane production through anaerobic digestion. Although biochemical methane potentials were consistent with median values reported in the literature, few generalisations could be made: there was no evidence that marine species were better candidates compared to freshwater species or vice versa; the percentage of volatile carbon convertible to biogas differed considerably, as did rates of degradation under anaerobic conditions; and similar species grown in different conditions (laboratory or large-scale cultivation) showed little uniformity. The results clearly indicate that a much deeper knowledge of the factors affecting the degradability of micro-algal biomass is desirable for understanding the heterogeneity of this material as a potential renewable energy source via this route. The current work went some way towards establishing a potential protocol for the screening of algal biomass taking into account not only its inherent anaerobic biodegradability but also its likely productivity as expressed by the growth yield, under standard conditions in each case.

T. pseudonana had the highest BMP of all the species examined, followed by *I. galbana*, *N. oculata* and *D. salina*. When growth yield was considered, however *I. galbana* gave the greatest methane production $L\ CH_4\ L^{-1}\ day^{-1}$. *T. pseudonana* cultures regularly experienced culture crashes, and it was therefore decided to examine *I. galbana* due to the high biomass and methane production and *D. salina* due to its higher BMP than *N. oculata*. *N. oculata* has been widely studied by others under batch and continuous conditions (Schwede et al., 2013, Park and Li, 2012, Frigon et al., 2013, Alzate et al., 2012), with only batch studies for *D. salina* (Mottet et al., 2014, Mussnug et al., 2010).

4.2 Acclimatisation of municipal wastewater bio-solids to salt

4.2.1 Introduction

The focus of this research was to distinguish the effects of salinity from chloride and sulphate salts, and the adaption of readily available municipal wastewater bio-solids to estuarine/marine concentrations of Na, Mg, Ca, K, Cl and SO₄, for the subsequent use as an inoculum source for the AD of marine microalgae. It was identified within the literature review that these ions could become inhibitory/ toxic at the concentrations observed within a marine system. Municipal sewage sludge was gradually adapted to the high inorganic solid content with the specific methodology and results outlined below.

Objective: Determine the effect of marine concentrations of Na, Mg, Ca, K, Cl and SO₄ on inoculum from a mesophilic municipal wastewater bio solids treatment plant, and develop an inoculum for the AD of marine microalgae.

Methodology: The experiment was divided into four main phases:

Phase 1 – This was an initial preliminary experiment. In Phase 1 the inoculum from a mesophilic anaerobic digester treating municipal sewage sludge was decanted into five pairs of reactors (R), with four pairs augmented with different loading regimes of Cl, Na, Mg, Ca and K at molar ratios of 1:0.83:0.05:0.02:0.02, similar to mean ocean values. Reactors R1 and R2 were augmented to 8g L⁻¹ of total salt within the feedstock only, reactors R3 and R4 to 16 g L⁻¹ within the feedstock only, reactors R5 and R6 to 10g L⁻¹ as a spike and maintained within the feedstock, R7 and R8 to 8 g L⁻¹ via the feedstock only using the commercial salt mix USSS, and R9 and R10 as controls with no added salt (Table 28). All reactors were then fed on a synthetic wastewater made up to the same salinities as the original salt spike or required salt concentration, at an organic loading rate (OLR) of 2.1 ± 0.1 g VS L⁻¹ and a HRT of 15 days in mesophilic conditions (35±0.5°C). On day 13 R5-6 was adjusted (spiked) on day 13 to a salt concentration of 10 g L⁻¹ and the reactors were fed with Synthetic wastewater made up to a 10% concentration of mixed chloride salts. In R1-4 and R7-8 there was no spiking of the inoculum, and salt was introduced as part of the daily feed at the concentrations shown in

Table 28. R1-4 received dilutions of the stock mixed chloride salts, and R7-8 USSS mix. R9-10 were maintained as controls using Synthetic wastewater without any salt addition.

Phases 2 and 3 - After the preliminary trial (Phase 1) the ten reactors were emptied and re inoculated with fresh inoculum starting Phase 2. Reactors 1-8 (R1-R8) were initially spiked and supplemented to between 6–9 g L⁻¹ of salt. This concentration was maintained for an initial period of 64 days to allow adaption to the change to the synthetic wastewater feedstock. R9 and R10 were maintained as controls at 0 g L⁻¹ throughout the duration of the experiment. During Phase 3 (days 65-400) R1-R8 were increased by 1.0 g L⁻¹ HRT⁻¹ until day 347 where all reactors were brought up to a total salt concentration of 31.1 g L⁻¹. The details of each phase are given in

Table 28 and the incremental increases in total salt are shown in Figure 49.

Table 28 – experimental design for each of the four main phases.

Phase	Day	Added	R1&2	R3&4	R5&6	R7&8	R9&10			
1	1-40	Salt g L ⁻¹	8 (feed only) ^a	16 (feed only) ^a	10 (spike and feed) ^a	8 (feed only) ^b	0 (control)			
2	1-64	Salt g L ⁻¹	6	7	8	9	0 (control)			
3	65-400	Salt g L ⁻¹	Additional salt in salt-supplemented digesters and in feed increased by 1 g L ⁻¹ every 14 days up to day 350, then raised to 31.1 g L ⁻¹							
			F1	F2	F3	F4	F5	F6	F7	F8
4	400-580	Salt g L ⁻¹	31.1	31.1	31.1	31.1	31.1	31.1	31.1	31.1
		SO ₄ g L ⁻¹	0	0.16	0.79	1.58	2.36	3.15	3.94	4.73

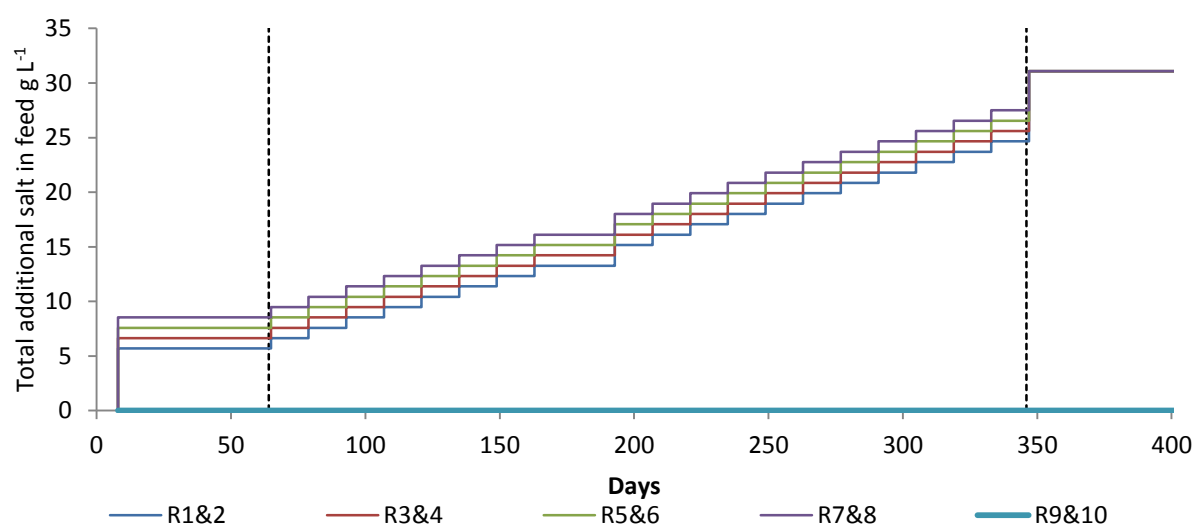


Figure 49 incremental increases in total salt content in feed and in digester contents during Phase 2 and Phase Three.

Phase 4 - In Phase 4 effluent from Phase 3 at 375 days was homogenised from R1-R8 and stored within a 4 L CSTR operated under the same conditions until use. 400 ml of the effluent was decanted into eight 500 ml Erlenmeyer flasks. The flasks were spiked with MgSO₄ to give initial SO₄ concentrations as shown in

Table 28. The flasks were then fed in the same way as the CSTRs to give the same HRT and OLR, the only difference being the adjustment of the sulphate concentration in the salt mix added to the Synthetic wastewater.

4.2.2 Substrate characteristics

Measured values for key properties of the Synthetic wastewater are shown in Table 29. The TKN value was 10.54% of the VS, almost double that of the elemental analysis result at 6.52%. This is likely to be due to the use of inorganic nitrogen as urea and ammonia which is observed in the TKN analysis but not the elemental analysis (EA). As a high proportion of inorganic nitrogen was added to the Synthetic wastewater as urea and ammonia it was decided to use the elemental analysis result for nitrogen rather than the TKN value for the TMP and theoretical calorific value (TCV) calculations as this would give a more representative analysis of the organic nitrogen content. Based on these results the maximum TMP according to the Buswell equation was 0.452 L CH₄ g⁻¹ VS added, and the TCV was around 20.0 MJ kg⁻¹ VS.

Table 29 Results of characterisation of the Synthetic wastewater.

Parameter	Unit	Value	
COD	g L ⁻¹	46.1	± 1.00
TS	g kg ⁻¹ WW	32.2	± 0.04
VS	%TS	90.1	± 0.01
TKN	g kg ⁻¹ WW	3.9	± 0.10
<i>Elemental composition</i>			
C	% VS	49.59	± 2.12
H	% VS	6.2	± 0.06
N	% VS	6.52	± 0.22
S	% VS	0.31	± 0.03
	L CH ₄ g ⁻¹		
TMP	VS	0.452	
TCV	MJ kg ⁻¹	20.0	

4.2.2.1 Atomic absorption

The constituent salts for the artificial salt medium were dried in an oven at 105°C to determine the water content by weight. An artificial salt solution was made at 10 x the concentration described in section 3.2.5 and analysed via atomic absorption. The results from the atomic absorption of the artificial salt solution show a similar return of the total mass of the metal ions to the dry mass of the salt, with NaCl, KCl and MgCl₂ 6H₂O returning around 100%. CaCl₂ yields a return of 73% of the expected. Lanthanum chloride was added to reduce any depression in absorbance from Al, Be, P, Si, Ti and Zr but no KCl was added as this was being analysed within the sample, potentially reducing the absorbance (Table 30). The analysis of the salt content as a dried sample and via AA when made into a salt solution shows that NaCl and KCl were dried samples and their concentrations were correct in the formulation used. CaCl₂ and MgCl₂.6H₂O are both deliquescent and hygroscopic. For this reason the water content increased within the bulk chemical reducing the concentration of salts added. The sample from the AA is an original sample from the first formulation using the same salt bulk chemicals. The dried samples are the bulk chemicals several months after analysis had ceased. The similarity between AA to the ashed gives a high confidence that there was a uniform addition of salts to the reactors, with only CaCl₂ showing the greatest difference. This, however, is one of the minor salt constituents at ~3% of the total salt content and as such does not affect the overall total salinity. This has subsequently been corrected throughout the report.

Table 30 Dried salt samples correction and observed % mass of metal ions in salt stock solution measured using the AA.

Salt	%TS of WW	% after ash WW	Expected similarity ¹ %	Similarity ² %	AA % of expected ¹	% Similarity of AA to ashed
NaCl	100	100	100	100	97	97
MgCl ₂ 6H ₂ O	78	26	47	56	28	107
KCl	100	100	100	100	97	97
CaCl ₂	92	89	100	89	65	73

¹ is the calculated expected similarity between the measured value and the dried value calculated from the chemical composition.

² Measured similarity between wet weight value and dried value.

³ Similarity between the measured value of the salt solution using the AA and the dried weight.

4.2.3 Phase 1 – preliminary trial

A preliminary study was conducted to determine the maximum concentration of salt that can be added in an initial spike to the source inoculum. As a commercial salt mix (USSS) had been used in the marine microalgae (a brand recommended by the Culture Collection of Algae and Protozoa) growth trials and substrate characterisation in section 4.1 this was investigated alongside laboratory sourced salts.

Specific methane production (SMP) and volumetric biogas production (VBP) in R5 and R6 supplemented to 10 g L⁻¹ of salt fell as soon as the digesters were spiked to the target concentration (Figure 50a and b), and continued to decline steadily. VBP, SMP and biogas methane content in digesters R3 and R4 with feed-only supplementation to 16 g L⁻¹ began to fall from day 23, and declined even more rapidly. The start of this decline in biogas production corresponded to an estimated dilute-in salt concentration of 9 g L⁻¹. These changes were accompanied by a steady fall in pH and a rise in IA/PA ratio caused by a decrease in partial alkalinity and an increase in intermediated alkalinity (Figure 51a – e). This was accompanied by an increase in VFA concentration (Figure 52), and on day 35 feeding of digesters R3-6 was stopped. In the following days there was little or no recovery in biogas production or pH. Gas production and other parameters in digesters R1 and R2 and R7 and R8 supplemented at 8 g L⁻¹ was similar to that in the controls, with no obvious difference between the laboratory and commercial sea salt. TAN stabilised for all reactors at between 2.5-2.7 g N L⁻¹ (Figure 51f). There was a small increase in VFA concentration in these digesters from around day 30 (Figure 52): the reasons for this are not known, but similar transient VFA peaks of this type have previously been observed when inoculum from this source is acclimated to a new feedstock (unpublished data, University of Southampton). g TS L⁻¹ for the all reactors decreased prior to the addition of salt to 1.9-2.1 g TS L⁻¹, remaining constant for R1 and R2 at ~ 2% TS of WW, and ~1.8% TS of WW for R7 and R8. R5 and R6 initially increase to ~2.7 g TS L⁻¹ with the initial addition of salt, decreasing to ~2.3% TS of WW as the TS from the inoculum is diluted out. R3 and R4 TS% of WW increases after salt addition over 20 days to ~2.5% TS of WW. R9 and R10 showed a reduction in TS concentration over the 40 day period to 1.3% TS of WW. VS content for all reactors decreased for all reactors over the 40 day period from 2.0% VS of WW to 0.9% VS of WW (Figure 53). Based on these results, it was concluded that the inoculum was unable to adapt to shock salt additions of ≥ 10 g L⁻¹ and it was therefore decided to test a range of initial salt additions

from 6-9 g L⁻¹ in Phase 2 of the work using a synthetic sea salt mixture using mean ocean concentrations of the six main ions. The results supported the findings of McCarty (1964) that salt concentrations ≥ 10 g L⁻¹ total salt cause strong inhibition of the methanogens, however, fermentative bacteria showed no noticeable decline in activity with increases in VFA concentration show in Figure 52.

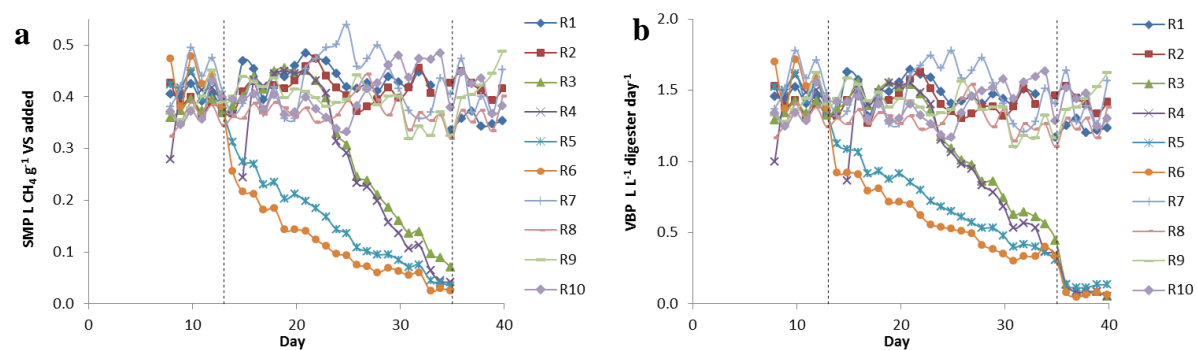


Figure 50 SMP and VBP for Phase 1 reactors. Vertical dotted lines indicate salt spiking and/or start of salt supplementation to feed on day 13 and cessation of feeding for R3-6 on day 35

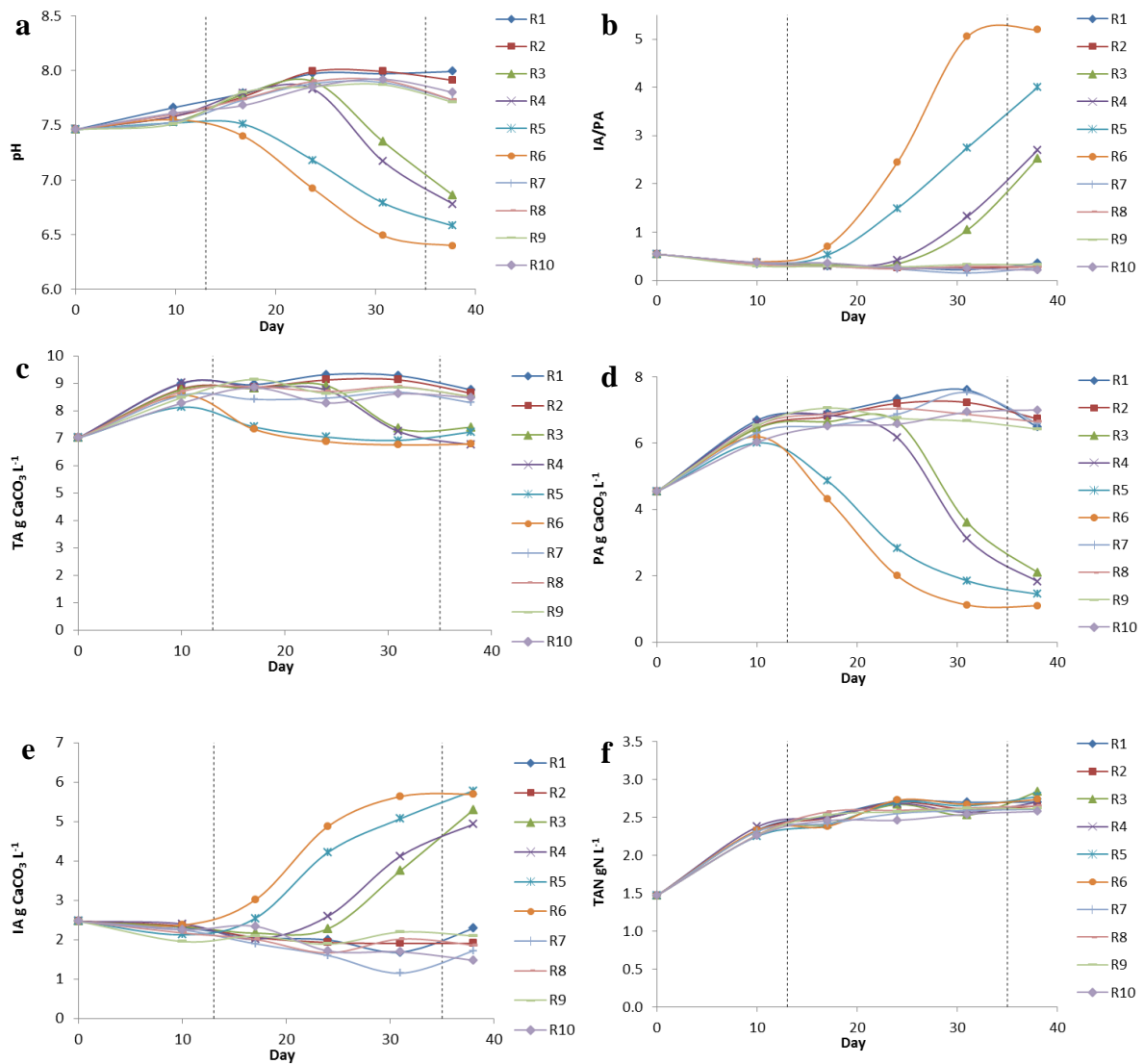
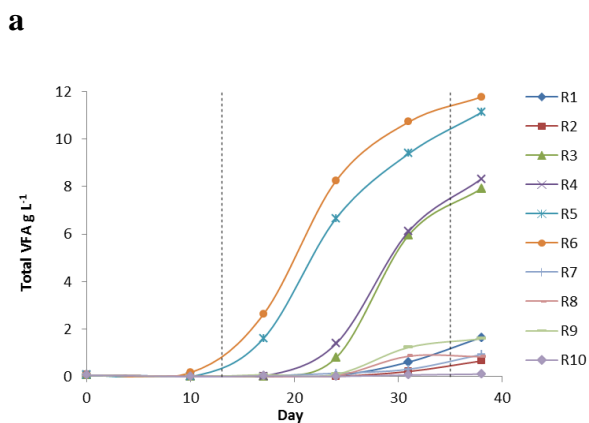
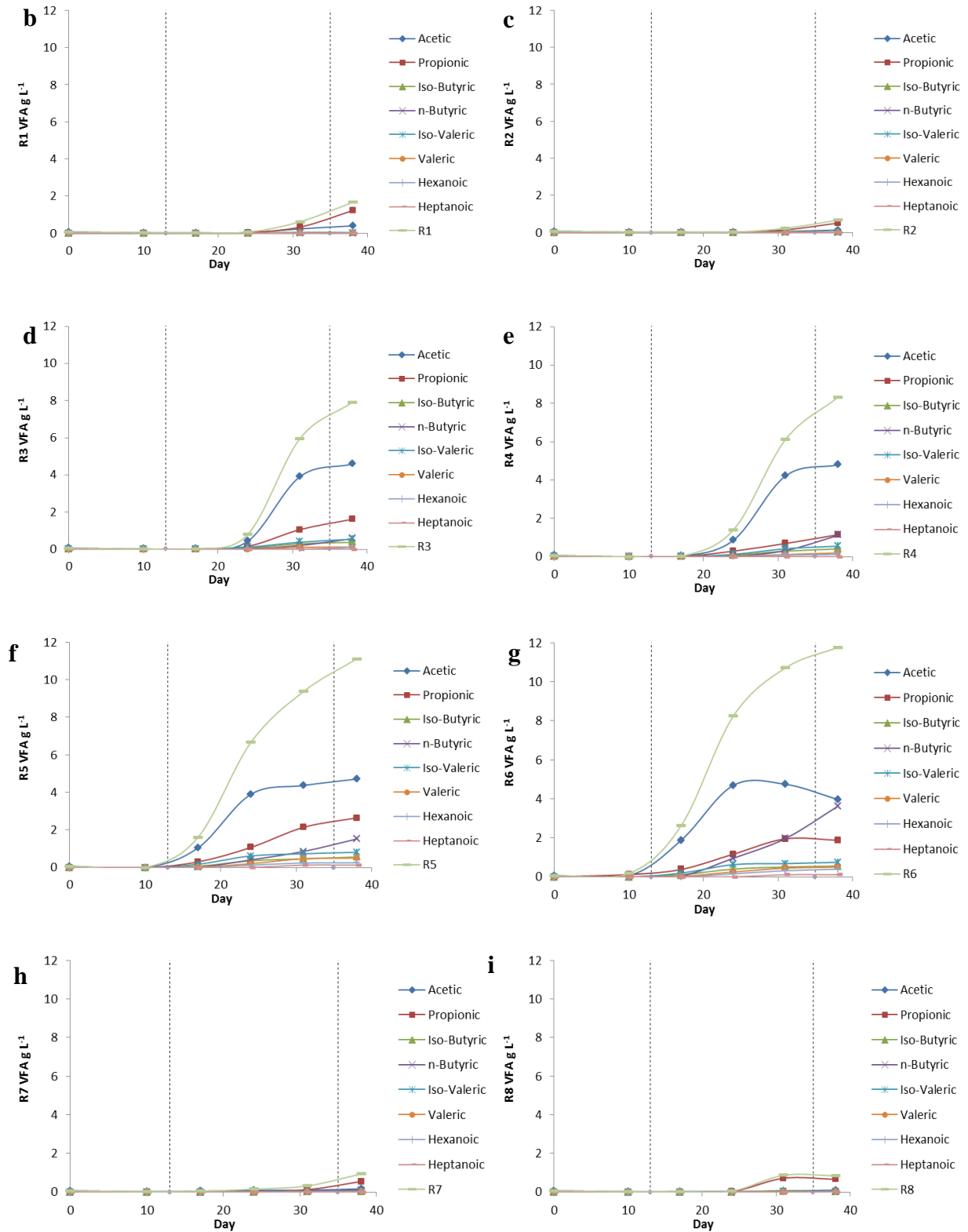


Figure 51 pH (a), TAN (b), IA/PA ratio (c), Total alkalinity (d), Partial alkalinity (e), Intermediate alkalinity (f). Vertical dotted lines indicate salt spiking and/or start of salt supplementation to feed on day 13 and cessation of feeding for R3-6 on day 35.





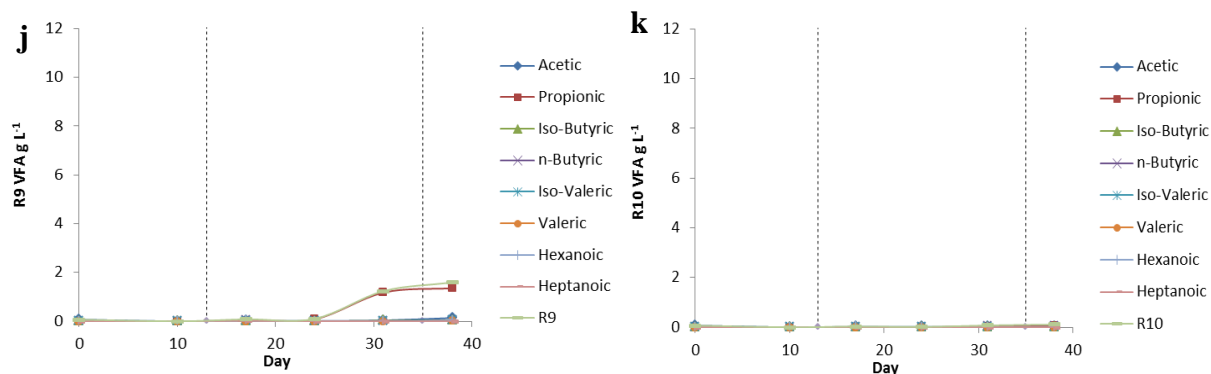


Figure 52 (a) Total VFA g L^{-1} , VFA species for reactors: R1 (b), R2 (c), R3 (d), R4 (e), R5 (f), R6 (g), R7 (h), R8 (i), R9 (j) and R10 (k). Vertical dotted lines indicate salt spiking and/or start of salt supplementation to feed on day 13 and cessation of feeding for R3-6 on day 35

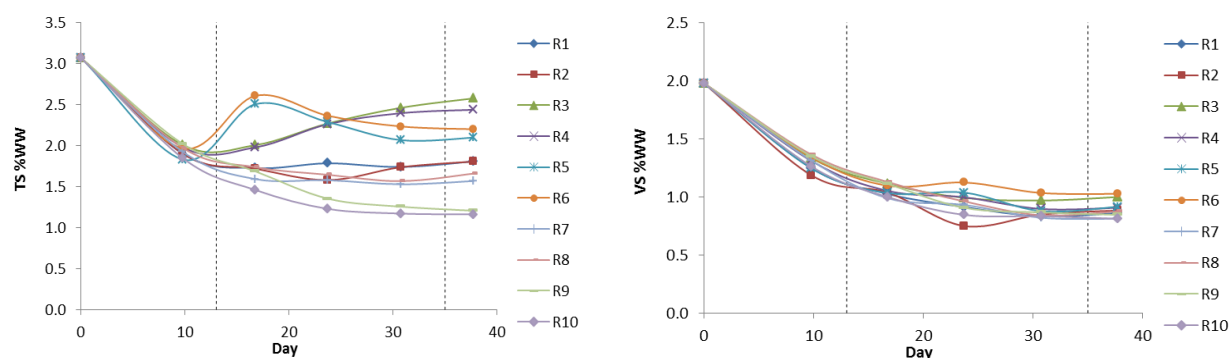


Figure 53 TS % WW and VS % WW

4.2.4 Phase 2 and Phase 3

4.2.4.1 Biogas production and methane yield

During the initial start-up of Phase 2 volumetric biogas production (VBP) increased to between $1.6 - 1.7 \text{ L L}^{-1} \text{ day}^{-1}$, from the low value of $\sim 0.75 \text{ L L}^{-1} \text{ day}^{-1}$, as the inoculum was starved for 24 hours prior to inoculation and start up (Figure 54a). At day eight all reactors exhibited a slight decrease in VBP to day 41, increasing towards the end of Phase 2 at day 68. Percentage methane content decreased from $\sim 67\%$ to 62% over the initial ten days, increasing to $66.1 - 67.8\% \text{ CH}_4$. All duplicate reactors showed a stable SMP, with R1 and R2 at 0.42 , R3 and R4 at 0.40 , R5 and R6 at 0.40 , R7 and R8 at 0.39 and R9 and R10 at 0.38 L

$\text{CH}_4 \text{ g}^{-1} \text{ VS}$ added. The lower SMP of the control reactors may be due to a stimulating effect caused by the addition of salt increasing methane production in the salt spiked reactors (Chen et al., 2008). Reasons for the lower SMP, however, are difficult to attribute over the initial start-up period due to the adaption of the inoculum to a new feedstock, organic loading rate and the addition of salt. At the end of Phase 2 average volumetric biogas production (VBP) and specific methane production (SMP) in all digesters apart from R7 appeared to show a slight downward trend with increasing salt addition (Figure 54c and d). The controls R9 and 10 achieved 92% of the TMP and conversion of 83% of the TCV into CH_4 . The SMP of digesters R1 and 2 supplemented at 6 g L^{-1} was equal to that of the controls, while R8 with 9 g L^{-1} salt addition achieved 83% of the TMP and 76% conversion of TCV.

After Phase 2 reactors were spiked with an increase in total salt by 0.9 g L^{-1} every 14 days in both the reactor and feed. Each increase in total salt caused a slight decrease in VBP and SMP before returning towards the controls. The average weekly SMP remained relatively stable throughout Phase Three with the average VBP and SMP of the salt-supplemented reactors was lower than that of the controls, although R1 and especially R5 showed good gas production. R1 and R2 observed a decrease in VBP and SMP between days 225 and 274 as they were not fed. Percentage methane content also remained relatively stable throughout all experimental phases between 63 and 68% CH_4 , with small fluctuations in the composition during Phase 2 due to a greater sampling rate (Figure 54b).

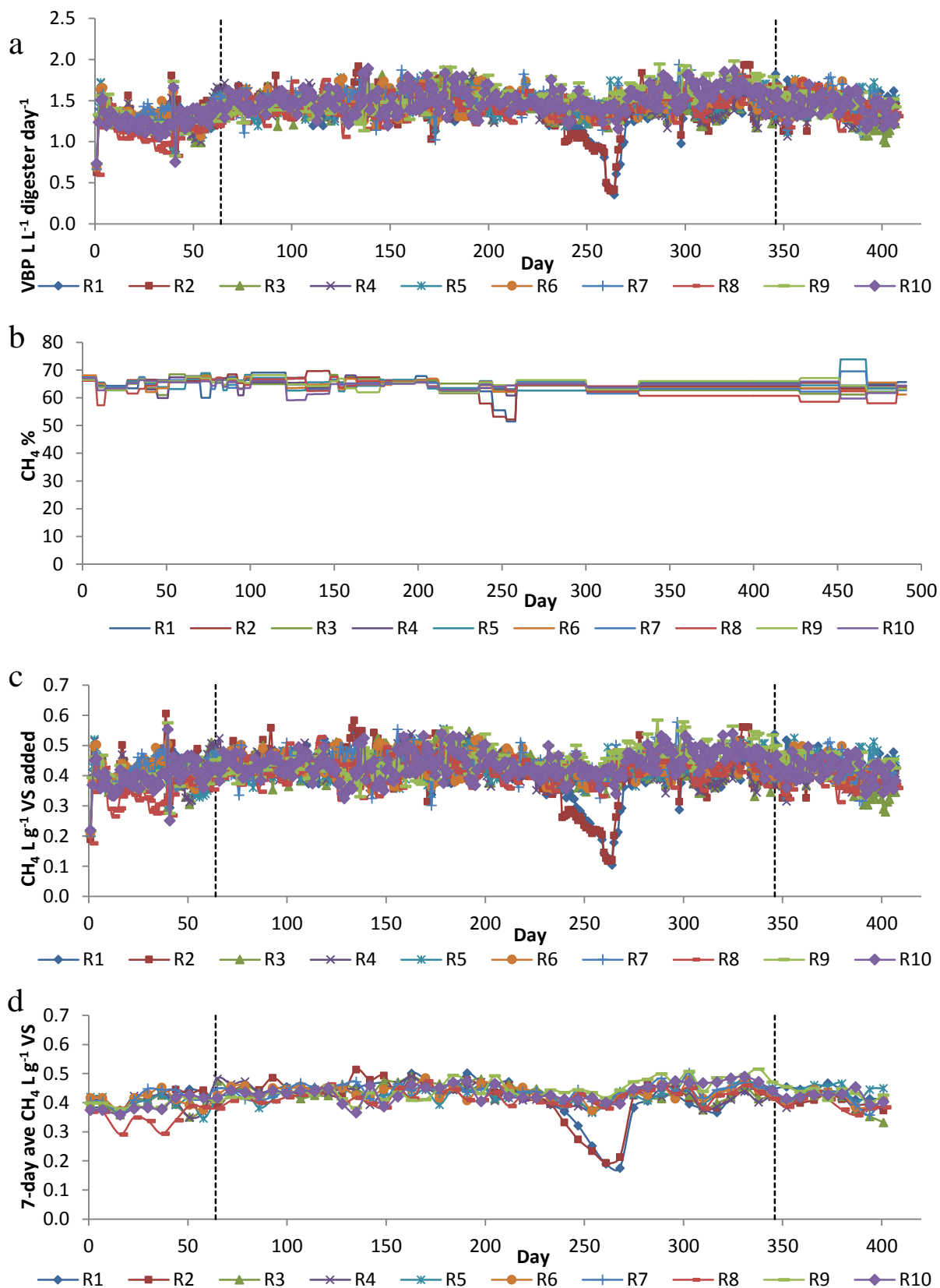


Figure 54 (a) VBP, (b) %CH₄, (c) SMP, (d) Average SMP. Black vertical lines denote the end of Phases. The first line is the end of Phase 2 where reactors 1-8 are spiked with chloride salts, with the right line the point where reactors R1 – R8 are brought up to 31.1g L⁻¹ total salt.

4.2.4.2 TS and VS

TS and VS (Figure 55a and b) decreased over an initial period of four days when the digestate was initially fed with a 90:10 mix of Synthetic wastewater and DI water. After four days the reactors were augmented to their respective target salt concentrations. A gradual reduction in TS was observed in all reactors over the initial 60 day acclimatisation period of Phase 2 in line with the lower solids concentration and higher digestibility of the feedstock to the source inoculum. After Phase 2 R1 – R8 total salt concentration was increased by $1.0 \text{ g L}^{-1} \text{ HRT}^{-1}$ to day 347 where all reactors were increased to 31.1 g L^{-1} following the addition graph in Figure 49. Slight decreases in %TS were observed between additions of up to 0.1% for R1 – R8. Figure 55a shows the increase in total solids with the increase in total salt concentration, with R9 and R10 remaining relatively stable throughout the duration of the experiment at between 0.99 – 1.09%. The percentage of VS as TS remains stable for R9 and R10, decreasing with the salt addition reactors (Figure 55).

All reactors have a similar %VS and VS destruction over the initial 100 days before the salt reactors decouple with increasing VS concentrations between 1.09 and 1.17 %TS and decreasing VS destruction from ~76 % VS destruction to ~63 % VS Destruction (Figure 55d). %VS decreases and %VS destruction increases within the last 40 days of operation for salt supplemented reactors from ~66% to 73% VS destruction and ~1.10 to ~0.90 VS % WW.

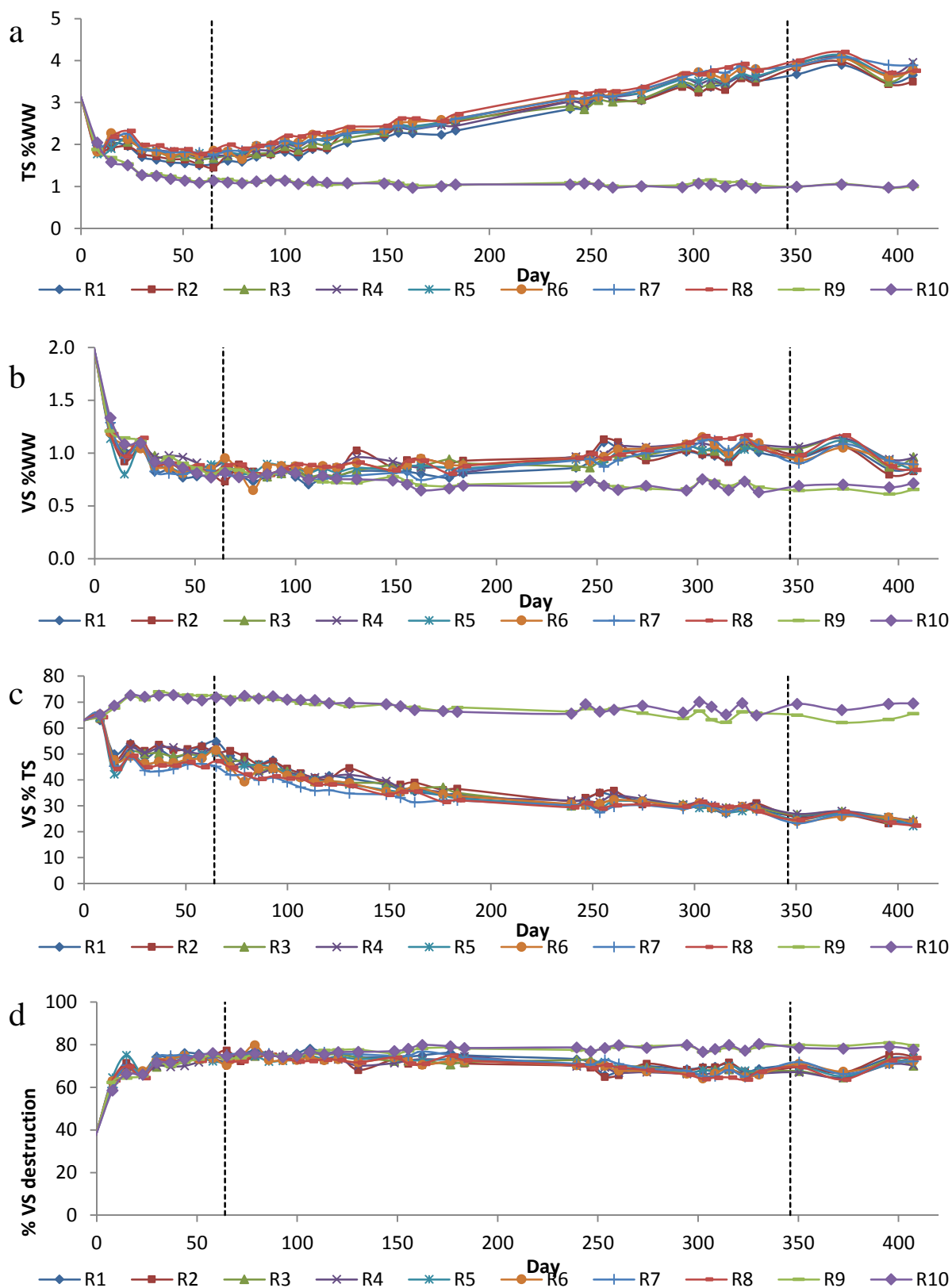


Figure 55 (a) TS %WW, (b) VS% WW, (c) VS as a % of TS and (d) % VS destruction. Black vertical lines denote the end of Phases. The first line is the end of Phase 2 where reactors 1-8 are spiked with chloride salts, with the right line the point where reactors R1 – R8 are brought up to 31.1g L⁻¹ total salt.

4.2.4.3 pH, Alkalinity, Ammonia and VFA

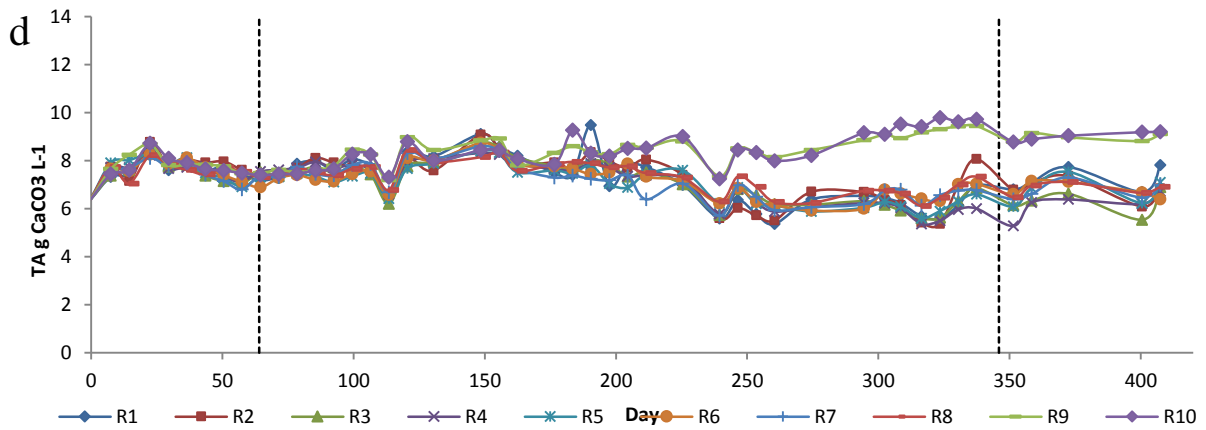
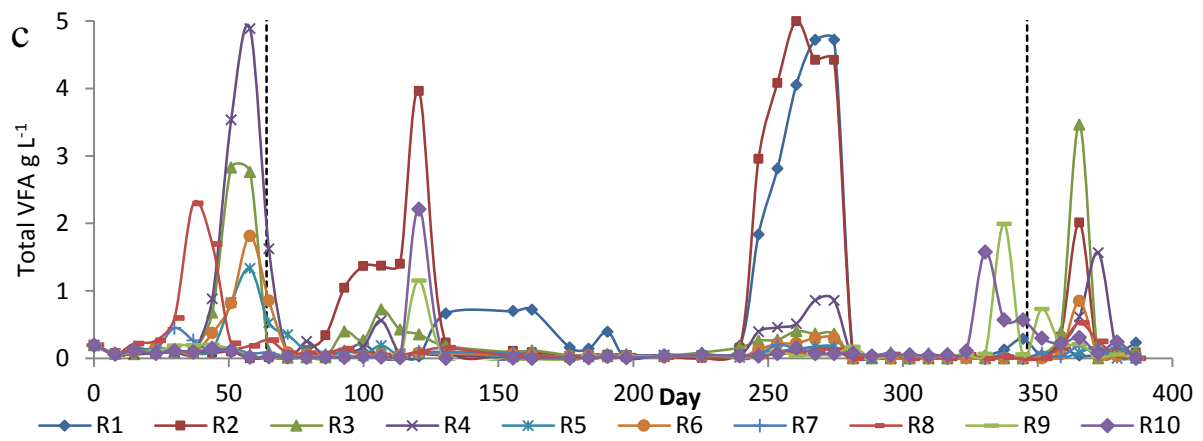
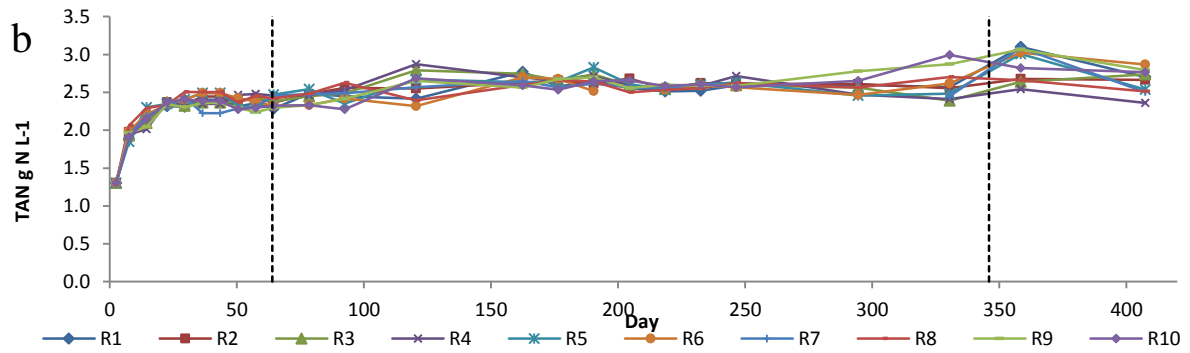
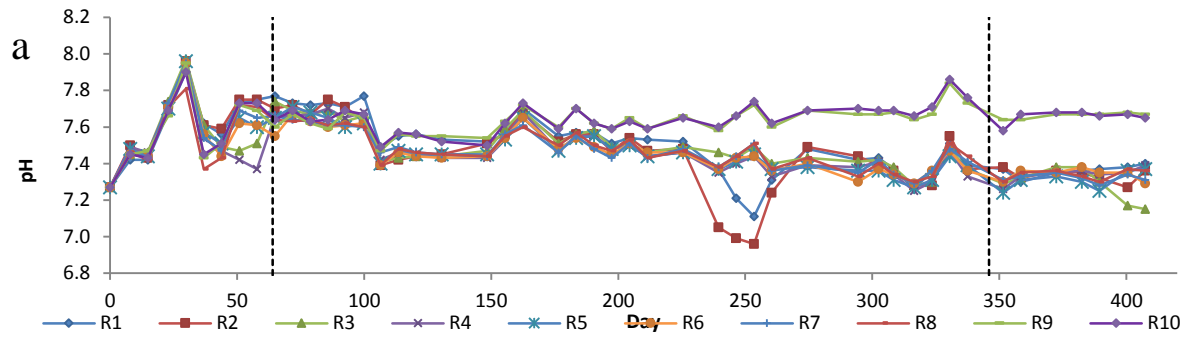
During Phase 2 the pH for all reactors increased from 7.27 to between 7.8 – 7.9 within 30 days before declining to a pH of between 7.4 – 7.7. All reactors follow a similar pattern with fluctuations potentially due to variations in the calibration of the pH probe (Figure 56a). From day 148 the salt reactors R1 – R8 decouple from the control reactors with a gradual decrease in pH for the salt reactors to between 7.3 - 7.37 and an increase in the controls to a pH of 7.65. A decrease in pH was observed in R1 and R2 between days 225 and 272.

Total ammonia nitrogen (TAN) increased over Phase 2 for all reactors in response to the feedstock composition but stabilised rapidly around 2.4 g N L⁻¹ for salt supplemented and 2.3 g N L⁻¹ for the controls. Concentrations for all the salt supplemented reactors remained relatively constant up to day 294 where the TAN was generally higher within the controls at 2.7 g N L⁻¹. There was some disturbance in TAN concentrations after salt incrimination began, perhaps indicating changes in the concentration of biomass in the reactor (Lindorfer et al., 2012).

Total alkalinity (TA) for all reactors increased to around 7.4 – 7.5 g CaCO₃ L⁻¹ reflecting the increase in TAN content (Figure 56b). Between days 43 and 64 the TA concentration decreased for all reactors exhibiting a similar effect to that observed in the preliminary study, where the inoculum is adapting to the new feedstock. Once adaption had occurred the TA increased. This is also reflecting in the total VFA concentration with digesters R3-R8 with salt supplementation above 6 g L⁻¹ showing transient VFA peaks between day 30-60 (Figure 56c), reaching as high as 4.8 g L⁻¹ in R4. The VFA peaks were reflected in the partial alkalinity and in the IA/PA ratio with increases due to acetic acid (Figure 56d-g); by the end of Phase 2 VFA concentrations were again close to the control values in R9&10.

During Phase 3 TA within the salt supplemented reactors R1 – R8 decreased in TA around day 200 stabilising towards the end of the experiment, with a slight increase in the control reactors R9 – R10 (Figure 56d). IA and PA ratio remains relatively constant throughout Phase 3 between 0.26 and 0.5 for all reactors except R1 and R2 (Figure 56g). TA and PA in the salt-supplemented digesters fell from around day 200, corresponding to salt concentrations of 16-19 g L⁻¹. The fall was especially sharp in R1 and 2, where PA dropped to 2.1 and 2.5 g CaCO₃ L⁻¹ over the next 60 days, with an IA/PA ratio above 1 (Figure 56d-g). VFA peaks of around 5 g L⁻¹ appeared in both digesters in this period, consisting primarily of acetic acid but also 1.0-1.3 g L⁻¹ of propionic, 0.7 g L⁻¹ iso-valeric and small

increases in butyric, iso-butyric and valeric acids. VFA concentrations fell rapidly after day 274, reaching values below 0.1 g L^{-1} by day 281 (Figure 57). Similar but much smaller VFA peaks were observed in the digesters at higher salt loadings, with the magnitude corresponding inversely to added salt concentration. In R1&2 there were accompanying falls in pH, VBP, SMP and biogas methane content, which then recovered to at or near their previous values by day 270. No significant changes occurred in the other salt-supplemented digesters. It is not known what caused this decrease, but reactors R1 and R2 were not fed between days 239 and 253 until the intermediate and partial alkalinity ratio and VFA concentrations had declined, resuming the regime described in the methodology (Figure 56c). After day 350 when the added salt concentration was equalised in all of the supplemented digesters, transient VFA peaks were seen in the digesters that had previously been at slightly lower loadings, but these had disappeared by day 400 close to the control values in R9 and R10. (Figure 57).



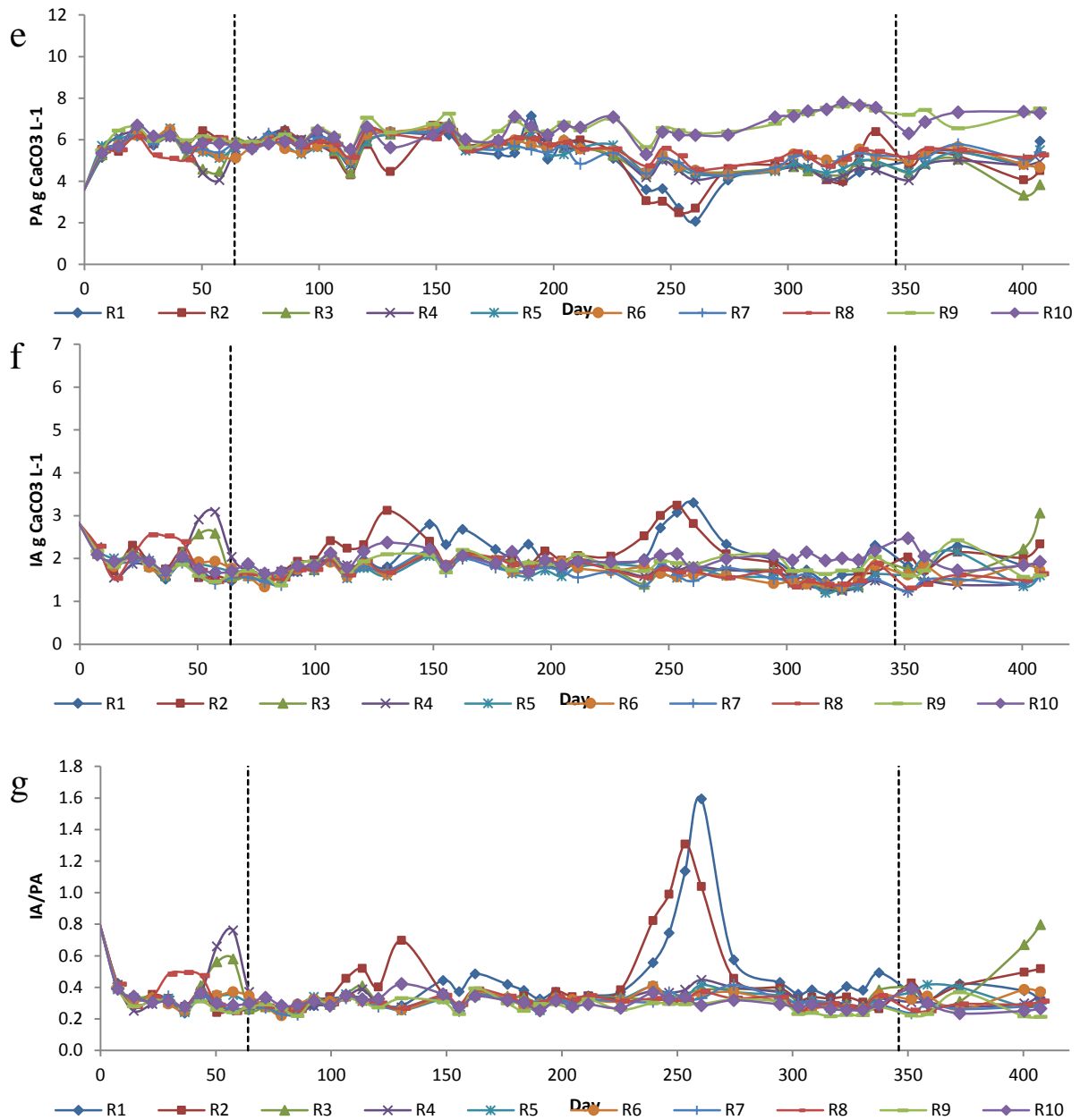
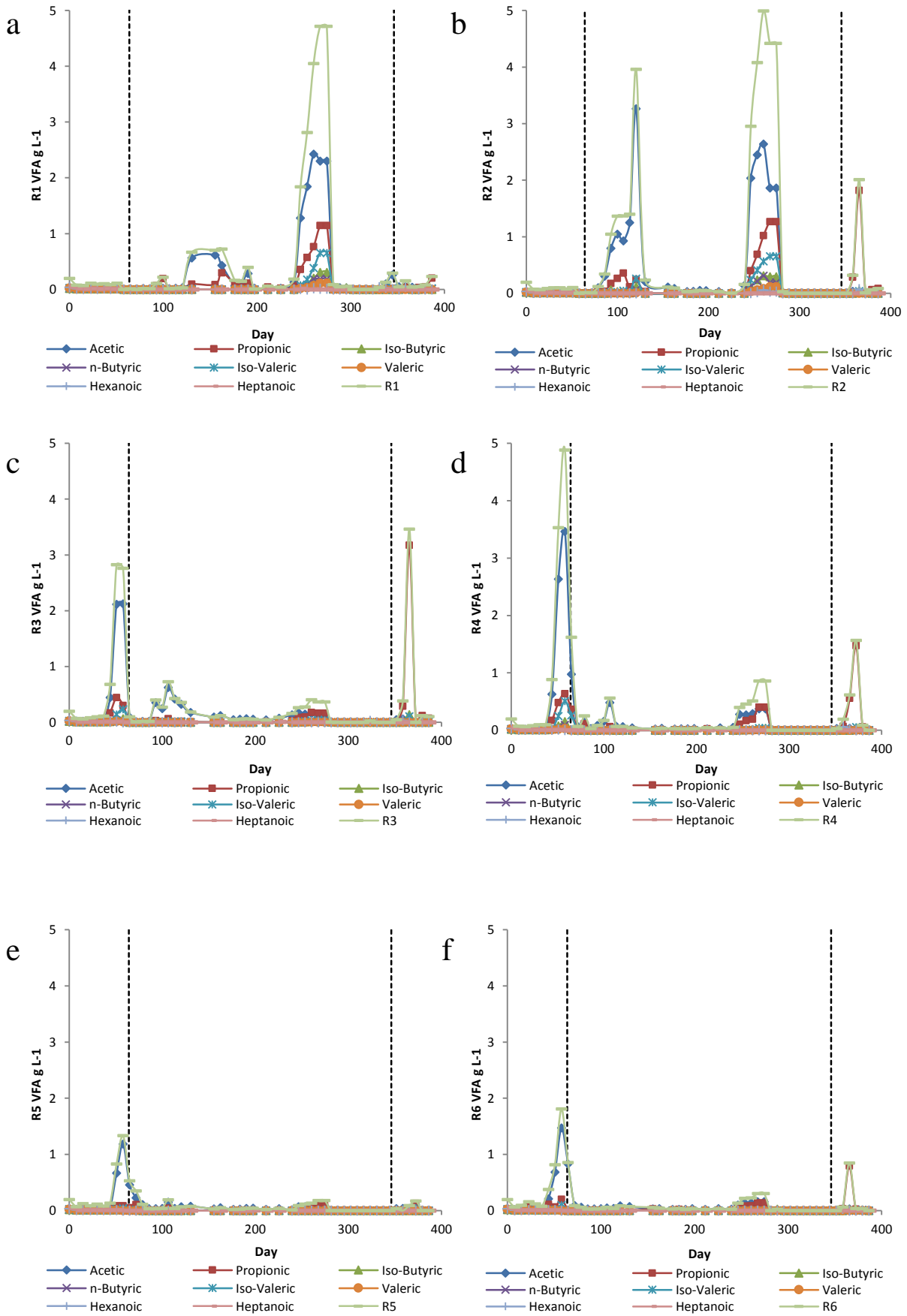


Figure 56 (a) pH, (b) Ammonia, (c) total VFA content, (d) total alkalinity, (e) partial alkalinity, (f) Intermediate alkalinity and (g) IA/PA ratio. Black vertical lines denote the end of Phases. The first line is the end of Phase 2 where reactors 1-8 are spiked with chloride salts, with the right line the point where reactors R1 – R8 are brought up to 31.1g L⁻¹ total salt.



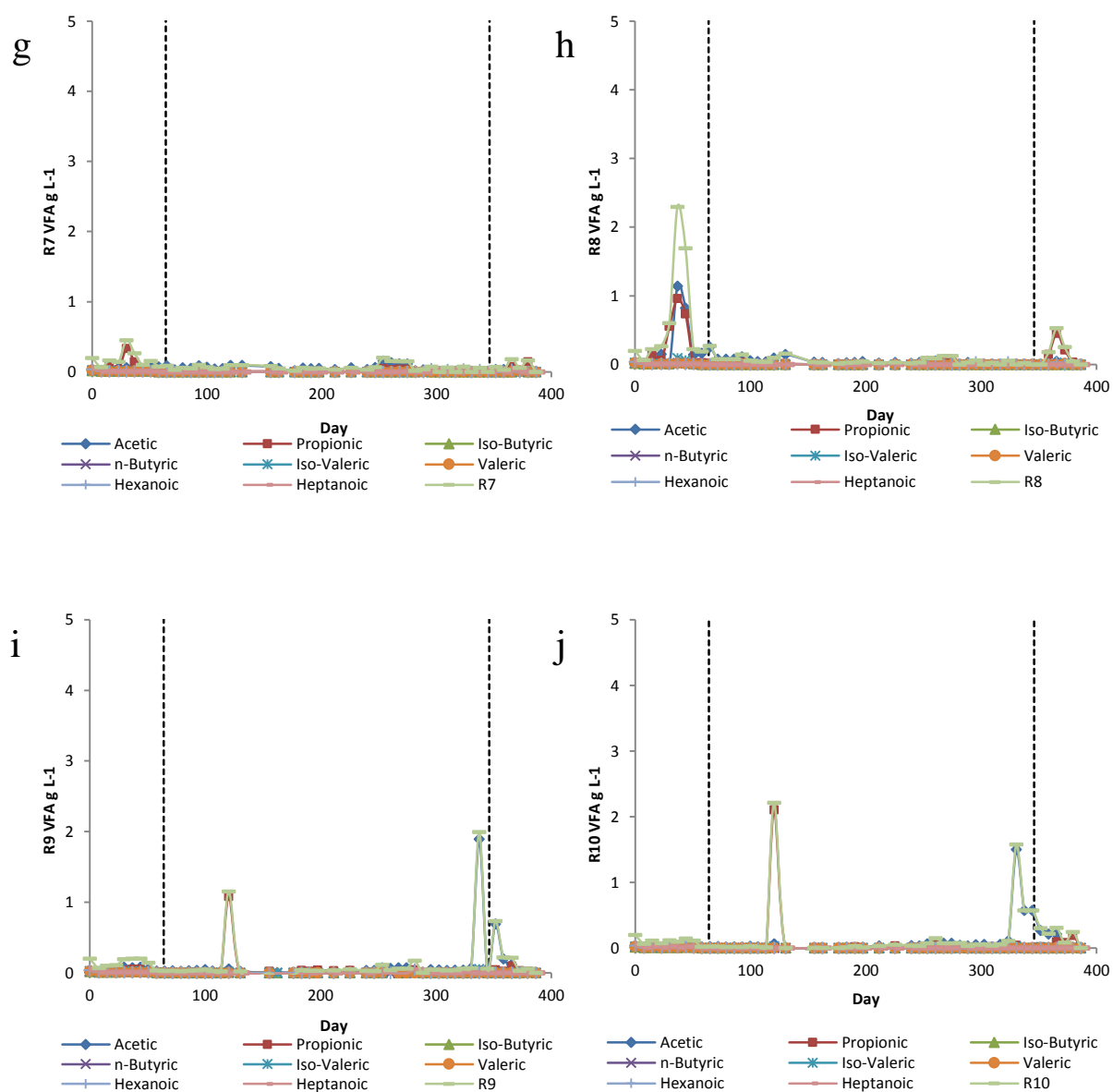


Figure 57 VFA profiles for R1 – R10. Black vertical lines denote the end of Phases. The first line is the end of Phase 2 where reactors 1-8 are spiked with chloride salts, with the right line the point where reactors R1 – R8 are brought up to 31.1 g L⁻¹ total salt.

4.2.5 Digestate solids content

All of the digesters acclimated successfully to the feedstock and the initial salt additions, with only minor signs of stress or instability. Digestate solids contents (Figure 55) reflected both acclimatisation to the feedstock and the amount of salt addition in each pair of digesters, with TS contents rising in response to the initial salt addition as expected, then gradually declining. A mass balance approach and visual observation at the end of the run indicated this may have been due to precipitation of struvite.

Declining inorganic solids content could be clearly observed during Phase 2 as shown in Figure 55a. When the value for the TS from the control is subtracted from the TS value of the salt reactors there is a loss of added salt of up to 2 g L^{-1} on the final set of measurements, which is highlighted in Figure 58. During Phase 3 each addition exhibited a slight decline in excess ash within seven days. The measured amount of additional salt, calculated by subtracting the control TS content from that in the salt-supplemented reactors, was less than the theoretical value in all CSTR's dosed with additional salt, with a reduction of between $4\text{-}5 \text{ g L}^{-1}$ inorganic TS at the end of the operational run. Using the measured inorganic TS difference to that of the control combined with the difference to the expected salt concentration a missing salt mass can be calculated. By calculating the loss of salt on a cumulative basis based on measured TS and VS values for the duration of operation compared to the predicted salt content an overall loss of $\sim 25.8 \text{ g TS}$ has occurred (for the highest salt reactor). This can be explained by the precipitation of struvite.

At the end of the experimental run it was observed that a whiteish crystalline salt had precipitated across all parts of the reactor which were in contact with the digestate (Figure 59a-b). Unfortunately all the reactors were cleaned, initially with hot water and detergents to remove an outer layer of organic sludge, then with 20% sulphuric acid to remove the precipitate, before any of the precipitate could be recovered for analysis. The difficulty in removing the precipitate suggests that it may be struvite, however, due to the low solubility of the precipitate in excess hot water and its eventual removal only with sulphuric acid, which is commonly used in struvite removal in industrial wastewater treatment systems (Williams, 1999, Wilsenach et al., 2007). The observed thickness of precipitate layer on the reactor surfaces was between $0.1 - 0.5 \text{ mm}$, giving a volume of precipitate of between $8.5 - 42.8 \text{ cm}^3$. The density of struvite is 1.7 g cm^3 at 56% TS (Kern et al., 2008), and this would potentially account for between $8.1 - 40.9 \text{ g}$ of inorganic solids deposited on the surfaces of the reactor.

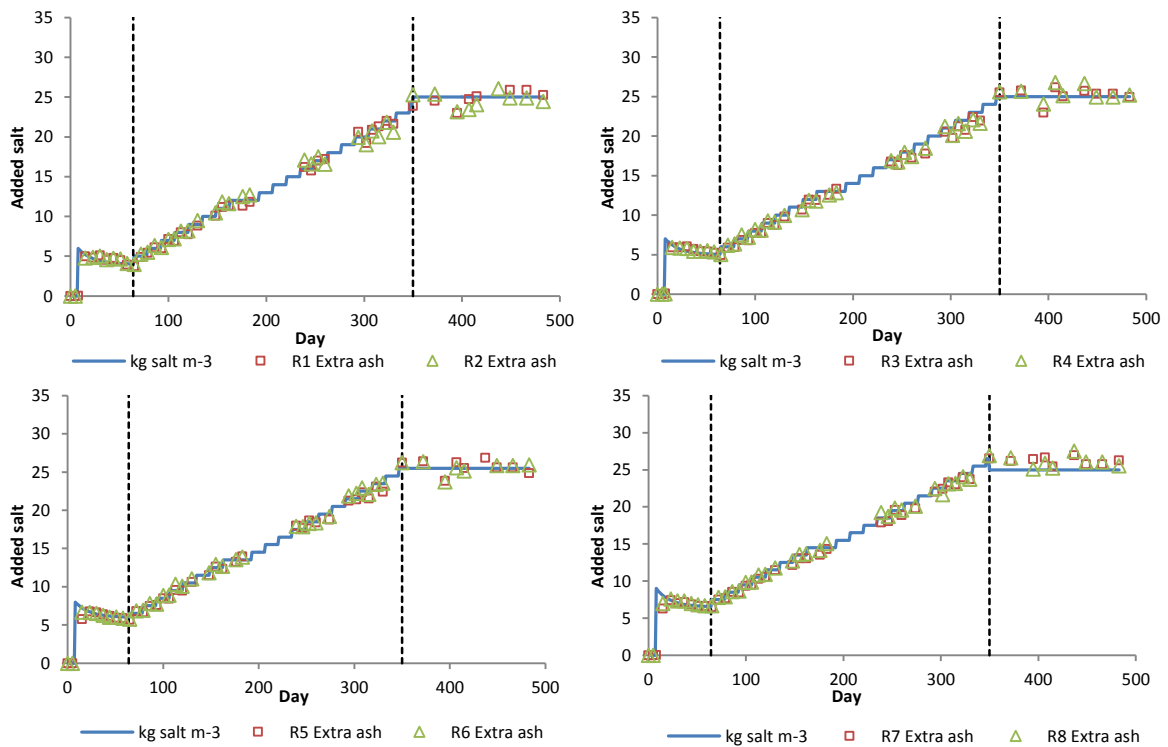


Figure 58 Modelled salt loss data with actual additional ash content compared to control for each duplicate of the salt supplemented reactors. Where extra ash is the difference between the control group TS and the salt spiked reactors TS.



Figure 59a shows fouling of reactor surfaces prior to cleaning with detergent and hot water. Figure 59b shows salt deposits after detergent, hot water, mechanical cleaning and an initial rinse with sulphuric acid.

Struvite precipitation occurs when the concentrations of Mg^{2+} , NH_4^+ and PO_4^{3-} are greater than the solubility limit of struvite. Struvite solubility decreases as pH increases due to a decrease in ammonia ion concentration and increasing phosphate ion concentration. The addition of ammonium phosphate dibasic as a component of the synthetic wastewater with the high salt media containing $MgCl_2$ would provide enough free ions to exceed the saturation limit. This with the breakdown of proteins producing free ammonia, and the lysing of cells releasing phosphate and magnesium would increase the ion concentration further driving precipitation.

Maximum solubility of struvite within deionised water is $212.7 (\pm 3.8)$ $mg L^{-1}$ at $35^\circ C$ and a pH of 7.4, similar to the pH of the high salt reactors in this research (Bhuiyan et al., 2007). The formation of struvite causes the release of hydrogen decreasing the reactor pH (Equation 4.1), which is observed in all the salt addition reactors which have a lower pH than that of the control reactors, in which no precipitation onto the reactor surfaces occurred. Precipitation of struvite can also occur with potassium as a replacement for NH_4^+ (Wilsenach et al., 2007), but as potassium concentrations are relatively low within the feedstock (Syazwani, 2013) and salt medium, and ammonia concentrations are high it is likely that precipitation occurred with ammonia .



It has been shown that within a wastewater treatment environment at a pH below 10 magnesium ions are the limiting factor in struvite formation and precipitation, with a minimum suggested Mg^{2+} , NH_4^+ and PO_4^{3-} ratio of 1:1:1 (Stratful et al., 2001). The molar ratio of Mg^{2+} added, NH_4^+ and PO_4^{3-} within the feed show an excess of Mg^{2+} , with greater concentrations of all ions than required for oversaturation of the reactor. As ammonia is produced as a by-product of anaerobic digestion, however, it is present in excess making Mg the limiting ion. Within the feedstock there are $1300 mg L^{-1}$ of Mg alone compared to struvites solubility of $212.7 mg L^{-1}$ enabling precipitation to occur as shown in Table 31. The removal of phosphate via precipitation of struvite along with magnesium would reduce the total salt concentration by between $3.05 - 6.3g L^{-1}$ compared to the control, depending on phosphate release from organics within the reactor and assuming all magnesium is precipitated. These values fall within the range required to correct the reported excess ash content. Phosphate precipitation would not occur in the control reactors, further increasing the inorganic TS content of these reactors with regards to the salt reactors, and increasing the apparent TS difference. Without a sample of the precipitate it is not possible to directly

identify the compound, however, the evidence clearly suggests that struvite precipitation could have occurred and that the nature of its adhesion and difficulty in removal support the view that the precipitation found was struvite.

Table 31 Mass of components within the synthetic feed required for struvite formation determined from the synthetic wastewater recipe in section 3.

Component	Mass added (g L ⁻¹)	Moles	Molar ratio
Mg ²⁺	1.3	0.053	1.00
NH ₄ ⁺	0.9	0.051	0.97
PO ₄ ⁺	2.4	0.026	0.48

The implications of this are that there is a greater probability of struvite formation within an anaerobic digester treating high saline waste waters at marine concentrations, than digesting wastes with relatively low Mg concentrations. This means great care must be taken in designing the reactor to ensure a reduced turbulence in piping, as turbulent conditions are likely to cause a reduction in pressure and a subsequent release of CO₂ reducing the pH, and ultimately the maintenance of the pH to reduce the precipitation potential (Borgerding, 1972). As the increase in Mg ions with wastewater strength NH₄ and PO₄ will cause struvite formation and precipitation.

It has been suggested that the precipitation of struvite could be used as a mechanism for the removal of phosphate from waste streams for subsequent capture and use as a fertiliser. This will be of increasing importance as the supply and reserves of accessible phosphate decline and costs increased. This could be incorporated into the design of a digester treating high Mg waste streams whereby the reactors pH is increased and temperature decreased to enable greater precipitation post digestion within a container that can be easily cleaned (Doyle and Parsons, 2002).

Recommendations based on these observations are that any future work with regards to synthetic wastewater utilises a different source of ammonia and phosphate if magnesium is utilised in abundance as the precipitation occurring may not be representative of the processes that occur within a large reactor.

4.2.5.1 Reactor performance and gas production

Table 32 shows the average values of key monitoring parameters for the last 20 days of Phase 2, after three HRT at the additional salt doses used. Gas production in the salt-supplemented digesters was similar to that in the controls (Figure 54), with exception of R8 which showed a temporary drop of around 20% between days 3-34. The high SMP in R3&4 at the end of phase 1 reflects the decline in accumulated VFA (Figure 1 j and d).

At the end of Phase 2 average volumetric biogas production (VBP) and specific methane production (SMP) in all digesters apart from R7 appeared to show a slight downward trend with increasing salt addition (Table 32). The controls R9 and 10 achieved 92% of the TMP and conversion of 83% of the TCV into CH₄. The SMP of digesters R1&2 supplemented at 6 g L⁻¹ was equal to that of the controls, while R8 with 9 g L⁻¹ salt addition achieved 83% of the TMP and 76% conversion of TCV. These results indicated that after >3 HRT of operation at their respective salinities there were small differences in performance between the controls and the more heavily salt-supplemented digesters, but that the anaerobic consortium could successfully adapt to an initial step in salinity to 9 g L⁻¹, with the preliminary study suggesting inhibition at initial concentrations greater than this.

Table 32 Average values for key monitoring parameters in the last 20 days of Phase 2.

Parameter	Unit	R1	R2	R3	R4	R5	R6	R7	R8	R9	R10
Salt	g L ⁻¹	6	6	7	7	8	8	9	9	0	0
pH		7.70	7.70	7.55	7.48	7.60	7.56	7.62	7.63	7.63	7.65
TAN	g N L ⁻¹	2.34	2.40	2.39	2.44	2.39	2.40	2.32	2.44	2.30	2.32
TA	g CaCO ₃ L ⁻¹	7.49	7.72	7.27	7.43	7.25	7.28	7.19	7.50	7.63	7.53
PA	g CaCO ₃ L ⁻¹	5.77	6.02	5.05	4.91	5.43	5.36	5.57	5.70	6.00	5.74
IA	g CaCO ₃ L ⁻¹	1.71	1.70	2.22	2.52	1.82	1.92	1.62	1.80	1.63	1.79
IA/PA		0.30	0.28	0.45	0.54	0.34	0.36	0.29	0.32	0.27	0.31
TS	% WW	1.54	1.57	1.69	1.76	1.77	1.78	1.80	1.85	1.17	1.13
VS	% WW	0.80	0.81	0.84	0.91	0.86	0.87	0.82	0.86	0.85	0.81
VFA	mg L ⁻¹	52	49	1591	2730	706	965	104	594	99	76
VBP	L L ⁻¹ day ⁻¹	1.32	1.33	1.28	1.28	1.26	1.27	1.33	1.22	1.30	1.33
CH ₄	% volume	66.2	66.1	65.5	65.0	64.6	65.7	66.7	66.3	66.5	65.6
SMP	L CH ₄ g ⁻¹ VS	0.421	0.422	0.400	0.395	0.388	0.396	0.423	0.384	0.413	0.420
	% ave control	1.01	1.01	0.96	0.95	0.93	0.95	1.02	0.92	0.99	1.01
	% of TCV	0.84	0.84	0.80	0.79	0.77	0.79	0.84	0.76	0.82	0.84

4.2.5.2 Phase 3 Discussion

Table 33 shows the average values of key monitoring parameters for the last 20 days of Phase 3. The pH in the salt-supplemented digesters was lower than in the controls, with average values of 7.33 and 7.67 respectively. TAN concentrations were also slightly lower on average. The IA/PA ratio of the salt-supplemented digesters was slightly higher than in the controls, at 0.37 and 0.26 respectively, although both were within the range considered as indicating stability. The average VBP and SMP of the salt-supplemented reactors was lower than that of the controls, although R1 and especially R5 showed good gas production. This difference was supported by the slightly higher VS content in the salt-supplemented digesters compared to the controls, corresponding to average VS destructions of 70 and 79% respectively.

Table 33 Average values for key monitoring parameters in the last 20 days of Phase 3.

Parameter	Unit	R1	R2	R3	R4	R5	R6	R7	R8	R9	R10
Salt	g L ⁻¹	31.1	31.1	31.1	31.1	31.1	31.1	31.1	31.1	0	0
pH		7.37	7.33	7.31	7.35	7.31	7.36	7.32	7.34	7.67	7.67
TAN	g N L ⁻¹	2.70	2.66	2.74	2.36	2.54	2.87	2.50	2.51	2.80	2.77
TA	g CaCO ₃ L ⁻¹	7.41	6.76	6.35	6.43	6.95	6.72	6.91	6.89	8.96	9.14
PA	g CaCO ₃ L ⁻¹	5.41	4.60	4.07	4.91	5.25	5.04	5.41	5.30	7.10	7.31
IA	g CaCO ₃ L ⁻¹	2.01	2.16	2.28	1.53	1.70	1.68	1.50	1.58	1.86	1.83
IA/PA		0.37	0.47	0.59	0.31	0.32	0.34	0.28	0.30	0.27	0.25
TS	% WW	3.68	3.64	3.83	3.91	3.86	3.82	3.96	3.89	1.01	1.02
VS	% WW	0.92	0.89	0.99	1.01	0.96	0.95	0.97	0.96	0.64	0.70
VS destr	% VS	71.3	72.2	69.2	68.5	70.0	70.3	69.9	70.1	80.0	78.3
VFA	mg L ⁻¹	121	55	73	553	57	24	73	99	28	109
VBP	L L ⁻¹ day ⁻¹	1.40	1.34	1.28	1.31	1.46	1.38	1.39	1.35	1.41	1.42
CH ₄	% volume	65.4	64.1	62.7	65.4	65.9	63.6	63.3	60.8	66.1	64.7
SMP	L CH ₄ g ⁻¹ VS	0.413	0.390	0.362	0.386	0.434	0.398	0.396	0.372	0.422	0.416
	% ave control	0.99	0.93	0.87	0.92	1.04	0.95	0.95	0.89	1.01	0.99
	% of TCV	0.82	0.78	0.72	0.77	0.86	0.79	0.79	0.74	0.84	0.83

By the end of Phase 3 all reactors appeared to be operating stably in terms of pH, alkalinity and gas production. The salt-supplemented reactors on average showed a 6-7% reduction in SMP and percentage conversion of TCV compared to the controls showing successful adaption of the seed feedstock to the high ion concentration. The results support the suggestions from Feijoo et al. (1995) and de Baere et al. (1984) that non-halo tolerant anaerobic bacteria can adapt to high salinity within a relatively short operating time.

4.2.6 Phase 4 – Sulphate addition

4.2.6.1 Biogas and specific methane production

Reactors F1 – F4 exhibit a slight decline in VBP and SMP over the initial 15 days, stabilising within 60 days at between 1.4 – 1.5 L L⁻¹ d⁻¹ of biogas and 0.44 – 0.48 L CH₄ g⁻¹ VS added (Figure 60a and b). The VBP and SMP for reactor F8 decreased over the initial 42 days before gradually increasing towards the control values. Biogas and methane production for reactors F5 – F7 declined after the addition of SO₄ from 1.28 -1.38 L L⁻¹ d⁻¹ of biogas at day 0 to 0.54 – 0.78 L L⁻¹ d⁻¹ of biogas by day 49. This was accompanied with a drop in SMP from 0.41-0.47 L CH₄ g⁻¹ VS added at day 0 to between 0.15–0.20 L CH₄ g⁻¹ VS added by day 49. After day 49 reactors F5-F8 increased towards the control reactor F1 VBP and SMP values (Figure 60a-c).

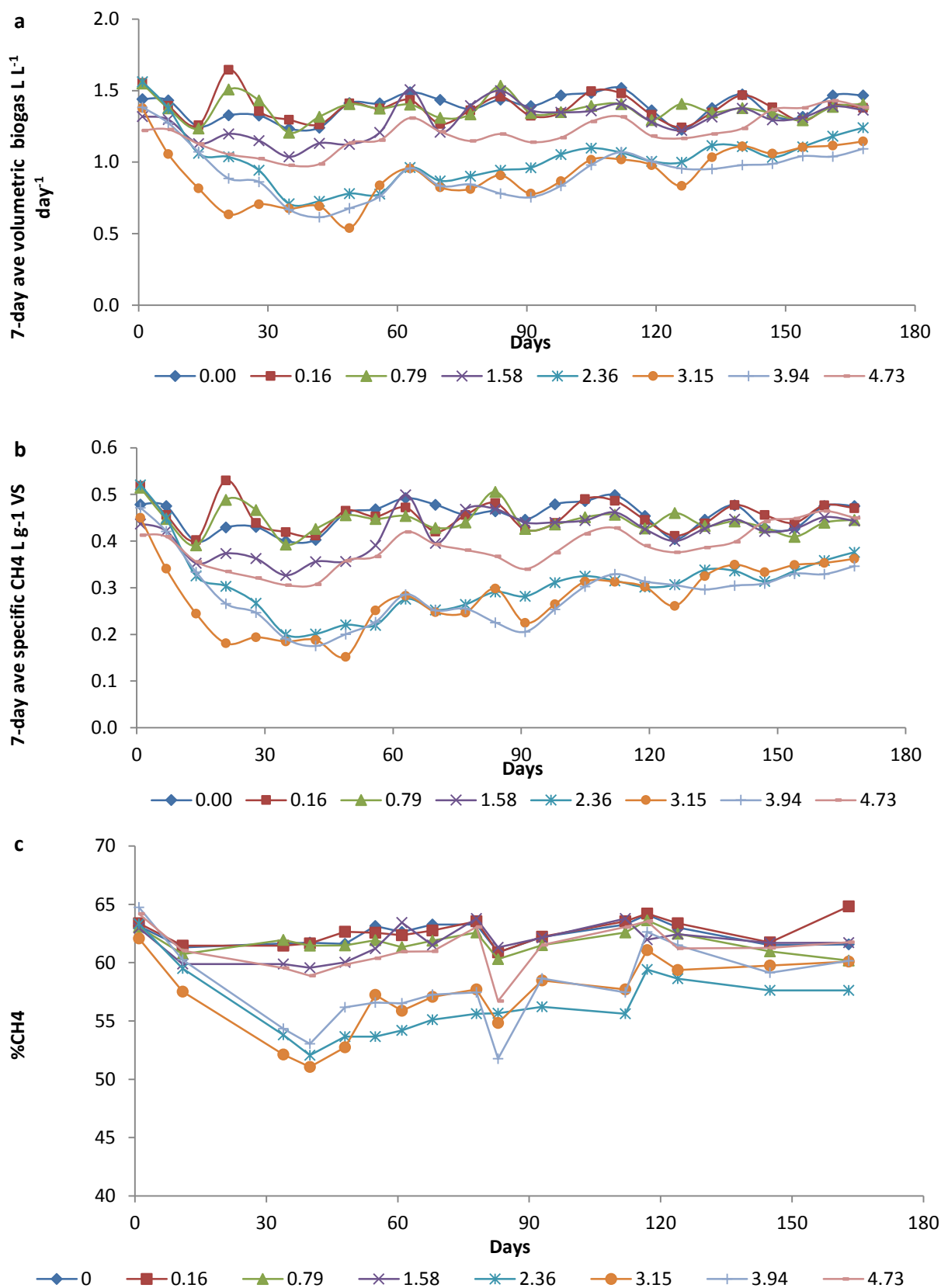


Figure 60 average weekly VBP (a), and SMP (b), and weekly %CH₄ content of the biogas (c) for the sulphate addition reactors.

4.2.6.2 TS and VS

Addition of MgSO_4 to reactors 0.16 – 4.73 caused a slight increase in TS %WW reaching relative stability for all reactors after three HRT (Figure 61a). Increases in VS% WW were observed in reactors with $>2.36 \text{ g L}^{-1}$ addition of SO_4 , with reactor F5 exhibiting the greatest increase from 0.9% to 1.8% within 60 days (Figure 61b). The control remained relatively constant between 0.8 and 0.9%. %VS destruction decreases with the addition of sulphate over the initial start-up period of 100 days (Figure 61c). Within the last 21 days %VS destruction is similar for all reactors at between 64 – 66% with the exception of F5 and F7 at 52 and 58% respectively.

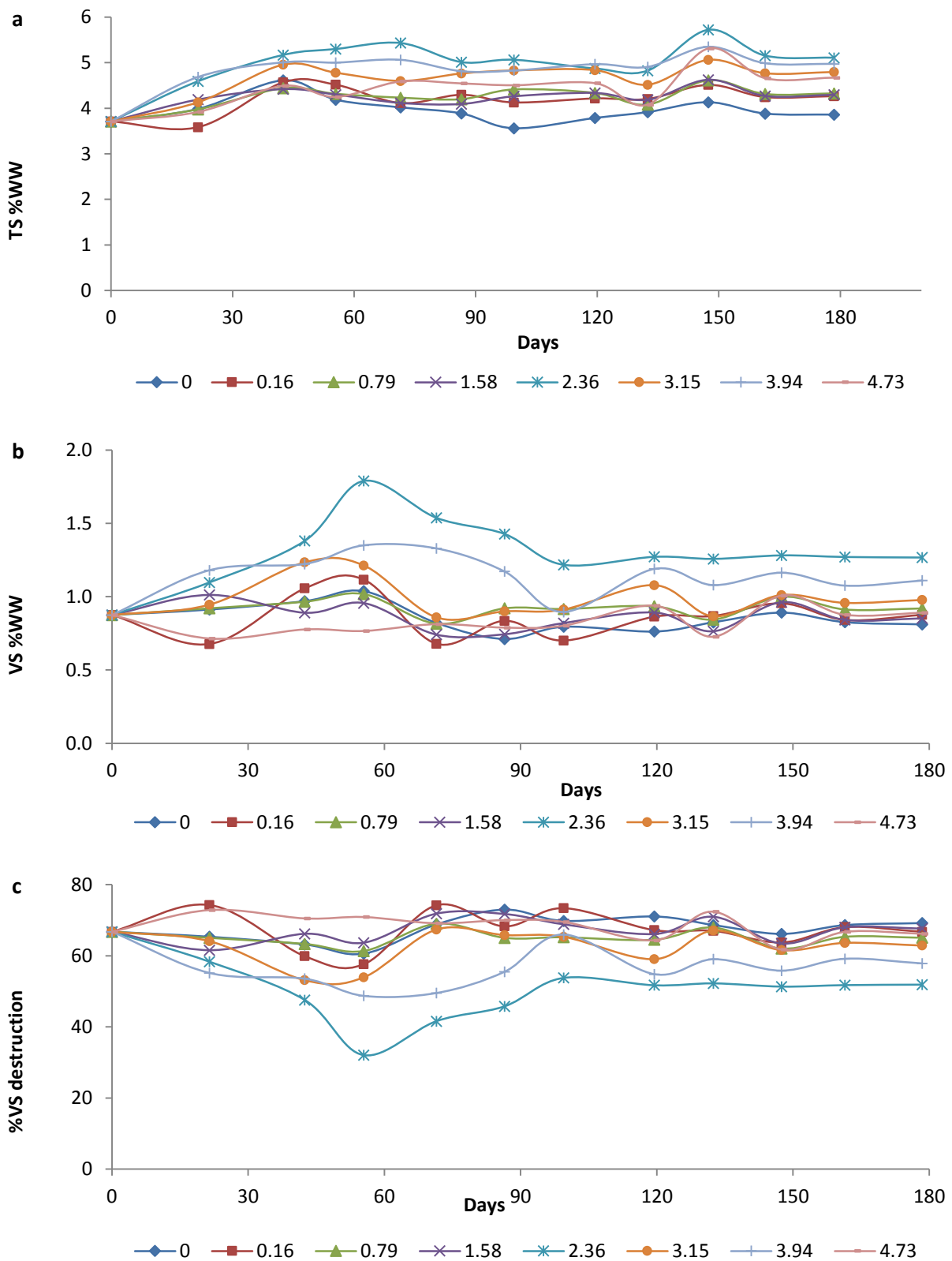


Figure 61 (a) TS% WW, (b) VS% WW and (c) %VS destruction.

4.2.6.3 pH, Alkalinity, Ammonia and VFA

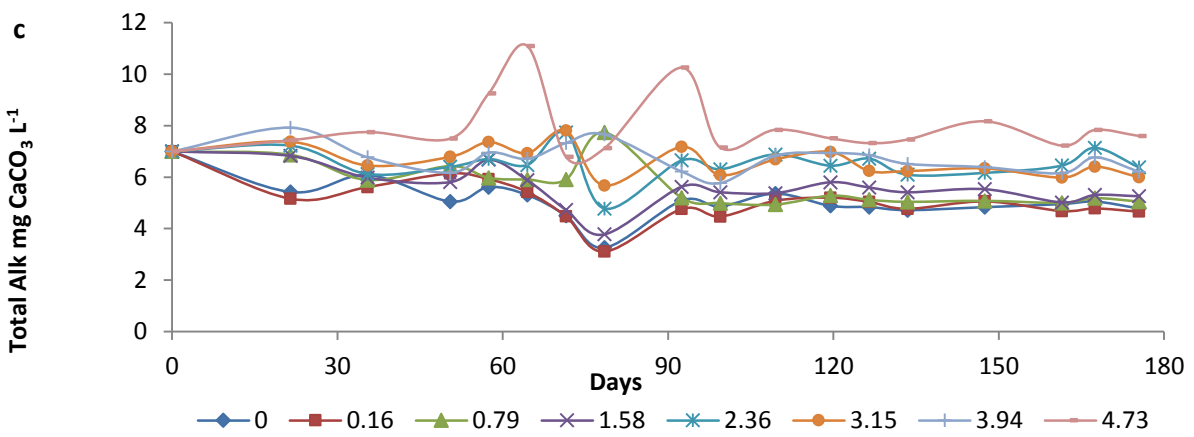
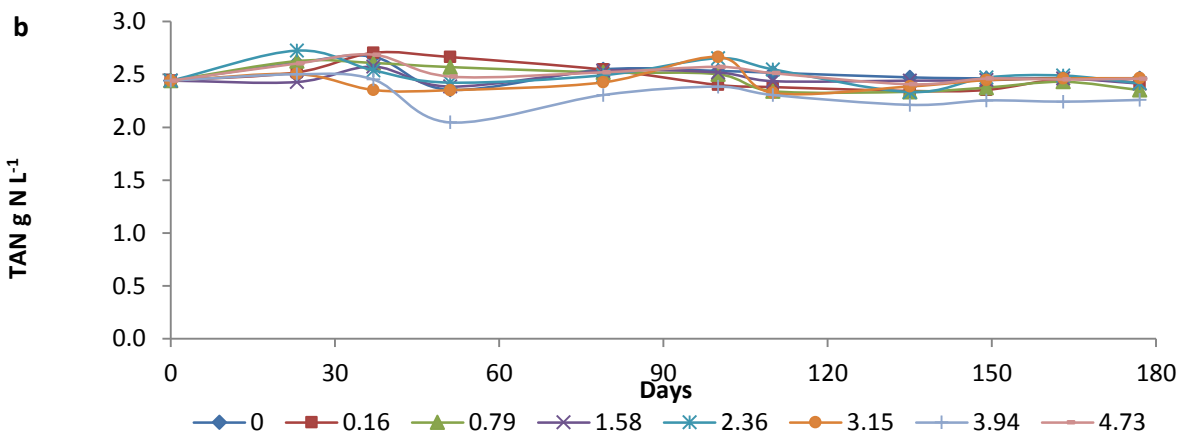
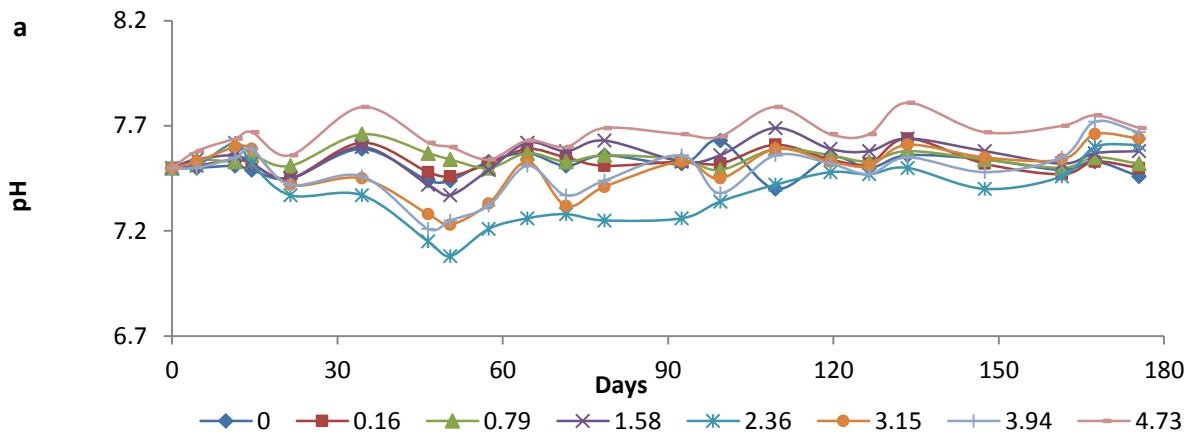
The control reactor F1 showed a stable pH and TAN averaging around 7.5 and 2.5 g N L⁻¹, with a small rise in IA/PA ratio concentration and VFA, possibly due to disturbances during the transfer of the inoculum from phase 3; but no longer-term changes were seen Figure 62a-h.

TAN concentrations in all reactors were similar, averaging around 2.5 g N L⁻¹, with the exception of F7 (2500 mg SO₄ L⁻¹) which stabilised at 2.2 g N L⁻¹ (Figure 62b).

Reactors F2 and F3 with the lowest concentrations of added sulphate showed little or no effect from the sulphate supplementation: the pH remained steady at an average value of 7.5 (Figure 63a), while TA and IA/PA stabilised at average values of 4.8 and 5.0 g CaCO₃ L⁻¹ and 0.34 and 0.35, respectively (Figure 62c - f). VFA concentrations remained below 0.2 g L⁻¹ (Figure 63g). In F4, supplemented at 1000 mg SO₄ L⁻¹, the pH also remained around 7.5 and TA stabilised at 5.3 g CaCO₃ L⁻¹, with an IA/PA ratio of 0.36. In this reactor, however, the VFA concentration rose to 2.5-2.7 g L⁻¹ between days 14-28, then declined to the same range as in the control (Figure 62g).

Reactors F5-8 with increasing sulphate concentrations showed more marked reactions to the sulphate addition. Between day 0-50 the pH fell to 7.1 in F5 and to 7.2 in F6 and 7 (Figure 62), before gradually returning to around 7.5 by the end of the run. VFA rose rapidly until day 14 and remained high until day 68, before declining towards control values. Average VFA concentrations during this period were in reverse order of added sulphate concentration, at around 5.9, 5.0, 4.3 and 2.5 g L⁻¹ in F5, 6, 7 and 8 respectively (Figure 63g). The main component in each case was acetic acid, with iso-valeric acid present in concentrations of up to 1 g L⁻¹ and small amounts of iso-butyric acid (Figure 63a - h). The effect of the VFA was reflected in the IA/PA ratios for each reactor (Figure 62f). TA in F5-7 stabilised from day 126 on at 6.2-6.5 g CaCO₃ L⁻¹, while in F8 the average TA was much higher at 7.6 g CaCO₃ L⁻¹ (Figure 62c). IA/PA ratios for F5-7 fell as the VFA accumulation declined, but were still 0.5 or above by the end of the run, while the IA/PA ratio in F8 was below 0.4 from day 100 on (Figure 62f).

Chapter 4



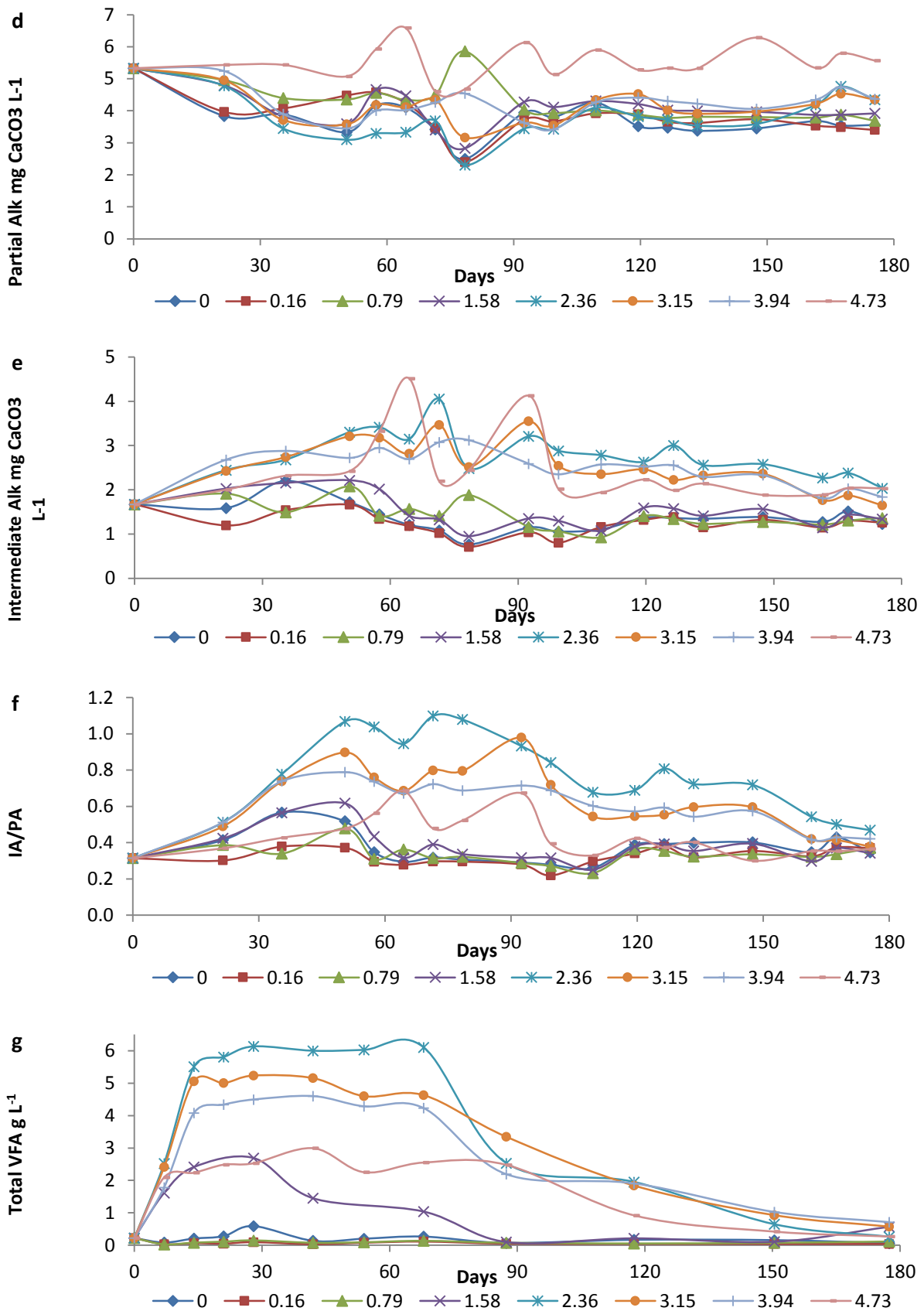
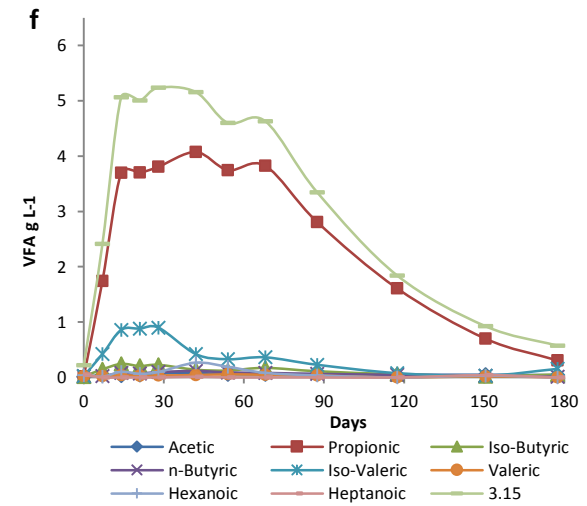
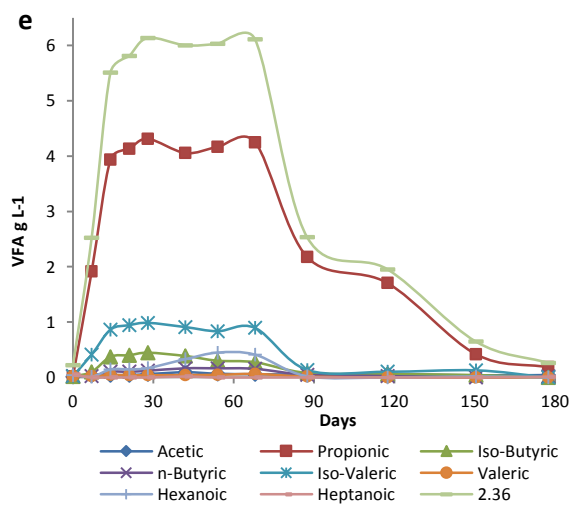
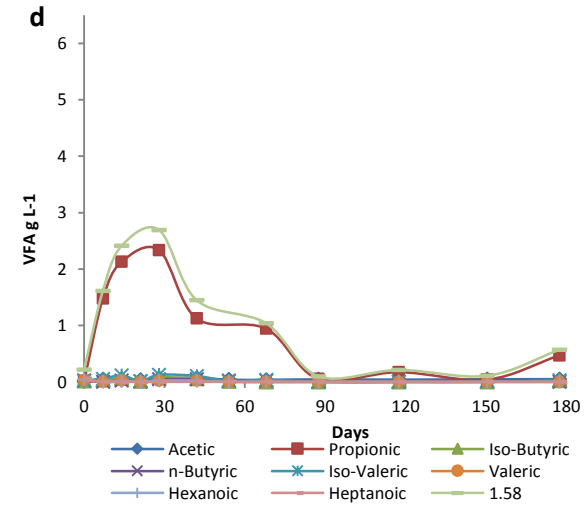
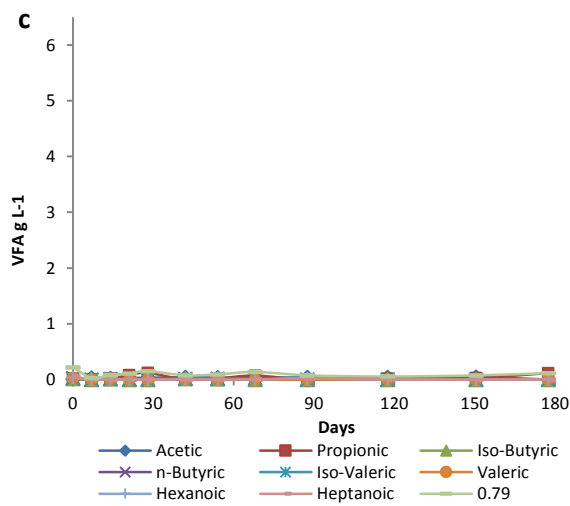
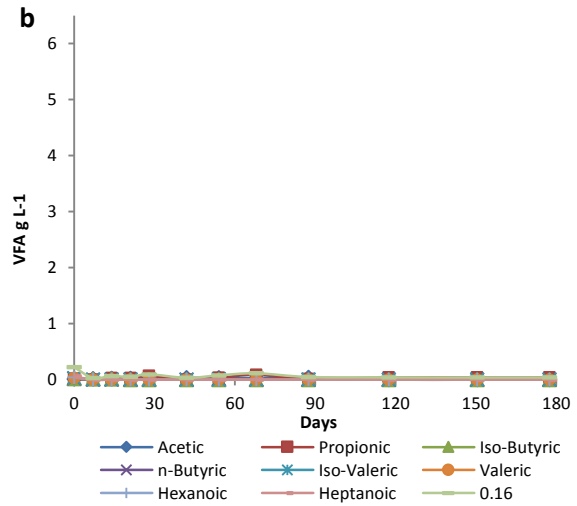
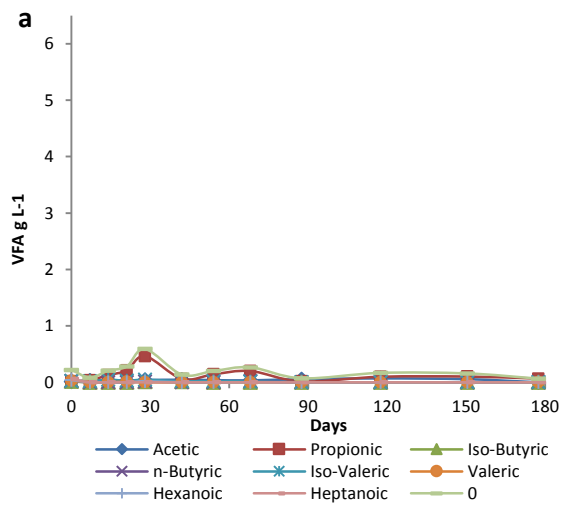


Figure 62 (a) pH, (b) TAN, (c) total alkalinity, (d) partial alkalinity, (e) intermediate alkalinity, (f) IA/PA and (g) total VFA for the reactors within Phase 4.

Chapter 4



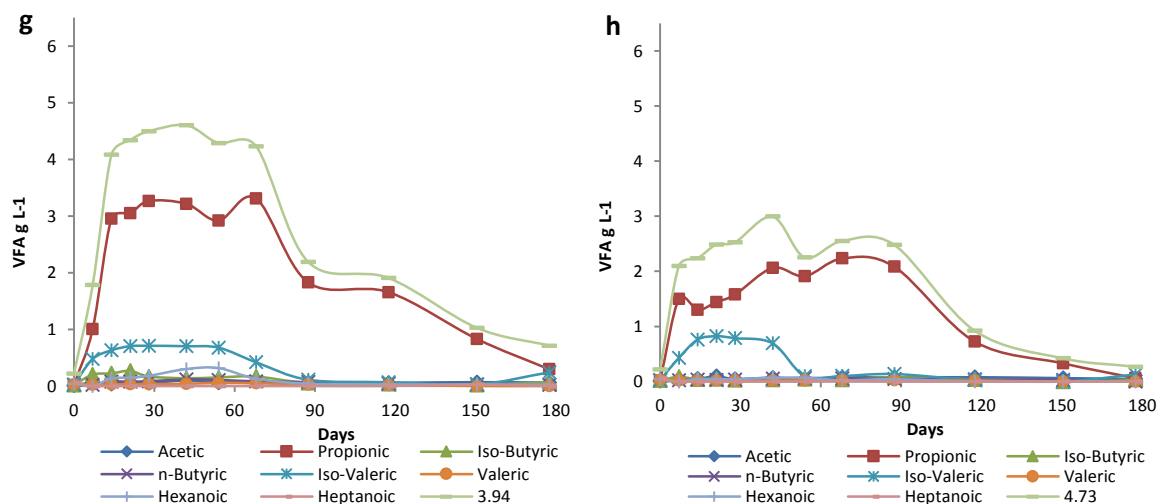


Figure 63 (a) VFA F1, (b) VFA F2, (c) VFA F3, (d) VFA F4, (e) VFA F5, (f) VFA F6, (g) VFA F7 and (h) VFA F8 for Phase 4.

4.2.6.4 Sulphur and sulphides

4.2.6.4.1 Determination of soluble sulphide method development

The determination of soluble sulphide via the ion selective probe gave precise but not accurate values for the sulphide present with potentially an order of magnitude less sulphide observed. This is potentially due to the preparation of the samples rather than the method itself. Analysis of the standards results in a precise and accurate linear response with an average R^2 of 0.989 that is repeatable with the concentrations checked by standardisation via titration and the electrode performance operating within the operating limits (Figure 64a). However samples from digesters in steady state produce different values on a weekly basis.

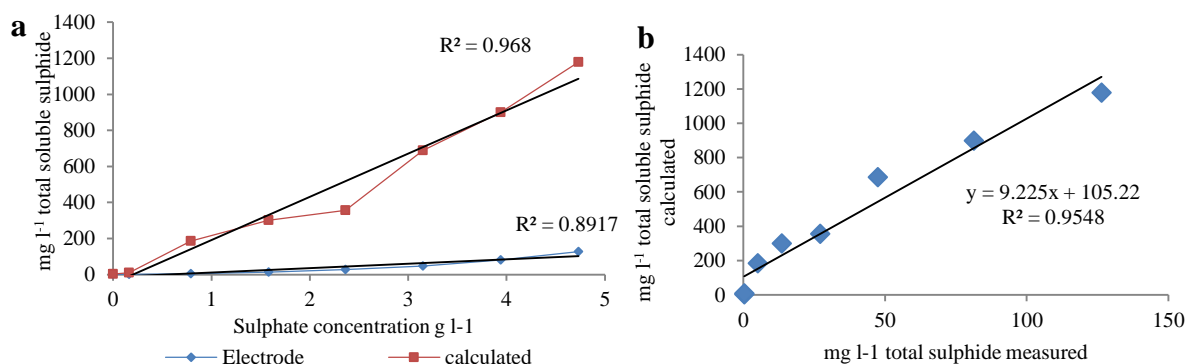


Figure 64 Measured and calculated values for soluble sulphide at different sulphate concentrations.

The preparation of the samples involves the removal of particulate material via centrifugation and filtration, before dilution and the addition of an alkaline anti-oxidant reagent (AAR) which alters the speciation of all soluble sulphide present to S^{2-} which is less likely to degas from the solution. The AAR must be added after the centrifugation and filtration as at high concentrations a precipitate containing the sulphide can form which would be removed by these processes it could re-dissolve. The processes themselves reduce the temperature of the sample from the initial 35°C , alters the pH by allowing the degassing of carbon dioxide and hydrogen sulphide into the atmosphere changing the partial pressure within the sample. This removes some of the soluble hydrogen sulphide present giving a lower, false result, that cannot be compensated for as environmental conditions during the preparation process affect the quantity of sulphide removed.

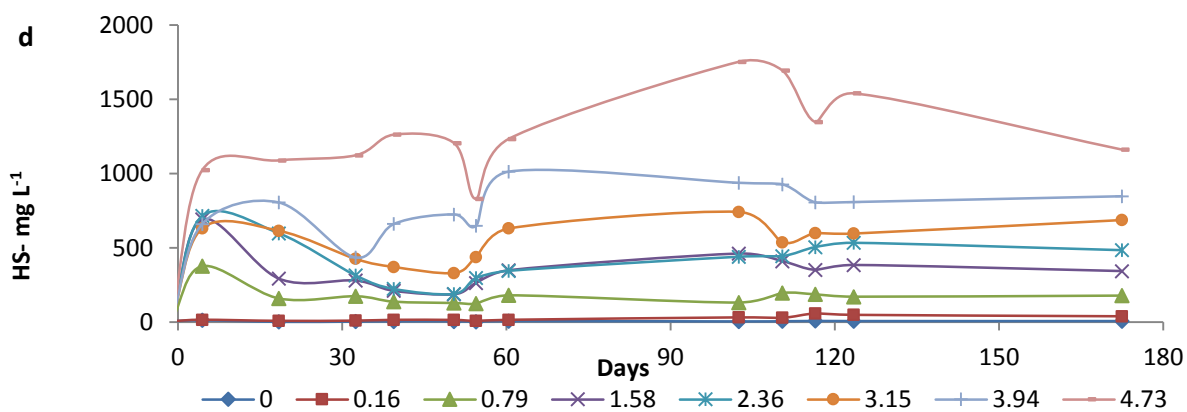
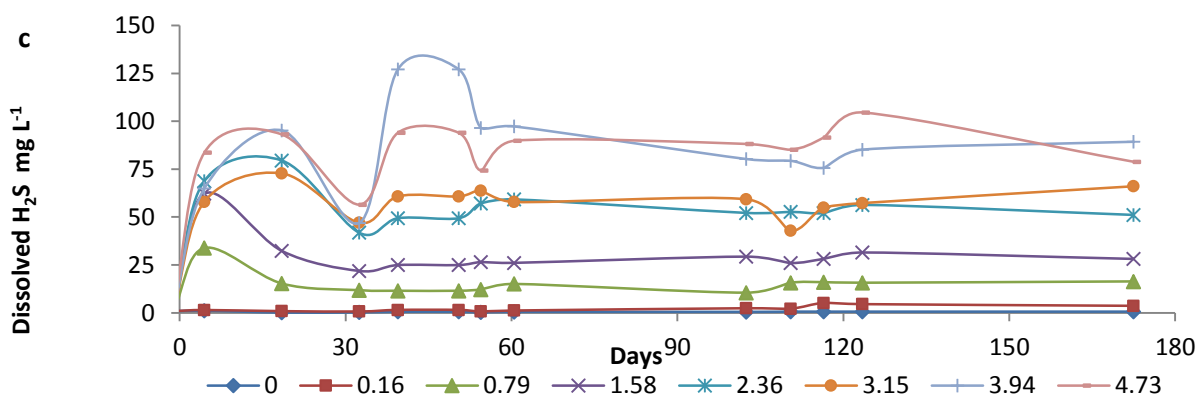
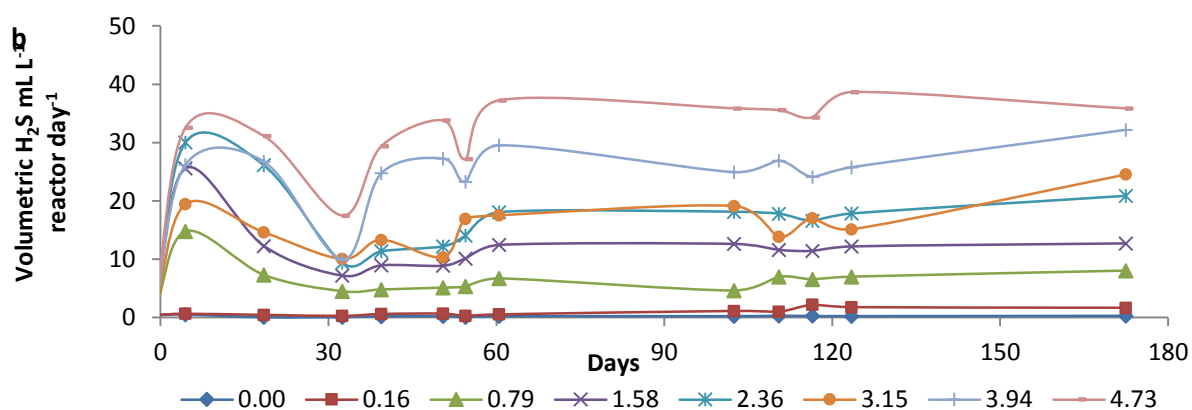
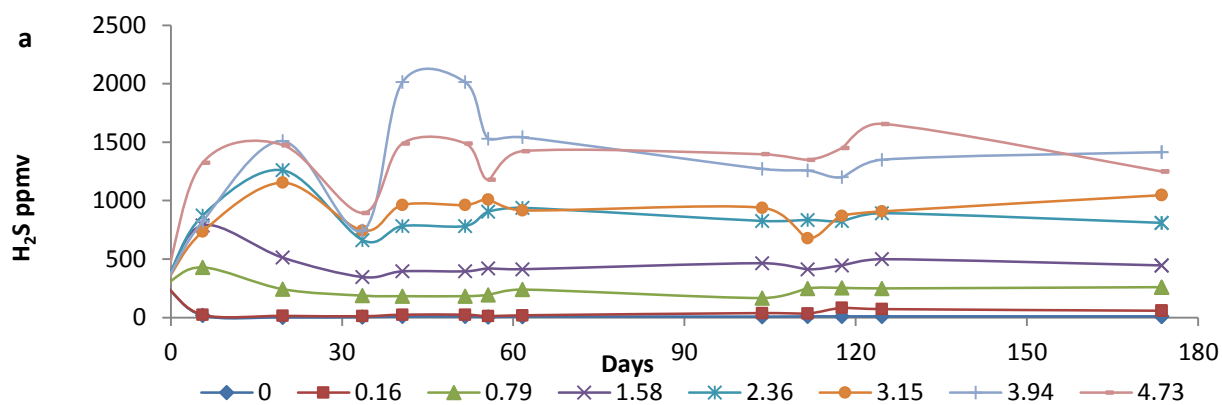
The methyl blue method was considered for the determination of soluble sulphide but due to the colour of the filtrate being similar to that needed for analysis and potential losses in preparation this method was rejected.

Figure 64b shows the relationship between a calculated and measured total soluble sulphide. This data was measured using three individuals and brand new equipment. The relationship is linear with an R^2 of 0.955 giving a high degree of confidence to the calculated value. This relationship is only possible when the samples are rapidly analysed with new equipment and fresh reagents, and is highly labour intensive. In contrast the gas sample is less labour intensive and time consuming. Due to these issues it was decided to use the volume of hydrogen sulphide produced in combination with Henry's Law and a calculation of the speciation of hydrogen sulphide taking into account the solids, salt and pH of the reactor. This was found to give a better mass balance within the reactor.

4.2.6.4.2 Hydrogen sulphide

Hydrogen sulphide production for the reactors F3 – F8 increased after the addition of sulphate within the first 20 days (Figure 65a-e). Increasing concentration of H_2S present in the biogas with increasing concentration of SO_4 producing a linear relationship (Figure 65f and g). H_2S gas production remained stable after 33 days for F1 – F4 and stable for reactors F5 – F8 after 62 days (Figure 65a, f). Dissolved H_2S and HS^- increased with the initial spike of sulphate gradually decreasing over the next 50 days before rising and remaining stable for the remainder of the experiment (Figure 65c, d and e). Sulphur removal for all reactors was

above 100% with the initial addition of the SO_4 augmentation, declining towards 100% within three HRT (Figure 65h).



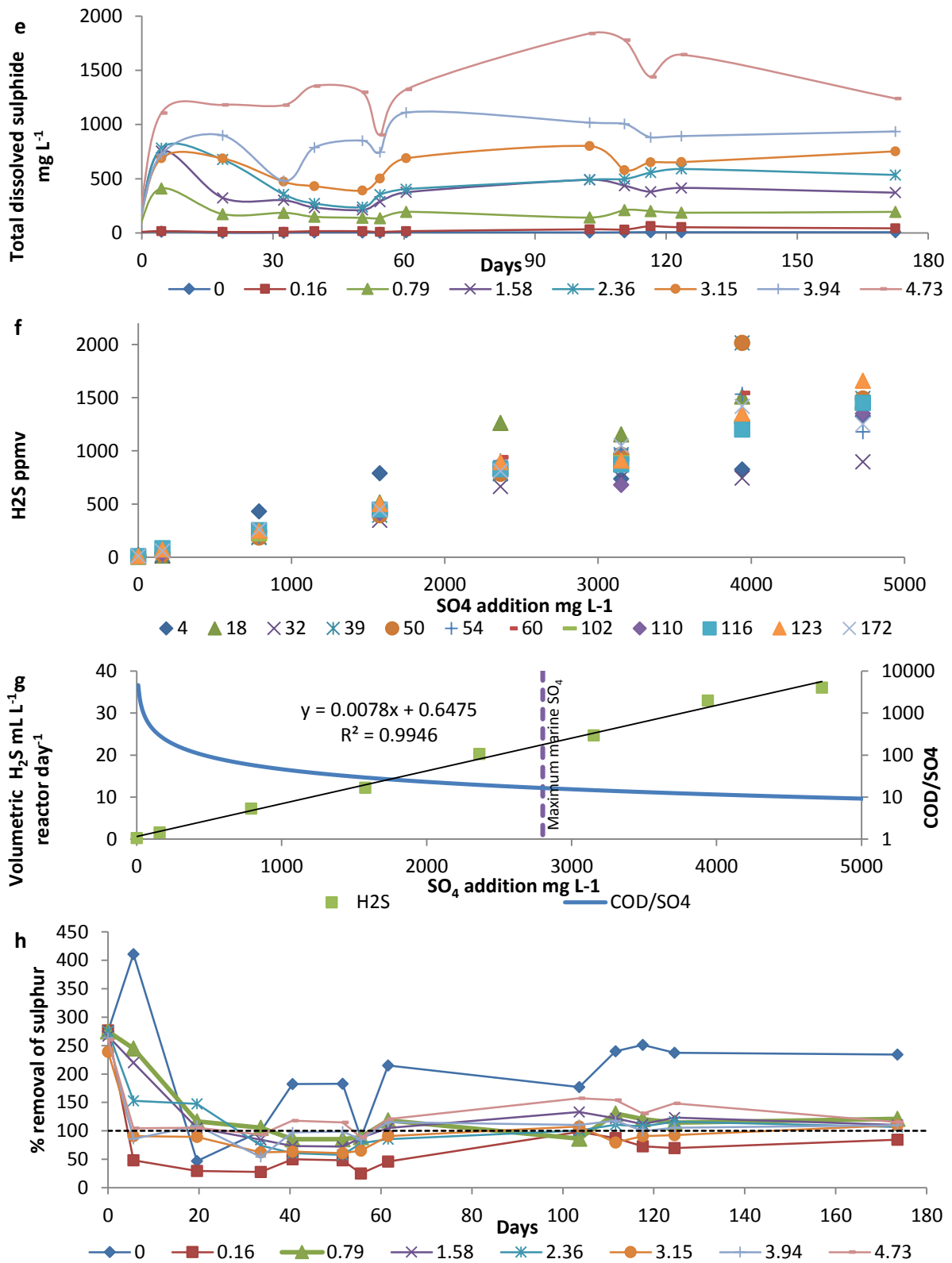


Figure 65 Hydrogen sulphide production graphs for Phase 4. (a) H₂S PPMV (b) Volumetric H₂S production (c) Soluble H₂S (d) Soluble HS⁻ (e) Total dissolved sulphide (f) H₂S ppmv/SO₄ addition (g) COD/ SO₄ (h) % removal of sulphur

Table 34 Average values for key monitoring parameters in the last 21 days of Phase 4.

Parameter	Unit	SO4 concentration/ reactor number							
		0	0.16	0.79	1.58	2.36	3.15	3.94	4.73
		F1	F2	F3	F4	F5	F6	F7	F8
Salt	g L ⁻¹	31.1	31.26	31.89	32.68	33.46	34.25	35.04	35.83
pH		7.49	7.50	7.52	7.56	7.56	7.61	7.65	7.71
TAN	g N L ⁻¹	2.46	2.41	2.39	2.44	2.46	2.46	2.25	2.46
TA	g CaCO ₃ L ⁻¹	4.93	4.71	5.08	5.19	6.66	6.13	6.38	7.55
PA	g CaCO ₃ L ⁻¹	3.59	3.47	3.78	3.89	4.43	4.37	4.48	5.57
IA	g CaCO ₃ L ⁻¹	1.34	1.24	1.30	1.31	2.23	1.76	1.89	1.99
IA/PA		0.37	0.36	0.34	0.34	0.50	0.40	0.42	0.36
TS	% WW	3.96	4.34	4.42	4.40	5.33	4.88	5.10	4.88
VS	% WW	0.84	0.89	0.94	0.89	1.27	0.98	1.12	0.92
VS Destruction	% VS	68.00	66.18	64.16	66.38	51.65	62.70	57.61	64.89
VFA	mg L ⁻¹	130	40	80	30	950	1110	1210	540
VBP	L L ⁻¹ day ⁻¹	0.57	0.55	0.56	0.55	0.48	0.45	0.43	0.56
CH ₄	% volume	61.53	63.28	60.57	61.70	57.62	59.92	59.65	61.51
SMP	L CH ₄ g ⁻¹ VS	0.46	0.46	0.43	0.44	0.36	0.35	0.34	0.45
H ₂ S	PPMV	200	1417	5087	9278	16856	18833	26433	29049
Volumetric H ₂ S	ml L ⁻¹ day ⁻¹	0.27	1.89	7.22	12.12	18.44	18.90	27.36	36.28
Dissolved H ₂ S	mg L ⁻¹	0.6	4.5	16.1	29.3	53.2	59.4	83.4	91.7
HS ⁻	mg L ⁻¹	6.6	48.3	178.4	359.7	507.4	626.8	820.5	1349.6
Total dissolved Sulphide	mg L ⁻¹	7.3	52.7	194.4	389.0	560.6	686.2	903.9	1441.2

4.2.6.5 Sulphate addition discussion

The differences between the more heavily sulphate-loaded reactors were evident in the gas production, with VBP in F5-7 falling to half that of the controls by around day 50, accompanied by a drop of 8-10% in biogas methane content and corresponding decreases in SMP (Figure 4e and f). Gas production in these reactors then gradually recovered, although it was still only 85-90% of the control value at the end of the run. In contrast gas production in F8 was only slightly reduced up to day 38 and had recovered to the control value by day ~120. The lower gas production in F5 was reflected in a fall in VS destruction, to around 32% on day 55 (Figure 4g). By the end of the run VS destruction in F1-4 and F8 had stabilised at between 65-69%, while F5-7 still showed reduced values ranging from 53-63%.

The reduction in biogas production and VS destruction was accompanied by an increase in propionic acid concentrations within the high sulphate reactors which are often attributed to the onset of reactor failure (Fischer et al., 1984, Pullammanappallil et al., 2001, Kaspar and Wuhrmann, 1977, van den Berg and Lentz, 1971). It has been suggested that a propionic acid concentration greater than 800 mg L⁻¹ or a propionic to acetic acid ratio greater than 1.4 may indicate reactor instability and potential failure (Hill et al., 1987). For the reactors F4 –F8, this ratio increased from ~1.4 to 100 within the first 21 days well above the recommended value, before gradually declining to between 1.3 and 10 after eleven HRT. The total VFA concentration was below 800 mg L⁻¹, however, at a maximum of 310 mg L⁻¹ in F6, indicating minimal reactor stress (Hill et al., 1987, Marchaim and Krause, 1993). Propionate is an important fermentation product in the anaerobic sulphate reduction process which can be directly consumed by SRB as shown in equation 2 (Speece, 1996, Widdel, 1988, Thauer et al., 1977). The degradation of propionate can be significantly enhanced by the presence of SRB, with the rate of oxidation higher at high sulphate concentrations (Liamleam and Annachatre, 2007).



The observed patterns in H₂S production may also help to indicate the reasons for the behaviour of the different reactors. In the process of sulphate reduction by SRB hydrogen ions are consumed, thus increasing the alkalinity and providing additional buffering. The initial addition of sulphate caused rapid production of H₂S and an increase in soluble sulphide concentrations to 1200 mg L⁻¹ or more, within reported values for the toxicity threshold of 200-1500 mg L⁻¹ (Chen et al., 2008, Koster et al., 1986, Parkin et al., 1990). This resulted in partial inhibition of methanogenesis, leading to the observed rise in VFA concentrations in reactors with sulphate additions ≥ 1.58 g SO₄ L⁻¹. At 1.58 g SO₄ L⁻¹ (F4) pH remained stable and the VFA accumulation was consumed fairly rapidly. At 2.36, 3.15 and 3.94 g SO₄ L⁻¹ (F5-7) the VFA increase led to a fall in pH, whereas at 4.73 g SO₄ L⁻¹ (F8) the pH increased slightly. Once a stable SRB population had grown excess propionic acid could be gradually consumed reducing the total VFA concentrations to between 1.2 and 0.54 g L⁻¹ of the high SO₄ reactors and increasing the pH.

pH is a major controlling factor in relation to sulphide speciation and a reduction can shift the equilibrium between HS⁻ and the more toxic H₂S, potentially causing inhibition of methanogenesis. Reactors F5-7 with intermediate sulphate addition had lower initial conversion of H₂S, less consumption of H⁺ and therefore lower partial alkalinity and greater

pH change. In contrast in F8, the reactor with the highest sulphate conversion, the consumption of H^+ was sufficient to buffer pH change and reduce VFA formation. pH values in F5-7 were in the critical range for sulphide toxicity: in F6 and F7 the minimum pH was around 7.2, where 88% of sulphide is present as HS^- ; whereas in F5 at a minimum pH of 7.1 the fraction of H_2S increases to 19%. Parkin et al. (1990) reported inhibitory sulfide concentrations in the range of 100–800 mg L^{-1} dissolved sulfide or approximately 50–400 mg L^{-1} undissociated H_2S . O'Flaherty et al. (1998b) observed that sulfide inhibition for both SRB and methanogens was related to the un-ionized sulfide concentration in the pH range 6.8–7.2 and to total sulfide concentrations above pH 7.2. The apparent fall in VS destruction observed in F5 during the period of low pH may also indicate some sulphide inhibition of hydrolytic and acidogenic organisms, in addition to methanogenesis.

As H_2S production in the reactors with intermediate sulphate addition stabilised after two HRT, the alkalinity and pH recovered, allowing the VFA accumulation to be reduced. By the end of the experimental period gas production in F2, 3 and 8 was equal to that in the control while that in digesters F5-7 was approaching the control value. Figure 65g shows the relationship between sulphate addition, volumetric H_2S production and substrate COD/ SO_4 ratio: it can be seen that the reactors were successfully able to convert the maximum marine sulphate concentration at the COD: SO_4 ratios applied; suggesting that the reactors could produce greater sulphide concentrations at a lower COD: SO_4 ratio.

Final sulphate concentrations in the digestate ranged from 16-257 mg $SO_4 L^{-1}$, corresponding to conversion of 94-95% of the added sulphate in reactors F3-8 (500-3000 mg $SO_4 L^{-1}$), and of 84% for F2 (100 mg $SO_4 L^{-1}$) (Figure 65h). These values are similar to the conversion efficiencies of 90-96% reported by (Omil et al., 1995). The high conversion rate of sulphate suggests the reactors have become stable with regards to sulphur production, which is further confirmed with the biogas productions trending towards the control and a decrease in VFA and IA/PA in all reactors. Reactor F1 had fluctuating removal efficiencies between 50 – 400%, potentially due to the difficulty in determining the states of sulphur at low concentrations, with a few mg of sulphur increasing the % removal by up to 300%.

4.2.7 Concluding remarks

These results demonstrated successful acclimatization of a methanogenic consortium to a high salinity feedstock starting with a municipal biosolids derived inoculum. Shock loadings of total salt exceeding 10 g L^{-1} showed inhibition of the methanogenic archaea, but little impact of the fermentative bacteria, with increases in total VFA coupled with a decrease in pH. This led to the reactors becoming “sour”, and the decision to cease operation at these initial high concentrations. At concentrations below 10 g L^{-1} there was little difference in the SMP to that of the control, suggesting that 10 g L^{-1} is potentially the critical concentration for inhibition of non-acclimatised methanogens

Gradual increase in total chloride salt concentration of the spiked reactors showed some fluctuations during acclimatisation, but became stable at a final chloride salt concentration of 31.1 g L^{-1} with the SMP reduced by around 6-7%. There appeared to be no other detrimental effects. The acclimatisation period could have been potentially reduced by spiking the reactors to 9 g L^{-1} , and increasing the salt concentration by $>1 \text{ g L}^{-1} \text{ HRT}^{-1}$ if the reactors are already adapted to their feedstock. This, however, will require further study to determine the maximum rate of acclimatisation.

On substitution of a proportion of the chloride for sulphate some initial instability was noted at the higher SO_4^{2-} concentrations dosed, which could be attributed to the predominant forms of reduced sulphur present as influenced by pH and its effect on the equilibrium concentrations. Sulphate addition also showed a further reduction in specific methane production but at marine concentrations this loss was less than 5%, and other than this digester performance and stability were comparable to the non-salt supplemented control. The acclimated digestate was considered suitable as an inoculum for digestion of marine microalgae harvested at around 5% TS which would result in 95% of the inoculum feed being undiluted seawater.

4.3 Large scale algal growth and continuous digestion

4.3.1 Introduction

The purpose of this part of the research was to determine the digestibility of marine microalgae suspended within their original salt water growth media at both low and high SO₄ concentrations. Prior to digestion strains of marine microalgae selected for their suitability for AD were continuously cultivated within a PBR with a medium containing either 20 or 4730 mg L⁻¹ of sulphate. After harvesting, the substrate was characterised to determine its chemical content, calorific content, biochemical methane potential and the specific methane potential utilising the salt adapted inoculum outlined in the previous chapter.

4.3.2 Continuous algal growth

Objective: To cultivate marine microalgae continuously in low and marine sulphate media for subsequent continuous digestion analysis, to determine the specific methane potential and effects of SRB.

Methodology: Two strains of marine algae were cultivated continuously within the 300 L tubular PBR as described in section 3.3.1 on JM with marine concentrations of Na, Mg, K, Ca, Cl (Section 3.2.3) (Table 19 and 20). *I. galbana* was cultivated between October and November 2013 at low sulphate concentrations, while *D. salina* was cultivated at low sulphate concentrations between March and April 2014 and at high sulphate concentrations between April and May 2014. Each run was inoculated with 160 L of a pure culture of the relevant microalga cultivated within the laboratory for ten days as described in Section 3.3. This was subsequently pumped into the PBR and topped up with fresh culture medium to fill the reactor and enable the airlift to work. The reactor was allowed to run for two days before dilution via feeding began at 70 L day⁻¹, with collection of displaced effluent via the overflow. Samples of the culture were monitored for TSS content and observed under the microscope to determine whether contamination had occurred. The collected effluent was centrifuged and the paste frozen at -17°C until use. *I. galbana* was harvested using a Powerfuge Pilot continuous centrifuge and the *D. salina* cultures were harvested using a milk creamer disk stack continuous centrifuge as described in Section 3.3.4.

4.3.3 Cultivation results and discussion

During each cultivation attempt some contamination and biofouling occurred within the reactor (Figure 66), which reduced the growth yield. *I. galbana* exhibited minor biofouling within 15 days, with invasive pennate microalgae observed after 19-21 days. *D. salina* grown on a low sulphate medium remained a pure culture for longer, exhibiting biofouling within 10 days which became growth limiting after 25 days, with an invasive pennate microalgae observed after 31 days. Biofouling of the high sulphate *D. salina* began within five days. Between days 12-15 a blockage to the overflow and foaming caused by the lysing of cells led to a leak of water onto a raised power supply. This caused the peristaltic pump that supplied the fresh culture medium to switch off, and thus the culture was not fed or harvested during this period.

High levels of biofouling were noted on the Perspex tubing in areas prior to a bend. In these regions the plastic followers used for cleaning the internal surface of the PBR tended to congregate at the base or top of the Perspex tubing preventing any scouring on the middle of the tubes (Figure 66c). This enabled a biofilm to grow, which reduced the light reaching the culture, and potentially the harvested algal yield of the reactor. Harris et al. (2013) observed a decrease in algal production with an increase in biofouling regardless of thickness of the biofilm, and attributed this to reduced irradiance. Arbib et al. (2013) reported similar findings using a PBR, with severe biofouling reducing algal yields from >0.7 g TSS L⁻¹ to <0.2 g TSS L⁻¹. In the current work any reduction in flow rate reduced the cleaning effect enough to allow rapid biofilm formation, such as occurred when the airlift failed.

A redesign of the reactor would be beneficial for future operation due to the difficulty of cleaning and maintaining the reactor when cultures crash. A flat plate reactor of equal or greater working volume could be utilised for simplicity, with several used to enable growth of cultures at the same time. Plastic could be replaced by glass if a flat plate reactor is used, reducing fouling and facilitating cleaning without damaging the surface.

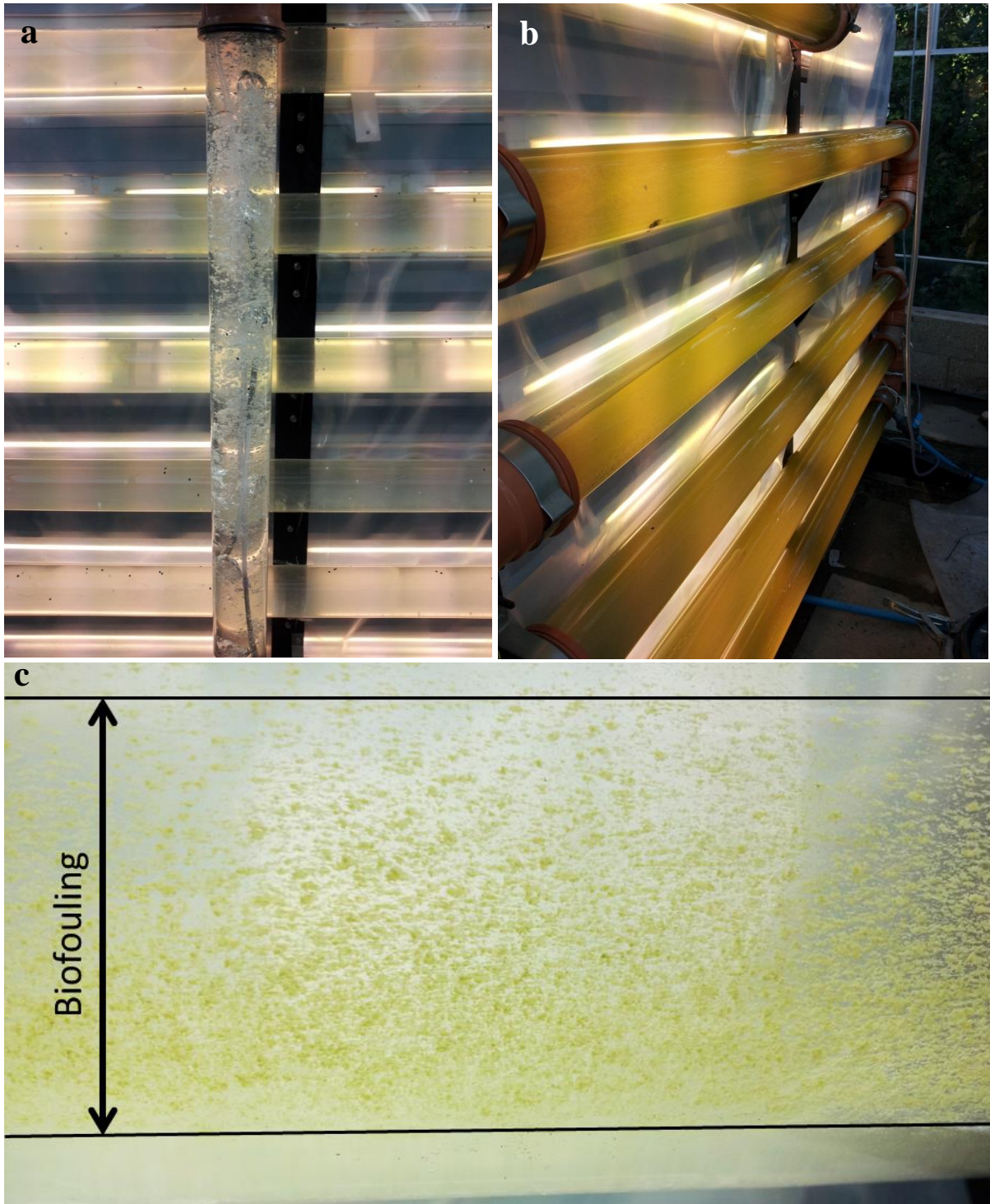


Figure 66 (a), pre inoculation with *I. galbana* showing the airlift, (b) post inoculation with *I. galbana*, (c) Fouling has begun to occur where the plastic followers are failing to clean the reactor in the central part of the tubes.

Seasonal variations were obvious for the growth yields of the reactors. The greatest overall yield came from the *D. salina* species grown between the spring and start of summer where

irradiances are greatest. Daily TSS concentrations in this period were 0.62 g L^{-1} ; almost double that of *I. galbana* within the same time span (Figure 67). The *I. galbana* run produced similar TSS concentrations to the first *D. salina* run possibly due to similar irradiance levels for the months in which they were cultured. When the airlift failed, however, temperature and oxygen became potentially toxic within the PBR to microalgae.

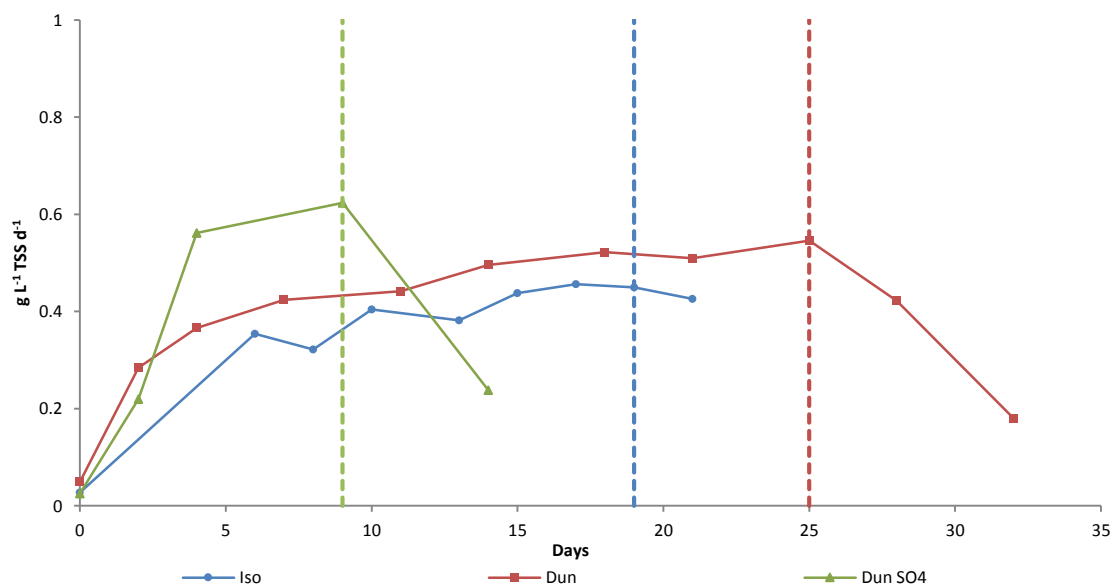


Figure 67 TSS of PBR for the species *I. galbana* and *D. salina*. Dotted vertical lines represent points where biofouling occurred sufficiently to reduce yields prior to stopping.

The airlift enabled degassing of excess oxygen from the culture media and dissolution of ambient atmospheric CO_2 into the culture media as the primary source of carbon. The airlift also passed through a thermo-regulator that chilled an enclosed section of the reactor to maintain an internal temperature of $\sim 25^\circ\text{C}$. Movement of the culture media through the PBR provided some turbulence and scouring effect with regards to the plastic follower beads to aid in the prevention and removal of bio fouling. Once the system failed all these processes ceased, allowing bio fouling and the potential build-up of dissolved oxygen. This could denature the RUBISCO enzyme within the chloroplasts due to the high concentrations of oxygen present, reducing the rate of photosynthesis and ultimately leading to photooxidative death (Molina et al., 2001, Abeliovich and Shilo, 1972, Powles, 1984). Overheating of the algae with the prolonged ambient temperatures exceeding 50°C towards mid-day could also denature algal proteins and enzymes causing death. Westerhoff et al. (2010) reported culture

failure at temperatures exceeding 42°C within a PBR. As dissolved oxygen and internal temperature were not continuously logged it is not possible to state definitively what caused the culture crash, but it is likely a combination of toxicity from oxygen, stress from the heat and reduced dissolved carbon all played a part.

4.3.3.1 Partial conclusion

Several potential inhibitory parameters need to be controlled within future experiments using the PBR outlined within this report. Oxygen toxicity and temperature shock were probable causes of culture shock and require a greater level of control and continued measurement during operation in future studies. Increasing irradiance from the spring to the summer shows a distinct difference between the growth yields of the *D. salina* samples, highlighting the need to cultivate samples at the same time to prevent differences in potential biomass composition that can occur when algae reach different phases within their lifecycle. The gradual increase in TSS over the growth period shows that the dilution rate could be increased for each species once an optimum solids concentration has been reached. This would enable a greater volume of biomass to be harvested per unit volume of reactor.

4.3.4 Continuous algal digestion

Objective: To determine the methane yield and digestion performance of microalgae cultured in low and high sulphate concentrations in continuous digestion under mesophilic conditions.

Methodology: Waste digestate removed daily from the eight salt-acclimatised reactors in section 4.2 was transferred into a 4 L CSTR digester maintained at 35°C, and fed with the same feed of 90% synthetic wastewater and 10% concentrated chloride salt solution at the same OLR as before. Once 3.5 L of digestate had accumulated in daily 800 ml aliquots, it was then decanted into six CSTR digesters each with a working volume of 0.5 L. 33 ml of digestate was removed from each of these digesters daily and 33 ml of feedstock added via a syringe through the feed hole in the top plate giving a HRT of 15 days. Digester feedstock was prepared by re-suspending the harvested algal paste (Section 3.3.4) in the centrate to a known solids content, which differed between the species depending on the mass harvested, to ensure that the system could be run for at least three HRT. Two reactors were fed on *I. galbana*, and the other four on *D. salina* at OLRs of 1.0 and 1.6 g VS L⁻¹ day⁻¹ respectively. Feeding with algal biomass commenced on day 7 of operation. After three HRT, the

feedstock to two of the *D. salina* reactors was switched to the *D. salina* grown in high sulphate conditions at an OLR of 1.9 g VS L⁻¹. Feeding with *D. salina* continued for six HRT, with *D. salina* SO₄ for three HRT, and with *I. galbana* for four HRT due to restrictions from the mass of biomass cultivated.

Biogas volume was determined using gas bags and the gasometer method, and gas composition was analysed weekly for CH₄, CO₂ and H₂S content along with pH on the same day. When H₂S was analysed all the gas produced was required for analysis and the previous day's gas production was therefore used as an estimate for the gas production volume.

4.3.5 Results and discussion

4.3.5.1 Substrate characterisation

Table 35 shows the results of characterisation of the three algal samples. VS content as a proportion of TS was 55.8% for *I. galbana* and between 77.8-80.5% for the *D. salina*. The differences in VS content are likely to be due to several factors including species, growth conditions and changes in centrifugation method. *I. galbana* was cultivated during winter with decreasing irradiance and ambient temperature and harvested using a 1 L Powerfuge Pilot; whereas the cultures of *D. salina* were cultivated with a milk creamer disk stack centrifuge. The VS content of the *I. galbana* is lower than that of the laboratory grown cultures (67.2% VS, Table 38): A simple correction for the inorganic salt content increases the VS content of the continuously grown sample to 61.5% VS of TS and the laboratory cultivated sample to 71% VS of TS, suggesting that this may be due to growth at lower irradiances and temperatures, and continuous operation with harvested concentrations lower at a maximum 0.45 g L⁻¹ TSS (Figure 67). In contrast the VS content of the laboratory grown *D. salina* at 50.4% of TS was much lower than both the low and high sulphate cultures grown in the PBR. This may be associated with an increased irradiance and temperature during continuous culture.

Carbon content ranged from 51.6 – 54.2% on a VS basis, with both *D. salina* cultures found to have similar carbon contents. As expected, the resulting C:N ratios of between 5.3 and 6.2 are all below the recommended range of 20-30 for anaerobic digestion, and similar to those reported in the literature (Ward et al., 2014). The low sulphate species had 0.4 - 0.9% sulphur, similar to the fresh water laboratory-grown algae of between 0.4 – 1.0% (Section

4.1.5, TABLE 3). High sulphate *D. salina* had a sulphur content of 2.4%, in the range of that for the laboratory-grown marine species (1.8 – 5.5%) (Section 4.1.5, TABLE 3). The total sulphur content was markedly lower than that of the laboratory grown species of *D. salina* at 5.5%, however, possibly due to the change in growth media salt source from a commercial combined brand to individual bulk chemicals, and a change in growth regime from batch to continuous. Harvesting of the algae during the exponential phase of growth rather than the stationary phase of growth could also change the composition of the feedstock, with microalgae reducing reproduction and protein synthesis in favour of carbohydrate and lipid storage (Rodolfi et al., 2009, Pal et al., 2011, Mata et al., 2010). Calorific values ranged from 12.9 MJ g⁻¹ TS for *I. galbana* to 18.3-19.3 MJ g⁻¹ TS for *D. salina* and *D. salina* SO₄ respectively, reflecting the different proportions of inorganic material present within the samples. On a VS basis the calorific values were more uniform at between 23.2 – 24 MJ kg⁻¹ VS reflecting the similarity between the elemental compositions of the organic fraction.

Table 35 Characteristics of the algal paste harvested from continuous growth.

Species	TS	VS	TKN	CV	Elemental composition (% of VS)					C:N ^b
	(%TS of WW)	(%TS)	%N of VS	MJ kg ⁻¹ VS	C	H	O ^a	N	S	
<i>I. galbana</i>	33.02 ± 0.50	55.8 ± 0.79	8.52 ± 0.01	23.2	51.59 ± 0.41	6.52 ± 0.18	33.02	5.95 ± 0.05	0.35 ± 0.01	6.1
<i>Dunaliella</i> sp.	32.65 ± 0.25	77.8 ± 0.41	8.75 ± 0.01	23.6	54.20 ± 0.41	6.89 ± 0.18	29.28	6.17 ± 0.05	0.88 ± 0.01	6.2
<i>Dunaliella</i> sp. <i>SO</i> ₄	28.51 ± 0.71	80.5 ± 0.18	10.18 ± 0.01	24.0	54.17 ± 1.16	6.89 ± 0.20	26.35	8.61 ± 0.09	2.40 ± 0.03	5.3

^a Oxygen calculated by difference based on determination of C, H and S by elemental analysis and N by TKN.

^b C/N ratio calculated using TKN on a VS basis

4.3.6 Continuous digestion study

4.3.6.1 Biogas production, and methane yield

Volumetric biogas production (VBP) for *I. galbana*, *D. salina* and high sulphate *D. salina* stabilised at 0.31, 0.62 and 0.54 L biogas L⁻¹ day⁻¹ respectively after three HRT (Figure 68a). The VBP in the high sulphate *D. salina* decrease slightly from 0.64 to 0.54 L⁻¹ day⁻¹ after three HRT (Figure 68a), corresponding respectively to specific biogas production (SBP) values of 0.29, 0.39 and 0.29 L biogas g⁻¹ VS added (Figure 68b). The CH₄ content of the biogas for *I. galbana* and *D. salina* stabilised within five days of switching to the algal feedstock at 64-68% and 58-62% for *D. salina* (Figure 68c). The CH₄ content for the high sulphate *D. salina* stabilised more slowly at 62% within one HRT (Figure 68c). The SMP for *D. salina* stabilised after 20 days at 0.24 L CH₄ g⁻¹ VS, with *I. galbana* and the high sulphate *D. salina* stabilising more slowly at 0.19 and 0.185 L CH₄ g⁻¹ VS after three HRT of feeding (Figure 68c). There was a temporary increase in biogas and methane production from the *I. galbana* digesters between days 19 and 31: this was probably due to a mis-feeding with the *D. salina* feedstock into the *I. galbana* reactors, as CH₄ production increased sharply from 0.21 to 0.28 L CH₄ g⁻¹ VS within one day, falling back to and stabilising at 0.21 L CH₄ g⁻¹ VS after five days. The switch to the high sulphate *D. salina* thus led to a slight decrease in VBP; coupled with a decrease in SMP.

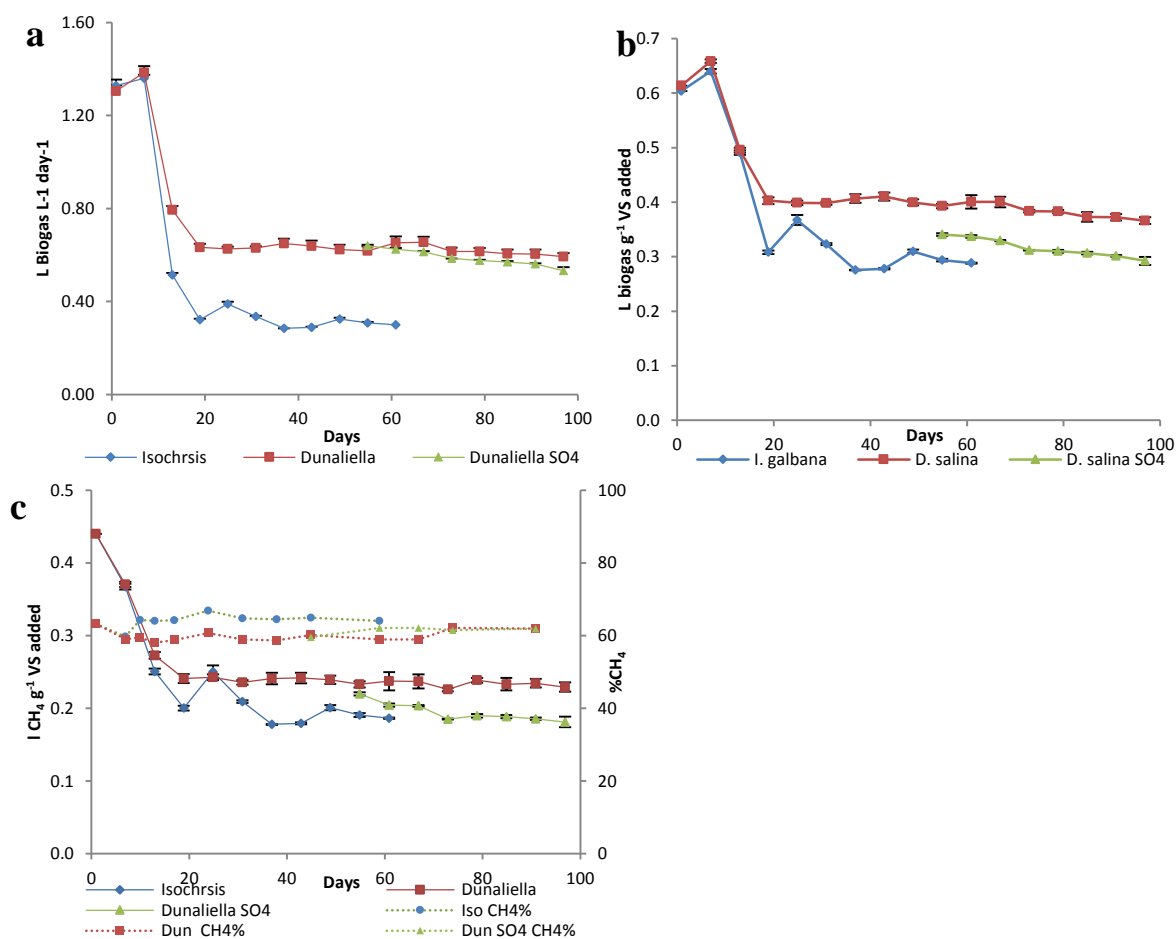


Figure 68 Weekly averages (a) Biogas, (b) Biogas g^{-1} VS, (c) SMP, (d) residual biogas production. Error bars show the range of the data.

4.3.6.2 TS and VS

As seen in Figure 69a TS content as a proportion of wet weight increased over the initial two weeks after switching from the synthetic wastewater feed to the algal substrate, from 3.7% to 4.8% and 4.5% for *I. galbana* and *D. salina*, respectively. This reflected the high inorganic solids of the substrate compared to that of the synthetic wastewater at 90.1% VS of TS. VS content as a proportion of wet weight increased for all substrates from an initial low of 0.87% prior to algal digestion to between 1.13% and 1.31% at the end of each run. This is due to a decrease in VS destruction, from ~71% for the synthetic wastewater fed inoculum to ~32% for *I. galbana*, ~48% for *D. salina* and 53% for *D. salina* SO₄ as shown in Figure 69b.

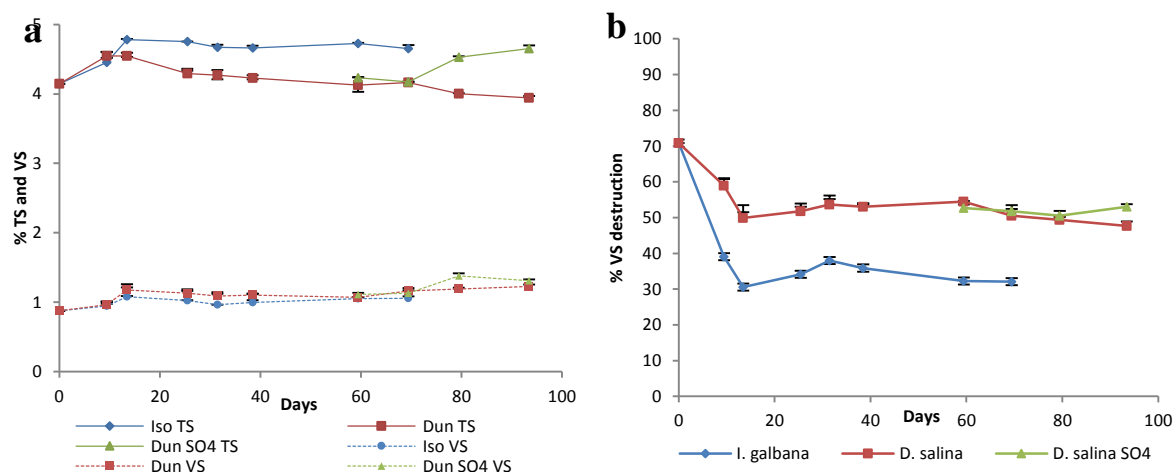
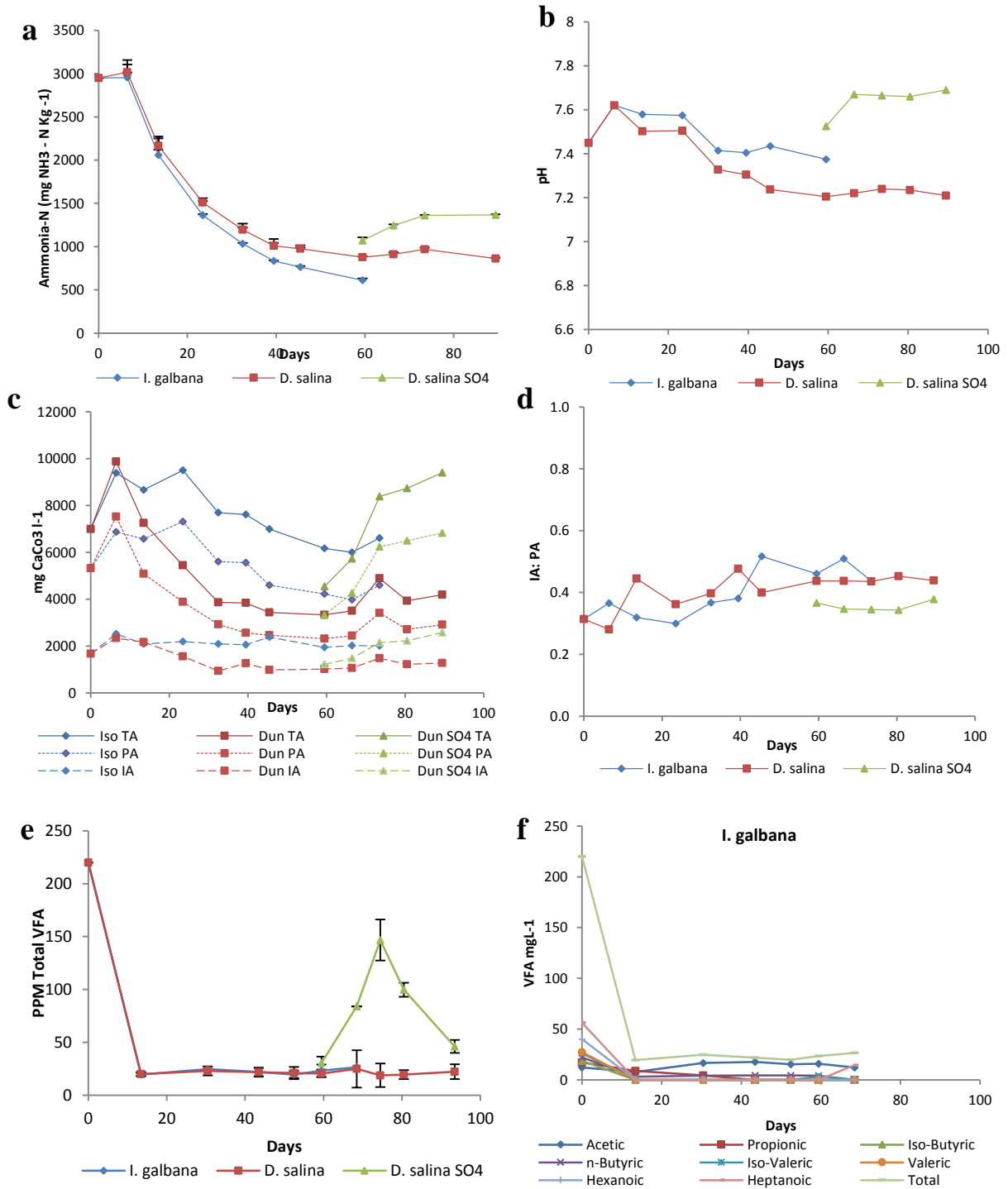


Figure 69 (a) %TS and VS of the digestate WW, (b) % VS destruction. Error bars show the range of the data.

4.3.6.3 Alkalinity, pH, Ammonia and VFA

Digestate total ammonia nitrogen (TAN) concentrations decreased in the digesters fed on *I. galbana* and *D. salina* from 3.0 g NH₃ N kg⁻¹ WW to 0.61 and 0.87 g NH₃ N kg⁻¹ WW respectively after 53 days (Figure 70a). The TAN concentration for the high SO₄ *D. salina* rose to 1.37 g NH₃ N kg⁻¹ WW after three HRT. The initial reduction is due to a combined effect of reducing the OLR, which reduces the loading of N to the digester; and the reduced digestibility of the feedstock, decreasing the conversion of organic N to inorganic ammonia. The higher OLR of the high sulphate *D. salina* feedstock reflects an increase in organic N loading within the digester; this enabled a greater proportion of nitrogen to be converted to TAN.

pH for both *I. galbana* and *D. salina* decreases from 7.62 stabilising at 7.38-7.4 and 7.20-7.23 respectively after three HRT. The addition of the high sulphate *D. salina* increased pH from an initial 7.23 to a stable 7.67 within one HRT (Figure 70b).



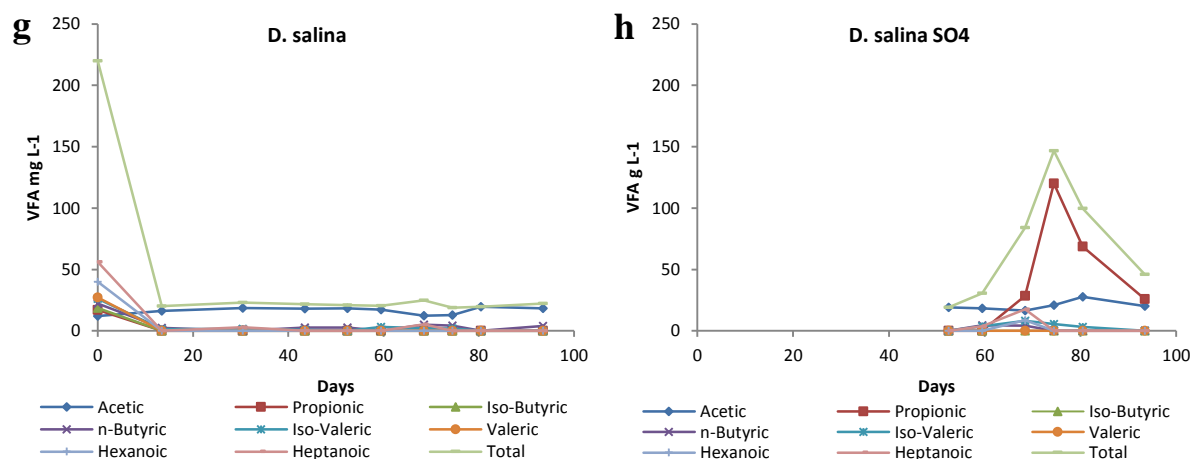


Figure 70 (a) ammonia, (b) pH, (c) alkalinity, (d) IA:PA, (e) total VFA, (f) *I. galbana* VFA, (g) *D. salina* VFA, (h) *D. salina* SO₄ VFA. Errorbars show the range of the data.

Total alkalinity for *I. galbana* and *D. salina* showed a small initial increase, then fell gradually over the next 2-3 HRT to stabilise at around 4.0 and 3.4 g CaCO₃ L⁻¹ respectively (Figure 70c). An increase in total alkalinity from 3.4 g CaCO₃ L⁻¹ to 9.4 g CaCO₃ L⁻¹ was observed following the switch to high sulphate *D. salina*. The IA/PA ratio remained relatively constant for all reactors, with a slight increase over the run from 0.3 to 0.5 for *I. galbana* and *D. salina*; the value of the high sulphate *D. salina* was slightly lower at around 0.35, reflecting possible hydrogen consumption; which is reflected in the increase in pH (Figure 70b and c)

Volatile fatty acid concentrations remained low throughout the digestion period (see Figure 70e). Total VFA for *I. galbana* and *D. salina* decreased from a stable 220 mg L⁻¹ in the salt-adapted inoculum to a stable 20 mg L⁻¹ within seven days of switching to the algal substrate, remaining low from then on. The introduction of the high sulphate *D. salina* led to a small increase in acetic, propionic and iso-valeric acid concentrations. The greatest increase was for propionic acid, which rose from 0 to 120 mg L⁻¹ within 14 days of introducing the new feedstock, before declining to 26 mg L⁻¹ 20 days later.

4.3.6.4 BMP and theoretical energy value

The BMP was determined using the algal paste prior to dilution with centrate, with inoculum taken from the same source as that used for algal screening, and for the salt adaption trial. Each sample was analysed in triplicate with triplicate cellulose controls and inoculum-only blanks. The cellulose control for this test gave a methane yield of 0.433 ± 0.004 L CH₄ g⁻¹ VS

added, less than <5% different from the values found in previous BMP tests, giving some confidence in the comparability of results for these assays (Figure 71a).

The results of the BMP are shown in Figure 71b and Table 37, with the theoretical values for methane potential and calorific value. *I. galbana* had the highest value at 0.326 L CH₄ g⁻¹ VS, equal to 93.4% of the BMP value for the original laboratory grown sample described in section 4.1.6 *D. salina* and *D. salina* SO₄ produced similar methane volumes at 0.269 and 0.281 L CH₄ g⁻¹ VS, respectively; in line with that of the original *D. salina* BMP value of 0.276 L CH₄ g⁻¹ VS. It is possible that the cumulative specific methane yield for *I. galbana* was still increasing very slightly at the end of the 87-day run period. As the increase over a 5-day period was less than 0.6% of the total methane production by *I. galbana*, however, the BMP was stopped at this point. After 30 days the *I. galbana* sample had produced around 94.5% of its final methane potential. Both *D. salina* samples had produced >98.2% of their methane potential, suggesting that the *I. galbana* sample contained a higher proportion of less readily degradable material than *D. salina*.

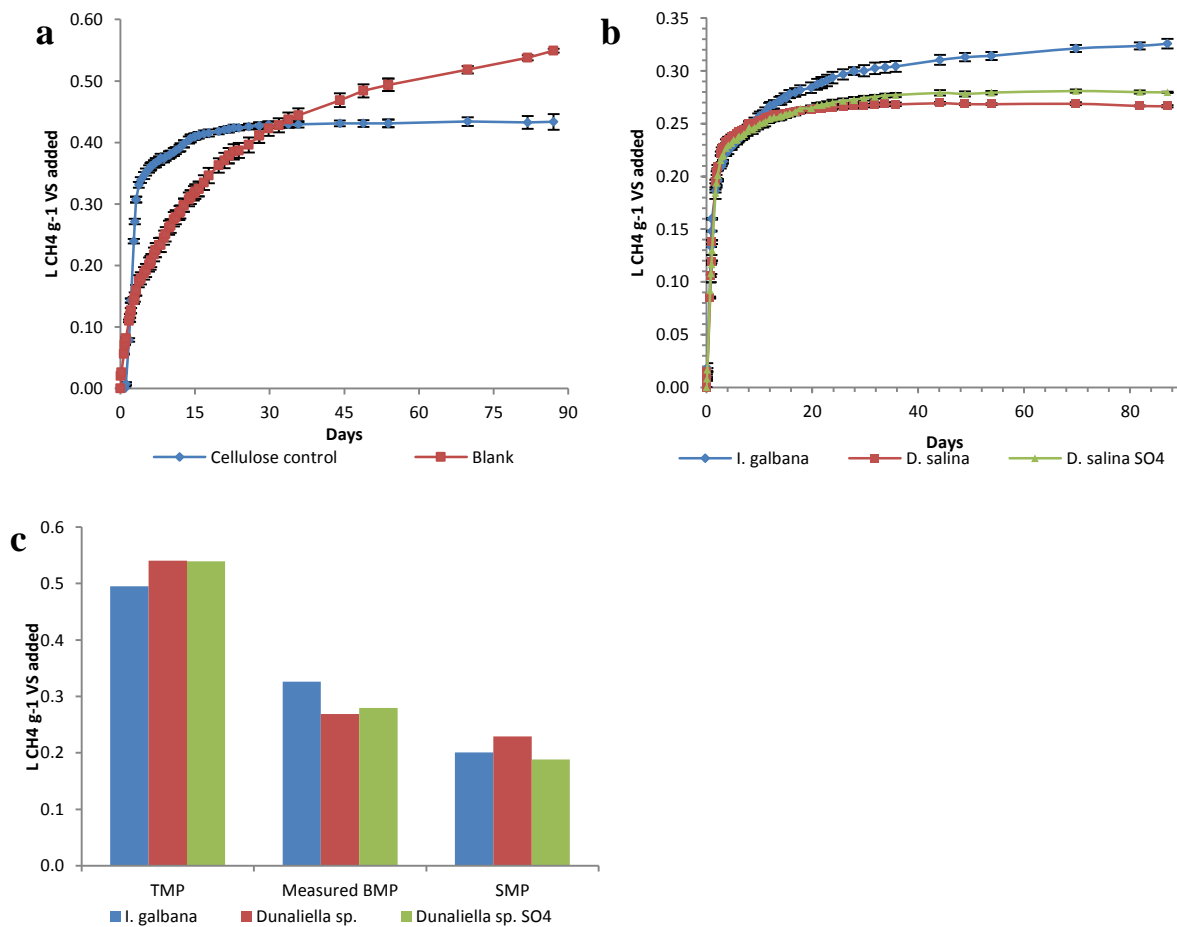


Figure 71 (a) Biochemical methane potential of cellulose control and Millbrook digestate as a blank. (b) Biochemical methane potential of *I. galbana*, *D. salina* and *D. salina* SO₄ continuously cultivated in a PBR. (c) Methane production for the TMP calculated from the EA, the final BMP values from graph b, and the average for the last HRT for the SMP from the continuous digestion analysis within this section. Error bars show the range of the data.

4.3.6.5 Methane production kinetics

The kinetic coefficients obtained from the methane potential tests are shown in Figure 72 and Table 36. As before in section 4.1.7 the kinetics are derived from the static BMP they cannot be used directly for continuous or semi continuous digestion, but they do indicate the degree of digestibility of the substrate.

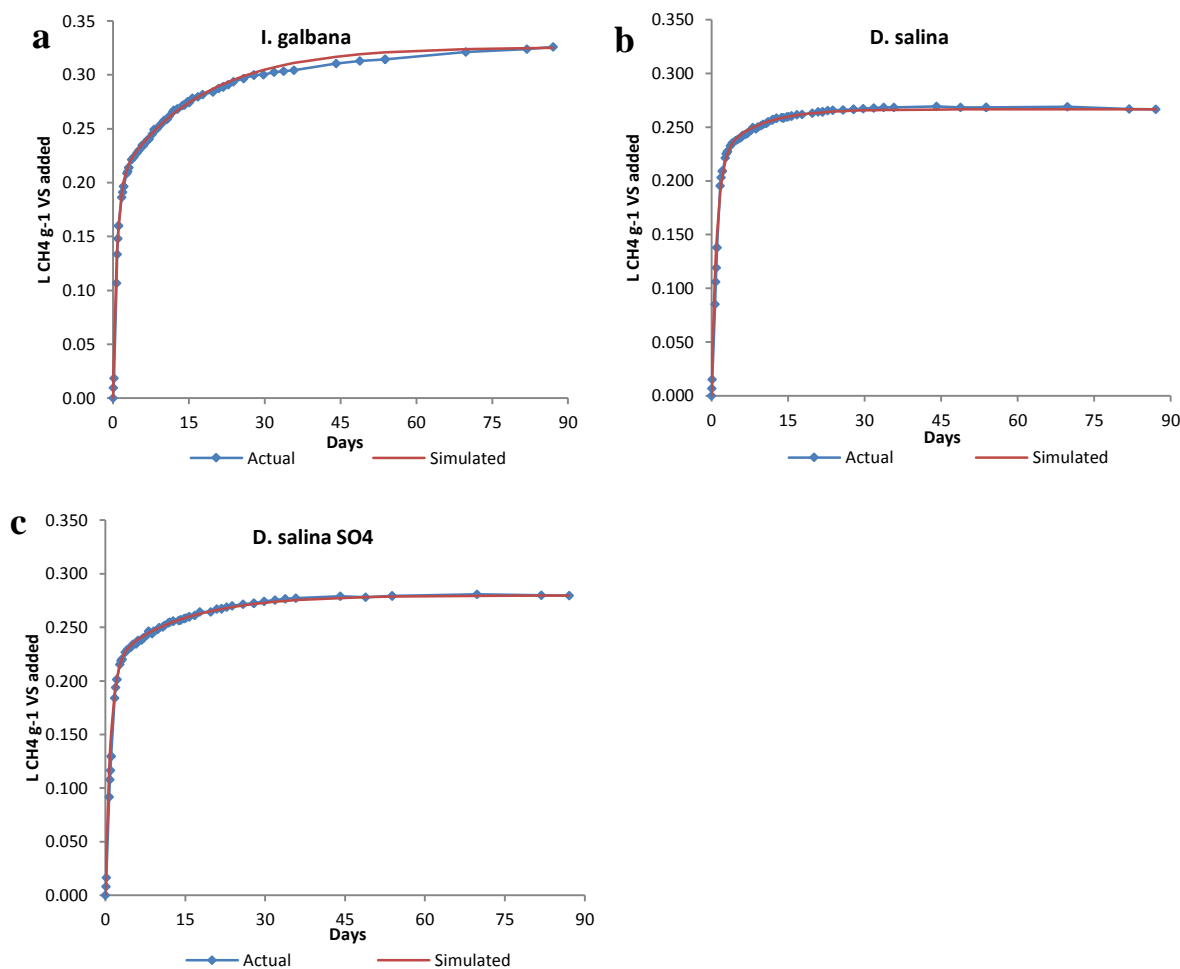


Figure 72 Cumulative net specific methane yield of marine microalgae (average of experimental data points for replicates) with kinetic models. (a) *I. galbana*, (b) *D. salina* and (c) *D. salina* SO₄.

The kinetic coefficients varied from those obtained in the algal screening in section 4.1. There was a decrease in biodegradable material from 71% for the laboratory cultivated *I. galbana* to 61% for the continuously cultivated substrate. For *D. salina* the proportion of readily biodegradable material was between 77-82%, similar to the value for the laboratory-grown *D. salina*. Values for k_1 were between 1.0 and 1.36 day⁻¹ for the three algal cultures, indicating that the properties of the readily degradable fraction were similar in all cases. Values for k_2 showed the least variability between 0.06 and 0.08 day⁻¹ again showing similar properties in the non-readily degradable fraction.

Table 36 Methane yields and kinetic constants obtained from modelling

Species	Y_{\max} (L CH ₄ g ⁻¹ VS)	P	k_1 day ⁻¹	k_2 day ⁻¹	R^2 ^a
<i>I. galbana</i>	0.326	0.61	1.28	0.06	0.998
<i>D. salina</i>	0.269	0.82	1.00	0.06	0.998
<i>D. salina SO4</i>	0.280	0.77	1.05	0.08	0.997

^a R^2 values indicate correlation between experimental and modelled data

4.3.6.6 Residual biogas production

Residual biogas potential (RBP) was measured in-situ after continuous operation had ended. *D. salina* and *I. galbana* have similar low RBP values at 0.81 and 1.03 L biogas g⁻¹ VS respectively, as shown in Figure 73. *D. salina* SO₄ at 1.08 L biogas g⁻¹ VS has a greater RBP than *D. salina* reflecting the lower specific biogas yields. All reactors showed a high degradable organic matter content post digestion due to the low VS destruction, retaining a high percentage of VS post digestion. Residual gas production for the *I. galbana* digestate took longer to plateau than for either of the *D. salina* samples, suggesting that the material present is slower to degrade. This is also observed in the BMP, with *I. galbana* gas production still rising after 88 days. This feedstock could benefit from an increased HRT. The BMP shows at 30 days a percentage CH₄ production of the maximum for *I. galbana*, of 94.2, compared to 83% within 15 days. *D. salina* and the high sulphate *D. salina* produced 97%, and 94% of their maximum CH₄ production respectively within 15 days, and would likely not benefit from an increased HRT. An increased HRT combined with a low energy pre-treatment step could perhaps increase the SMP and reduce the RBP for *I. galbana*. Currently the breakdown of organics is not maximising the SMP per unit of feedstock produced reducing the efficiency of the process. Increasing the SMP would be a requirement for disposal of the digestate as the biogas production post digestion is too high for conventional disposal (Banks et al., 2013). RBP includes all gases produced and does not reflect the methane potential of the residual biomass in this instance. Residual biogas production could be used to compare the SMP and BMP of each feedstock using a mass balance approach for all the materials entering the digester. This could then help explain the discrepancies between the batch and continuous operation due to the longer retention time of the batch analysis. In

this case, however, it was not possible as only residual biogas volume was measured, and not methane content.

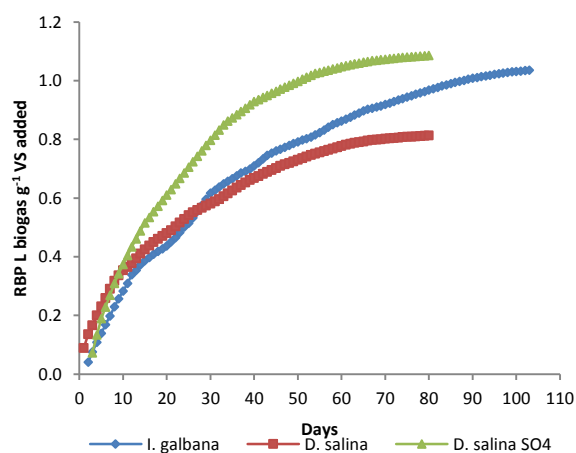


Figure 73 average in-situ residual biogas production post-feeding for the digesters *D. salina*, *D. salina* SO₄ and *I. galbana*.

Table 37 TMP, BMP, SMP and calorific values

Species	TMP	Measured BMP	SMP	Theoretical CV	BMP as % of TMP	SMP as % of BMP	Energy value of CH ₄ from BMP	% of CV converted to CH ₄ ^c
	L CH ₄ g ⁻¹ VS	L CH ₄ g ⁻¹ VS		L CH ₄ g ⁻¹ VS	kJ g ⁻¹ VS	%	%	kJ g ⁻¹ VS
<i>I. galbana</i>	0.495	0.326 ± 0.004	0.201	22.6	65.8	61.6	13.0	55.9
<i>Dunaliella</i> sp.	0.541	0.269 ± 0.017	0.229	24.5	49.7	85.2	10.7	45.5
<i>Dunaliella</i> sp. SO ₄	0.539	0.280 ± 0.011	0.188	25.0	51.9	67.4	11.1	46.4

TMP values predicted from the Buswell equation were 0.495, 0.541 and 0.539 L CH₄ g⁻¹ VS for *I. galbana*, *D. salina* and *D. salina* SO₄ respectively. Measured BMP values ranged from 49.3 - 51.9% of the TMP for the *D. salina* samples to 62.2% of the TMP for *I. galbana*, again indicating differences in the degree of VS breakdown. *I. galbana* had the greatest apparent conversion efficiency of measured CV into methane at 55.9%, similar to the result of 59.5% for the laboratory grown sample. The conversion efficiencies of 45.1 and 46.4% for the low and high sulphate *D. salina* respectively were lower than the 55.1% achieved in the laboratory-grown sample of *D. salina* (section 4.1.6, TABLE 4), due to the higher carbon content of the biomass increasing the overall calorific value (Table 37).

As expected, TMP, BMP and SMP show a declining trend with TMP showing the highest methane yield and SMP the lowest. The TMP is calculated assuming that all organic carbon

and hydrogen is converted to biogas, thus giving a maximum upper threshold. The BMP value shows the maximum methane production that can occur within the operating conditions over a prolonged period; in this instance, 87 days. The SMP shows the actual methane production under continuous conditions. The reason for the decrease in methane potential from the TMP to the BMP is due to the presence of recalcitrant material, such as highly polymerised glycoproteins and sporopollenin-like polymer within cell membranes that is not consumed and converted to biogas within the BMP, but is included within the TMP (Labatut et al., 2011). The difference between the BMP and SMP may be due to the following: continuous operation, which removes a proportion of biomass and non-digested substrate daily; potential inhibition from the high salt content in the feedstock and possible competition from SRB and other microorganisms for fermentative products.

The TMP value can be adjusted if the fraction of anaerobically biodegradable material is known. The mass of highly recalcitrant material which breaks down at a slower rate than the residence time of the feedstock could be excluded from the TMP, reducing it towards the BMP. When the TMP is corrected for the %VS destruction under CSTR operation, however, the agreement between the gas production value is still poor (Table 38). *I. galbana* has a lower corrected TMP than the SMP suggesting a higher proportion of readily degradable lipids, whereas both *D. salina* samples have a higher corrected biogas production suggesting they have a higher recalcitrant proportion.

Table 38 Correction of TMP using VS destruction under CSTR operation

Species	% VS destruction	TMP	SMP	TMP x VS destruction	% Agreement
		L CH ₄ g ⁻¹ VS	L CH ₄ g ⁻¹ VS	L CH ₄ g ⁻¹ VS	
<i>I. galbana</i>	32.1	0.495	0.201	0.159	79
<i>D. salina</i>	50.5	0.541	0.229	0.273	119
<i>D. salina SO4</i>	51.8	0.539	0.188	0.279	148

There is currently a lack of published BMP values for both of the marine microalgae *I. galbana* and *D. salina*. The BMP value for *I. galbana* obtained in the current work is below a previously reported value of 0.408 L CH₄ g⁻¹ VS (Frigon et al., 2013), with the BMP value for *D. salina* falling into the lower range of reported values between 0.204-0.505 L CH₄ g⁻¹ VS (Mussnug et al., 2010, Mottet et al., 2014). As already noted, however, it is clear that different algal growth conditions, harvesting techniques, BMP inoculum sources and assay

procedures can all contribute to differing results. These differences can be due to each algal substrate having potential differences in percentage lipid content, cell wall structure, and any potential pre-treatments applied increasing the degradability of the material.

4.3.6.7 Sulphate and sulphide

For the low sulphate algal substrates *I. galbana* and *D. salina*, hydrogen sulphide production remained low at below 250 ppmv $\text{H}_2\text{S}_{(\text{g})}$ and $<0.001 \text{ L H}_2\text{S g}^{-1} \text{ VS}$, with total soluble sulphide concentrations $<10 \text{ mg L}^{-1}$ throughout the experiment, as shown in the sulphur equation within Section 3.4. The addition of high sulphate *D. salina* caused a rapid increase in hydrogen sulphide production, stabilising at $0.031 \text{ L H}_2\text{S g}^{-1} \text{ VS}$ within three HRT. This caused an increase in the soluble H_2S and total sulphide from 1.0 and 9.2 mg L^{-1} to 67 and 1130 mg L^{-1} respectively after three HRT from addition. The increase in sulphide production is likely due to the growth of SRB caused by the gradual washing in of sulphate within the feedstock, which stabilised when it reached equilibrium, contrasting with response to the sudden sulphate addition in the previous experiment in section 4.2. the observed increase in pH from 7.44 to 7.7 in the high sulphate *D. salina* reactors (Figure 70b) would alter the speciation of sulphide, enabling up to one order of magnitude more HS^- to remain dissolved within the digestate than $\text{H}_2\text{S}_{(\text{aq})}$.

An attempt was made to calculate a sulphur mass balance; taking into account sulphur added within the organic fraction and sulphate dissolved in the feedstock fed per day; the sulphur within the total soluble sulphide removed, and hydrogen sulphide gas produced daily as outlined in Figure 74. Influent concentrations of sulphur exist as SO_4 within the liquid fraction and elemental sulphur within the organic fraction. Headspace gas contain H_2S , with effluent sources presumed to contain aqueous H_2S , HS^- as calculated from the H_2S gas concentration, and a small fraction of un-digested SO_4 and organic sulphur. These values were used to estimate the proportion of sulphur removed within the reactor. High concentrations of anions and cations from the salt solution made the use of ion chromatography unsuitable for the determination of sulphate remaining within the digestate, due to the high dilutions required and the fouling that occurred within the packed column. Turbidimetric methods gave anomalous results due to the reddish colour of the feedstock caused by the presence of blood absorbing the wavelength examined at 420 nm, and to the presence of soluble organics interfering with the formation barium salts precipitates. As the majority of sulphur present within the feed for the high sulphate *D. salina* originates from

sulphate, at 97.4% of the total sulphur, with only 2.6% of the total sulphur added within the feedstock from the organic fraction it was considered reasonable to assume the remaining excess fraction consisted primarily of non-digested sulphur as sulphate.

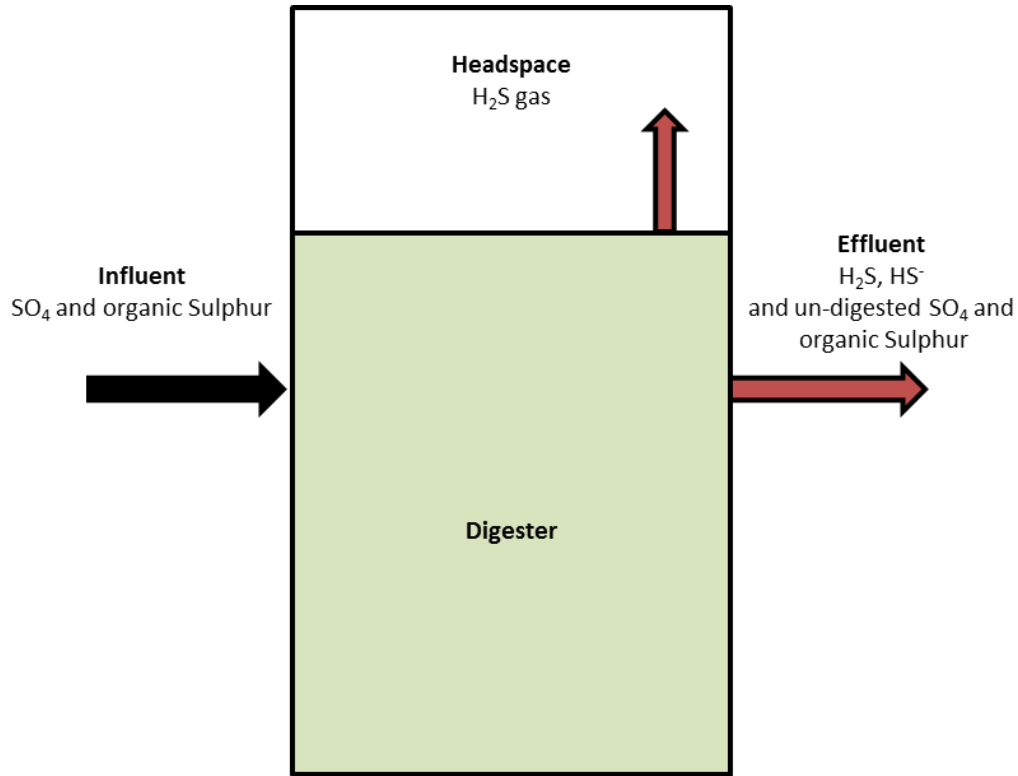


Figure 74 Design of mass balance implemented to determine the removal rate of sulphur equations within section 3.4.

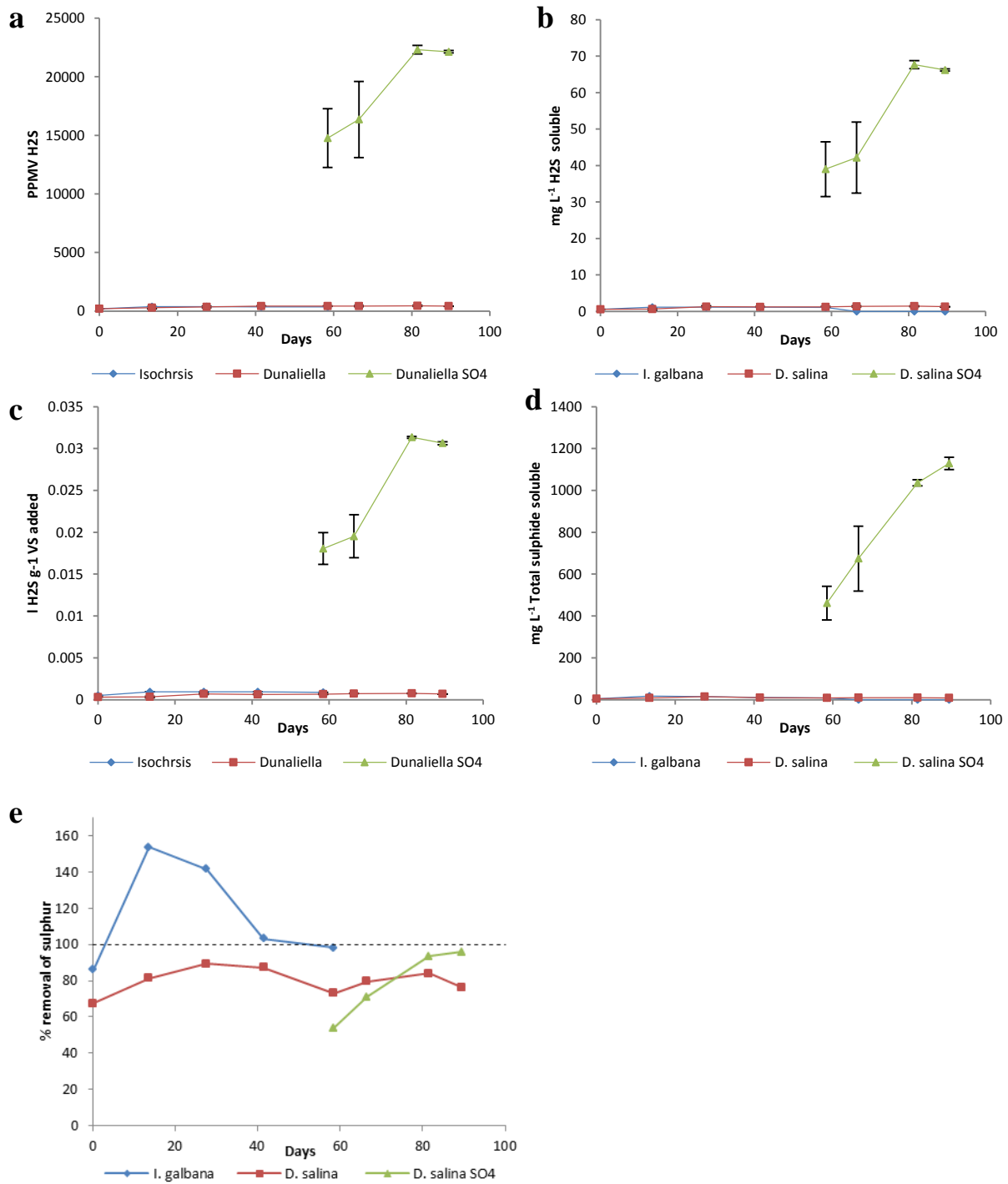


Figure 75 (a) PPMV H₂S, (b) L H₂S g⁻¹ VS added, (c) mg L⁻¹ H₂S soluble, (d) mg L⁻¹ total sulphide soluble, (e) percentage removal of sulphur. Error bars show the range of the data.

4.3.7 Continuous digestion discussion

4.3.7.1 Biogas and methane production

The lower SMP of the high sulphate *D. salina* reactors at 0.188 L CH₄ g⁻¹ VS added compared to that of the *D. salina* reactors at 0.23 L CH₄ g⁻¹ VS added is likely caused by the consumption of fermentative products by SRB and the subsequent production of H₂S, reducing the methane yield. The decrease in specific biogas production may be due to several factors relating to the production of hydrogen sulphide; Inhibition of methanogens and fermentative bacteria due to the presence of H₂S in aqueous solution and competitive inhibition from the SRB to the methanogenic archaea. When compared to the previous study on the addition of SO₄ there is no noticeable inhibition occurring. The slight increase in propionic acid may suggest some inhibition of propionic utilising bacteria, as seen in the salt acclimatisation experiment in section 4.2, but in the current trial this occurred only briefly. If there is competition for fermentative products by SRB and methanogens then the volume of H₂S gas produced combined with dissolved sulphide as a gas and with SMP should equal the SMP of the low sulphate reactors under steady state. The final values of SMP and H₂S produced for the *D. salina* reactors were within 2% for both conditions, suggesting that this is true. This suggests that the reactors are not severely inhibited, but rather SRB are directly competing for fermentative products. There is a significant difference between the SMP of the *D. salina* SO₄ and *D. salina* reactors of 0.0006, suggesting that the difference was not by chance, supporting the argument that the reduction is due to the activity of SRB.

4.3.7.2 Competition and inhibition

Several studies have reported inhibition or reactor failure due to low C: N ratios when digesting micro algae at OLR of 3 - 5 g and HRT between 10-20 days similar to the HRT in this study (Samson and Leduyt, 1986, Yen and Brune, 2007, Samson and LeDuy, 1983a). The present study showed no signs of inhibition, possibly due to the low OLR.

The addition of the *D. salina* SO₄ likely stimulated the growth of SRB, which rapidly produced hydrogen sulphide, and altered the chemistry within the reactor. Prior to switching feed-stocks, the pH within the *D. salina* reactors remained constant, at around 7.24 - 7.3, before increasing to a stable 7.6-7.7 pH following the input of the high sulphur feedstock, showing little effect from the increasing VFA concentration on pH as observed in the

sulphate addition reactors outlined in Chapter 4.2. This is explained by the fact that sulphide compounds, similar to carbonate compounds, exhibit a buffering capacity within anaerobic reactors through the production and emission of H₂S through the following reversible reaction: $\text{H}_2\text{O} + \text{CO}_2 + \text{HS}^- \leftrightarrow \text{H}_2\text{S} + \text{HCO}_3^-$ (Mehdizadeh and Shayegan, 2003). Increasing concentrations of soluble sulphide due to SRB activity will drive gas off as H₂S into the headspace, favouring the forward reaction increasing the reactor alkalinity and pH, with pH also affected by TAN.

It has been reported that the degradation of propionate can be inhibited at concentrations of undissociated H₂S_(aq) above 100 mg L⁻¹, with the poor degradation attributed to the inhibition of either the propionate splitting microorganisms obligate hydrogen producers or the hydrogen oxidising methanogens (Rinzema and Lettinga, 1988). O'Flaherty and Colleran (1999) found inhibition of the syntrophic propionate-degrading activity and severe inhibition of the methanogenic acetate-degrading microorganisms under a high sulphate loading of 4g L⁻¹ similar to the concentrations used in this study. The results support these observations, with increasing sulphate concentrations accompanied with a decrease in propionic acid degradation, potentially due to a combined effect from the SRB competing for fermentative products, such as acetate and inhibiting methanogens with the production of undissociated sulphide, reducing methane yields. In contrast, reactors low in sulphate experienced no decline in SMP and propionic acid concentrations remained consistently low.

4.3.7.3 Sulphur removal

The percentage sulphur removal rate for *I. galbana* was variable, highlighting the difficulty in determining a sulphur balance at low sulphur concentrations with removal efficiencies initially exceeding the mass of sulphur added by up to 55% shown in Figure 75e. The method used to estimate a sulphur balance and removal rate is potentially vulnerable to errors from several sources. The calculation for soluble H₂S is reliant on an accurate pH, temperature and known concentration of H₂S within the headspace. At the pH range operated within the CSTR's the speciation of H₂S can vary greatly by two and three orders of magnitude, representing a dramatic change in ionised sulphide. The time between sample removal and pH analysis is critical as the degassing of CO₂ can increase the sample pH shifting the equilibrium; with slight differences at lower concentrations resulting in a greater variation in % removal than that at higher concentrations. However at these low concentrations sulphur is

of little concern within the reactor as there is adequate organics present to dilute out any effects from competition by SRB and inhibition from H₂S.

D. salina had a variable removal efficiency under low sulphur conditions, initially between 73 - 90%. This was likely due to the system adapting to an increase in sulphate and changes to organic sulphur content before reaching stability (Figure 75e). After three HRT, the low sulphur *D. salina* reactors had a relatively stable sulphur removal rate of between 73 – 80% suggesting the reactors were in steady state with regards to sulphur breakdown. Harada et al. (1994) reported a 85 – 88% removal of sulphur from UASB reactors treating waste waters with low COD/ SO₄ ratios of 0.8 – 16.7, without reactor failure. Rizvi et al. (2013) reported a lower sulphur removal rate of 76% possibly due to operating at lower temperatures between 25 and 30°C. However, Ali (2014) using a diluted synthetic waste water as described in section 4.2 under ambient temperature conditions, observed an 87% removal rate for sulphur. The current work exceeds the removal efficiencies of these reported figures. When the feedstock was switched from the low to high sulphate grown substrate and culture media there is an increase in sulphur removal from ~80% increasing towards 96% after three HRT, as shown in Figure 75e. This reduction in removal is due to an excess of sulphate within the feedstock to the population of SRB present. The subsequent addition of high sulphate stimulates the growth of SRB which consume the excess sulphate present to produce H₂S, with a large proportion remaining dissolved within the effluent. The remaining % sulphur in the *D. salina* SO₄ could be attributed to non-digested sulphate as mentioned above. If ~ 50%+ of the organics is assumed converted to biogas as shown in the VS destruction in Figure 69, it could be assumed that a maximum of 50% of the sulphur contained within the organics has been liberated and converted to H₂S via SRB activity, with the remaining organic sulphur removed with the digestate reducing the organic fraction further with <25% of the remaining sulphur potentially organic. This may not necessarily be true, as it is not known what fraction of proteins were digested.

The reactors at higher sulphate appeared to enter steady state conditions towards the end of the experiment, with between 92 and 97% removal rates. Balances remain within 20% of the maximum for the low sulphur phase and an increase towards 100% for the high sulphur phase providing some support for the validity of the method used. Due to rapid changes with regards to the chemistry of H₂S within the reactors over the initial period of acclimatisation to

the high sulphate feedstock a greater rate of sampling should be undertaken. However, due to the small volumes of gas produced this could not feasibly occur.

The results suggest that SRB were directly competing for fermentative products with methanogens with an average % sulphur removal of 95% and a decrease in SMP. As Sulphur removal is close to 100%, and there is a linear relationship between sulphate addition and hydrogen sulphide production shown in section 4.2.6.4.2 (Figure 65), sulphur is likely a limiting nutrient at the high marine concentrations examined, with potential for greater sulphide production dependent on the toxicity of sulphide to the fermentative and SRB. This was also observed in the high sulphate reactors described in section 4.2, where a linear production of H₂S was observed with regards to the addition of sulphate. However, reactors remained relatively unaffected by the addition of excess sulphate to the digester, suggesting that reactors can become stable and maintain biogas production under high sulphur loadings.

4.3.7.4 Solids precipitation

Post operation the reactors were opened for cleaning, revealing a thin biofilm within the reactors where high sulphate concentrations were introduced. Figure 76a - d displays a low sulphur *D. salina* reactor (Figure 76a and c) and a high sulphur *D. salina* reactor post operation. The low sulphur reactor exhibits a slight thin deposit of crystals, potentially struvite as mentioned above, whereas the high sulphur has a thin (1 - 2 mm) white/ yellow biofilm with occasional crystals observable. This film is likely due to the high concentrations of H₂S gas being produced combined with oxygen when the reactor is opened for feeding acting as a feedstock for chemotrophic oxidation with sulphide oxidising bacteria (SOB) (Muyzer and Stams, 2008, Kobayashi et al., 2012). Kobayashi et al. (2012) observe a thick white biofilm growth within the headspace of an agricultural AD plant treating cattle slurry. By addition of 1% V/V oxygen to biogas produced they reduced the H₂S within the headspace by >50%. It is likely the method of feeding enabled sufficient intrusion of oxygen in the air to enable the oxidation of H₂S to occur. 10 – 15% of the biogas content prior to correction did not contain CH₄, CO₂ or H₂S. this is potentially water vapor from the reactor (Walker et al., 2009) with air from within the laboratory containing ~21% oxygen, sufficiently greater than the 1% volume added by Kobayashi et al. (2012). However this is not a gradual addition and will be rapidly removed from the headspace within a few hours reducing the oxygen concentration.

Chapter 4

The addition of low concentrations of oxygen has been used to scrub the biogas of high concentrations H_2S reducing upstream processing costs and potentially harvesting useful sulphur products (van den Bosch et al., 2007). This also increases the partial pressures between the headspace and digestate drawing out a greater volume of H_2S from solution reducing the concentration and potential inhibitory effects (Kobayashi et al., 2012). White biofilm build-up was not observed in the sulphate addition experiments outlined in Section 4.2, possibly due to the use of a submerged feed tube preventing the intrusion of air into the reactor which prevented sulphide oxidation.



Figure 76 Images of deposits within the anaerobic digesters for low sulphate *D. salina* on the left (a and c), and high sulphate fed *D. salina* reactors on the right (b and d).

4.3.7.5 Cell breakdown

Figure 77 provides a qualitative view of the breakdown of the cellular material pre and post digestion. There is a distinct difference between pre and post digestion, with fewer identifiable whole cells present after digestion has occurred. As the material has already undergone pre-treatments in the harvesting and storage process via centrifugation and freezing, some lysing of cells may have occurred pre-digestion (Samson and Leduy, 1983b, Gerken et al., 2013). Post-digestion images show some identifiable cellular material present, particularly with the *D. salina* samples, suggesting that in some cases the cell walls have either not been ruptured or digested causing the reduction in digestion of the organics over the HRT used reducing the methane production compared to the BMP. *I. galbana* appears to have the greatest breakdown of cellular material but has the lowest SMP. This could be due to rupturing of the cells but a thick recalcitrant cell wall reducing the available organic carbon for methane production (Leeuw et al., 2006, Syrett and Thomas, 1973, González-Fernández et al., 2012a, Gunnison and Alexander, 1975a, Gunnison and Alexander, 1975b, Mussnug et al., 2010), although this is not considered within the current study. These images are only qualitative and further examination using electron microscopes should be implemented to fully observe the effects of digestion on algal cells wall structure.

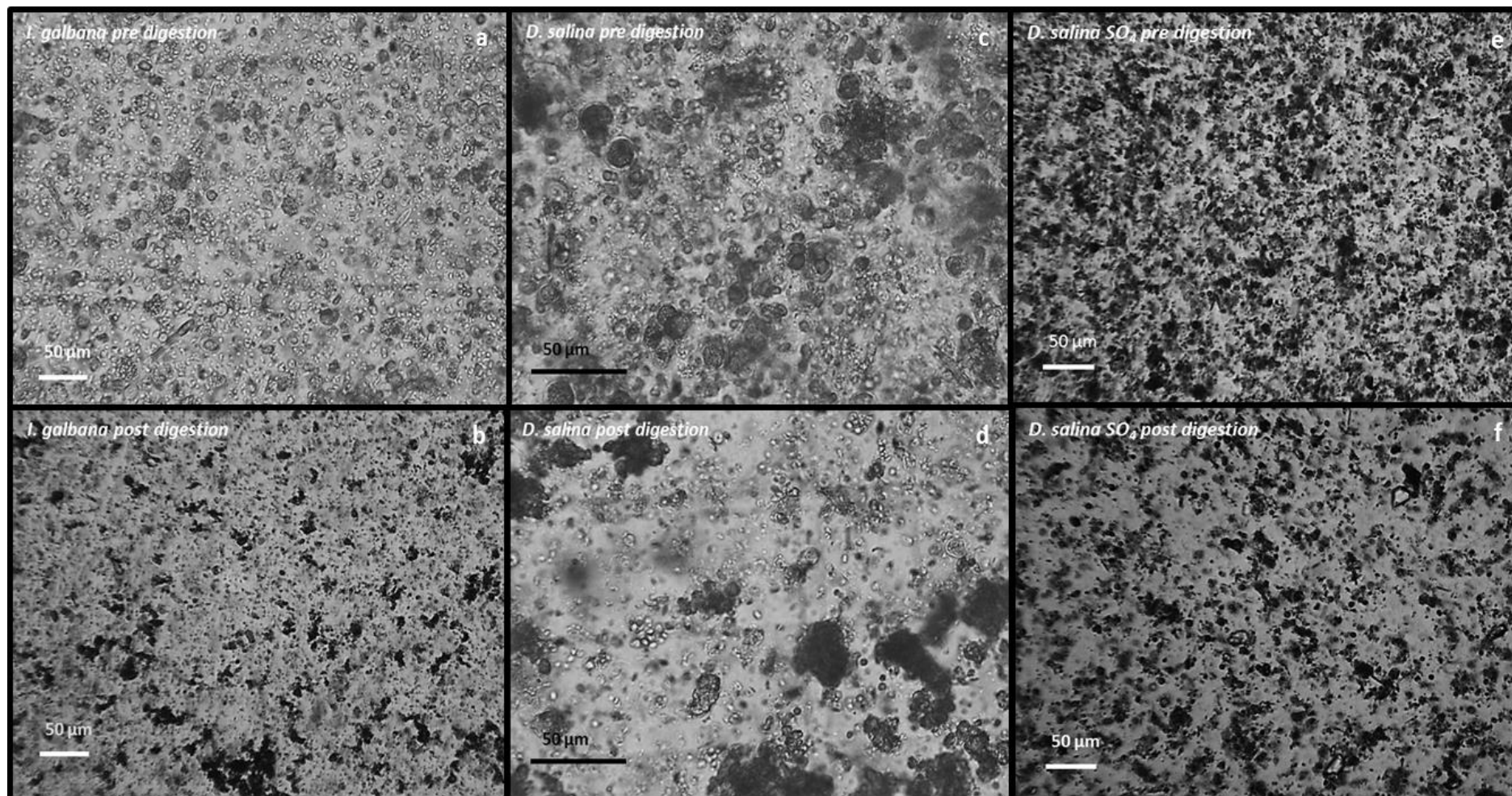


Figure 77 Optical microscope images of the feedstock's pre and post digestion.

Continuous digestion of the marine microalgae investigated within this work produced greater SMP than that reported in previous studies for non-pre-treated marine microalgae, and towards the higher end for fresh water species. At present *N. salina* is the only saline species for which continuous digestion has been reported, producing 0.13 L CH₄ g⁻¹ VS before pre-treatment, increasing to 0.27 L CH₄ g⁻¹ VS after thermal pre-treatment (Schwede et al., 2013). For the fresh water species *Chlorella*, Ehimen et al. (2011) reported a high SMP at 0.302 L CH₄ g⁻¹ VS primarily due to pre-treatment to the algae to remove lipids and co-digest with the extracted lipids, rupturing the cells prior to digestion and increasing digestibility. *C. vulgaris* cultivated on waste water was reported to have a lower SMP at 0.240 L CH₄ g⁻¹ VS. the highest SMP in continuous digestion was reported for *Spirulina maxima* at 0.35 L CH₄ g⁻¹ VS, however due to the OLR ammonia inhibition occurred resulting in reactor failure (Samson and Leduyt, 1986). *Scenedesmus spp* had the lowest reported SMP at 0.139 L CH₄ g⁻¹ VS. This low value was tentatively attributed to the recalcitrant cell wall and the high inorganic solids present (Tran et al., 2014).

As mentioned previously there is the possibility that struvite precipitation can occur within high salt anaerobic digesters (Wilsenach et al., 2007, Stratful et al., 2001). The addition of sulphate to a high salt reactor will increase the reactors pH enabling a greater proportion of struvite to precipitate. This would exacerbate the situation further under full scale operation, requiring a complete redesign of reactors to enable ease of cleaning and extraction of struvite. This can be used to reduce the salt content of the digestate to improve the quality of the effluent. The struvite extracted can then be subsequently sold as a fertiliser.

4.3.8 Concluding remarks

Continuous anaerobic digestion of marine microalgae yielded lower gas productions than the TMP and BMP as expected due to the presence of recalcitrant material and the relatively short HRT applied. Methane yields for the *D. salina* culture were close to the BMP at 86%, with the other algal cultures below 67% of the BMP. Differences between the BMP of the laboratory-grown cultures, the BMP of the biomass cultivated continuously and the subsequent SMP varied. This highlights the importance of

conducting continuous studies as opposed to traditional batch BMP assays for determination of the feasibility of algae as a feedstock for AD. All reactors showed a stable SMP within one week of altering feedstocks, and stable characteristics after three HRT. A higher TMP than the SMP suggests that the microalgae examined could possibly benefit from potential pre-treatment methods, as outlined in Chapter 2, to increase the SMP and reduce the RBP improving the digestate quality and energy recovery.

The addition of high sulphate media reduces the SMP mainly due to the stimulation of SRB producing high concentrations of H_2S within the biogas. The short-term increase in propionic acid may suggest that there is slight initial inhibition of fermentative bacteria due to the presence of un-ionised soluble sulphide, but adaption will likely occur within three HRT with sulphate gradually washing into the reactors. In contrast, reactors spiked to the high sulphate concentration, as described in section 4.2, showed a prolonged VFA build up, with a decrease in SMP and taking more than ten HRT to recover. This indicates that more gradual addition of SO_4 at high concentrations can allow reactors to maintain a stable SMP.

As these reactors used feedstock cultivated in a high energy environment to ensure adequate growth of biomass and a pure culture of algae, it was considered unrealistic to conduct a whole life cycle energy balance.

Overall stable anaerobic digestion of marine microalgae can occur with minimal effects to the methanogenic consortium once an adapted inoculum is used. A gradual increase in SO_4 enables the consortium to adapt to increases in H_2S production with only a decrease in SMP caused by competition for fermentative products. The differences in methane production between batch and continuous study show that it is crucial to undertake continuous analysis prior to starting pilot or large scale studies, as issues with regards to precipitation and inhibition are only made apparent within the continuous studies.

CHAPTER 5

5. Conclusions and further work

5.1 Conclusions

There is currently limited reported data on the continuous digestion of marine microalgae. To date *Nannochloropsis Sp.* is the only species of algae to be investigated for its methane potential under continuous operation. This research examined the methane production of the marine microalgal species *I. galabana* and *D. salina* using a salt adapted inoculum under mesophilic and continuous operation conditions. This study also addressed the effects of marine concentrations of sulphate on a methanogenic consortium with a comparison between high and low sulphate cultivated *D. salina* re-suspended within their saline culture medium. All were successfully digested with no noticeable negative effects on the methanogenic consortium, suggesting that marine microalgae and possibly other marine feedstocks can be suitable for anaerobic digestion. The following main findings and conclusions can be drawn from the work carried out:

5.1.1 Algal growth and characterisation

- Continuous cultivation of the marine species of micro algae *D. salina*, *N. oculata* and *I. galbana* at concentrations lower than $3.9 \text{ mg SO}_4 \text{ L}^{-1}$ caused a decrease in growth yield and growth rate ultimately leading to culture failure. this supported the findings by Giordano et al. (2000) with *D. salina* exhibiting the greatest growth yield and rates at the lowest concentrations.
- Increasing the concentration of JM up to three times of that recommended increased the growth rate; however, the increase was not linearly proportional. The results showed the optimum concentration of JM to growth rate to be at the recommended concentration.
- The work showed a wide variation in the energy recovery via anaerobic digestion between marine and freshwater microalgae under batch analysis. The marine species *T. pseudonana* had the highest BMP of all the species examined, followed by *I. galbana*.

- This research determined the highest volumetric methane productivity of each algal species using the growth rate under standard conditions and the BMP. A low BMP could be increased if the growth yield per unit volume of culture vessel was high. This enables a combined comparison of methane production with growth yield for different species, suggesting that individual species could produce different volumes of methane per unit of culture vessel, but that the difference between freshwater and marine are reduced. Taking the average of a group of species is most likely to be consistent with the use of open systems and mixed species growth.

5.1.2 Acclimatisation to chloride and sulphate salts

- Increasing the salinity at or above 10 g L⁻¹ of total salt causes inhibition and reactor failure to non-acclimatised inoculum, supporting the findings of the literature. However, this work demonstrated that inoculum from anaerobic digestion of municipal wastewater biosolids could be successfully acclimatised to marine concentrations of chloride salts. Under continuous operation at a HRT of 15 days all reactors supplemented with 31.1 g L⁻¹ of chloride salts reactors remained stable under steady state operating conditions (> 3 HRT). This suggests that marine substrates could be digested using a readily available inoculum source which could have a greater stability than marine sourced inoculum as shown by the literature.
- Acclimatised inoculum showed a minimal reduction of 6-7% in stable SMP between the reactors supplemented with chloride salts and the control reactors, with all other parameters showing reactor stability similar to that of the control. This suggests there is some slight inhibition occurring with the hydrolysing bacteria in the salt adapted reactors as VFA's remain consistent with the controls, however, VS destruction decreases.
- This work found that high salinity reactors developed a thin whitish precipitate in areas in contact with digestate. Based on to the high concentration of Mg²⁺ ions present in combination with the phosphate and ammonia ions from within the feedstock it was inferred that this precipitate was struvite. This highlights the

importance of undertaking continuous studies over batch analysis, as this precipitation would not be observed within a batch assay. This work also suggests that the potential for solids precipitation is taken into account when digesting high salinity feedstocks, by controlling pH, temperature and reducing turbulence in small piping.

- This work showed that initially after spiking sulphate concentrations within a high salinity anaerobic digester the H₂S production was not proportional to loading, providing insight into the ability of the microbial community to adapt in step changes of different concentrations of sulphate. After adaption had occurred the H₂S production was proportional to sulphate addition up to 4800 mg SO₄ L⁻¹, suggesting that the rate of H₂S production is limited by SO₄.
- Increasing SO₄ concentrations increased propionic acid concentrations suggesting that the fermentative bacteria that convert propionic acid to acetic acid were inhibited by the presence of H₂S, however, other fermentative bacteria were not inhibited by the presence of high concentrations of H₂S.
- This work found that reactors initially augmented to high sulphate concentrations showed initial instability, with increases in total VFA concentration and H₂S production, with decreases in pH SMP. The reactors, however, at COD:SO₄ ratios lower than stated in the literature as potentially toxic and inhibitory were able to recover after an adaption period towards reactor parameters similar to the control. This shows that there is a high buffering capacity of the inoculum to H₂S once adaption has occurred, and that the addition of sulphate will not be problematic for digestion of the feedstock. This does, however, raise concerns with regards to downstream treatment of H₂S produced.

5.1.3 Continuous digestion of *D. salina* and *I. galbana*

- *D. salina* and *I. galbana* were successfully converted to biogas via semi-continuous anaerobic digestion without any observable negative effects on the methanogenic consortium that have been highlighted within the literature.
- The SMP for all substrates was lower than the BMP and up to 50% of the TMP, suggesting that the microalgae examined could benefit from pre-treatment methods to improve the energy recovery.

- Microscope observations indicated that there was a high proportion of cell lysing post digestion. Suggesting that recalcitrant material is not only present within the cell wall but within the cell itself. This will require further work to identify the cause of these lower SMP values.
- The addition of a high SO₄ algal feedstock reduced the SMP, which is possibly due to the consumption of fermentative products for the production of H₂S by SRB.
- This work highlights the importance of conducting continuous studies as opposed to traditional batch BMP assays alone for determination of the feasibility of algal and other marine biomass as a feedstock for AD.

5.2 Further work

Algal characterisation and continuous digestion studies both from the literature and from this body of work have highlighted the recalcitrant nature of various species of both fresh water and marine microalgae; all failing to reach their maximum methane potential.

Further work should focus on a combined approach of determining what parts of the microalgae are recalcitrant and why. This could be conducted using batch analysis and scanning electron microscope imaging to locate areas of the cell that remain post-digestion. These regions can then be isolated prior to digestion and analysed for their composition.

After determining what regions of the microalgae are recalcitrant, methods to improve their digestibility should be examined, with successful methods implemented at laboratory scale.

D. salina has no rigid cell wall and as such can alter its volume accordingly with osmotic pressures. It is likely that the reduced SMP of *D. salina* is due to the composition of its cell membrane. It would be interesting to determine why *D. salina* does not have a higher SMP towards that of the TMP and the composition of its membrane in comparison to highly recalcitrant species such as *Scenedesmus* that have a thick rigid cell wall.

6. References

- USA Congress 2007. Energy Independence and Security Act. *110th Congress ed.* USA.
- ABELIOVICH, A. T. & SHILO, M. 1972. Photooxidative death in blue-green algae. *Journal of bacteriology*, 111, 682-689.
- ACIEN FERNANDEZ, F. G., GARCIA CAMACHO, F., SANCHEZ PEREZ, J. A., FERNANDEZ SEVILLA, J. M. & MOLINA GRIMA, E. 1998. Modeling of biomass productivity in tubular photobioreactors for microalgal cultures: Effects of dilution rate, tube diameter, and solar irradiance. *Biotechnology and Bioengineering*, 58, 605-616.
- ADAMS, C. & BUGBEE, B. 2014. Nitrogen retention and partitioning at the initiation of lipid accumulation in nitrogen-deficient algae. *Journal of Phycology*, 50, 356-365.
- AJANOVIC, A. 2011. Biofuels versus food production: Does biofuels production increase food prices? *Energy*, 36, 2070-2076.
- ALAERTS, G. J., VEENSTRA, S., BENTVELSEN, M. & VAN DUIJL, L. 1993. Feasibility of anaerobic sewage treatment in sanitation strategies in developing countries. *Water Science & Technology*, 27, 179-186.
- ALI, M. A. G. 2014. *Energy recovery from treatment of a synthetic municipal-type wastewater in UASB reactors at ambient temperatures and elevated sulphate concentrations.* University of Southampton.
- ALZATE, M. E., MUÑOZ, R., ROGALLA, F., FDZ-POLANCO, F. & PÉREZ-ELVIRA, S. I. 2012. Biochemical methane potential of microalgae: Influence of substrate to inoculum ratio, biomass concentration and pretreatment. *Bioresource Technology*, 123, 488-494.
- ANDERSON, L. A. 1995. On the hydrogen and oxygen content of marine phytoplankton. *Deep Sea Research Part I: Oceanographic Research Papers*, 42, 1675-1680.
- ANDERSON, R. A. (ed.) 2005. *Algal Culturing Techniques*: Elsevier Academic Press.
- ANGELIDAKI, I., ALVES, M., BOLZONELLA, D., BORZACCONI, L., CAMPOS, J. L., GUWY, A. J., KALYUZHNYI, S., JENICEK, P. & VAN LIER, J. B. 2009. Defining the biomethane potential (BMP) of solid organic wastes and energy crops: a proposed protocol for batch assays. *Water Science and Technology*, 59, 927-934.
- ANGELIDAKI, I. & SANDERS, W. 2004. Assessment of the anaerobic biodegradability of macropollutants. *Re/Views in Environmental Science & Bio/Technology*, 3, 117-129.
- APHA 2005. *Standard Methods for the examination of water & wastewater*, American Public Health Organisation.
- APPELS, L., BAEYENS, J., DEGRÈVE, J. & DEWIL, R. 2008. Principles and potential of the anaerobic digestion of waste-activated sludge. *Progress in Energy and Combustion Science*, 34, 755-781.
- ARBIB, Z., RUIZ, J., ÁLVAREZ-DÍAZ, P., GARRIDO-PÉREZ, C., BARRAGAN, J. & PERALES, J. A. 2013. Long term outdoor operation of a tubular airlift pilot photobioreactor and a high rate algal pond as tertiary treatment of urban wastewater. *Ecological Engineering*, 52, 143-153.
- ARCHER, D. B. & KIRSOP, B. H. 1991. The microbiology and control of anaerobic digestion. . In: WHEATLEY, A. (ed.) *Anaerobic digestion: a waste treatment technology*.
- ASINARI DI SAN MARZANO, C. M., LEGROS, A., NAVEAU, H. P. & NYNS, E. J. 1983. Biomethanation of the marine algae *Tetraselmis*. *International Journal of Solar Energy*, 1, 263-72.
- ASPE, E., MARTI, M. C. & ROECKEL, M. 1997. Anaerobic treatment of fishery wastewater using a marine sediment inoculum. *Water Research*, 31, 2147-2160.
- ASTM 1992. E1196-92 Standard Test Method for Determining the Anaerobic Biodegradation Potential of Organic Chemicals. West Conshohocken: PA.

References

- BAK, F. & PFENNIG, N. 1987. Chemolithotrophic growth of *Desulfovibrio sulfodismutans* sp. nov. by disproportionation of inorganic sulfur compounds. *Archives of Microbiology*, 147, 184-189.
- BANKS, C. J., HEAVEN, S., CORONA, L. E. S. & ROGALLA, F. 2011. Energy production from integration of high rate anaerobic and algal wastewater treatment: the EU FP7 All-Gas project. *9th IWA Specialist Group on Waste Stabilisation Ponds*. Adelaide.
- BANKS, C. J., HEAVEN, S., ZHANG, Y., SAPP, M. & THWAITES, R. 2013. Review of the application of the Residual Biogas Potential test. WRAP.
- BARTON, L. L. & FAUQUE, G. D. 2009. Chapter 2 Biochemistry, Physiology and Biotechnology of Sulfate - Reducing Bacteria. In: ALLEN I. LASKIN, S. S. & GEOFFREY, M. G. (eds.) *Advances in Applied Microbiology*. Academic Press.
- BECKER, E. W. 2004. Microalgae in human and animal nutrition. In: RICHMOND, A. (ed.) *Handbook of Microalgal Culture Biotechnology and Applied Phycology*. Oxford: Blackwell Publishing.
- BECKER, E. W. 2007. Micro-algae as a source of protein. *Biotechnology Advances*, 25, 207-210.
- BELCHER, J. H. & SWALE, E. M. F. 1977. Species of *Thalassiosira* (Diatoms, Bacillariophyceae) in the plankton of English rivers. *British Phycological Journal*, 12, 291-296.
- BENEMANN, J. R. 2008. Opportunities and challenges in algae biofuels production. *Algae World*. Singapore.
- BERGES, J. A., VARELA, D. E. & HARRISON, P. J. 2002. Effects of temperature on growth rate, cell composition and nitrogen metabolism in the marine diatom *Thalassiosira pseudonana* (Bacillariophyceae). *Marine Ecology Progress Series*, 225, 139-146.
- BHATNAGAR, A., BHATNAGAR, M., CHINNASAMY, S. & DAS, K. C. 2010. *Chlorella minutissima*-A Promising Fuel Alga for Cultivation in Municipal Wastewaters. *Applied Biochemistry and Biotechnology*, 161, 523-536.
- BHUIYAN, M. I. H., MAVINIC, D. S. & BECKIE, R. D. 2007. A solubility and thermodynamic study of struvite. *Environmental Technology*, 28, 1015-1026.
- BILLER, P. & ROSS, A. B. 2011. Potential yields and properties of oil from the hydrothermal liquefaction of microalgae with different biochemical content. *Bioresource Technology*, 102, 215-225.
- BIRD, K. T. & BENSON, P. H. 1987. Seaweed cultivation for renewable resources. *Developments in Aquaculture and Fisheries Science*.
- BLUNDEN, J. & ANEJA, V. P. 2008. Characterizing ammonia and hydrogen sulfide emissions from a swine waste treatment lagoon in North Carolina. *Atmospheric Environment*, 42, 3277-3290.
- BOARDMAN, G. D., TISINGER, J. L. & GALLAGHER, D. L. 1995. Treatment of clam processing wastewaters by means of upflow anaerobic sludge blanket technology. *Water Research*, 29, 1483-1490.
- BOHUTSKYI, P., BETENBAUGH, M. J. & BOUWER, E. J. 2014. The effects of alternative pretreatment strategies on anaerobic digestion and methane production from different algal strains. *Bioresource Technology*, 155, 366-372.
- BORGERDING, J. 1972. Phosphate deposits in digestion systems. *J. Wat. Pollut. Control Fed.*, 44, 813-819.
- BÖTTCHER, M. E., THAMDRUP, B., GEHRE, M. & THEUNE, A. 2005. 34S/32S and 18O/16O Fractionation During Sulfur Disproportionation by *Desulfobulbus propionicus*. *Geomicrobiology Journal*, 22, 219-226.
- BRENNAN, L. & OWENDE, P. 2010. Biofuels from microalgae—A review of technologies for production, processing, and extractions of biofuels and co-products. *Renewable and Sustainable Energy Reviews*, 14, 557-577.
- BRIAND, X. & MORAND, P. 1997. Anaerobic digestion of *Ulva* sp. 1. Relationship between *Ulva* composition and methanisation. *Journal of Applied Phycology*, 9, 511-524.

- BROWN, E., COLLING, A., JAMES, R., PARK, D., PHILLIPS, J., ROTHERY, D. & WRIGHT, J. 2005. *Marine Biogeochemical Cycles*, Oxford, Elsevier.
- BUXY, S., DILTZ, R. & PULLAMMANAPPALLIL, P. 2012. Biogasification of Marine Algae *Nannochloropsis Oculata*. *Materials Challenges in Alternative and Renewable Energy II*. John Wiley & Sons, Inc.
- BUYUKKAMACI, N. & FILIBELI, A. 2004. Volatile fatty acid formation in an anaerobic hybrid reactor. *Process Biochemistry*, 39, 1491-1494.
- CARRÈRE, H., DUMAS, C., BATTIMELLI, A., BATSTONE, D. J., DELGENÈS, J. P., STEYER, J. P. & FERRER, I. 2010. Pretreatment methods to improve sludge anaerobic degradability: A review. *Journal of Hazardous Materials*, 183, 1-15.
- CECCHI, F., PAVAN, P. & MATA-ALVAREZ, J. 1996. Anaerobic co-digestion of sewage sludge: Application to the macroalgae from the Venice lagoon. *Resources, Conservation and Recycling*, 17, 57-66.
- CHANDRA, R., TAKEUCHI, H. & HASEGAWA, T. 2012. Methane production from lignocellulosic agricultural crop wastes: A review in context to second generation of biofuel production. *Renewable and Sustainable Energy Reviews*, 16, 1462-1476.
- CHEN, P. H. & OSWALD, W. J. 1998. Thermochemical treatment for algal fermentation. *Environment International*, 24, 889-897.
- CHEN, W., HAN, S. & SUNG, S. 2003. Sodium Inhibition of Thermophilic Methanogens. *Journal of Environmental Engineering*, 129, 506-512.
- CHEN, Y., CHENG, J. J. & CREAMER, K. S. 2008. Inhibition of anaerobic digestion process: A review. *Bioresource Technology*, 99, 4044-4064.
- CHENG-WU, Z., ZMORA, O., KOPEL, R. & RICHMOND, A. 2001. An industrial-size flat plate glass reactor for mass production of *Nannochloropsis* sp. (Eustigmatophyceae). *Aquaculture*, 195, 35-49.
- CHERNICHARO, C. A. D. L. 2007. *Anaerobic Reactors*, IWA Publishing.
- CHISTI, Y. 2007. Biodiesel from microalgae. *Biotechnology Advances*, 25, 294-306.
- CHISTI, Y. 2008. Biodiesel from microalgae beats bioethanol. *Trends in Biotechnology*, 26, 126-131.
- CHISTI, Y. & MOOYOUNG, M. 1993. Improve the performance of airlift reactors. *Chemical Engineering Progress*, 89, 38-45.
- CHIU, S.-Y., KAO, C.-Y., TSAI, M.-T., ONG, S.-C., CHEN, C.-H. & LIN, C.-S. 2009. Lipid accumulation and CO₂ utilization of *Nannochloropsis oculata* in response to CO₂ aeration. *Bioresource Technology*, 100, 833-838.
- CHUM, H., FAALJ, A., MOREIRA, J., BERNDEN, G., DHAMIJA, P., DONG, H., GABRIELLE, B., ENG, A. G., LUCHT, W., MAPAKO, M., CERUTTI, O. M., MCINTYRE, T., MINOWA, T. & PINGOUD, K. 2011. Bioenergy. In: EDENHOFER, O., PICHS-MADRUGA, R., SOKONA, Y., SEYBOTH, K., MATSCHOSS, P., KADNER, S., ZWICKEL, T., EICKEMEIER, P., HANSEN, G., SCHLÖMER, S. & VON STECHOW, C. (eds.) *IPCC Special Report on Renewable Energy Sources and Climate Change Mitigation*. Cambridge, United Kingdom and New York, NY, USA: Cambridge University Press.
- CHYNOWETH, D. P., OWENS, J. M. & LEGRAND, R. 2001. Renewable methane from anaerobic digestion of biomass. *Renewable Energy*, 22, 1-8.
- COLE, T. M. & WELLS, S. A. 2008. CE-QUAL-W2: a two-dimensional, laterally averaged, hydrodynamic and water quality model. *US Army Corps of Engineers*. Washington DC.
- COLLET, P., HÉLIAS, A., LARDON, L., RAS, M., GOY, R.-A. & STEYER, J.-P. 2011. Life-cycle assessment of microalgae culture coupled to biogas production. *Bioresource Technology*, 102, 207-214.
- CONVERTI, A., CASAZZA, A. A., ORTIZ, E. Y., PEREGO, P. & DEL BORGHI, M. 2009. Effect of temperature and nitrogen concentration on the growth and lipid content of *Nannochloropsis oculata* and *Chlorella vulgaris* for biodiesel production. *Chemical Engineering and Processing: Process Intensification*, 48, 1146-1151.

References

- DE BAERE, L. A., DEVOCHT, M., VAN ASSCHE, P. & VERSTRAETE, W. 1984. Influence of high NaCl and NH₄Cl salt levels on methanogenic associations. *Water Research*, 18, 543-548.
- DE FRAITURE, C., GIORDANO, M. & LIAO, Y. 2008. Biofuels and implications for agricultural water use: blue impacts of green energy. *Water Policy*, 10, 67.
- DE SCHAMPHELAIRE, L. & VERSTRAETE, W. 2009. Revival of the biological sunlight-to-biogas energy conversion system. *Biotechnology and Bioengineering*, 103, 296-304.
- DEMIRBAŞ, A. 2001. Biomass resource facilities and biomass conversion processing for fuels and chemicals. *Energy Conversion and Management*, 42, 1357-1378.
- DEMIREL, B. & SCHERER, P. 2008. The roles of acetotrophic and hydrogenotrophic methanogens during anaerobic conversion of biomass to methane: a review. *Reviews in Environmental Science and Bio/Technology*, 7, 173-190.
- DOYLE, J. D. & PARSONS, S. A. 2002. Struvite formation, control and recovery. *Water Research*, 36, 3925-3940.
- EHIMEN, E. A., SUN, Z. F., CARRINGTON, C. G., BIRCH, E. J. & EATON-RYE, J. J. 2011. Anaerobic digestion of microalgae residues resulting from the biodiesel production process. *Applied Energy*, 88, 3454-3463.
- ELSER, J. J., FAGAN, W. F., DENNO, R. F., DOBBERFUHL, D. R., FOLARIN, A., HUBERTY, A., INTERLANDI, S., KILHAM, S. S., MCCAULEY, E., SCHULZ, K. L., SIEMANN, E. H. & STERNER, R. W. 2000. Nutritional constraints in terrestrial and freshwater food webs. *Nature*, 408, 578-580.
- FALKOWSKI, P. G. & RAVEN, J. A. 2007. *Aquatic Photosynthesis*, Princeton University Press.
- FANG, C., BOE, K. & ANGELIDAKI, I. 2011. Anaerobic co-digestion of desugared molasses with cow manure; focusing on sodium and potassium inhibition. *Bioresource Technology*, 102, 1005-1011.
- FEIJOO, G., SOTO, M., MÉNDEZ, R. & LEMA, J. M. 1995. Sodium inhibition in the anaerobic digestion process: Antagonism and adaptation phenomena. *Enzyme and Microbial Technology*, 17, 180-188.
- FERNÁNDEZ, F. A., SEVILLA, J. F., PÉREZ, J. S., GRIMA, E. M. & CHISTI, Y. 2001. Airlift-driven external-loop tubular photobioreactors for outdoor production of microalgae: assessment of design and performance. *Chemical Engineering Science*, 56, 2721-2732.
- FERNANDEZ, F. G. A., SEVILLA, J. M. F., PEREZ, J. A. S., GRIMA, E. M. & CHISTI, Y. 2001. Airlift-driven external-loop tubular photobioreactors for outdoor production of microalgae: assessment of design and performance. *Chemical Engineering Science*, 56, 2721-2732.
- FERNANDEZ, N. & FORSTER, C. F. 1994. Anaerobic digestion of a simulated coffee waste using thermophilic and mesophilic upflow filters. *Process Safety and Environmental Protection: Transactions of the Institution of Chemical Engineers, Part B*, 72, 15-20.
- FERREIRA, R. M. B. & TEIXEIRA, A. R. N. 1992. Sulfur starvation in lemna leads to degradation of ribulose-bisphosphate carboxylase without plant death. *Journal of Biological Chemistry*, 267, 7253-7257.
- FERRER, I., VÁZQUEZ, F. & FONT, X. 2010. Long term operation of a thermophilic anaerobic reactor: Process stability and efficiency at decreasing sludge retention time. *Bioresource Technology*, 101, 2972-2980.
- FISCHER, J. R., IANNOTTI, E. L. & PORTER, J. H. 1984. Anaerobic digestion of swine manure at various influent solids concentrations. *Agricultural Wastes*, 11, 157-166.
- FLEISCHER, C., BECKER, S. & EIGENBERGER, G. 1996. Detailed modeling of the chemisorption of CO₂ into NaOH in a bubble column. *Chemical Engineering Science*, 51, 1715-1724.
- FLETCHER, L. E. 1998. Potential explosive hazards from hydrogen sulfide production in ship ballast and sewage tanks.

- FP7. 2015. *FP7 - Algae Cluster* [Online]. Available: <http://www.all-gas.eu/Pages/default.aspx> [Accessed 20/4/2015 2015].
- FRICKE, K., SANTEN, H., WALLMANN, R., HÜTTNER, A. & DICHTL, N. 2007. Operating problems in anaerobic digestion plants resulting from nitrogen in MSW. *Waste Management*, 27, 30-43.
- FRIGON, J.-C., MATTEAU-LEBRUN, F., HAMANI ABDU, R., MCGINN, P. J., O'LEARY, S. J. B. & GUIOT, S. R. 2013. Screening microalgae strains for their productivity in methane following anaerobic digestion. *Applied Energy*, 108, 100-107.
- GARRELS, R. & CHRIST, C. 1965. *Solutions, Minerals and Equilibria*. Harper and Row. New York.
- GE, H., JENSEN, P. D. & BATSTONE, D. J. 2011. Temperature phased anaerobic digestion increases apparent hydrolysis rate for waste activated sludge. *Water Research*, 45, 1597-1606.
- GEBAUER, R. 2004. Mesophilic anaerobic treatment of sludge from saline fish farm effluents with biogas production. *Bioresource Technology*, 93, 155-167.
- GEORGACAKIS, D., SIEVERS, D. M. & IANNOTTI, E. L. 1982. Buffer stability in manure digesters. *Agricultural Wastes*, 4, 427-441.
- GERARDI, M. H. 2003. *The Microbiology of Anaerobic Digesters*, New Jersey, John Wiley & Sons.
- GERKEN, H., DONOHOE, B. & KNOSHAUG, E. 2013. Enzymatic cell wall degradation of *Chlorella vulgaris* and other microalgae for biofuels production. *Planta*, 237, 239-253.
- GILBERT, S. M., CLARKSON, D. T., CAMBRIDGE, M., LAMBERS, H. & HAWKESFORD, M. J. 1997. SO₂- deprivation has an early effect on the content of ribulose-1,5-bisphosphate carboxylase/oxygenase and photosynthesis in young leaves of wheat. *Plant Physiology*, 115, 1231-1239.
- GIORDANO, M., PEZZONI, V. & HELL, R. 2000. Strategies for the allocation of resources under sulfur limitation in the green alga *Dunaliella salina*. *Plant Physiology*, 124, 857-864.
- GOLDMAN, J. C. & GRAHAM, S. J. 1981. Inorganic Carbon Limitation and Chemical Composition of Two Freshwater Green Microalgae. *Applied and Environmental Microbiology*, 41, 60-70.
- GOLDTHAU, A. & SOVACOO, B. K. 2012. The uniqueness of the energy security, justice, and governance problem. *Energy Policy*, 41, 232-240.
- GOLUEKE, C. G., OSWALD, W. J. & GOTAAS, H. B. 1957. Anaerobic digestion of algae. *Appl Microbiol*, 5, 47-55.
- GONZÁLEZ-FERNÁNDEZ, C., MOLINUEVO-SALCES, B. & GARCÍA-GONZÁLEZ, M. C. 2011. Evaluation of anaerobic codigestion of microalgal biomass and swine manure via response surface methodology. *Applied Energy*, 88, 3448-3453.
- GONZÁLEZ-FERNÁNDEZ, C., SIALVE, B., BERNET, N. & STEYER, J.-P. 2012a. Impact of microalgae characteristics on their conversion to biofuel. Part II: Focus on biomethane production. *Biofuels, Bioproducts and Biorefining*, 6, 205-218.
- GONZÁLEZ-FERNÁNDEZ, C., SIALVE, B., BERNET, N. & STEYER, J. P. 2012b. Comparison of ultrasound and thermal pretreatment of *Scenedesmus* biomass on methane production. *Bioresource Technology*, 110, 610-616.
- GOUVEIA, L. & OLIVEIRA, A. 2009. Microalgae as a raw material for biofuels production. *Journal of Industrial Microbiology & Biotechnology*, 36, 269-274.
- GRAHAM, L. E., GRAHAM, J. M. & WILCOX, L. W. 2009. *Algae*, San Fransico, Pearson.
- GROBBELAAR, J. U. 2007. Algal Nutrition – Mineral Nutrition. In: RICHMOND, A. (ed.) *Handbook of Microalgal Culture: Biotechnology and Applied Phycology*. Oxford: Blackwell Publishing Ltd.
- GUERRERO, L., OMIL, F., MENDEZ, R. & LEMA, J. M. 1997. Treatment of saline wastewaters from fish meal factories in an anaerobic filter under extreme ammonia concentrations. *Bioresource Technology*, 61, 69-78.
- GUILLARD, R. & RYTHER, J. 1962. Studies of marine planktonic diatoms. I. *Cyclotella nana* Hustedt and *Detonula confervaceae* (Cleve). *Journal of Microbiology*, 8, 229-239.

References

- GUNNISON, D. & ALEXANDER, M. 1975a. Basis for the susceptibility of several algae to microbial decomposition. *Canadian journal of microbiology*, 21, 619-628.
- GUNNISON, D. & ALEXANDER, M. 1975b. Resistance and susceptibility of algae to decomposition by natural microbial communities. *Limnol. Oceanogr*, 20, 64-70.
- HANSEN, T. 1993. Carbon Metabolism of Sulfate-Reducing Bacteria. In: ODOM, J. M. & SINGLETON, R., JR. (eds.) *The Sulfate-Reducing Bacteria: Contemporary Perspectives*. Springer New York.
- HARADA, H., UEMURA, S. & MOMONOI, K. 1994. Interaction between sulfate-reducing bacteria and methane-producing bacteria in UASB reactors fed with low strength wastes containing different levels of sulfate. *Water Research*, 28, 355-367.
- HARKER, M., TSAVALOS, A. J. & YOUNG, A. J. 1996. Autotrophic growth and carotenoid production of *Haematococcus pluvialis* in a 30 liter air-lift photobioreactor. *Journal of Fermentation and Bioengineering*, 82, 113-118.
- HARRIS, L., TOZZI, S., WILEY, P., YOUNG, C., RICHARDSON, T.-M. J., CLARK, K. & TRENT, J. D. 2013. Potential impact of biofouling on the photobioreactors of the Offshore Membrane Enclosures for Growing Algae (OMEGA) system. *Bioresource Technology*, 144, 420-428.
- HARUN, R., DAVIDSON, M., DOYLE, M., GOPIRAJ, R., DANQUAH, M. & FORDE, G. 2011. Technoeconomic analysis of an integrated microalgae photobioreactor, biodiesel and biogas production facility. *Biomass and Bioenergy*, 35, 741-747.
- HAVLÍK, P., SCHNEIDER, U. A., SCHMID, E., BÖTTCHER, H., FRITZ, S., SKALSKÝ, R., AOKI, K., CARA, S. D., KINDERMANN, G., KRAXNER, F., LEDUC, S., MCCALLUM, I., MOSNIER, A., SAUER, T. & OBERSTEINER, M. 2011. Global land-use implications of first and second generation biofuel targets. *Energy Policy*, 39, 5690-5702.
- HEASMAN, M. P., SUSHAMES, T. M., DIEMAR, J. A., O'CONNOR, W. A. & FOULKES, L. A. 2001. Production of Micro-algal Concentrates for Aquaculture Part 2: Development and Evaluation of Harvesting, Preservation, Storage and Feeding Technology. *NSW Fisheries Final Report Series*. NSW Fisheries.
- HEAVEN, S., MILLEDGE, J. & ZHANG, Y. 2011. Comments on 'Anaerobic digestion of microalgae as a necessary step to make microalgal biodiesel sustainable'. *Biotechnology Advances*, 29, 164-167.
- HEDGES, J. I., BALDOCK, J. A., GÉLINAS, Y., LEE, C., PETERSON, M. L. & WAKEHAM, S. G. 2002. The biochemical and elemental compositions of marine plankton: A NMR perspective. *Marine Chemistry*, 78, 47-63.
- HIERHOLTZER, A. & AKUNNA, J. C. 2012. Modelling sodium inhibition on the anaerobic digestion process. *Water Science and Technology*, 66, 1565-1573.
- HILL, D. T., COBB, S. A. & BOLTE, J. P. 1987. Using volatile fatty acid relationships to predict anaerobic digester failure. *Journal Name: Trans. ASAE; (United States); Journal Volume: 30:2, Medium: X; Size: Pages: 496-501.*
- HILL, J., NELSON, E., TILMAN, D., POLASKY, S. & TIFFANY, D. 2006. Environmental, economic, and energetic costs and benefits of biodiesel and ethanol biofuels. *Proceedings of the National Academy of Sciences*, 103, 11206-11210.
- HILLS, D. J. 1979. Effects of carbon: Nitrogen ratio on anaerobic digestion of dairy manure. *Agricultural Wastes*, 1, 267-278.
- HILTON, B. L. & OLESZKIEWICZ, J. A. 1988. Sulfide-induced inhibition of anaerobic-digestion. *Journal of Environmental Engineering-Asce*, 114, 1377-1391.
- HO, D., JENSEN, P. & BATSTONE, D. 2014. Effects of Temperature and Hydraulic Retention Time on Acetotrophic Pathways and Performance in High-Rate Sludge Digestion. *Environmental Science & Technology*, 48, 6468-6476.
- HOOGENHOUT, H. & AMESZ, J. 1965. Growth rates of photosynthetic microorganisms in laboratory cultures. *Archiv für Mikrobiologie*, 50, 10-25.

- HUGHES, A. D., KELLY, M. S., BLACK, K. D. & STANLEY, M. S. 2012. Biogas from Macroalgae: is it time to revisit the idea. *Biotechnol Biofuels*, 5, 86.
- HULSHOFF POL, L., LENS, P. L., STAMS, A. M. & LETTINGA, G. 1998. Anaerobic treatment of sulphate-rich wastewaters. *Biodegradation*, 9, 213-224.
- IAEA. 2014. <http://www.iaea.org/PRIS/WorldStatistics/NuclearShareofElectricityGeneration.aspx> [Online]. [Accessed 08/10/2014 2014].
- IEA. 2006. *World Energy Outlook 2006* [Online]. Paris: International Energy Agency. [Accessed 07/11/ 2011].
- ISA, M. H. & ANDERSON, G. K. 2005. Molybdate inhibition of sulphate reduction in two-phase anaerobic digestion. *Process Biochemistry*, 40, 2079-2089.
- J. HEERENKLAGE, T. MAXFIELD, A. ZAPF, H. ADWIRAAH, N. W. & KOERNER, I. 2010. Anaerobic Digestion of Microalgae - Possibilities and limits. *Third International Symposium on Energy from Biomass and Waste*. Venice, Italy.
- JIANG, Y., HEAVEN, S. & BANKS, C. J. 2012. Strategies for stable anaerobic digestion of vegetable waste. *Renewable Energy*, 44, 206-214.
- JITTS, H. R., MCALLISTER, C. D., STEPHENS, K. & STRICKLAND, J. D. H. 1964. The Cell Division Rates of Some Marine Phytoplankters as a Function of Light and Temperature. *Journal of the Fisheries Research Board of Canada*, 21, 139-157.
- JOEL C, G. 1979. Outdoor algal mass cultures—II. Photosynthetic yield limitations. *Water Research*, 13, 119-136.
- KAISER, M. J., ATTRILL, M. J., JENNINGS, S., THOMAS, D. N., BARNES, D. K. A., BRIERLEY, A. S., POLUNIN, N. V. C., RAFFAELLI, D. G. & WILLIAMS, P. J. (eds.) 2005a. *Marine Ecology*: Oxford University Press.
- KAISER, M. J., ATTRILL, M. J., JENNINGS, S., THOMAS, D. N., BARNES, D. K. A., BRIERLEY, A. S., POLUNIN, N. V. C., RAFFAELLI, D. G. & WILLIAMS, P. J. 2005b. *Marine Ecology, Processes, Systems and Impacts*. Oxford: Oxford University Press.
- KARGI, F. & DINCER, A. R. 1997. Biological Treatment of Saline Wastewater by Fed-Batch Operation. *Journal of Chemical Technology & Biotechnology*, 69, 167-172.
- KARRAY, R., HAMZA, M. & SAYADI, S. 2015. Evaluation of ultrasonic, acid, thermo-alkaline and enzymatic pre-treatments on anaerobic digestion of *Ulva rigida* for biogas production. *Bioresource Technology*, 187, 205-213.
- KASPAR, H. & WUHRMANN, K. 1977. Product inhibition in sludge digestion. *Microbial Ecology*, 4, 241-248.
- KAYHANIAN, M. 1999. Ammonia Inhibition in High-Solids Biogasification: An Overview and Practical Solutions. *Environmental Technology*, 20, 355-365.
- KERN, J., HEINZMANN, B., MARKUS, B., KAUFMANN, A. C., SOETHE, N. & ENGELS, C. 2008. Recycling and assessment of struvite phosphorus from sewage sludge. *Agricultural Engineering International: CIGR Journal*.
- KHALID, A., ARSHAD, M., ANJUM, M., MAHMOOD, T. & DAWSON, L. 2011. The anaerobic digestion of solid organic waste. *Waste Management*, 31, 1737-1744.
- KIMATA-KINO, N., IKEDA, S., KUROSAWA, N. & TODA, T. 2011. Saline adaptation of granules in mesophilic UASB reactors. *International Biodeterioration and Biodegradation*, 65, 65-72.
- KIRIYAMA, E. & KAJIKAWA, Y. 2014. A multilayered analysis of energy security research and the energy supply process. *Applied Energy*, 123, 415-423.
- KIRK, J. T. O. 1994. *Light & photosynthesis in aquatic ecosystems*, Cambridge University Press.
- KIRST, G. O. 1990. Salinity tolerance of eukaryotic marine-algae. *Annual Review of Plant Physiology and Plant Molecular Biology*, 41, 21-53.
- KLEINJAN, W. 2005. *Biologically Produced Sulphur Particles and Polysulphide Ions. Effects on a Biotechnological Process for the Removal of Hydrogen Sulphide from Gas Streams*. Ph. D. Thesis, Wageningen Universiteit, Wageningen.

References

- KLEMM, D., HEUBLEIN, B., FINK, H. P. & BOHN, A. 2005. Cellulose: Fascinating biopolymer and sustainable raw material. *Angewandte Chemie-International Edition*, 44, 3358-3393.
- KOBAYASHI, T., LI, Y.-Y., KUBOTA, K., HARADA, H., MAEDA, T. & YU, H.-Q. 2012. Characterization of sulfide-oxidizing microbial mats developed inside a full-scale anaerobic digester employing biological desulfurization. *Applied Microbiology and Biotechnology*, 93, 847-857.
- KOSTER, I. W. & LETTINGA, G. 1988. Anaerobic digestion at extreme ammonia concentrations. *Biological Wastes*, 25, 51-59.
- KOSTER, I. W., RINZEMA, A., DE VEGT, A. L. & LETTINGA, G. 1986. Sulfide inhibition of the methanogenic activity of granular sludge at various pH-levels. *Water Research*, 20, 1561-1567.
- KUGELMAN, L. J. & MCCARTY, P. L. 1965. Cation toxicity and stimulation in anaerobic waste treatment. *J Water Pollut Contr Federation*, 37, 97-116.
- LABATUT, R. A., ANGENENT, L. T. & SCOTT, N. R. 2011. Biochemical methane potential and biodegradability of complex organic substrates. *Bioresource Technology*, 102, 2255-2264.
- LAFARGA-DE LA CRUZ, F., VALENZUELA-ESPINOZA, E., MILLÁN-NÚÑEZ, R., TREES, C. C., SANTAMARÍA-DEL-ÁNGEL, E. & NÚÑEZ-CEBRERO, F. 2006. Nutrient uptake, chlorophyll a and carbon fixation by *Rhodomonas* sp. (Cryptophyceae) cultured at different irradiance and nutrient concentrations. *Aquacultural Engineering*, 35, 51-60.
- LAKANIEMI, A.-M., HULATT, C. J., THOMAS, D. N., TUOVINEN, O. H. & PUHAKKA, J. A. 2011a. Biogenic hydrogen and methane production from *Chlorella vulgaris* and *Dunaliella tertiolecta* biomass. *Biotechnol Biofuels*, 4, 34.
- LAKANIEMI, A.-M., HULATT, C. J., THOMAS, D. N., TUOVINEN, O. H. & PUHAKKA, J. A. 2011b. Biogenic hydrogen and methane production from *Chlorella vulgaris* and *Dunaliella tertiolecta* biomass. *Biotechnology for Biofuels*, 4.
- LAKANIEMI, A.-M., TUOVINEN, O. H. & PUHAKKA, J. A. 2013. Anaerobic conversion of microalgal biomass to sustainable energy carriers – A review. *Bioresource Technology*, 135, 222-231.
- LANGEVELD, J. W. A., DIXON, J., VAN KEULEN, H. & QUIST-WESSEL, P. M. F. 2014. Analyzing the effect of biofuel expansion on land use in major producing countries: evidence of increased multiple cropping. *Biofuels, Bioproducts and Biorefining*, 8, 49-58.
- LAWS, E. A. 1991. Photosynthetic quotients, new production and net community production in the open ocean. *Deep Sea Research Part A. Oceanographic Research Papers*, 38, 143-167.
- LEE, A. K., LEWIS, D. M. & ASHMAN, P. J. 2012. Disruption of microalgal cells for the extraction of lipids for biofuels: Processes and specific energy requirements. *Biomass and Bioenergy*, 46, 89-101.
- LEE, A. K., LEWIS, D. M. & ASHMAN, P. J. 2013. Force and energy requirement for microalgal cell disruption: An atomic force microscope evaluation. *Bioresource Technology*, 128, 199-206.
- LEE, R. E. 2008. *Phycology*, Cambridge, Cambridge University Press.
- LEEUW, J., VERSTEEGH, G. & BERGEN, P. 2006. Biomacromolecules of algae and plants and their fossil analogues
- Plants and Climate Change. In: ROZEMA, J., AERTS, R. & CORNELISSEN, H. (eds.). Springer Netherlands.
- LEFEBVRE, O. & MOLETTA, R. 2006. Treatment of organic pollution in industrial saline wastewater: A literature review. *Water Research*, 40, 3671-3682.

- LEFEBVRE, O., VASUDEVAN, N., TORRIJOS, M., THANASEKARAN, K. & MOLETTA, R. 2006. Anaerobic digestion of tannery soak liquor with an aerobic post-treatment. *Water Research*, 40, 1492-1500.
- LENS, P. & KUENEN, J. 2001. The biological sulfur cycle: novel opportunities for environmental biotechnology. *Water Science & Technology*, 44, 57-66.
- LETTINGA, G., REBAC, S. & ZEEMAN, G. 2001. Challenge of psychrophilic anaerobic wastewater treatment. *Trends in Biotechnology*, 19, 363-370.
- LIAMLEAM, W. & ANNACHHATRE, A. P. 2007. Electron donors for biological sulfate reduction. *Biotechnology Advances*, 25, 452-463.
- LINDORFER, H., RAMHOLD, D. & FRAUZ, B. 2012. Nutrient and trace element supply in anaerobic digestion plants and effect of trace element application. *Water Science and Technology*, 66, 1923-1929.
- LIU, C.-Z., WANG, F., STILES, A. R. & GUO, C. 2012. Ionic liquids for biofuel production: Opportunities and challenges. *Applied Energy*, 92, 406-414.
- LIU, X., DING, H., SREERAMACHANDRAN, S., STABNIKOVA, O. & WANG, J. 2008. Enhancement of food waste digestion in the hybrid anaerobic solid-liquid system.
- LIU, Y. & BOONE, D. R. 1991. Effects of salinity on methanogenic decomposition. *Bioresource Technology*, 35, 271-273.
- LONG, S. P., HUMPHRIES, S. & FALKOWSKI, P. G. 1994. Photoinhibition of photosynthesis in nature. *Annual Review of Plant Physiology and Plant Molecular Biology*, 45, 633-662.
- LÜ, F., JI, J., SHAO, L. & HE, P. 2013. Bacterial bioaugmentation for improving methane and hydrogen production from microalgae. *Biotechnology for biofuels*, 6, 92.
- LUITEN, E. E. M., AKKERMAN, I., KOULMAN, A., KAMERMANS, P., REITH, H., BARBOSA, M. J., SIPKEMA, D. & WIJFFELS, R. H. 2003. Realizing the promises of marine biotechnology. *Biomolecular Engineering*, 20, 429-439.
- LUNDQUIST, T. J., WOERTZ, I. C., QUINN, N. W. T. & BENEMANN, J. R. 2010. A Realistic Technology and Engineering Assessment of Algae Biofuel Production. Berkeley, California: Energy Biosciences Inst.
- MAMAI, D., PITT, P. A., CHENG, Y. W., LOIACONO, J. & JENKINS, D. 1994. Determination of ferric-chloride dose to control struvite precipitation in anaerobic sludge digesters. *Water Environment Research*, 66, 912-918.
- MARA, D. & HORAN, N. J. 2003. *Handbook of water and wastewater microbiology*, Academic press.
- MARCHAIM, U. & KRAUSE, C. 1993. Propionic to acetic acid ratios in overloaded anaerobic digestion. *Bioresource Technology*, 43, 195-203.
- MARKOU, G., ANGELIDAKI, I. & GEORGAKAKIS, D. 2012. Microalgal carbohydrates: an overview of the factors influencing carbohydrates production, and of main bioconversion technologies for production of biofuels. *Applied Microbiology and Biotechnology*, 96, 631-645.
- MARTIN, C. L. & TORTELL, P. D. 2006. Bicarbonate Transport and Extracellular Carbonic Anhydrase Activity in Bering Sea Phytoplankton Assemblages: Results from Isotope Disequilibrium Experiments. *Limnology and Oceanography*, 51, 2111-2121.
- MATA, T. M., MARTINS, A. A. & CAETANO, N. S. 2010. Microalgae for biodiesel production and other applications: A review. *Renewable and Sustainable Energy Reviews*, 14, 217-232.
- MAYERS, J. J., FLYNN, K. J. & SHIELDS, R. J. 2014. Influence of the N:P supply ratio on biomass productivity and time-resolved changes in elemental and bulk biochemical composition of *Nannochloropsis* sp. *Bioresource Technology*, 169, 588-595.
- MCCARTY, P. L. 1964. Anaerobic waste treatment fundamentals. *Public Works*, 95, 91-99.
- MEDINA, A. R., GRIMA, E. M., GIMÉNEZ, A. G. & GONZÁLEZ, M. J. I. 1998. Downstream processing of algal polyunsaturated fatty acids. *Biotechnology Advances*, 16, 517-580.
- MEEHL, G. A., STOCKER, T. F., COLLINS, W. D., FRIEDLINGSTEIN, P., GAYE, A. T., GREGORY, J. M., KITOH, A., KNUTTI, R., MURPHY, J. M., NODA, A., RAPER, S.

References

- C. B., WATTERSON, I. G., WEAVER, A. J. & ZHAO, Z.-C. 2007. Global Climate Projections. In: *Climate Change 2007: The Physical Science Basis. Contribution of Working Group I to the Fourth Assessment Report of the Intergovernmental Panel on Climate Change*
- MEHDIZADEH, H. & SHAYEGAN, J. 2003. The effect of sulfate concentration on COD removal and sludge granulation in UASB reactors. *International Journal of Engineering Transaction B: Applications*, 16, 1-10.
- MENDOZA, J. L., GRANADOS, M. R., DE GODOS, I., ACIÉN, F. G., MOLINA, E., HEAVEN, S. & BANKS, C. J. 2013. Oxygen transfer and evolution in microalgal culture in open raceways. *Bioresource Technology*, 137, 188-195.
- MIGLIORE, G., ALISI, C., SPROCATI, A. R., MASSI, E., CICCOLI, R., LENZI, M., WANG, A. & CREMISINI, C. 2012. Anaerobic digestion of macroalgal biomass and sediments sourced from the Orbetello lagoon, Italy. *Biomass and Bioenergy*, 42, 69-77.
- MILLEDGE, J. 2011. Commercial application of microalgae other than as biofuels: a brief review. *Reviews in Environmental Science and Bio/Technology*, 10, 31-41.
- MILLEDGE, J. 2013. *Energy balance and techno-economic assessment of algal biofuel production systems*. University of Southampton.
- MILLEDGE, J. J. 2010a. The challenge of algal fuel : economic processing of the entire algal biomass. *Condensed Matter -Materials Engineering Newsletter*, 4-6.
- MILLEDGE, J. J. 2010b. The challenge of algal fuel: economic processing of the entire algal biomass. *Condensed Matter Materials Engineering Newsletter*, 1, 4-6.
- MILLERO, F. J. 1986. The thermodynamics and kinetics of the hydrogen sulfide system in natural waters. *Marine Chemistry*, 18, 121-147.
- MOEN, E., HORN, S. & ØSTGAARD, K. 1997. Alginate degradation during anaerobic digestion of *Laminaria hyperborea* stipes. *Journal of Applied Phycology*, 9, 157-166.
- MOLINA, E., FERNANDEZ, J., ACIEN, F. G. & CHISTI, Y. 2001. Tubular photobioreactor design for algal cultures. *Journal of Biotechnology*, 92, 113-131.
- MONNET, F. 2003. An introduction to anaerobic digestion of organic wastes. *Final Report*. pp, 1-43.
- MONOD, J. 1949. The growth of bacterial cultures. *Annual Reviews in Microbiology* 3, 371-394.
- MOREL, F. M. M. & HERING, J. G. 1993. *Principles and Applications of Aquatic Chemistry*, John Wiley & Sons.
- MOSQUERA-CORRAL, A., SANCHEZ, M., CAMPOS, J. L., MENDEZ, R. & LEMA, J. M. 2001. Simultaneous methanogenesis and denitrification of pretreated effluents from a fish canning industry. *Water Research*, 35, 411-418.
- MOTTET, A., HABOUZIT, F. & STEYER, J. P. 2014. Anaerobic digestion of marine microalgae in different salinity levels. *Bioresource Technology*, 158, 300-306.
- MÜLLER, V. 2003. Energy conservation in acetogenic bacteria. *Applied and environmental microbiology*, 69, 6345-6353.
- MUSSGUNG, J. H., KLASSEN, V., SCHLÜTER, A. & KRUSE, O. 2010. Microalgae as substrates for fermentative biogas production in a combined biorefinery concept. *Journal of Biotechnology*, 150, 51-56.
- MUYZER, G. & STAMS, A. J. M. 2008. The ecology and biotechnology of sulphate-reducing bacteria. *Nat Rev Micro*, 6, 441-454.
- NIELSEN, H. & HEISKE, S. 2011. Anaerobic digestion of macroalgae: methane potentials, pre-treatment, inhibition and co-digestion. *Water Science & Technology*, 64, 1723-1729.
- NKEMKA, V. N. & MURTO, M. 2010. Evaluation of biogas production from seaweed in batch tests and in UASB reactors combined with the removal of heavy metals. *Journal of Environmental Management*, 91, 1573-1579.

- O'FLAHERTY, V. & COLLERAN, E. 1999. Effect of sulphate addition on volatile fatty acid and ethanol degradation in an anaerobic hybrid reactor. I: process disturbance and remediation. *Bioresource Technology*, 68, 101-107.
- O'FLAHERTY, V., COLOHAN, S., MULKERRINS, D. & COLLERAN, E. 1999. Effect of sulphate addition on volatile fatty acid and ethanol degradation in an anaerobic hybrid reactor. II: microbial interactions and toxic effects. *Bioresource Technology*, 68, 109-120.
- O'FLAHERTY, V., LENS, P., LEAHY, B. & COLLERAN, E. 1998a. LONG-TERM COMPETITION BETWEEN SULPHATE-REDUCING AND METHANE-PRODUCING BACTERIA DURING FULL-SCALE ANAEROBIC TREATMENT OF CITRIC ACID PRODUCTION WASTEWATER. *Water Research*, 32, 815-825.
- O'FLAHERTY, V., MAHONY, T., O'KENNEDY, R. & COLLERAN, E. 1998b. Effect of pH on growth kinetics and sulphide toxicity thresholds of a range of methanogenic, syntrophic and sulphate-reducing bacteria. *Process Biochemistry*, 33, 555-569.
- OBATA, O., AKUNNA, J. C. & WALKER, G. 2015. Hydrolytic effects of acid and enzymatic pre-treatment on the anaerobic biodegradability of *Ascophyllum nodosum* and *Laminaria digitata* species of brown seaweed. *Biomass and Bioenergy*, 80, 140-146.
- OLESZKIEWICZ, J. A. & SHARMA, V. K. 1990. Stimulation and inhibition of anaerobic processes by heavy metals—A review. *Biological Wastes*, 31, 45-67.
- OMIL, F., MENDEZ, R. & LEMA, J. M. 1995. Anaerobic treatment of saline wastewaters under high sulphide and ammonia content. *Bioresource Technology*, 54, 269-278.
- ORTIZ, J., ROMERO, N., ROBERT, P., ARAYA, J., LOPEZ-HERNÁNDEZ, J., BOZZO, C., NAVARRETE, E., OSORIO, A. & RIOS, A. 2006. Dietary fiber, amino acid, fatty acid and tocopherol contents of the edible seaweeds *Ulva lactuca* and *Durvillaea antarctica*. *Food Chemistry*, 99, 98-104.
- PACHECO-RUIZ, S., HEAVEN, S. & BANKS, C. J. 2015. Development and testing of a fully gravitational submerged anaerobic membrane bioreactor for wastewater treatment. *Environmental Technology*, 36, 2328-2339.
- PAL, D., KHOZIN-GOLDBERG, I., COHEN, Z. & BOUSSIBA, S. 2011. The effect of light, salinity, and nitrogen availability on lipid production by *Nannochloropsis* sp. *Applied Microbiology and Biotechnology*, 90, 1429-1441.
- PARK, S. & LI, Y. 2012. Evaluation of methane production and macronutrient degradation in the anaerobic co-digestion of algae biomass residue and lipid waste. *Bioresource Technology*, 111, 42-48.
- PARKIN, G. F., LYNCH, N. A., KUO, W. C., VANKEUREN, E. L. & BHATTACHARYA, S. K. 1990. Interaction between sulfate reducers and methanogens fed acetate and propionate. *Research Journal of the Water Pollution Control Federation*, 62, 780-788.
- PARKIN, G. F. & OWEN, W. F. 1986. Fundamentals of Anaerobic Digestion of Wastewater Sludges. *Journal of Environmental Engineering*, 112, 867-920.
- PASSOS, F., SOLÉ, M., GARCÍA, J. & FERRER, I. 2013. Biogas production from microalgae grown in wastewater: Effect of microwave pretreatment. *Applied Energy*, 108, 168-175.
- PATARRA, R., PAIVA, L., NETO, A., LIMA, E. & BAPTISTA, J. 2011. Nutritional value of selected macroalgae. *Journal of Applied Phycology*, 23, 205-208.
- PATE, R., KLISE, G. & WU, B. 2011. Resource demand implications for US algae biofuels production scale-up. *Applied Energy*, 88, 3377-3388.
- PERRY ROBERT, H., GREEN DON, W. & MALONEY JAMES, O. 1997. Perry's Chemical Engineers' Handbook. *Mc Graw-Hills New York*.
- PEU, P., SASSI, J. F., GIRAULT, R., PICARD, S., SAINT-CAST, P., BÉLINE, F. & DABERT, P. 2011. Sulphur fate and anaerobic biodegradation potential during co-digestion of seaweed biomass (*Ulva* sp.) with pig slurry. *Bioresource Technology*, 102, 10794-10802.
- POLAKOVIČOVÁ, G., KUŠNÍR, P., NAGYOVÁ, S. & MIKULEC, J. 2012. Process integration of algae production and anaerobic digestion. *CHEMICAL ENGINEERING*, 29.

References

- POWLES, S. B. 1984. Photoinhibition of photosynthesis induced by visible light. *Annual Review of Plant Physiology*, 35, 15-44.
- PULLAMMANAPPALLIL, P. C., CHYNOWETH, D. P., LYBERATOS, G. & SVORONOS, S. A. 2001. Stable performance of anaerobic digestion in the presence of a high concentration of propionic acid. *Bioresource Technology*, 78, 165-169.
- RAJESHWARI, K. V., BALAKRISHNAN, M., KANSAL, A., LATA, K. & KISHORE, V. V. N. 2000. State-of-the-art of anaerobic digestion technology for industrial wastewater treatment. *Renewable and Sustainable Energy Reviews*, 4, 135-156.
- RANADE, D. R., DIGHE, A. S., BHIRANGI, S. S., PANHALKAR, V. S. & YEOLE, T. Y. 1999. Evaluation of the use of sodium molybdate to inhibit sulphate reduction during anaerobic digestion of distillery waste. *Bioresource Technology*, 68, 287-291.
- RAO, M. S., SINGH, S. P., SINGH, A. K. & SODHA, M. S. 2000. Bioenergy conversion studies of the organic fraction of MSW: assessment of ultimate bioenergy production potential of municipal garbage. *Applied Energy*, 66, 75-87.
- RAPOSO, F., DE LA RUBIA, M., FERNÁNDEZ-CEGRÍ, V. & BORJA, R. 2012. Anaerobic digestion of solid organic substrates in batch mode: an overview relating to methane yields and experimental procedures. *Renewable and Sustainable Energy Reviews*, 16, 861-877.
- RAS, M., LARDON, L., BRUNO, S., BERNET, N. & STEYER, J.-P. 2011a. Experimental study on a coupled process of production and anaerobic digestion of *Chlorella vulgaris*. *Bioresource Technology*, 102, 200-206.
- RAS, M., LARDON, L., BRUNO, S., BERNET, N. & STEYER, J. P. 2011b. Experimental study on a coupled process of production and anaerobic digestion of *Chlorella vulgaris*. *Bioresource Technology*, 102, 200-206.
- RASI, S., VEIJANEN, A. & RINTALA, J. 2007. Trace compounds of biogas from different biogas production plants. *Energy*, 32, 1375-1380.
- RCEP, ROYAL COMMISSION ON ENVIRONMENTAL POLLUTION 2004. Biomass as a renewable energy source. Published by the Royal Commission on Environmental Pollution. London SW1P 3JS.
- REBOLLOSO-FUENTES, M. M., NAVARRO-PÉREZ, A., GARCÍA-CAMACHO, F., RAMOS-MIRAS, J. J. & GUIL-GUERRERO, J. L. 2001. Biomass Nutrient Profiles of the Microalga *Nannochloropsis*. *Journal of Agricultural and Food Chemistry*, 49, 2966-2972.
- REDFIELD, A. C. 1958. The biological control of the chemical factors in the environment. *American Scientist*, 46, 230A-221.
- RENAUD, S. M., THINH, L.-V., LAMBRINIDIS, G. & PARRY, D. L. 2002. Effect of temperature on growth, chemical composition and fatty acid composition of tropical Australian microalgae grown in batch cultures. *Aquaculture*, 211, 195-214.
- RICHMOND, A. (ed.) 2004. *Handbook of Microalgal Culture Biotechnology and Applied Phycology*, Oxford: Blackwell Publishing.
- RINZEMA, A. & LETTINGA, G. 1988. The effect of sulphide on the anaerobic degradation of propionate. *Environmental Technology*, 9, 83-88.
- RINZEMA, A., VAN LIER, J. & LETTINGA, G. 1988. Sodium inhibition of acetoclastic methanogens in granular sludge from a UASB reactor. *Enzyme and Microbial Technology*, 10, 24-32.
- RIPLEY, L. E., BOYLE, W. C. & CONVERSE, J. C. 1986. Improved alkalimetric monitoring for anaerobic-digestion of high strength wastes. *J. Water Pollution*, 58, 406-411.
- RIZVI, H., AHMAD, N., ABBAS, F., BUKHARI, I. H., YASAR, A., ALI, S., YASMEEN, T. & RIAZ, M. 2013. Start-up of UASB reactors treating municipal wastewater and effect of temperature/sludge age and hydraulic retention time (HRT) on its performance. *Arabian Journal of Chemistry*.

- ROBERTS, K. 1974. Crystalline Glycoprotein Cell Walls of Algae: Their Structure, Composition and Assembly. *Philosophical Transactions of the Royal Society of London. Series B, Biological Sciences*, 268, 129-146.
- ROCHA, J. M. S., GARCIA, J. E. C. & HENRIQUES, M. H. F. 2003. Growth aspects of the marine microalga *Nannochloropsis gaditana*. *Biomolecular Engineering*, 20, 237-242.
- RODOLFI, L., ZITTELLI, G. C., BASSI, N., PADOVANI, G., BIONDI, N., BONINI, G. & TREDICI, M. R. 2009. Microalgae for Oil: Strain Selection, Induction of Lipid Synthesis and Outdoor Mass Cultivation in a Low-Cost Photobioreactor. *Biotechnology and Bioengineering*, 102, 100-112.
- ROGALLA, F. 2014. FP & Project All-Gas: From urban waste water to biofuel. *4th UK Algae Conference*. Cranfield.
- ROVIROSA, N., SANCHEZ, E., CRUZ, VEIGA, M. C. & BORJA, R. 2004. Coliform concentration reduction and related performance evaluation of a down-flow anaerobic fixed bed reactor treating low-strength saline wastewater. *Bioresour. Technol.*, 94, 119-127.
- RUBIO, F. C., FERNÁNDEZ, F. G. A., PÉREZ, J. A. S., CAMACHO, F. G. & GRIMA, E. M. 1999. Prediction of dissolved oxygen and carbon dioxide concentration profiles in tubular photobioreactors for microalgal culture. *Biotechnology and Bioengineering*, 62, 71-86.
- RUI, X., PAY, E., TIANRONG, G., FANG, Y. & WUDI, Z. 2009. The Potential of Blue-Green Algae for Producing Methane in Biogas Fermentation. In: GOSWAMI, D. Y. & ZHAO, Y. (eds.) *Proceedings of ISES World Congress 2007 (Vol. I – Vol. V)*. Springer Berlin Heidelberg.
- SALERNO, M., NURDOGAN, Y. & LUNDQUIST, T. J. 2009. *Biogas Production from Algae Biomass Harvested at Wastewater Treatment Ponds*.
- SALTER, A. & BANKS, C. 2009. Establishing an energy balance for crop-based digestion.
- SAMSON, R. & LEDUY, A. 1983a. Improved performance of anaerobic digestion of *Spirulina maxima* algal biomass by addition of carbon-rich wastes. *Biotechnology Letters*, 5, 677-682.
- SAMSON, R. & LEDUY, A. 1983b. Influence of mechanical and thermochemical pretreatments on anaerobic digestion of *Spirulina maxima* algal biomass. *Biotechnology Letters*, 5, 671-676.
- SAMSON, R. & LEDUY, A. 1983c. Influence of mechanical and thermochemical pretreatments on anaerobic digestion of *Spirulina maxima* algal biomass. *Biotechnology Letters*, 5, 671-676.
- SAMSON, R. & LEDUYT, A. 1986. Detailed study of anaerobic digestion of *Spirulina maxima* algal biomass. *Biotechnology and Bioengineering*, 28, 1014-1023.
- SÁNCHEZ HERNÁNDEZ, E. P. & TRAVIESO CÓRDOBA, L. 1993. Anaerobic digestion of *Chlorella vulgaris* for energy production. *Resources, Conservation and Recycling*, 9, 127-132.
- SANDNES, J. M., KÄLLQVIST, T., WENNER, D. & GISLERØD, H. R. 2005. Combined influence of light and temperature on growth rates of *Nannochloropsis oceanica*: linking cellular responses to large-scale biomass production. *Journal of Applied Phycology*, 17, 515-525.
- SANTELICES, B. 2007. The discovery of kelp forests in deep-water habitats of tropical regions. *Proceedings of the National Academy of Sciences*, 104, 19163-19164.
- SANTOS, N. O., OLIVEIRA, S. M., ALVES, L. C. & CAMMAROTA, M. C. 2014. Methane production from marine microalgae *Isochrysis galbana*. *Bioresource Technology*, 157, 60-67.
- SARMIENTO, J. L. & GRUBER, N. 2006. *Ocean Biogeochemical Dynamics*, Oxfordshire, Princeton University Press.
- SCHERER, P. & SAHM, H. 1981. Influence of sulphur-containing compounds on the growth of *Methanosarcina barkeri* in a defined medium. *European journal of applied microbiology and biotechnology*, 12, 28-35.
- SCHLARB-RIDLEY, B. 2011. Algal research in the UK. BBRSC.

References

- SCHWEDE, S., REHMAN, Z.-U., GERBER, M., THEISS, C. & SPAN, R. 2013. Effects of thermal pretreatment on anaerobic digestion of *Nannochloropsis salina* biomass. *Bioresource Technology*, 143, 505-511.
- SHAFIEE, S. & TOPAL, E. 2009. When will fossil fuel reserves be diminished? *Energy Policy*, 37, 181-189.
- SHAFIEE, S. & TOPAL, E. 2010. A long-term view of worldwide fossil fuel prices. *Applied Energy*, 87, 988-1000.
- SIALVE, B., BERNET, N. & BERNARD, O. 2009. Anaerobic digestion of microalgae as a necessary step to make microalgal biodiesel sustainable. *Biotechnology Advances*, 27, 409-416.
- SIEGRIST, H., VOGT, D., GARCIA-HERAS, J. L. & GUJER, W. 2002. Mathematical Model for Meso- and Thermophilic Anaerobic Sewage Sludge Digestion. *Environmental Science & Technology*, 36, 1113-1123.
- SIMS, R. E. H., R.N. SCHOCK, A. ADEGBULULGBE, J. FENHANN, I. KONSTANTINAVICIUTE, W. MOOMAW, H.B. NIMIR, B. SCHLAMADINGER, J. TORRES-MARTÍNEZ, C. TURNER, Y. UCHIYAMA, S.J.V. VUORI, N. WAMUKONYA & X. ZHANG 2007. Energy supply. In *Climate Change 2007: Mitigation. Contribution of Working Group III to the Fourth Assessment Report of the Intergovernmental Panel on Climate Change*. In: B. METZ, O.R. DAVIDSON, P.R. BOSCH, R. DAVE & MEYER, L. A. (eds.). Cambridge, United Kingdom and New York, NY, USA.
- SINGH, R. N. & SHARMA, S. 2012. Development of suitable photobioreactor for algae production – A review. *Renewable and Sustainable Energy Reviews*, 16, 2347-2353.
- SOTO, M., MÉNDEZ, R. & LEMA, J. M. 1991. Biodegradability and toxicity in the anaerobic treatment of fish canning wastewaters. *Environmental Technology*, 12, 669-677.
- SOTO, M., MÉNDEZ, R. & LEMA, J. M. 1993. Sodium inhibition and sulphate reduction in the anaerobic treatment of mussel processing wastewaters. *Journal of Chemical Technology & Biotechnology*, 58, 1-7.
- SOWERS, K. R. & GUNSALUS, R. P. 1988. Adaptation for growth at various saline concentrations by the archaeobacterium *methanosarcina-thermophila*. *Journal of Bacteriology*, 170, 998-1002.
- SPEECE, R. E. 1983. Anaerobic biotechnology for industrial wastewater treatment. *Environmental Science & Technology*, 17, 416A-427A.
- SPEECE, R. E. 1996. Anaerobic biotechnology for industrial wastewaters. *Anaerobic biotechnology for industrial wastewaters*.
- SPEECE, R. E. & PARKIN, G. F. The response of methane bacteria to toxicity. In: R. L. WENTWORTH, D. A. STAFFORD, B. I. WHEATLEY, W. E. EDELMANN, G. LETTINGA, Y. MINODA, P. MULAS DEL POZO, E. J. NYNS, F. G. POHLAND, J. F. REES, L. VAN DEN BERG, W. VERSTRAETE & WARD, R. F., eds. 3rd International Symposium on Anaerobic Digestion, 1983 Watertown, Mass., 23-35.
- SPICER, M. 1988. Renewable energy in the UK: The way forward. In: ENERGY, D. O. (ed.). London: Her Majesties Stationary Office.
- SPOLAORE, P., JOANNIS-CASSAN, C., DURAN, E. & ISAMBERT, A. 2006. Commercial applications of microalgae. *Journal of Bioscience and Bioengineering*, 101, 87-96.
- STADTMAN, T. C. & BARKER, H. A. 1951. STUDIES ON THE METHANE FERMENTATION IX. : The Origin of Methane in the Acetate and Methanol Fermentations by *Methanosarcina*. *Journal of Bacteriology*, 61, 81-86.
- STEPHENSON, A. L., KAZAMIA, E., DENNIS, J. S., HOWE, C. J., SCOTT, S. A. & SMITH, A. G. 2010. Life-Cycle Assessment of Potential Algal Biodiesel Production in the United Kingdom: A Comparison of Raceways and Air-Lift Tubular Bioreactors. *Energy & Fuels*, 24, 4062-4077.

- STEPHENSON, P. G., MOORE, C. M., TERRY, M. J., ZUBKOV, M. V. & BIBBY, T. S. 2011. Improving photosynthesis for algal biofuels: toward a green revolution. *Trends in Biotechnology*, 29, 615-623.
- STEUDEL, R. 1996. Mechanism for the Formation of Elemental Sulfur from Aqueous Sulfide in Chemical and Microbiological Desulfurization Processes. *Industrial & Engineering Chemistry Research*, 35, 1417-1423.
- STRATFUL, I., SCRIMSHAW, M. D. & LESTER, J. N. 2001. Conditions influencing the precipitation of magnesium ammonium phosphate. *Water Research*, 35, 4191-4199.
- SUGGETT, D. J., LE FLOC'H, E., HARRIS, G. N., LEONARDOS, N. & GEIDER, R. J. 2007. Different strategies of photoacclimation by two strains of *Emiliana huxleyi* (Haptophyta)1. *Journal of Phycology*, 43, 1209-1222.
- SYAZWANI, I. 2013. *Washing of wheat straw to improve its combustion properties with energy recovery by anaerobic digestion of the washwater*. University of Southampton.
- SYMONS, G. E. & BUSWELL, A. M. 1933. The Methane Fermentation of Carbohydrates1,2. *Journal of the American Chemical Society*, 55, 2028-2036.
- SYRETT, P. J. & THOMAS, E. M. 1973. The Assay of Nitrate Reductase in Whole Cells of *Chlorella*: Strain Differences and the Effect of Cell Walls. *New Phytologist*, 72, 1307-1310.
- TABARSA, M., REZAEI, M., RAMEZANPOUR, Z. & WAALAND, J. R. 2012. Chemical compositions of the marine algae *Gracilaria salicornia* (Rhodophyta) and *Ulva lactuca* (Chlorophyta) as a potential food source. *Journal of the Science of Food and Agriculture*, 92, 2500-2506.
- TAKAGI, M., KARSENO & YOSHIDA, T. 2006. Effect of salt concentration on intracellular accumulation of lipids and triacylglyceride in marine microalgae *Dunaliella* cells. *Journal of Bioscience and Bioengineering*, 101, 223-226.
- TEDESCO, S., BENYOUNIS, K. & OLABI, A. 2013. Mechanical pretreatment effects on macroalgae-derived biogas production in co-digestion with sludge in Ireland. *Energy*, 61, 27-33.
- THAUER, R. K., JUNGERMANN, K. & DECKER, K. 1977. Energy conservation in chemotrophic anaerobic bacteria. *Bacteriological Reviews*, 41, 100-180.
- THOMAS, W. H., SEIBERT, D. L. R., ALDEN, M., NEORI, A. & ELDRIDGE, P. 1984. Yields, photosynthetic efficiencies and proximate composition of dense marine microalgal cultures. II. *Dunaliella primolecta* and *Tetraselmis suecica* experiments. *Biomass*, 5, 211-225.
- THOMPSON, P. 1999. THE RESPONSE OF GROWTH AND BIOCHEMICAL COMPOSITION TO VARIATIONS IN DAYLENGTH, TEMPERATURE, AND IRRADIANCE IN THE MARINE DIATOM *THALASSIOSIRA PSEUDONANA* (BACILLARIOPHYCEAE). *Journal of Phycology*, 35, 1215-1223.
- THRONDSSEN, J. 1997. *Identifying Marine Phytoplankton*, San Diego, Academic Press.
- TRAN, K. C., MENDOZA MARTIN, J. L., HEAVEN, S., BANKS, C. J., ACIEN FERNANDEZ, F. G. & MOLINA GRIMA, E. 2014. Cultivation and anaerobic digestion of *Scenedesmus* spp. grown in a pilot-scale open raceway *Algal Research*.
- UPHAM, P., THORNLEY, P., TOMEI, J. & BOUCHER, P. 2009. Substitutable biodiesel feedstocks for the UK: a review of sustainability issues with reference to the UK RTFO. *Journal of Cleaner Production*, 17, Supplement 1, S37-S45.
- VAN DEN BERG, L. & LENTZ, C. P. 1971. Anaerobic Digestion of Pear Waste: Laboratory Equipment Design and Preliminary Results. *Canadian Institute of Food Technology Journal*, 4, 159-165.
- VAN DEN BOSCH, P. L. F., VAN BEUSEKOM, O. C., BUISMAN, C. J. N. & JANSSEN, A. J. H. 2007. Sulfide oxidation at halo-alkaline conditions in a fed-batch bioreactor. *Biotechnology and Bioengineering*, 97, 1053-1063.
- VAVILIN, V. A., RYTOV, S. V. & LOKSHINA, L. Y. 1996. A description of hydrolysis kinetics in anaerobic degradation of particulate organic matter. *Bioresource Technology*, 56, 229-237.

References

- VAVILIN, V. A., RYTOV, S. V. & LOKSHINA, L. Y. 1997. A balance between hydrolysis and methanogenesis during the anaerobic digestion of organic matter. *Microbiology*, 66, 712-717.
- VERGARA-FERNÁNDEZ, A., VARGAS, G., ALARCÓN, N. & VELASCO, A. 2008. Evaluation of marine algae as a source of biogas in a two-stage anaerobic reactor system. *Biomass and Bioenergy*, 32, 338-344.
- VIDAL, G., ASPE, E., MARTI, M. C. & ROECKEL, M. 1997. Treatment of recycled wastewaters from fishmeal factory by an anaerobic filter. *Biotechnology Letters*, 19, 117-121.
- VIVEKANAND, V., EIJSINK, V. G. & HORN, S. J. 2012. Biogas production from the brown seaweed *Saccharina latissima*: thermal pretreatment and codigestion with wheat straw. *Journal of Applied Phycology*, 24, 1295-1301.
- VOGELS, G. D., KELTJENS, J. T. & VAN DER DRIFT, C. 1988. Biochemistry of methane production. *Biology of anaerobic microorganisms*, 707-770.
- VOROSMARTY, C. J., MCINTYRE, P. B., GESSNER, M. O., DUDGEON, D., PRUSEVICH, A., GREEN, P., GLIDDEN, S., BUNN, S. E., SULLIVAN, C. A., LIERMANN, C. R. & DAVIES, P. M. 2010. Global threats to human water security and river biodiversity. *Nature*, 467, 555-561.
- VYRIDES, I. & STUCKEY, D. C. 2009. Adaptation of anaerobic biomass to saline conditions: Role of compatible solutes and extracellular polysaccharides. *Enzyme and Microbial Technology*, 44, 46-51.
- WALKER, M., ZHANG, Y., HEAVEN, S. & BANKS, C. 2009. Potential errors in the quantitative evaluation of biogas production in anaerobic digestion processes. *Bioresource Technology*, 100, 6339-6346.
- WANG, Z. J. & BANKS, C. J. 2006. Report: Anaerobic digestion of a sulphate-rich high-strength landfill leachate: the effect of differential dosing with FeCl₃. *Waste Management & Research*, 24, 289-293.
- WARD, A. J., LEWIS, D. M. & GREEN, F. B. 2014. Anaerobic digestion of algae biomass: A review. *Algal Research*, 5, 204-214.
- WEILAND, P. 2010. Biogas production: current state and perspectives. *Applied Microbiology and Biotechnology*, 85, 849-860.
- WESTERHOFF, P., HU, Q., ESPARZA - SOTO, M. & VERMAAS, W. 2010. Growth parameters of microalgae tolerant to high levels of carbon dioxide in batch and continuous - flow photobioreactors. *Environmental Technology*, 31, 523-532.
- WEYER, K., BUSH, D., DARZINS, A. & WILLSON, B. 2010. Theoretical Maximum Algal Oil Production. *BioEnergy Research*, 3, 204-213.
- WHALLEY, C. 2008. *Performance of variable climate waste stabilisation pond systems during critical spring warm-up period*. PhD, University of Southampton.
- WHALLEY, C. P., BANKS, C. J. & HEAVEN, S. (In preparation) Formulation of a synthetic sewage for use in laboratory-scale biological treatment studies.
- WHEELER, A. E., ZINGARO, R. A., IRGOLIC, K. & BOTTINO, N. R. 1982. The effect of selenate, selenite, and sulfate on the growth of six unicellular marine algae. *Journal of Experimental Marine Biology and Ecology*, 57, 181-194.
- WIDDEL, F. 1988. Microbiology and ecology of sulfate- and sulfur-reducing bacteria. *Biology of Anaerobic Microorganisms*, 469-585.
- WIJFFELS, R. H. & BARBOSA, M. J. 2010. An Outlook on Microalgal Biofuels. *Science*, 329, 796-799.
- WILHELM, C. & JAKOB, T. 2011. From photons to biomass and biofuels: evaluation of different strategies for the improvement of algal biotechnology based on comparative energy balances. *Applied Microbiology and Biotechnology*, 92, 909-919.
- WILLIAMS, P. J. L. B. & LAURENS, L. M. L. 2010. Microalgae as biodiesel & biomass feedstocks: Review & analysis of the biochemistry, energetics & economics. *Energy & Environmental Science*, 3, 554-590.

- WILLIAMS, S. 1999. Struvite Precipitation in the Sludge Stream at Slough Wastewater Treatment Plant and Opportunities for Phosphorus Recovery. *Environmental Technology*, 20, 743-747.
- WILSENACH, J. A., SCHUURBIERS, C. A. H. & VAN LOOSDRECHT, M. C. M. 2007. Phosphate and potassium recovery from source separated urine through struvite precipitation. *Water Research*, 41, 458-466.
- WISE, D. L., AUGENSTEIN, D. C. & RYTHER, J. H. 1979. Methane fermentation of aquatic biomass. *Resource Recovery and Conservation*, 4, 217-237.
- WORM, P., FERMOSE, F. G., STAMS, A. J. M., LENS, P. N. L. & PLUGGE, C. M. 2011. Transcription of *fdh* and *hyd* in Syntrophobacter spp. and Methanospirillum spp. as a diagnostic tool for monitoring anaerobic sludge deprived of molybdenum, tungsten and selenium. *Environmental Microbiology*, 13, 1228-1235.
- YEN, H.-W. & BRUNE, D. E. 2007. Anaerobic co-digestion of algal sludge and waste paper to produce methane. *Bioresource Technology*, 98, 130-134.
- YENIGÜN, O. & DEMIREL, B. 2013. Ammonia inhibition in anaerobic digestion: A review. *Process Biochemistry*, 48, 901-911.
- ZAMALLOA, C., BOON, N. & VERSTRAETE, W. 2012a. Anaerobic digestibility of *Scenedesmus obliquus* and *Phaeodactylum tricornutum* under mesophilic and thermophilic conditions. *Applied Energy*, 92, 733-738.
- ZAMALLOA, C., DE VRIEZE, J., BOON, N. & VERSTRAETE, W. 2012b. Anaerobic digestibility of marine microalgae *Phaeodactylum tricornutum* in a lab-scale anaerobic membrane bioreactor. *Applied Microbiology and Biotechnology*, 93, 859-869.
- ZAMALLOA, C., VULSTEKE, E., ALBRECHT, J. & VERSTRAETE, W. 2011. The techno-economic potential of renewable energy through the anaerobic digestion of microalgae. *Bioresource Technology*, 102, 1149-1158.
- ZANDVOORT, M. H., VAN HULLEBUSCH, E. D., FERMOSE, F. G. & LENS, P. N. L. 2006. Trace Metals in Anaerobic Granular Sludge Reactors: Bioavailability and Dosing Strategies. *Engineering in Life Sciences*, 6, 293-301.
- ZAYED, G. & WINTER, J. 2000. Inhibition of methane production from whey by heavy metals - Protective effect of sulfide. *Applied Microbiology and Biotechnology*, 53, 726-731.
- ZENG, S., YUAN, X., SHI, X. & QIU, Y. 2010. Effect of inoculum/substrate ratio on methane yield and orthophosphate release from anaerobic digestion of *Microcystis* spp. *Journal of Hazardous Materials*, 178, 89-93.
- ZHANG, L., HAPPE, T. & MELIS, A. 2002. Biochemical and morphological characterization of sulfur-deprived and H₂-producing *Chlamydomonas reinhardtii* (green alga). *Planta*, 214, 552-561.
- ZHANG, R., EL-MASHAD, H. M., HARTMAN, K., WANG, F., LIU, G., CHOATE, C. & GAMBLE, P. 2007. Characterization of food waste as feedstock for anaerobic digestion. *Bioresource Technology*, 98, 929-935.
- ZHANG, Y., ZHANG, Z., SUZUKI, K. & MAEKAWA, T. 2003. Uptake and mass balance of trace metals for methane producing bacteria. *Biomass and Bioenergy*, 25, 427-433.
- ZHAO, B., MA, J., ZHAO, Q., LAURENS, L., JARVIS, E., CHEN, S. & FREAR, C. 2014. Efficient anaerobic digestion of whole microalgae and lipid-extracted microalgae residues for methane energy production. *Bioresource Technology*, 161, 423-430.
- ZHONG, W., ZHANG, Z., LUO, Y., QIAO, W., XIAO, M. & ZHANG, M. 2012. Biogas productivity by co-digesting Taihu blue algae with corn straw as an external carbon source. *Bioresource Technology*, 114, 281-286.
- ZHU, C. J. & LEE, Y. K. 1997. Determination of biomass dry weight of marine microalgae. *Journal of Applied Phycology*, 9, 189-194.